REMOTE DETERMINATION OF DISEASE, PHENOLOGY, PHENOTYPE, AND NITROGEN ON THE WILD BLUEBERRY FIELD

By

Kenneth Eteme Anku

Submitted in partial fulfillment of the
requirements for the degree of Doctor of Philosophy

at

Dalhousie University
Halifax, Nova Scotia
May 2024

TABLE OF CONTENTS

LIST OF TABLES

LIST OF FIGURES

ABSTRACT

Utilizing remote sensing for research and development is essential in enhancing site-specific management practices and estimations of wild blueberry field characteristics. This research aimed to address challenges with site-specific management practices by enhancing productivity, promoting sustainability, reducing production costs, and minimizing environmental impact through decreased agrochemical use. This was achieved partly by identifying plant phenotypes, phenology, and early detection of Monilinia and Botrytis floral diseases, and nitrogen use. An increase in N significantly improved plant growth due to the perennial nature and potential nutrient carryover in wild blueberries. Effective estimations of LNC and LAI were achieved using VIs. Further monitoring and estimation of the growth and development parameters of the plant revealed that LAI, floral, and vegetative bud stages can be estimated at the tight cluster (F4/F5) and bloom (F6/F7) stages with R^2/Lin's CCC values of 0.90/0.84, respectively, although there were challenges in estimating floral and vegetative bud numbers. Additionally, NDVI, ENDVI, GLI, VARI, and GRVI significantly contributed to achieving the predicted values, while NDRE had minimal effects. A pixel classification method successfully identified *Vaccinium angustifolium* f. nigrum, a disease-susceptible phenotype, with an overall accuracy (OA) of 80%. Estimating the incidence and severity of Monilinia and Botrytis blight on the field posed a challenge, although, the VIS-VIs performed better compared to the NIR-VIs. Classification assessment using hyperspectral data showed that discrimination of MB and BB disease from healthy plants was achieved with an OA of about 96.6% using an SVM or RF classifier. This influences production costs by adopting a spot application of fungicides rather than a blanket application. These findings underscore the utility of remote sensing in discerning floral diseases, assessing phenology, identifying phenotypes, and monitoring nitrogen utilization in wild blueberries.

LIST OF ABBREVIATIONS AND SYMBOLS

% - Percent

< - Less than

> - More than

ALE – Accumulated local effect

BB – Botrytis blossom blight

CB – Cubist

CCC – Lin's concordance correlation coefficient

cm – centimeter

ENDVI – Enhanced NDVI

FBN or FN – Floral bud number

FBS or FS – Floral bud stage

g – Gram

g/m^2 – gram per meter square

GLI – Green light index

GRVI – Green red vegetation index

ha – hectare

kg – Kilogram

KNN – K-Nearest Neighbour

kPa – Kilopascal

L – litre

LAI – Leaf Area Index

LNC – Leaf nitrogen concentration

m – meter

MB – Monilinia blight

ML – Machine Learning

mL – milliliter

NDRE – Normalized difference red edge

NDVI – Normalized difference vegetation index

NIR – Near Infra-red

NIR–VIs – Near Infra-red vegetative indices

nm – nanometer

OA – Overall accuracy

ºC – Degrees Celsius

PD – Plant Density

PH – Plant height

Px – pixel

R – Correlation

R^2 - Coefficient of regression

RF – Random Forest

RGB – Red green blue

RMSE – Root means square error

SAVI – Soil atmospheric vegetative index

SE – Standard error

SMLR – Stepwise multilinear regression

SVM – Support Vector Machine

UAV – Unmanned aerial vehicle

Va – *Vaccinium angustifolium*

VARI – Visible atmospheric red index

VBN or VN – Vegetative bud number

VBS or VS – Vegetative bud stage

VIs – Vegetative Indices

VIS – Visible Light Region

VIS–VIs – Visible light vegetative indices

Vm – *Vaccinium myrtilloides*

ACKNOWLEDGEMENT

My first thanks go to the Almighty God for his faithfulness in strength, grace, and ability towards me in this journey. It's been an interesting journey full of memories and most importantly an opportunity to learn.

I would also like to express my sincere gratitude and thanks to my supervisor, Dr. David Percival, for his invaluable contribution to making this a success. Most importantly, I'm grateful for the belief, patience, and opportunities he gave me throughout this program. I also want to express my sincere appreciation to my committee members, Dr. Rajasekaran Lada, Dr. Brandon Heung, and Dr. Mathew Vankoughnett for their relentless efforts in pushing me every step of the way. I appreciate your constant guidance, contributions, and tireless work around the clock to help me get things done. I cannot thank you enough but wish God's blessings upon your life and ask that the future be kind to you. Without your efforts, this project would not have been possible.

I am also grateful to Joel Langdon, Wayne Reid, and all the research assistants and research interns for their contributions to flying the drone and helping with field activities. Without your help and contribution, I would not have been successful.

Finally, I'm grateful to my family and friends, especially my dad (late), Nancy Kotei-Sass, Joel Abbey, Alex Cornel, Truro friends, Dr. Temidayo, Dr. Lord Abbey, Dr. Yiridoe, and Dr. Asiedu for their direct and indirect support and contributions toward this success. To the many unnamed persons, a special thanks to you for your unconditional support, love, care, and encouragement on this journey.

CHAPTER 1: INTRODUCTION

The wild blueberry plant is native to the northeastern North of America with large hectares of land for production (Drummond, 2019; Drummond & Rowland, 2020). Cultivation of blueberries is generally divided into two forms (i) lowbush blueberry and (ii) highbush blueberry production with the industry focusing predominantly on processing and production of individual quick freeze (IQF) berries (Drummond, 2019). Canada remains one of the largest producers of blueberries, second to the United States (US) with about 80, 657 ha of land, producing 195,892 tons of berries valued at about $363.948 million in 2022 (Eaton & Nams, 2012a; Statistics Canada, 2023).

The wild blueberry plant which is also referred to as "lowbush" blueberry comprises several species, but the two commonly known species are *Vaccinium angustifolium* (Aiton) and *Vaccinium myrtilloides* (Michx.) (Abbey et al., 2018; Kinsman, 1993). The production system is unique, as it is not planted, no tillage practices are used and there's a dependency on using pre-existing population. The plant is managed by the removal of competing vegetation, stumps, and rocks (McIsaac, 1997; Zhang et al., 2010). The wild blueberry plant is well adapted as a stress-tolerating shrub that thrives in naturally acidic soils that are low in nutrients with high proportions of bare spots and weed patches with different topographic elevations (Eaton & Nams, 2012a; Zaman et al., 2008). The regular management practice of pruning forces the plant into a 2-year production cycle. Thus, vegetative, and floral bud development occurs in the first year after pruning has taken place. This is followed by a year of bloom, pollination, fruit set, and berry harvesting (Eaton & Nams, 2012a; Fournier et al., 2020; Zhang et al., 2010). Despite these practices, the development of the plant is met with diseases and stress-limiting challenges.

Several diseases affect the wild blueberry plant, prevalent among them are Monilinia blight (MB) and Botrytis blight (BB) disease. MB is capable of affecting all susceptible tissue shortly

after bud break with BB affecting mainly flowers (Hildebrand & Braun, 1991; Penman & Annis, 2005). Monilinia blight disease is a yield-limiting fungal disease caused by *Monilinia vaccinii-corymbosi* (Reade) Honey (M.vc). The two phases of infection of the fungal organism result in a loss of foliage, floral tissue, yield, and berry quality (Percival et al., 2018). As an economically important disease, the first disease infection takes place in spring at bud break (F2 and V2 stage), while the second infection results from berries that overwinter on the field serving as primary spores for infection (Delbridge & Hildebrand, 1997a; Percival & Beaton, 2012). The fungus colonizes the developing leaves and fruits of the berry plants. Several weeks after infection, symptoms appear as dark brown areas along the veins and midrib of leaves (Delbridge & Hildebrand, 1997a; Hildebrand & Braun, 1991). The disease is not only important to wild blueberries but also to highbush and rabbiteye blueberries (Delbridge & Hildebrand, 1997a; Thompson & Annis, 2014). Each year blueberry loss because of Monilinia blight may vary in their severity depending on the levels of condition present on the field (Thompson & Annis, 2014).

Botrytis cinerea Pers.: Fr, the causative organism of the grey mold and blossom blight, is another commonly encountered pathogen in wild blueberries affecting mainly flowers (Delbridge & Hildebrand, 1997a; Reeh & Cutler, 2013). The organism infects flowers beginning at the F5 stage (tight but expanded corollas) with the F6 and F7 stage being the most susceptible to the organism (Abbey et al., 2018). Generally, the organism infects the expanded corolla until flowers drop and become attached to other plant parts, thus establishing new infection sites (Abbey et al., 2018). The length of time for disease infection is largely dependent on long periods of wet weather conditions, inoculum levels, and temperature during bloom (Delbridge & Hildebrand, 1997a; Oudemans et al., 2018; Reeh & Cutler, 2013). The organism causes high yield losses of about 30 – 35% through infected flowers turning brown and shriveling up with premature abscission of

fruits (Delbridge & Hildebrand, 1997a; Reeh, 2012). Thus, an entire year's crop of blueberries can be lost to Monilinia and Botrytis infection of leaves and flowers in a lowbush field. Because of the devastation caused by diseases, measures are adopted to mitigate these challenges.

The varying pattern of disease damage observed throughout commercial wild blueberry fields points to the potential to reduce fungicide application on tolerant and resisting phenotypes. Wild blueberry fields are naturally heterogeneous with distinctly different phenotypes (Abbey et al., 2018). The different phenotypes of *Vaccinium angustifolium* and *Vaccinium myrtilloides* vary in their physiological and morphological traits, which include stem length, leaves, flowers, and fruit colour (Abbey et al., 2018; Penman & Annis, 2005). Distinctively, these recognizable traits help with identifying the major three, *Vaccinium angustifolium, Vaccinium angustifolium* f. nigrum*,* and *Vaccinium myrtilloides*, and by extension all six phenotypes in commercial fields. Abbey et al., (2018) established that the nature of growth and development observed in the different phenotypes of *Vaccinium myrtilloides* makes them tolerant to Botrytis blossom blight with the prevalent *Vaccinium angustifolium* species being more susceptible to the disease. It is observed that the early stages of growth of *Vaccinium angustifolium* compared to *Vaccinium myrtilloides* differ, thus, the growth and development characteristics observed in *Vaccinium myrtilloides* may account for their tolerance or resistance to diseases on the field (Abbey et al., 2018; Fournier et al., 2020; Kinsman, 1993). It is therefore, significant that the different phenotypes and their phenology be given more consideration. As plant traits and growth stages contribute to the resistant or susceptible nature of the different phenotypes (Abbey et al., 2018; Fournier et al., 2020), there is a need to identify or differentiate between phenotypes and their phenological stages. Knowledge from this can be incorporated into the development of spot application of agrochemicals rather than the traditional method of a blanket application of these

products. Therefore, considering the progress made concerning diseases, phenology, and phenotypic differentiation in wild blueberry fields, there is a need to focus attention on exploring new methods to improve site-specific management practices to maximize production.

Increasing the quantity of blueberries to meet the increasing demands of the global market, while decreasing the carbon footprint on the environment needs the adoption of a more effective approach in assessing, monitoring, and tackling disease problems on the field. Remote sensing and near-range methods such as multi- and hyperspectral sensors provide multiple opportunities where agricultural productivity can be increased (Mahlein et al., 2013). Remote sensing technologies have rapidly developed becoming one of the most important directions in the development of Precision Agricultural Aviation Technology (PAAT), providing imagery data for crops, insects, pests, and diseases using different spatial, spectral, and temporal resolutions to guide decision making (Lan et al., 2017; Pajares, 2015). Unmanned Aerial Vehicles (UAVs) have shown their effectiveness in the field of precision agriculture by being used as one of the technologies for remote sensing of vegetation (Matese et al., 2015). The efficient use of spectral reflectance measurements on plants depends on identifying significant wavelengths of interest. Therefore, depending on the purpose and areas of application, short portions of the wavelength spectrum are considered. The visible region (400 nm – 700 nm) and the near-infrared regions (700 nm – 2500 nm) of the wavelength spectrum are mostly utilized in agricultural determinations. Structural leaf traits, water content, and composition of pigments have a significant impact on spectral signatures, thus, using sensors to concentrate on the visible light and near-infrared regions for agricultural use (Mahlein et al., 2013). These techniques have been demonstrated in fields and are currently being utilized in pathogen detection, phenotype classification, monitoring physiological traits such as biomass and nitrogen levels, plant phenology, and flower detection among other applications

(Maes & Steppe, 2019). This system allows for the collection of visual, multispectral, hyperspectral, and thermal imagery that cannot be obtained readily by ground methods (de Castro et al., 2018). Spectral vegetation indices or indicators used for the detection of plant phenotype and morphological traits range from several simple ratios obtained from wavelength responses through normalized indices to complex equations and algorithms (Walter et al., 2015). The most frequently used index on leaf vegetation in remote sensing is the normalized difference vegetation index (NDVI). The development of NDVI has been correlated with crop properties such as nitrogen status, biomass, chlorophyll content (Eitel et al., 2009; Erdle et al., 2011), and biotic and abiotic stress assessments (Lopes & Reynolds, 2012) in the field. The development of combining NDVI with some indices such as the Green/Red index has resulted in the use of spectral and UAV technologies to monitor disease pressures and phenological changes in the field (Walter et al., 2015).

Research and development activities using remote sensing are critical in improving the site-specific management practices and estimations on wild blueberry fields. Despite the successes achieved with other crops (Hassan et al., 2019; Liu et al., 2018; Penglei et al., 2020), very few studies have been conducted in wild blueberries using UAV and other remote sensing techniques (Barai et al., 2021; Marty et al., 2022). With no reported study on phenotype classification and disease assessment on wild blueberry fields, this study seeks to examine the potential of using remote sensing techniques to identify disease and *Vaccinium* species on the field, especially the disease-susceptible species.

1.1 Research goals, objectives, and hypotheses

This research aimed to address challenges with site-specific management practices by improving yield, sustaining production, and environmental protection by reducing the amount of

agrochemicals used, which reduces the overall cost of production. It is expected that this research develops and establishes a mapped population structure of the wild blueberry fields, identify phenotypes, monitor, and estimate growth and development parameters, and assess Monilinia and Botrytis blight disease pressures observed using remote sensing techniques. With the limited knowledge in these aspects of aerial determination of diseases and phenotypes, estimation of nitrogen using VIs, and phenology monitoring on wild blueberry fields, it was anticipated that findings from this research will culminate into improved predictive disease forecasting models, diagnostic and disease control technologies, and production systems sustainability using prescription maps for spot application rather than the blanket application of agrochemicals on the field. Stemming from the fact that UAVs present a platform for collecting detailed information, this research explored its limited use on commercial wild blueberry fields. It is estimated that developments from the study will improve management practices by reducing agrochemical usage and the overall cost of production by at least 20%.

The objectives of this research were:

1. To examine the potential impact of nitrogen on vegetative indices and plant growth parameters in wild blueberries.
2. To examine the ability to remotely monitor plant growth and the developmental stages in wild blueberries.
3. To remotely identify phenotypes (i.e., clones) and determine variability in wild blueberry fields.
4. To investigate the ability to remotely detect and assess the incidence and severity of Monilinia and Botrytis blossom blight disease in wild blueberries.

In achieving these objectives, we hypothesized that:

1. Nitrogen will have a significant impact on vegetative indices and measurable growth parameters can be estimated using VIs (Objective 1)
2. High predictability of growth parameters can be achieved at all phenological stages using remote sensing techniques (Objective 2).
3. Pubescence and leaf colour of *V. myrtilloides* and *V. angustifolium* are more likely to enable their remote identification and differentiation in the field (Objective 3).
4. Monilinia and Botrytis blight-infected plants will have a different but overlapping response pattern in disease infection and severity in the visible (400 nm – 700 nm) and near infra-red (700nm – 1200 nm) regions of light (Objective 4).

CHAPTER 2: LITERATURE REVIEW

2.1 Overview of the wild blueberry plant

Blueberries are important plants that belong to the family, Ericaceae, and genus, *Vaccinium,* with about 740 species (Kron et al., 2002; Luby et al., 1991; Stephens et al., 2012). Vaccinium is the third largest genus in the Ericaceae family aside from Erica and Rhododendron (Stephens et al., 2012). The genus, *Vaccinium*, consists of several sections which include *Cyanococcus, Oxycoccus, Myrtillus, Vitis idaea, Hemi-myrtillus, Pyxothamnus*, and *Oreades*, among many others (Vander Kloet & Avery, 2010; Yarborough, 2012). Among the sections of Vaccinium, (Stephens et al., 2012; Vander Kloet, 1988), 17 were identified of which Cyanococcus constitutes a majority of the species. There are several species of *Vaccinium* among which include, *V. corymbosum*, *V. oxycoccos*, *V. myrtillus*, *V. angustifolium* Aiton, *V. myrtilloides* Michx., *V. boreale* among other species (Griffin & Blazich, 2008; Luby et al., 1991; USGS, 2013). However, this review is centered on the tetraploid species *Vaccinium angustifolium* Aiton, and the diploid species *Vaccinium myrtilloides* Michx given their prevalence in wild blueberry fields.

Vaccinium angustifolium Aiton and *Vaccinium myrtilloides* Michx, capable of surviving the onslaught of flames (forest fires/burning), salts, cold, water-logged soils, and other harsh environmental conditions make the plant an excellent example of a stress resistant shrub (Vander Kloet & Avery, 2010). Notwithstanding its extreme multiple stress and tolerant nature, the plant is constantly faced with challenges, such as weeds, disease, and pest control problems in nature (Yarborough et al., 1986). Several diseases are associated with the plant, and these include Monilinia blight (*Monilinia vaccinii-corymbosi*), Botrytis blossom blight (*Botrytis cinerea* Pers.), blueberry rust (*Thekopsora vaccinii*) and Septoria leaf spot among other diseases (Abbey et al., 2020; Penman & Annis, 2005). Common to each disease is the fact that they cause severe yield

losses depending on the wet conditions of the location, the inoculum levels, and temperatures during bloom (Delbridge & Hildebrand, 1997a; Oudemans et al., 2018). However, the heterogeneous nature of the field affects the patterns of disease spread, leading to the blanket application of fungicides (Abbey et al., 2018). In addition, the growth and development timing of the two commercially dominant species, *Vaccinium angustifolium*, and *Vaccinium myrtilloides* influences their susceptibility or tolerance to these diseases (Fournier et al., 2020). Therefore, to increase production, several management practices like pruning, fertilization, fungicide application, and pollination have been adopted.

2.2 Production of *Vaccinium spp*.

Blueberry species are native to Northeastern North America (Maine), but the crop naturally grows in all provinces in Canada. Canada's main wild blueberry production centers are Nova Scotia, Quebec, New Brunswick, and Prince Edward Island, with over 69,016 hectares of land for production and 12,367 hectares for the cultivation of highbush blueberry (Agriculture and Agri-Food Canada, 2022; Drummond, 2019). The plant is regarded as the most important crop in value terms and it is valued at about $312 million in 2021 and $363.948 million in 2022, which are above the value of apples and cranberries (Agriculture and Agri-Food Canada, 2022; Statistics Canada, 2023).

Vaccinium. angustifolium (sweet lowbush blueberry) and *Vaccinium myrtilloides* (velvet-leaf blueberry) are the commonly known species on commercial fields (Abbey et al., 2018; Debnath, 2007; Kinsman, 1993). The term “lowbush” as it is popularly called, describes the short or low-growing deciduous and the rhizomatous nature of the shrub compared to a highbush plant that grows to heights typically greater than 1 m. The plant is unique, as it is not planted, no tillage

practices are used and there is a dependency on using pre-existing population of *Vaccinium angustifolium* and *Vaccinium myrtilloides* phenotypes and the removal of competing vegetation, stumps, and rocks (Aalders et al., 1972; McIsaac, 1997; Zaman et al., 2008; Zhang et al., 2010). The wild blueberry plant is well adapted as a stress-resistant perennial shrub that thrives in naturally acidic soils that are low in nutrients with high proportions of bare spots and weed patches with different topographic elevations (Eaton & Nams, 2012a; Zaman et al., 2008). The regular management practice of pruning forces the plant into a 2-year production cycle (Penman & Annis, 2005). Thus, vegetative, and floral bud development occurs in the first year after pruning has taken place. This is followed by a year of bloom, pollination, fruit set, and berry harvesting (Eaton & Nams, 2012; Zaman et al., 2008; Zhang et al., 2010). The presence of bare spots, weed patches, biotic and abiotic stress factors, fruit yield variability, and disease damage within the wild blueberry fields focuses attention on the importance of precision agriculture and site-specific management to maximize production.

2.3 History and background of *Vaccinium spp*.

Historically, wild blueberry species are believed to be the first blueberries to be "cultivated" after indigenous people of North America burned the plants to enhance the production of the plant (Moore, 1993). It is said that the First Nations people originally harvested berries from forested areas that suffered burns from lightning strikes. This activity was later encouraged by indigenous people as they deliberately set fire to picking areas, and this method of pruning led to improved growth and increased yield of the fruits (Wood, 2004). At this point, European settlers began tending stands of the wild plant in the 18th century (Moore, 1993), with large-scale production commencing in the late 1840s and early 1850s (McIsaac, 1997; Wood, 2004). It was around the

era of the 1900s to 1950s that the taxonomic scrabble/treatment of the lowbush blueberries became controversial (Vander Kloet, 1978; Vander Kloet & Dickinson, 2009). Despite the obvious limitations in resolving the phylogenetic tassel of species at the time, Vander Kloet & Dickinson, (2009) suggested that these species could be of hybrid origin. Stephens et al., (2012) stated that the only distinguishing characteristic of *Vaccinium* from the other 30 – 35 genera is their floral morphology. Since that time, several studies on the molecular and morphology of the plant have been conducted and resolved (Duy, 1999; Griffiths et al., 1971).

Early records of harvesting by handpicking and sale of blueberries date back to the 1800s. Around the 1866's, in Milbridge, Maine, a cannery was set up marking the beginning of blueberry processing and movements into the wider markets (Wood, 2004). This method was improved upon, and since the 1930s into recent times, blueberries have been frozen, and this has become a preferred method for shipping. Commercially, lowbush blueberries (V*accinium angustifolium,* and V*accinium myrtilloides*) are cultivated in northern New Hampshire and Maine in the United States, and the Maritime provinces, Quebec, and northern Ontario (Wood, 2004; Yarborough, 2012; Yarborough et al., 1986).

2.4 Clonal, physiological, and morphological variations on the wild blueberry field

2.4.1 *Vaccinium angustifolium* and *Vaccinium myrtilloides*

Vaccinium consists of several species, and these species are present mainly in North America, Europe, and Asia. The broad types of Vaccinium mainly harvested in Canada are the high-bush (*Vaccinium corymbosum* L.) and "wild" or lowbush blueberry (*Vaccinium angustifolium* Aiton. (Stephens et al., 2012; Yarborough et al., 1986). Among some of the species of *Vaccinium* cultivated in Canada are *Vaccinium angustifolium* Aiton, *V. myrtilloides* Michx., *Vaccinium*

corymbosum L., *V. angustifolium* x *V. corymbosum* hybrids, *V. boreale*, and *V. pallidum* Aiton, (Drummond, 2019; Tirmenstein, 1991). *Vaccinium angustifolium* and *Vaccinium myrtilloides* have colonized most areas of commercial fields. The wild blueberry industry is, therefore, based on a mixed field of these two species. Although *V. myrtilloides* is not the most abundant species (Drummond, 2019), they have shown levels of tolerance to diseases and also typically have poor berry yields, thus, a need to identify their population for management purposes.

A wild blueberry field is a composite of many phenotypically diverse clones (Duy, 1999) thus, the two most common wild species exhibit observational differences. The clones vary in their leaf and fruit colour, height, berry size, and leaf density (Ashley, 2020; Jamieson, 2008). These characteristics make it easy to identify clones; yet, this process can be challenging due to the level of variability in the field. It is interesting to note that adjacent clones on the field can have completely different morphological traits (Penman & Annis, 2005).

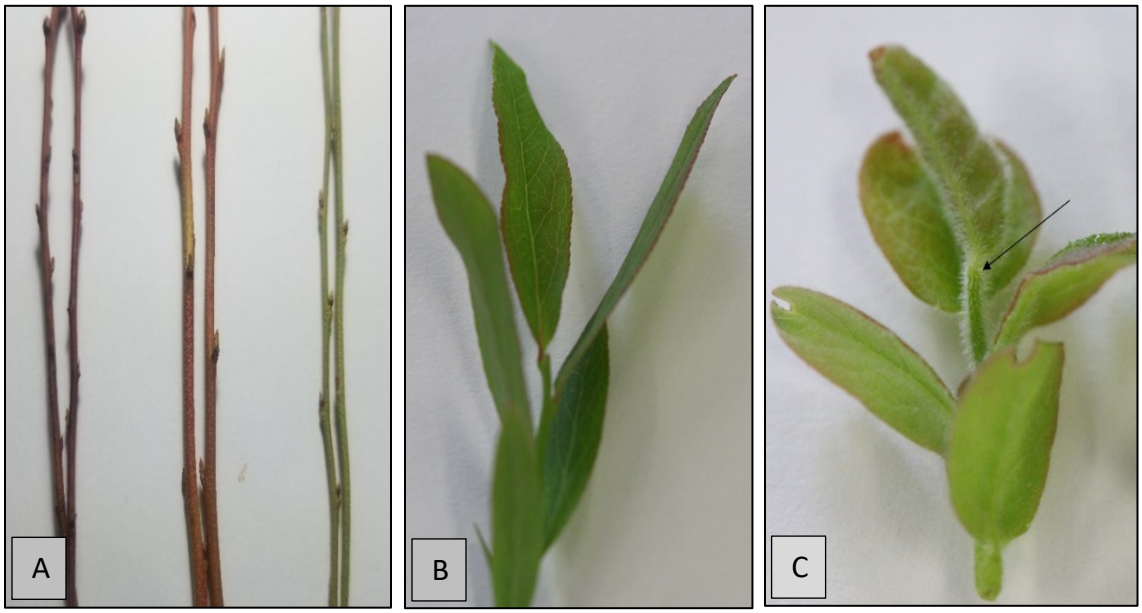

Figure 2.1. Well-developed stems and wild blueberry leaves. (A) Different stem colouration of *V. angustifolium*, (B) Leaves of *V. angustifolium*, and (C) Leave of *V. myrtilloides* with an arrow pointing to pubescence on stems and leaves

2.4.2 *Vaccinium angustifolium*

Vaccinium angustifolium Ait., popularly known as sweet lowbush blueberry, is the most abundant lowbush blueberry cultivated in the eastern North American regions (Drummond, 2019; Noormets & Olson, 2006). The stems are glabrous (without hairs) with fruits covered with powdery pellicules of epicutular wax called bloom. Within *V. angustifolium* f. nigrum, a sub-specie of *V. angustifolium* shows a black shiny fruit colour with *V. angustifolium* showing a blue fruit colour (Agriculture, Aquaculture, and Fisheries, 2010; Chiasson & Morin, 2011). The plant is a tetraploid (2n = 4x = 48) but may hybridize with some species including *Vaccinium myrtilloides* (Vander Kloet, 1978). Studies by Griffiths et al., (1971) showed that crosses between *V. angustifolium* and *V. myrtilloides* did germinate, however, the germination percentages were low. This may account for some level of clonal variability observed on the field.

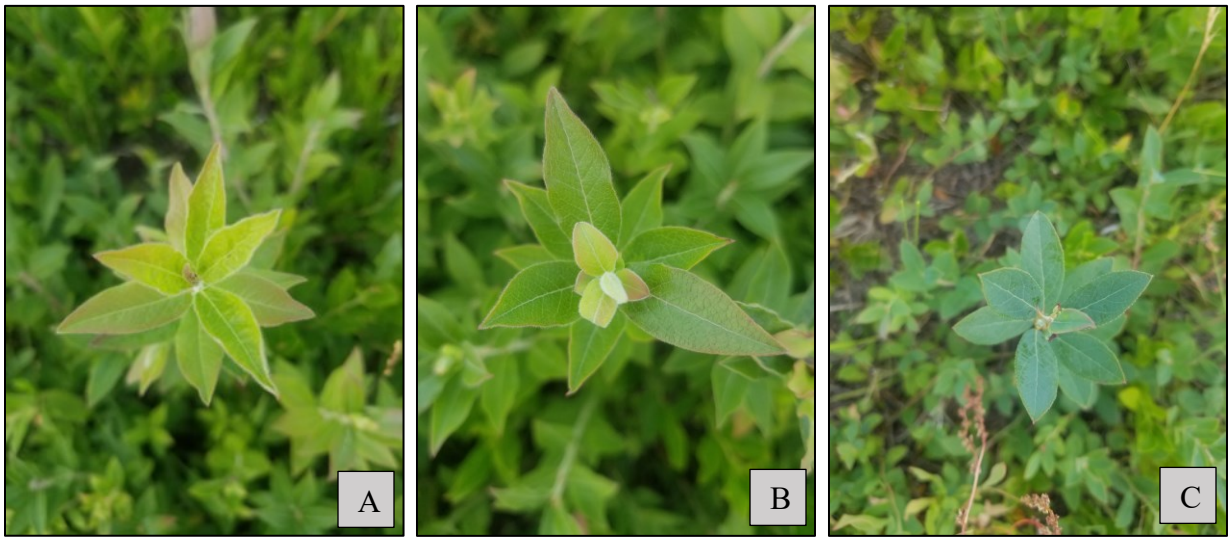

Figure 2.2. Leaf types of the 3 species on the wild blueberry field; (A) *V. myrtilloides*, (B) *V. angustifolium* and (C) *V. angustifolium* f. nigrum

Three morphological *V. angustifolium* phenotypes can be readily identified and present in fields that are distinguished by their leaves, berry, and stem colour characteristics (Duy, 1999; Penman & Annis, 2005). These types consist of (i) blue morphs with black fruits; (ii) green leaves with medium blue colour; and (iii) the hairy morphs that are shown on the underside of leaves (Duy, 1999). A more recent study by Abbey et al., (2023), clearly identified 6 phenotypes as being present on the wild blueberry field and these consisted of *Vaccinium angustifolium* (*Va)* green stem, *Va* brown stem, *Va* f. nigrum, *Vaccinium myrtilloides* (*Vm)* short, *Vm* medium, and *Vm* tall stems (Table 1).

Table 2.1. Classification of wild blueberry phenotypes on the field

Phenotypes	**Description**
V. angustifolium brown	Brown stem/white flower
V. angustifolium f. nigrum	Red/Brown stem/pink flower
V. angustifolium green	Green stem/white flower
V. myrtilloides (tall, medium & short)	Pubescence stems and leaves with white flowers
Vm Short	<15 cm plant height
Vm Medium	15 - 25 cm plant height
Vm Tall	>25 cm plant height

Vm - *Vaccinium myrtilloides*

Therefore, the stem colour variation of tan, green, and brown can be associated with *V. angustifolium* (Wood & Barker, 1963). However, studies have shown that these clones are not distinct biological entities, but only an inconsistent variation of a single polymorphic species, *V. angustifolium* (Duy, 1999; Wood & Barker, 1963). Hall et al., (1972) further state that, despite the

varying stem colours, there is no reported relationship established except for the varying concentrations of chemicals within the stems. The root system is a significant aspect of the plant which enhances increase by the expansion of rhizomes. The roots and rhizomes constitute about 75 – 85% dry weight of the plant (Kaur et al., 2012). These massive underground rhizomes serve as a stem base for the sprouting new shoots; and the greater their depth, the greater their lateral expansion (Hall, Aalders, et al., 1972; Jamieson, 2008). Rhizomes subjected to fire, or any other disturbance, develop a significantly greater number of shoots than untreated rhizomes (Jamieson, 2008; Tirmenstein, 1990).

2.4.3 *Vaccinium myrtilloides*

Vaccinium myrtilloides Michx., commonly known as velvetleaf blueberry is a wild shrub commonly found growing in the boreal forest, headlands, barrens, and meadows. *V. myrtilloides* is a diploid, which spreads vegetatively by forming ramets and can reproduce sexually by forming racemose inflorescences along with erect aerial shoots. Though the plants are predominantly outcrossing, self-pollination is also an option (Noormets & Olson, 2006). The plant is a low, green shrub with a perennial growth cycle. The plant can grow to a height between 10 to 50 cm. The leaves of the plant are entire alternate thin velvet elliptic which is 1 to 4 cm long. Flowers are pendulous and pentacyclic, and it is characterized by an urceolate corolla, clustered at the tip of the branch (Noormets & Olson, 2006; Tirmenstein, 1990). The flowers are about 5 mm long and are inverted with the opening of the corolla at the bottom with curled back edges (Wood et al., 2013). Flower coloration varies from greenish white to pink flowers (Duy, 1999). The plant has a complex root structure, consisting of a taproot and rhizomes with branch-like structures (Wood et al., 2013). The plant is more erect (“stool like”) than *V. angustifolium* and its leaves and stems are

covered with pubescence (hairs; Figure 1C) from which it obtained its name 'velvet-leaf blueberry' (Agriculture, Aquaculture, and Fisheries, 2010; Chiasson & Morin, 2011). The pubescence or trichomes may function as water repellants, deterrents to herbivores, and reducing agents of inoculum loads on plant surfaces (Brewer et al., 1991; Mmbaga et al., 1994; Riddick & Simmons, 2014). This feature of the plant may contribute to the disease variation observed on the field (Figure 1C & 2B).

Phenotypic differences in *V. myrtilloides* have been known, but limited documentation was present until the recent study conducted by Abbey et al., (2023). However, the population structure of these plants on the field indicates notable height variations (Table 1). The observational differences in the field may suggest possible clonal differences and a future categorization of the plant. There is limited study in this aspect, however, field observations suggest a possible categorization based on the height difference that characterizes the clone, *V. myrtilloides.* However, these differences in height may be associated with their genetic or environmental variations. There has been no recent study examining the intra-variations within the *V. myrtilloides* species apart from the work conducted by Abbey et al., (2023), which primarily focused on height differences. Despite these facts, the difference between the "short" *V. myrtilloides* and the "tall" *V. myrtilloides* is striking with *V. myrtilloides* "medium" assuming some similarity with the tall *V. myrtilloides*.

2.5 Phenology of the wild blueberry plant

2.5.1 Growth dynamics of the plant

Genetic characteristics and the local climate are key components regulating the timing of phenological events in Vaccinium species. This phenomenon may lead to early or late phenological events in leaves and flowers, which ultimately influences the susceptibility of the plant to

pathogens and weather conditions (Fournier et al., 2020). Phenology is an important aspect of plant growth and abundance, with temperature, light (hours of sunshine), and rainfall (moisture) being integral aspects, that account for the development processes of the plant (Anadon-Rosell et al., 2014; Hall et al., 1982). Development stages of the plant are common to both *V. angustifolium* and *V. myrtilloides*, and the introduction of pruning into the commercial management system restricts the plant to a two-year growth cycle. The two-year developmental cycle consists of pruning/mowing, plant emergence/sprouting, floral and vegetative bud initiation, tip dieback, and senescence, all occurring within the first-year cycle. The second-year cycle of the plant is characterized by floral and vegetative bud breaking, flower and leaf development, pollination, fruit set, fruit development, and harvest (Fournier et al., 2020; White et al., 2012).

After pruning, plants redevelop naturally from rhizomes which serve as a start for the plant's vegetative growth phase. Most stems develop from auxiliary buds on shoots when burning is not used, however, when burning is used, more shoots tend to develop from the rhizomes (Gibson, 2011; Lambert, 1990; White et al., 2012). As rhizomes expand, new roots are formed, and aerial shoots emerge (Fournier et al., 2020; Gibson, 2011; White et al., 2012). With a base temperature of 0°C, these new shoots emerge rapidly between 222 and 265 growing degree-days (GDD) (White et al., 2012). Up to 90% of the shoots emerge rapidly and this is followed by a period of growth from 2132 to 2768 GDD (13 September to 20 October) (White et al., 2012). After shoots emerge, the plant continues to grow until mid-June. The plant grows in a wide variety of habitats and is tolerant to a wide range of temperatures between 0 °C to 15 °C (Tirmenstein, 1991; White et al., 2012). Sunlight, like other factors, plays an important role in the growth and development of the plant (Tirmenstein, 1991). With temperature contributing to the development process, longer days of warm temperatures enhance the rapid growth of shoots (Tirmenstein, 1991;

White et al., 2012). Apical shoot abortion also referred to as tip dieback, is a prerequisite to the initiation of flower buds on the blueberry plants. Tip dieback is an important process prominent not only in blueberry plants but also in many other species. These developmental processes hinge on several factors, which are necessary and crucial in the establishment of plant density and biomass to support floral bud development (Hall et al., 1970; White et al., 2012). Therefore, vegetative shoot ceases to expand during mid-summer, following the death of the apical meristem. Flower bud initiation starts between June and July of the first year, primordia development (7 – 10 flower primordia per inflorescence), overwinters and resumes growth after dormancy and opens in spring of the second year (Bell, 1950; Gibson, 2011). Therefore, as buds located around the upper part of the stem gradually differentiate into floral parts, the lower buds remain vegetative (Barker & Collins, 1963; Chiasson & Morin, 2011). The process of floral and vegetative bud development and differentiation begins and carries through into the crop year. The plants and their developed buds go into a state of dormancy, where buds develop hardiness to survive winter conditions.

The forms of dormancy can be categorized based on the factors of initiation, which include, endodormancy (self-imposed), paradormancy (factors outside of bud), and ecodormancy (environmental factors) (Faust et al., 1997; Lang et al., 1987). With the resumption of growth, several metabolic processes, like the hydrolysis of stored starch may account for breaking dormancy. The breaking of endodormancy has been attributed to exposure to low temperatures, however, this can be genotype dependent. This requirement is referred to as the chilling requirement (CR) (Parmentier et al., 1998). Afterward, the plants undergo leaf senescence during the fall season, and this constitutes the first-year cycle or the “vegetative growth phase” (Chiasson & Morin, 2011; Fournier et al., 2020; Kaur et al., 2012). Usually, the stem assumes an unequal

proportion of floral and vegetative bud numbers, with considerable variation in the number of floral buds. The stem length significantly affects the number of floral buds and vegetative buds on the plant (Chiasson & Morin, 2011; Fournier et al., 2020). It is observed that *V. angustifolium* has a higher floral bud number than *V. myrtilloides*, with *V. myrtilloides* having more vegetative buds (leaves) than *V. angustifolium* (Fournier et al., 2020). By mid-May the following year, the formed floral buds assume a swollen state, and buds resume growth, producing flowers (fruits) and leaves (Moola & Mallik, 1998). In the shoot development stage, translocation of root carbohydrates is carried out to supply carbon and nutrients to the vegetative buds (Fournier et al., 2020; Kaur et al., 2012). Furthermore, the growth stages of the Vaccinium plant have been determined using developmental guides as described by Hildebrand & Braun, (1991). Therefore, the development process spans from floral bud stage 1 to 12 (F1 to F12) and from vegetative bud stage 1 to 6 (V1 to V6) (Fournier et al., 2020; Jensen & Specht, 2002), thus floral buds undergo several developmental stages compared to the vegetative buds (Fournier et al., 2020). This developmental scale for assessing floral and vegetative budbreak is similar to that of the highbush blueberry plant.

In several studies conducted, results have shown that vegetative bud development spanned stages 1 to 6, with floral bud development measured from stages 1 to 7 (fruiting) (Kovaleski et al., 2015; Williamson et al., 2001). This implies that from the fruiting stage till harvest, there are other developmental stages involved. After the dormancy stage, bud breaking (F1) commences the second cycle of growth leading to the harvest of blueberries later in that season. Studies have shown that flowering in the fruit-bearing year begins between 376 and 406 growing degree-days (GDD), which is estimated to be between 19 May to 30 May (White et al., 2012). However, this can vary depending on the location and climatic conditions prevailing (Tirmenstein, 1991; White et al., 2012). From the F1 stage, the flowering process of the plant continues for an average of 3 –

4 weeks until full bloom (Bell, 1950). Before the fruit set stage (F8), the pistil remains open and receptive for about a week; with a reduction in fertility observed as flowers get old (Gibson, 2011). However, this may vary depending on phenotype (Fournier et al., 2020). The percentage of flowering plants peaks between 692 and 748 GDD (16 June to 17 June) however, the maximum percentage of open flowering plants (F4 to F6) is achieved between 538 and 564 GDD (7 June) (White et al., 2012). According to Chiasson & Argall, (1996 as cited by White et al., 2012) they stated that the full bloom period is believed to last for about 1 to 3 weeks during which the activities of bees help in pollinating the plant (Wood, 1961). However, from the field perspective, studies have shown that there is a clonal difference in phenology with respect to bud break and anthesis between *V. angustifolium* and *V. myrtilloides*. Therefore, the delayed phenology (1 week – 7 days) observed in *V. myrtilloides* affects the phenological calendar when the whole field is considered (Fournier et al., 2020; Moola & Mallik, 1998).

2.5.2 Impact of complex environmental interactions on growth and development

It is evident that developments from the shoot stage until harvest are affected by field conditions which contribute significantly to the phenological dynamics of the plant (Hall et al., 1970). Though both *V. angustifolium* and *V. myrtilloides* demonstrate cold resilience and adaptation, low or freezing temperatures or frost cause damage during flower bloom, and this affects the reproductive structures of the plant by reducing fruit development and yield (Fournier et al., 2020). Hicklenton et al., (2002) in their studies, showed that exposure to 4 hours of -3.5°C resulted in 80% and 60% damage to open and closed flowers, respectively. Research has shown that the abysmally low fruit yield of lowbush blueberries from Nova Scotia is primarily due to the low temperatures within both growing seasons (Hall et al., 1970). In addition, light is a fundamental requirement for growth

and development, therefore a limited supply of light to the plant affects fruit yield. With rhizomes acting as a carbohydrate source, the developing berry crop appears as a strong sink for photoassimilates thus, sucrose is imported from leaf and stem tissues and converted into fructose and glucose during maturation (Kaur et al., 2012). Therefore, without this effective light-dependent process, the assimilation of carbon compounds for yield is affected. Higher temperatures (optimum temperature is around 23°C) create favourable conditions for yield growth, however, higher temperatures when combined with prolonged wetness increase the risk of disease infection (Delbridge & Hildebrand, 1995). Aside from the effect of temperature is the effect of light and how it affects blueberry development. The effects of photoperiod on the growth and development of blueberry have been well documented (Darnell, 1991; Hall & Ludwig, 1961; Spann et al., 2004).

The wild blueberry plant is reported to induce higher flower bud initiation at photoperiods <12 h, however, higher photoperiods between 14 and 16 h can produce limited amounts to no flower buds, with this occurrence being clonal specific (Hall & Ludwig, 1961). Conversely, plants kept under 14 to 16 h photoperiod observes high vegetative bud numbers, (Darnell, 1991; Hall & Ludwig, 1961). Despite some findings, there are difficulties or complexities in the interaction of temperature and photoperiod on blueberries. This was demonstrated when Hall & Ludwig, (1961), applied several photoperiods and temperatures to plants and their response was measured. It was observed that regardless of temperature flower bud initiation occurred between 11 and 13 h however, vegetative bud growth was significant at higher temperatures (21°C). Therefore, at 21°C and 15 h photoperiod, no flower buds were formed, at 10°C and 15 h photoperiod some clones produced flower buds with other clones producing abnormal inflorescence (Hall & Ludwig, 1961). This phenomenon was also reported when Spann et al., (2004) established similar limitations and complexity in the interaction between temperature and photoperiods. However, it was established

that plants grown under short days (SD), 8 h photoperiod with 21°C induced flower buds, compared to a higher temperature (28°C). In that study, the high photoperiod (8 h) led to a complete floral differentiation with an increased and enhanced bloom compared to a 4 h photoperiod (Spann et al., 2004).

Despite the phenotypic and phenological challenges associated with the plant; high variability, different growth habits, and about 80% of the plant being below ground, the growth dynamics of the plant have significantly been explored (Kaur et al., 2012; Penman & Annis, 2005), however, these challenges can affect the successional plant growth dynamics in the field. Irrespective of these facts, it can be stated that the success in growth and the developmental dynamics of the plant are largely dependent on the temperature within a given season.

2.6 Management practices

Field management practices are important aspects of the production process however, while some practices have evolved over the period other new practices have also been introduced. Over the past three decades, more than a four-fold increase in wild blueberry yield can be attributed to the improvements adopted in wild blueberry production (Yarborough, 2004, 2012). Thus, the relevance of these management practices cannot be underestimated. Several management practices have been adopted on the wild blueberry field, and these include, pruning, irrigation, pest and disease management, pollination, nutrient management, and harvesting (Drummond, 2019; Kinsman, 1993; Yarborough, 2012). In this document, some of these practices will be discussed.

2.6.1 Pruning

Pruning wild blueberries is the practice of cutting plant stems or removing the vegetative cover to allow for new growth. Pruning as a method has been adopted in management practices for several reasons: (i) to enhance vigorous and upright growth from underground stems (Kinsman, 1993), (ii) to control pests and diseases on the field (Drummond & Yarborough, 2014), and (iii) to increase production (Eaton et al., 2004) and harvest efficiency. Methods such as flail mowing, burning, chemical spray, and electrical pruning have been used over the years, but there is a heavy dependence on the use of mowing in several commercial fields because of its cost benefits. Chen et al. (2017) found a significant 20% difference in costs between flail mowing and oil-fired burning. Furthermore, a study conducted by Yarborough et al., (2017) established that burning as a method for pruning was associated with reduced plant stand. Therefore, despite the commercial success of using some of these methods, the beneficial effects of using flail mowing outweigh that of burning thus, its adoption in the production practice (Eaton et al., 2004).

2.6.2 Irrigation

Irrigation is a popular practice in many crops including wild blueberries, but it is mostly practiced in Maine. Although the crop has been described as a drought-tolerant plant, several studies and reports have shown that supplementary irrigation enhances berry quality and yield (Hunt et al., 2009). Barai et al., (2021) in a recent study established that irrigation improves plant vigor with a short- and long-term impact on the production system. However, the adoption of this method on these large blueberry fields will increase the cost of production. Despite the research trials conducted using approaches like drip and overhead irrigation, this set-up adds a layer of problem when it comes to pruning because the whole set will have to be removed and reinstalled (Hunt et al., 2009; Yarborough, 2012). There are consequences for excessive watering and underwatering

of the plant, however, efficient water management systems should be adopted. Wild blueberry fields are therefore deemed to require about 2.5 cm of water every week (Yarborough, 2012). In Nova Scotia, irrigation studies conducted have shown poor correlations, however, Maine remains the only wild blueberry area to have invested in irrigation on wild blueberry fields due to the presence of aquifers and sandy soils (Yarborough, 2004).

2.6.3 Nutrient management

Nutrient management in crops is vital for the growth and development of those plants. Thus, aside from the other factors (floral bud number, pollination, etc.) affecting blueberry yield, an improvement in yield depends on the nutrients available to the plant. Low pH soils by nature are low in nutrients, and because the plant thrives in low nutrient acidic soils, there is often less emphasis on fertilization (Agriculture, Aquaculture, and Fisheries, 2013). Despite the low nutrient requirements of the plant, the plant is highly sensitive to excess nutrient levels (Hanson & Lansing, n.d.). Studies have shown that the addition of organic or inorganic fertilizers increases yield (Agriculture, Aquaculture, and Fisheries, 2010; Yarborough, 2004). Over the years, studies have recommended different fertilizer types, diammonium sulfate/ urea, diammonium phosphate (DAP), and monoammonium phosphate (MAP) fertilizers, among others (Santiago, 2011; Santiago & Smagula, 2013; Yarborough, 2004) to be used on blueberry fields. This is because a constituent like urea helps maintain soil pH within the recommended range (Starast et al., 2007). It was established that optimal nitrogen for highbush blueberry is between 50 – 100 kg N/ha however, the acidity of the field must complement its fertility (Starast et al., 2007). Therefore, with acidity playing a significant role in soil fertility, it was recommended that a pH between 4.2 and 5.2 is acceptable for wild blueberry production (Agriculture, Aquaculture, and Fisheries, 2013; Yarborough, 2004).

Specific nutrient requirements of a field may vary; thus, an assessment of leaf nitrogen is carried out to determine the need for fertilization. However, according to Yarborough, (2004, 2012) there was no successful correlation between soil nutrients and productivity, thus testing of soils for nutrient constituents may yield no value. It was stated that highbush stands absorb about 32% of applied N, whereas lowbush absorbed between 45 to 67% of labeled N fertilizer; thus between 33 to 55% of N remains in the soil (Hanson, 2006). Fertilization of fields has focused mainly on macronutrients (nitrogen, phosphorus, and potassium) with some emphasis on the micronutrients.

Table 2.2. Standard reference values for leaf Nutrient levels in wild blueberry plants

Element	Trevett (1972)		Santiago (2011)		
	Min.	**Max**	**Min.**	**Max**	**Optimum**
Nitrogen (N)	1.7%	2.2%	1.55%	1.85%	1.76%
Phosphorous (P)	0.12%	0.18%	0.111%	0.143%	0.136%
Potassium (K)	0.40%	0.60%	0.31%	0.56%	0.44%
Calcium (Ca)	0.37%	0.65%	0.31%	0.40%	0.38%
Magnesium (Mg)	0.13%	0.25%	0.16%	0.18%	0.17%
Boron (B)	21ppm	40 ppm	2 ppm	44 ppm	23 ppm
Iron (Fe)	19 ppm	70 ppm	34 ppm	37 ppm	35 ppm
Manganese (Mn)	750 ppm	1490 ppm	710 ppm	2637 ppm	963 ppm
Zinc (Zn)	15 ppm	20 ppm	10 ppm	15 ppm	13 ppm
Copper (Cu)	3 ppm	6 ppm	3 ppm	6 ppm	4 ppm
Molybdenum (Mo)*	na	na	1.20 ppm	3.30 ppm	0.33 ppm
Aluminum (Al)	na	na	98 ppm	289 ppm	179 ppm

Sources: (Agriculture, Aquaculture, and Fisheries, 2013; Calderwood et al., 2020)

From the standard leaf nitrogen contents of lowbush blueberries established by Trevett, (1972), new standards (Table 2) have been determined by Santiago, (2011). Therefore, it was recommended that leaf testing should be conducted within the year of application to determine the leaf nitrogen level of the plant (Calderwood et al., 2020). However, in addressing the plant's specific needs, specific formulations are also required, thus, a focus on the macronutrient requirements of the wild blueberry plant specifically nitrogen.

2.6.3.1 Macronutrients

2.6.3.1.1 Nitrogen

Of the three major nutrients (N, P, K), nitrogen remains one of the largest nutrients needed for growth and development (Kumar et al., 2021). N is an important plant requirement utilized in the formation of compounds such as chlorophyll, enzymes, and amino acids/proteins (Calderwood et al., 2020; Santiago & Smagula, 2013). In addition, nitrogen enhances yield and vegetative growth (Kumar et al., 2021), but it's also seen to regulate other soil nutrients. Therefore, high amounts of nitrogen can lead to a loss of potassium and calcium (Calderwood et al., 2020). Application of nitrogen to the wild blueberry field has taken different forms with several studies comparing nitrate (NO_3^-) and ammonium (NH_4^+) ions. Despite the success of using NO_3^-, plants grew poorly under NO_3^- but showed a higher affinity for NH_4^+ types (Hanson, 2006; Santiago & Smagula, 2013) thus, the use of the ammonium product types in fertilization on the field (Percival & Privé, 2002). However, the combination of NH_4^+ and NO_3^- can be beneficial to plants (Hanson, 2006; Santiago, 2011). Despite the successes of using N forms, there are several challenges ranging from toxicity, sensitivity (Hanson, 2006), leaching, and volatilization of ammonia (Thyssen et al., 2006) faced on the field.

2.6.3.1.2 Phosphorus

P plays significant roles in plants including storage and the transfer of energy in plants. They enhance early growth, flowering, fruiting, seed production, root development, and the balancing of N effects (Agriculture, Aquaculture, and Fisheries, 2013; Calderwood et al., 2020). In addition, P is mostly used in the formation of nucleic acids (DNA, RNA) (Calderwood et al., 2020) and several cellular processes like signaling, photosynthesis, and energy production (Kumar et al., 2021), however, low pH can limit its availability to the plant by bonding with Fe and aluminum oxides in the soils (Agriculture, Aquaculture, and Fisheries, 2013). The association of *ericoid mycorrhiza* on the roots (69% to 72%) of *Vaccinium* species, enables the uptake of P and other organic nutrients (Percival & Sanderson, 2004). Though the deficiency of this nutrient is not very obvious, dark green with abnormally small leaves can be associated with this nutrient (Calderwood et al., 2020).

2.6.3.1.3 Potassium

K, like the two dominant nutrients, is also used in the synthesis of new compounds. The mobile nature of this nutrient causes it to move from older tissues to actively growing areas of the plant (Calderwood et al., 2020). A study conducted by Percival & Sanderson, (2004) showed that the levels of P increased by about 23% under high N concentrations but observed that about 13% increased under high P conditions. The study established that there is a complex interaction between P and K causing an increase in P to about 81% under K and P applications (Percival & Sanderson, 2004). Though limited studies have been conducted in wild blueberries, it is inferred that K contributes to winter hardiness and storage organs like rhizomes (Agriculture, Aquaculture, and Fisheries, 2013), protein, and chlorophyll formation (Calderwood et al., 2020). However, the

effects of K deficiency are diverse ranging from chlorosis, stunted growth, weak and lodging stems, reduced quality and production of seeds to several other effects (Uchida, 2000).

2.6.3.2 Micronutrients

Generally, these are nutrients that are needed in trace amounts for the growth and development of wild blueberry plants (Agriculture, Aquaculture, and Fisheries, 2013). These include boron (B), manganese (Mn), zinc (Zn), copper (Cu), iron (Fe), and molybdenum (Mo) (Santiago, 2011; Trevett, 1972). Despite the importance of these nutrients, there are rare occurrences of their deficiency on the field, however, other factors like high acidity, low soil temperature, and high soil Ca can trigger Fe and Mn deficiency. Furthermore, excessive application of B and Cu can also cause plant damage (Calderwood et al., 2020). However, a blend of boron and zinc is introduced in fertilizer applications to curb boron deficiency in leaves and enhance its concentration in acidic soils (Smagula & Litten, 2002).

2.6.4 Pollination

Pollination is the most expensive management practice adopted in wild blueberry production (5 hives/acre amounts to more than $150/acre) because it plays a key role in the phenological processes, leading to the yield determination of the plant. Generally, the wild blueberry is an entomophilic, obligate outcrossing plant, whose outcrossing compatibility appears to be non-reciprocal (Drummond, 2019; Drummond & Rowland, 2020; Javorek et al., 2002). This implies that the movement of pollen from clones may achieve fruit set in one direction, but low fruit set in the other direction (Drummond, 2019). This phenomenon is significant because pollen dilution results in ovules being aborted, and this prevents any further chance of the ovules being effectively

pollinated with compatible pollen (Aalders & Hall, 1961). Therefore, the process of pollination in wild blueberry production depends heavily on the use of supplementary and introduced bees (*Apis mellifera*) aside from the wild bee population (Drummond, 2019; Javorek et al., 2002). Though some insects and birds like beetles among other insects and the hummingbird contribute to this process, bees have been used commercially as the main actors in pollination (Drummond, 2019; Manning & Cutler, 2018). Vander Kloet, (1988, as cited in Noormets & Olson, 2006), also states that though *V. myrtilloides* falls into this category, self-pollination should not be excluded from the possibilities. The study established that all three scenarios, autogamy (pollen transfer among the same clone), geitonogamy (pollen transfer among flowers in the same inflorescence), and xenogamy (pollen transfer within a single flower) are genetically equivalent and may occur in the plant (Noormets & Olson, 2006). Studies have shown that high levels of fruit yield have been tied to bee pollination (Drummond, 2019). Given that most phenotypes have self-incompatibility mechanisms and pollen is present as large and sticky tetrads, there is a reliance on the presence of pollinators. This phase leads to fruit set, then ripening of berries begins and continues until harvest. The fruit size of the lowbush blueberry is an intermediate between high bush (*V. corymbosum*) or rabbiteye (*V. uliginosum*) and European bilberry (*V. myrtillus*) or bog blueberry (*V. virgatum*) (Yarborough, 2012). Studies have shown a correlation between seed number and fruit size, thus from the perspectives of pollination, good pollination leads to high seed numbers translating to an increase in fruit size (Isaacs & Kirk, 2010; Percival, personal communication, 2023). The fruit varies in size with a size ranging between 5 to 15 mm in diameter with an average weight of 0.5 grams (Agriculture, Aquaculture, and Fisheries, 2010). The fruit contains between 30 to 70 seeds, with an average of about 64 seeds of which about 50 of these seeds (78%) are considered imperfect

(Bell, 1957). A study by Drummond, (2019) establishes that berry size, fruit weight, and fruit set are factors that are dependent on pollination and fertilization events of the plant.

2.6.5 Weeds, pest and disease management: disease development and plant susceptibility

2.6.5.1 Weeds and insect pest management

Weed control is a major problem in lowbush production. In a study conducted between 2017 to 2019, it was discovered that the lowbush blueberry field in Nova Scotia is naturally home to around 211 weed species. These species include 89 herbaceous perennial forbs, 50 woody perennials, 24 annual broadleaf plants, and 20 perennial grassweeds (Lyu et al., 2021). Additionally, there are other weed flora species such as ferns, biennials, sedges, rushes, and orchids. Some of the most significant weeds in this field are hair fescue (*Festuca filiformis* Pourr.), red or sheep sorrel (*Rumex acetosella* L.), goldenrod (*Euthamia graminifolia*), poverty oat grass (Danthonia spicata L. Beauv.), and yellow hawkweed (*Hieracium caespitosum* Dumort), among others (Boyd & White, 2010; Farooq, 2018; Lyu et al., 2021). These plants compete with lowbush stands for nutrient resources, which can affect yields. However, management and control of these weeds have been carried out using several herbicides.

Similarly, the wild blueberry field also serves as grounds for many insects. Research conducted over six years indicates 3 insect pests as being consistent on the wild blueberry field. These insect pests include blueberry maggot fly (*Rhagoletes mendax*), blueberry thrips (*Frankliniella vaccinii* and *Catinathrips kainos*), and blueberry tips midge (*Dasineura oxycoccana*) (Yarborough et al., 2017). According to Drummond et al., (2009), blueberry spanworm, blueberry flea beetle, strawberry rootworm, and blueberry thrips are the most important insect pest that affects the leaves of wild blueberry plants. Therefore, this presents a scenario that

indicates that the presence of some insect pests may be dependent on location. However, other insect pests have been spotted, namely, spotted wing drosophila, grasshopper, strawberry rootworm, red-striped fireworm, blueberry sawfly, tarnished plant bug, and spiders (Drummond et al., 2009; Yarborough et al., 2017). Despite their presence, spiders have been shown to reduce the prevalence of blueberry thrips. Other insect pests like damsel bugs and lady beetles also contribute to lowering blueberry thrip populations. Spiders are also significant predators of different pests like grasshoppers and strawberry rootworms (Yarborough et al., 2017). However, the continuous use of inputs over the years affects the population density of beneficial insects like bees (*Apis mellifera*) (bumble bees, and honeybees).

2.6.5.2 Disease development and plant susceptibility

Several groups of diseases affect wild blueberries, and this consists of those that affect the flowers (floral blights), leaves (leaf spot diseases), and stems (e.g., stem blights including phomopsis). Among the most prevalent diseases affecting wild blueberry production are Monilinia blight disease (MB) and Botrytis blossom blight disease (BB), which affect mainly foliage and flowers, respectively (Jose et al., 2021; Penman & Annis, 2005; Percival et al., 2018). Monilinia blight disease is a yield-limiting fungal disease caused by *Monilinia vaccinii-corymbosi* (Reade) Honey (M.vc). The two phases of infection of the fungal organism result in a loss in foliage, floral tissue, yield, and berry quality (Abbey et al., 2018). The first disease infection starts in spring at bud break when the plants are at the F2 and V2 developmental stages. These stages are characterized by scales separating flower buds (F2) and vegetative buds showing 2 - 5 mm of green tissues. The second infection stage results from berries that overwinter on the field serving as primary spores for infection (Delbridge & Hildebrand, 1997; Percival & Beaton, 2012). The fungus colonizes the floral and vegetative nodes and fruits of the berry plants. Several weeks after infection, symptoms

appear as dark brown patches along the veins and midrib of leaves (Delbridge & Hildebrand, 1997a; Hildebrand & Braun, 1991). The disease is not only important to wild blueberries, but also to highbush blueberries (Delbridge & Hildebrand, 1997a; Thompson & Annis, 2014). Each year blueberry production records losses because the disease is endemic in most fields (Lambert, 1990) and thus, Monilinia blight may vary in its severity depending on the levels of condition present on the field (Thompson & Annis, 2014). Furthermore, the history of a field is considered necessary for disease management, thus, Delbridge & Hildebrand, (1997) states that "the decision to spray depends almost entirely on the past history of blight on that field". Despite this, the decision to spray also depends on other factors such as plant stage, environmental condition, and the status of the fungal organism (i.e., sporulation) (Abbey et al., 2018; Percival & Beaton, 2012).

The stages of growth of the blueberry plant are considered critical as the production system employs the use of predictive models and growth guides in the management practices on the field. There are several reasons for this development, and these include preventing or controlling disease, and the timely harvest of fruits on the field (Aalders et al., 1972). As part of control measures adopted, predictive models of both Monilinia and Botrytis blight diseases have been developed as alternative measures by monitoring temperature and leaf wetness duration (Delbridge & Hildebrand, 1997a). The susceptibility of the blueberry plant to diseases is a function of climate (temperature and prolonged wet conditions), the plant's developmental stage, and the history of the field with disease occurrence (Delbridge & Hildebrand, 1997a). Therefore, following bud break the plant becomes susceptible to Monilinia blight infection when vegetative buds and floral buds are at the V2 and F2 stage, respectively. Plant susceptibility becomes even more profound when wetness duration and high temperatures last for longer periods (Delbridge & Hildebrand, 1997a; McArt et al., 2016).

After Monilinia blight infection, Botrytis blight infects flowers starting from the corolla (bloom) and spreads to the peduncle of the flower clusters. The disease starts at the white petal stage (F5) and becomes worse at anthesis (F7) to fruit set (Hildebrand et al., 2001). Despite these disease challenges, it is noted that though both *V. angustifolium* and *V. myrtilloides* show similar growth patterns, reproductive budburst, and flowering are delayed by a week (7 days) in *V. myrtilloides* compared to *V. angustifolium* (Fournier et al., 2020; Moola & Mallik, 1998). This delayed process in *V. myrtilloides* may suggest that tolerance or resistance to blight diseases can be attributed to disease avoidance by the plant (Penman & Annis, 2005). This explains the observation made by Lambert, (1990) when he describes some clones in the field as not being affected by some diseases. However, some clones with early shoot also show resistance to some blight diseases (Penman & Annis, 2005). Studies have shown that *V. angustifolium* f. nigrum is the most susceptible phenotype to Monilinia and Botrytis blight disease (Abbey et al., 2018; Jose et al., 2021).

Considering the dependence of these management practices on heavy machinery, these activities involve the burning of fuels which leads to greenhouse gas emissions, soil compaction, time wastage, and the overall increase in production cost. Therefore, to enhance rapid monitoring and determination on the wild blueberry field, it is possible to employ remote sensing techniques to monitor phenology and geospatial identification of phenotypes and diseases in the field.

2.7 Precision agriculture: the potential of utilizing remote sensing in plants

2.7.1 General concept of remote sensing

Vegetation plays an important role in developing and sustaining humans, and its significance affects the global carbon cycle. However, many activities such as climate change, erosion, and

deforestation among others result in serious but continuous damage to vegetation, water, and land resources leading to a loss in biodiversity (Zhang et al., 2019). However, to monitor spatio-temporal phenomena, remote sensing has been adopted into many circles. The traditional methods of monitoring vegetation parameters and measurements, adopt a destructive sampling approach, which requires; longer time, intensive energy, material resources, and cannot be applied in large areas (Jones et al., 2007; Khaled et al., 2018; Tao et al., 2020). Therefore, remote sensing has been adopted to maintain accurate, rapid extraction of cover information and timely monitoring of changes in vegetation (Deng et al., 2018; Lee & Lee, 2018). All objects differentially absorb and reflect electromagnetic waves of different wavelengths. Therefore, since objects exhibit unique spectral characteristics different from other objects, it makes it possible to identify an object based on its reflectance spectra, leading to the concept of remote sensing (Tao et al., 2020).

Over the years, with the rapid development of remote sensing technologies, high-resolution remote sensing images have been widely adopted in the monitoring of vegetation (Zhang et al., 2019). Remote sensing has been adopted to monitor the growth and development of crops using various spatial, temporal, and spectral resolutions acquired through different platforms (Kokhan & Vostokov, 2020) such as ground platforms, unmanned aerial vehicles (UAVs) platforms, and satellite platforms (Tao et al., 2020).

Numerous studies devoted to crop growth and development have utilized crop growth indicators such as leaf area index and nitrogen status, and their relationship with the crop spectral properties to monitor vegetation (Kokhan & Vostokov, 2020). Findings from such studies have projected the use of vegetation indices especially, the normalized difference vegetation index (NDVI) as an important spectral index to monitor the physiological dynamics of key traits such as plant disease, leaf area index (Myneni et al., 2008), nitrogen, and biomass (Hassan et al., 2019).

The potential use of UAVs and other tools in remote sensing has been researched in several studies with high-performing results (Pajares, 2015). The range of their application and possibilities makes them suitable for use on the wild blueberry fields.

2.7.2 Different sensors in remote sensing

The commercial remote sensing industry is comprised of several platforms including satellites, UAVs, aerial, and terrestrial sensors. These platforms are broadly grouped into two major forms: active and passive sensor instruments (Lee & Lee, 2018; Maes & Steppe, 2019). Active sensors use their own energy like RADAR (radio detection and ranging) and LiDAR (light detection and ranging), and passive sensors like UAVs, satellites, and aerial, rely on reflected energy from the sun (Digital Globe, 2014; Weiss et al., 2020). Four kinds of sensors cover almost all applications of UAVs in remote sensing under precision agricultural research, red-green-blue (RGB), multi- and hyperspectral, and thermal sensors (Maes & Steppe, 2019; Nebiker et al., 2016). Each sensor type has a specific wavelength range, which determines the depth of data to be obtained. The RGB camera is a low-cost solution that can be used to generate vegetative indices (VI's), high-resolution digital elevation models (DEMs), and height maps (Maes & Steppe, 2019; Xue & Su, 2017a). Hyperspectral sensors can obtain more waveband information and better reflect biophysical and biochemical parameters and environmental stress, or plant diseases compared to the RGB and multispectral sensors (Aasen et al., 2015; Maes & Steppe, 2019; Tao et al., 2020). However, the applications from a multispectral sensor have extra bands which makes it more rewarding compared to an RGB sensor (Table 1). The multispectral sensor comes with additional wavelength bands, the red edge, and near-infrared wavebands, allowing for enhanced applications than an RGB sensor (Zhang et al., 2020). LIDAR is another powerful sensor that is used to measure spatial variations in canopy heights and other aspects of canopy vertical structure. The system estimates

the distance between the sensor and object by measuring the distance, time, and ranges of light that bounce back (Jones et al., 2007).

Table 2.3. Applications suitable for the different types of cameras/sensors

Application		Type of Camera/sensor[a]			
		RGB	Multispectral (broadband)	Hyperspectral (narrow band)	Thermal
Drought stress	Detection in early stages	-	-	S	HS
	Long-term consequences	-	HS	HS	S
Pathogen detection	Detection in early stages	-	-	HS	HS
	Severity of infection	HS	HS	HS	S
Weed detection	Spectral discrimination	-	S	HS	-
	Object-based	HS	HS	-	-
Nutrient status		S	HS	HS	S
Growth vigor	Growth stage	HS	-	S	-
	Canopy height and biomass	HS	HS	-	-
	Lodging	HS	-	-	S
Yield prediction		S	HS	-	-

[a]*Abbreviations: HS, highly suited; S, suited.* (Adapted from Maes, & Steppe, 2019)

2.7.3 The mechanics of light classification

Plants are phototrophs thus, light is an important survival component for every plant as it regulates their growth and development within a changing light environment (Huché-Thélier et al., 2016; Kami et al., 2010). Across the electromagnetic spectrum, the light sensitivity of a plant varies from the ultraviolet (UV) through the visible spectrum (VS) to the infrared (IR) spectrums (Huché-Thélier et al., 2016; Hunt et al., 2013; Figure 2.3 & 2.4). Although the specific limits of the various regions vary, there is a widely acceptable range for these light regions. However, this broad electromagnetic spectrum (Figure 4.4) can be classified into smaller groups, thus, UV light can be classified into UV-C (100-280 nm), UV-B (280-315 nm), and UV-A (315-400 nm) lights. Whereas UV-A and UV-B get to plants, UV-C light is absorbed within the ozone layer of the atmospheric

stratosphere (Huché-Thélier et al., 2016). Furthermore, the wavelength applications on vegetation at the visible regions are based on the following spectra regions: (i) blue light (450 to 495 nm); (ii) green light (495 to 570 nm); (iii) red light (620 to 750 nm); (iv) red-edge light (760 to 840 nm); and (v) the near and mid-infrared bands (850 to 1700 nm) (Hunt et al., 2013; Xue & Su, 2017a); Figure 2.3). However, significant light regions for plants lies within the VS and IR regions (Carvalho et al., 2011). Based on these wavelength regions, several vegetation indices are computed in the determination of different types of applications such as monitoring crop phenology and phenotype on the field (Table 2.3 and 2.4).

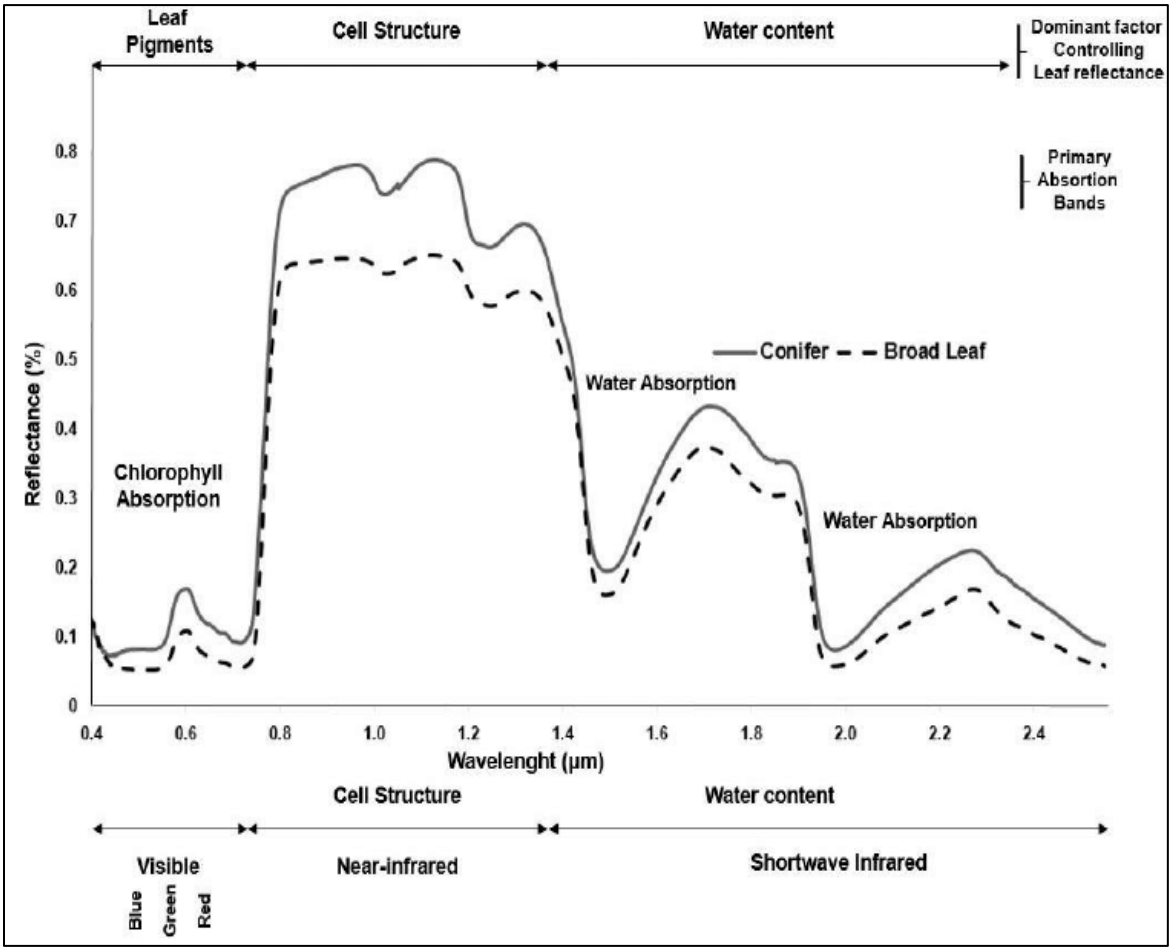

Figure 2.3. Significant wavelength regions in plant monitoring (Cárdenas et al., 2015).

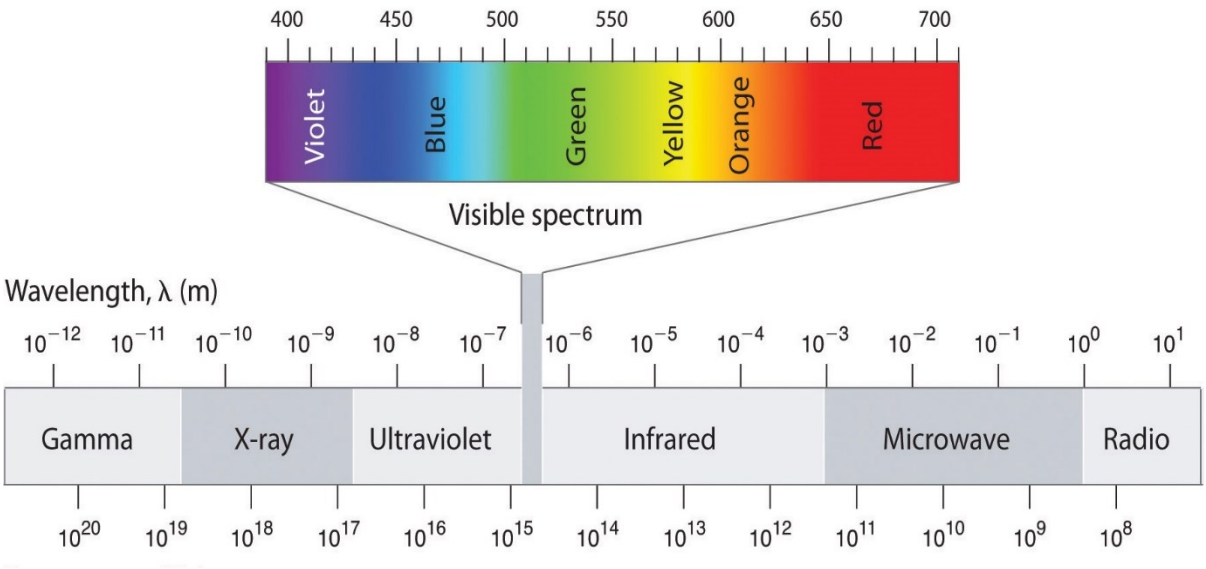

Figure 2.4. Broad electromagnetic spectrum showing the relevant light regions for plant growth and development (Gordon, 2017).

Light signature under a plant canopy differs in its absorption and reflectance, thus blue and red light are strongly reduced through absorption by photosynthetic pigments with high levels of green and near-infrared lights (Kami et al., 2010). Therefore, low reflectance is observed at the VS due to pigment absorption properties with high reflectance at the near-infrared (NIR) region due to the scattering effects of canopy traits (Ollinger, 2011; Woolley, 1971).

2.7.4 Pigmentation in plants

Plants contain several pigments ranging from chlorophyll (e.g. chlorophyll a and b), carotenoids, anthocyanins, flavonoids, and other auxiliary pigments significant in the light-harvesting processes for photosynthesis (Alkema & Seager, 1982; Carvalho et al., 2011; Ollinger, 2011). Therefore, the observance of strong absorption at the visible region indicates the abundance of pigments in healthy vegetation thus, chlorophyll, which is the major light-harvesting compound in plants strongly absorbs at the red (600-700 nm) and blue (400-500 nm) regions. Carotenoids, which

consist of carotenes and xanthophylls absorb at the blue region, with anthocyanins absorbing at the UV range and similar regions of chlorophyll. However, this absorption is rather slow with weak features of the red and yellow colours of autumn leaves. Anthocyanin is seen to protect the plant from stress factors like temperature, excess sunlight, and UV radiation, thus, it is often referred to as the stress pigment. Other pigments command specific colouration in plants, and these range from green to yellow and magenta (Ollinger, 2011; Table 2.4).

Table 2.4. Classification of pigments and their colours in plant leaves

Pigment Class	Compound Type	Colours Reflected
Porphyrin	Chlorophyll	Green
Carotenoid	Carotene (α, β, γ, and lycopene)	Yellow, orange, red
	Xanthophyll	yellow
Flavonoid	Flavone	Yellow
	Flavonol	Yellow
	Anthocyanin	Red, blue, purple, magenta

Adapted from: Alkema & Seager, (1982)

Therefore, colouration of plant leaves occurs through a complex combination of the different pigments (Table 2.4). Most plants produce green pigments called chlorophyll. This pigment reflects incoming light at the green region making most plants appear green during the sun-filled growing season, and this masks the other pigments (Alkema & Seager, 1982). However, growth and environmental conditions like autumn season and senescence unmask some of these pigments. Therefore, a complex interplay of endo- and exogenous conditions during the growing season results in the saturation or reduction of a pigment, and this affects the mechanics of light in leaves.

2.7.5 Reflectance and transmittance of light by leaves

Light that hits the surface of any object is either reflected, transmitted, or absorbed (Woolley, 1971). Reflectance is defined as the portion of light that is reflected from a diffused object/surface, while transmittance is the portion of light that goes through an object/surface (Woolley, 1971). Absorption is defined as when light is retained at a specific wavelength (Ritchie & Runcie, 2014) and transferred to the surface materials thus, it is established that the biochemical properties of plants regulate their absorption and otherwise their reflectance (Ollinger, 2011; Vilfan et al., 2016; Woolley, 1971). Absorption in plant leaves causes molecules to change from an excited state to a non-excited state, leading to the re-emission of light known as fluorescence.

Therefore, the absorption (fluorescence) and reflection of light from plants may vary depending on several factors. The structural properties of the plant, water absorption properties, and plant pigments can alter the absorption or reflectance of light (Ollinger, 2011). The characteristics of leaves and their impact on light have been greatly studied thus, the reflectance of light is primarily attributed to the arrangement of cells in the mesophyll tissues. Strehler & Arnold, (1951) indicated that the delayed reflectance of light was a result of early photosynthetic activity. Therefore, directing light onto the spongy mesophyll cells is the function of the palisade cells, which implies that more scattering/reflectance will occur when a higher proportion of cells in the spongy mesophyll is present compared to the palisade mesophyll cells (Ollinger, 2011).

2.7.6 Spectral vegetative indices

Spectral vegetation indices (SVIs) are important methods used to extract information from remotely sensed data (Hunt et al., 2013; Tilly et al., 2015). Rather than a wider section of the electromagnetic wavelength, only a section of the spectrum is considered relevant for agricultural

purposes (Mahlein et al., 2013). These SVIs are derived using ratios or normalized differences of two or three bands, usually compressed into a vegetation index (Hunt et al., 2013; Jones et al., 2007; Xue & Su, 2017a). The simple ratio index (SRI) is one of the widely used ratio combinations of near-infrared (NIR) and red (R) wavelength reflectance from vegetation (Myneni et al., 1995).

Of all vegetative indexes, normalized difference vegetation index (NDVI) is the most consistently used vegetation index (VI), based on the different ratios of light reflected at the near infra-red (NIR) region and the red (r) light region of the electromagnetic spectrum (Hassan et al., 2019; Jones et al., 2007). Several indices have been computed from different sensors and these may range into 100's of vegetative indices (Tilly et al., 2015; Xue & Su, 2017a) (Table 2.5). However, depending on the type of application a specific sensor can be considered suitable or otherwise (Table 2.3). The reflectance of light spectra changes with the type of plant, water content within the plant tissues, and other intrinsic factors of the plant. Therefore, reflectance from vegetation is generally determined by the chemical and morphological characteristics of the surface of organs or leaves (Xue & Su, 2017a).

Table 2.5. Some vegetative indices used in agriculture

Vegetative Index		Equation	Reference
Ratio analysis of reflectance spectral chlorophyll-a (RARSa)	Chlorophyll a	RARSa = $\frac{R675}{R700}$	(Chappelle et al., 1992)
Ratio Analysis of reflectance Spectral Chlorophyll-b (RARSb)	Chlorophyll b	RARSb = $\frac{R675}{(R700x\ R650)}$	(Chappelle et al., 1992)
Pigment specific simple ratio (PSSRa)	Pigment, chlorophyll	RARSa = $\frac{R800}{R680}$	(Blackburn, 1998)
Green NDVI (GNDVI)	Chla	GNDVI = $\frac{(R850 - R580)}{(R850 + R580)}$	(A. A. Gitelson & Merzlyak, 1996)
Photochemical Reflectance Index (PRI)	Isoprenoid emission, PS I and II	PRI = $\frac{(R532 - R570)}{(R532 + R570)}$	(Penuelas, Llusia, et al., 1997)
Simple Ratio Index (SR900)	Chlorophyll activity	SRI = $\frac{R900}{R680}$	(Jordan, 1969)

Water Index (WI)	Plant water concentration	WI = $\frac{R900}{R970}$	(Penuelas, Pinol, et al., 1997)
Soil atmospheric vegetation index (SAVI)	Correctional index	SAVI = $\frac{(1+0.5)(Rn-Rr)}{(Rn+Rr+0.5)}$	(Huete, 1988)
Structure Insensitive Pigment Index (SIPI)	Chlorophyll, Carotenoid	SIPI = $\frac{(R840-R450)}{(R840+R670)}$	(Penuelas et al., 1995)
Simple Ratio Index (SR 760)	Chlorophyll activity	SRI = $\frac{R761}{R650}$	(Jordan, 1969)
Simple Ratio Index (SR 850)	Chlorophyll activity	SRI = $\frac{R850}{R650}$	(Jordan, 1969)
Triangle Vegetation Index (TVI)		TVI = 0.5[120(R750-R550)-200(R670-R550)]	(Broge & Leblanc, 2001)
Transform chlorophyll absorption in reflectance index (TCARI)	Chlorophyll pigments	TCARI = 3[(R740-R651) - 0.2(R740-R581) ($\frac{R740}{651}$)]	(Haboudane et al., 2002)
Modified chlorophyll absorption in reflectance index (MCARI)	Green leaf area index	MCARI = [(R700 - R670) - 0.2 * (R700 - R550)] *(R700/R670)	(Daughtry, 2000)
Modified Chlorophyll Absorption in Reflectance Index (MCARI 1)	Leaf area index	MCARI 1 = $1.2[2.5(R761^{R651}) - 1.3(R761^{581})]$	(Haboudane, 2004)
Anthocyanin Reflectance Index (ARI)	Anthocyanin	ARI = ($\frac{1}{R550}$) – ($\frac{1}{R700}$)	(A. A. Gitelson et al., 2001)
Chlorophyll Index (CI green)	Chlorophyll activity	CI green = ($\frac{R840}{R570}$) – 1	(A. A. Gitelson, Gritz †, et al., 2003)
Chlorophyll-Index Red edge (CI rededge)	Chlorophyll estimation	CI rededge = ($\frac{R780}{R705}$) – 1	(A. A. Gitelson, Gritz †, et al., 2003)
Chlorophyll vegetation index (CVI)	Chlorophyll estimation	CVI = R840($\frac{R760}{R550^2}$)	(Vincini et al., 2007)
Green Leaf Index (GLI)	Leaf chlorophyll	GLI = $\frac{(2.Rg-Rr-Rb)}{(2.Rg+Rr+Rb)}$	(Louhaichi et al., 2001)
Green, Red Vegetation Index (GRVI)	Chlorophyll content	GRVI = $\frac{(Rg-Rr)}{(Rg+Rr)}$	(Sripada et al., 2006)
Normalized Difference Vegetation Index (NDVI)	Plant Health, biomass	NDVI = $\frac{(Rn-Rr)}{(Rn+Rr)}$	(Rouse et al., 1974)
Enhanced Normalized Difference Vegetation Index (ENDVI)	Leaf chlorophyll	ENDVI = $\frac{(Rn+Rr)-(2.Rb)}{(Rn+Rr)+(2.Rb)}$	(Strong et al., 2017)
Normalized Difference Red Edge (NDRE)	Plant health	NDRE = $\frac{(Rn-Rre)}{(Rn+Rre)}$	(A. Gitelson & Merzlyak, 1994)
Modified Simple Ratio (MSR)	Biophysical parameters	MSR = $\frac{(Rn-Rr-1)}{[(Rn+Rr)0.5+1]}$	(Chen, 1996)
Visible atmospheric red index (VARI)	Vegetation estimation	VARI = $\frac{(Rg-Rr)}{(Rg+Rr)}$	(A. A. Gitelson, Viña, et al., 2003)

[a] *Indices are grouped based on the major wavelengths (R): NIR (n), red edge (re), red (r), green (g), and blue (b).*

2.8. Phenology, phenotype, and disease estimations and assessments

2.8.1 Phenology monitoring and phenotype identification

The term 'phenology' refers to the timing of recurring biological events in the life of an organism (Vilhar et al., 2013) while phenotype reflects the main and interactive effects of a genotype with

the environment, producing characteristics perceived with a cultivar (Deng et al., 2018). Currently, there are two main methods for extracting data from the field: the destructive (manual approach) and the non-destructive method (remotely sensed approach) (Deng et al., 2018). The remotely sensed method having been adopted has aided in the rapid and accurate determination of field data; leaf area, soil moisture content, leaf area index, plant nutrient stress status, stress, yield, disease, and growth stage index among others, and these have been demonstrated through several studies using the non-destructive method (Vicente et al., 2019). The approach has been made possible using vegetative indices (VI's) and these have been generally used to monitor crop changes and other phenotypic traits like yield, biophysical characteristics, and other growth parameters in the field (Table 2.3).

Table 2.6. Some descriptions of phenological monitoring on the field using remote sensing

Type/Crop	Description	Reference
Maize (*Zea maize* L.)	Remote evaluation on phenological development of maize in biomass accumulation and reproductive organ appearance.	(Viña et al., 2004)
Vegetation	Tracking vegetation responses to climate variability in specific species and locations	(M. A. White et al., 2009)
Vegetation	Region to global monitoring of vegetation (phenology) to improve and understand variation in plant dynamics	(X. Zhang et al., 2003)

Several studies have demonstrated the use of remote sensing to assess the phenology and phenotypes of plants (Souza et al., 2017). Recent studies include, Wang et al., (2014), used NDVI to establish relationships and predict crop yield; Bush et al., (2020), monitored crown leaf turnover

using satellite data; Vicente et al., (2019), identified traits associated with barley yield determination of crop height, canopy cover and NDVI, and Hussain et al., (2020) adopted the use of a multispectral sensor to determine the biophysical parameters of the rapeseed crop.

These recent developments in research in contrast to some approaches (Table 2.6), shift focus from the broad scope of seasonal monitoring to crop monitoring at their specific growth stages. Therefore, several growth parameters have been predicted using VIs. The establishment of results from these studies is dependent on the relationship between specific vegetative indices (VI) and the field-measured data (growth parameter). Thus, it evaluates the strength of the relationship between two quantitative variables (Ranganathan et al., 2019). Therefore, data obtained using remotely sensed approaches are always compared with ground truth data. Though this may be a robust approach, there may often be drawbacks to this method. Largely, correlation and regression analysis are usually adopted in establishing these relationships. Therefore, higher correlation (r) and coefficient of determination (R^2) values establish a good relationship between variables. In this way, higher correlation (r) values in the range of 0.70 to 1.00 are considered the strongest relationship with ground data, and correlation values in the range of 0.10 to 0.39 and 0.40 to 0.69 are considered to have a low and medium correlation with ground data, respectively (Ranganathan et al., 2019). With these considerations, it becomes possible to assess growth parameters in the wild blueberry field.

Phenotype determination is another important aspect that considers the identification of species or clones based on their genetic makeup or the physical characteristics of the plant. In the past, the nature of this process focused attention on the laboratory determination of these clones. Over the years, the expansion in the use of remote sensing approaches focused attention on the combination of laboratory processes and remote sensing techniques (Vicente et al., 2019).

Currently, development in the use of remote sensing applications has led to a potential in the identification of phenotypes using UAV high throughput phenotyping platforms (UAV-HTTPs) (Han et al., 2018). These platforms use sensors like the RGB, multispectral, hyperspectral, and thermal cameras (Han et al., 2018; Nebiker et al., 2016). This approach has been used widely in wheat, sorghum, and maize, among other crops. Therefore, several studies have adopted different approaches including the use of UAV-HTTP, spectral radiometric approaches, hyperspectral imagery analysis, and some machine learning approaches like classification in phenotype determinations on the field (Bendig et al., 2015; Han et al., 2018; Panda et al., 2009; Peña et al., 2017; Vicente et al., 2019).

2.8.2 Disease determination

The effect of diseases on plants varies from one plant to another. These different responses emphasize pathogen-host interaction (Al-Saddik et al., 2017; Velásquez et al., 2018). However, the effects of these diseases are usually visible only after deterioration, which poses a challenge to plants, affecting food security. Early detection has been a challenge, and the detection process of these diseases is a function of when early discrimination could be achieved. As a result, it poses challenges to early detection until spectral differences can be achieved (Franke et al., 2005).

Drawing steps closer to disease detection, remote sensing techniques provide a means of visually assessing and identifying plant disease after deterioration had reached an advanced stage (Liu et al., 2018; Mahlein et al., 2013; Oerke, 2020; Vega et al., 2015). Information gathered from visible and near-infrared regions of the spectrum has been consistent in simulating biochemical and biophysical processes in plants (Bush et al., 2020; Hunt et al., 2013; Mahlein et al., 2013; Oerke, 2020; Yue et al., 2019). Narrowing it down, significant steps were taken to assign regions on the electromagnetic wavelength that control some of the plants' processes (Zhang et al., 2020).

It was revealed that the visible region (400 nm to 690 nm) has a dominant impact on pigmentation whereas infrared regions (700 nm to 1200 nm) have an impact on structural leaf traits and water content (Mahlein et al., 2013; Weingarten et al., 2022; Zhang et al., 2019). Though disease detection may be challenging, a recent study on the early detection of tree diseases and pathogens reveals some insight into the potential of using imaging spectroscopy in this identification process (Weingarten et al., 2022).

Several studies have also shown the possibility of using other approaches like thermal and hyperspectral techniques to detect an early start of diseases in crops (Calderón et al., 2015; Yang, 2020). Developments using spectral vegetative indices (SVIs) have been utilized to detect several physiological changes in plants. These indices combine ratios or normalized differences of two wavebands to specify different plant parameters (Bush et al., 2020; Hunt et al., 2013; Mahlein et al., 2013). This technique has been used to observe changes and detect pests and diseases in several crops; *Cnaphalocrocis medinalis* in rice (Huang et al., 2012), *Schizaphis graminum* in wheat (Yang et al., 2005), *Verticillium wilt* of Olive trees (Calderón et al., 2013, 2015), lodging in rice (Liu et al., 2018), Cercospora leaf spot in sugar beet plant (Mahlein et al., 2013) among other detections.

Remote determination of diseases depends on vegetative indices. Though these indices combine a few spectral bands, blue, green, red, and near-infrared bands in their computation, these are indirect measurements, and therefore, statistical methods are again adopted to establish findings. Several statistical approaches including, classification approaches like Support Vector Machine (SVM) and Maximum Likelihood Classification (MLC), stepwise discriminant methods like Fisher Linear Discriminant Analysis (FLDA) and Quadratic Discriminant Analysis (QDA), machine learning, correlation, and several regression methods such as Partial Least Squares Regression (PLSR), an Artificial Neural Network (ANN), Random Forest (RF), Multilinear

Regression (MLR) among other approaches have all been used to establish relationships in their determination (Maes & Steppe, 2019; Mahlein et al., 2013; Oerke, 2020; Su et al., 2018; Tao et al., 2020; Zhang et al., 2019). Regression techniques have greatly been explored and have achieved good results in the prediction of growth parameters (Tao et al., 2020).

2.9 Advancements and challenges of the technology in wild blueberries

2.9.1 Remote sensing in wild blueberry production

Despite challenges posed on the field, many gains have been made using remote sensing techniques. Having set the pace for other remote sensing approaches to be adopted on wild blueberry fields, a study by Michaud et al., (2006), employed aerial scans as a guide to optimize the delivery of pesticides to blueberry plants. Furthermore, Maqbool et al., (2010), employed reflectance measurements to estimate different yield components in the wild blueberry field. Subsequent advancements in the wild blueberry fields have adopted the use of remote sensing techniques, especially unmanned aerial vehicles (UAVs) for different applications. Currently, field mapping (Panda et al., 2016; Peltoniemi et al., 2005), identification of phenotype and bare areas (Percival et al., 2023), phenology monitoring (Anku et al., 2023), weed detection (Hennessy et al., 2022), geospatial difference in phenology (Sharpe, 2008), and yield estimates (Barai et al., 2021) among others are currently underway, with these technological applications at different levels of development. Current advancements point to the classification of orthomosaic maps, which are developed into prescription maps to be used by tractors (*Advancements on the Wild Blueberry Fields*, personal communication, 2021). These maps will help minimize the use of resources through the adoption of spot application rather than a blanket application of biofungicides and

other agrochemicals. This phase of development in the application of UAVs and remote sensing puts wild blueberry production on a path to great technological advancements.

2.9.2 Challenges with the plant and the remote sensing technique

Challenges associated with the blueberry plant are numerous, and this emanates from the different perspectives of field management and mechanization. Despite the challenges faced by the plant, some gains can be achieved. The nature of the plant being "short or small" introduces some challenges to flights conducted at high altitudes, except for sensors of high resolution. Despite these challenges, there are software packages that help in the determination of an appropriate altitude for flights. However, the plant structure and the type of application inform flight altitude, and this has an impact on flight coverage in the field. This is because flight altitude and type of application have a direct relationship. This implies that short plants will have a relatively low flight altitude, which would have a negative bearing on the UAV. However, this phenomenon varies from one application to another.

Berries are distributed along the stem of the plant, and this makes harvesting easy, however, aerial view and coverage using the UAV face difficulties in identifying these berries. This is because, though berries are usually clustered at the proximal region of the stem, an aerial view limits their detection or identification. However, this phenomenon may vary from field to field. In fruit distribution on the stem, some plants may observe about 60% clustering at the apical region, and the remaining 40% distributed along the plant stem. Just like any other plant the nadir angle of view makes it impossible to identify and account for all berries on the plant and on the field at large. Furthermore, the difficulty in identifying neighbouring plant stands and berries within a patch is another challenge posed in the detection process. This situation makes it difficult to detect berries hidden within the plant canopy.

The heterogeneous nature of plants in terms of height, fruit colour, leaf colour (Jamieson, 2008), and plant density raises some challenges with UAV data generated through remote sensing. Uniformly, an average height can be estimated for plants. However, this average would vary considerably across the field. Colour is an important aspect of remote sensing, and this is because the colour displayed depends on which wavelength is being reflected (Ashley, 2020; Duy, 1999). Therefore, considering the leaf colour variations displayed on the field, inferences made on such information may be misleading. These variations though can be managed, may pose serious challenges on some intended applications of the data.

Another heavy challenge of the blueberry field is bare areas and weed patches on the field. Research has it that young fields contain lots of bare areas (less than 50% cover) and weedy patches, but relatively old fields of about 50 years or more have less of such problems with nearly, 100% crop cover (Jamieson, 2008). Therefore, aerial estimations on such fields may lump both weeds and crops as one, and averages are calculated for those fields. Thus, the imbalanced density of plants on a plot somewhat puts some estimated higher-valued plots ahead of others containing bare areas. However, there are methods to control or manage such challenges, but these processes can be difficult and cumbersome.

One other challenge of wild blueberry studies as explained by Drummond, (2019) is that, because plants are not sown from seeds the spatial patterns of genotypes on the field cannot be defined or predetermined like in other experiments like maize, wheat, and apples among others (Drummond, 2019). Therefore, the unique situation that needs to be solved arises from combining the challenges of using remote sensing methods with the challenges presented by the plant.

CHAPTER 3: CANOPY NITROGEN AND GROWTH ESTIMATION USING REMOTE SENSING AND ITS IMPACT ON GROWTH PARAMETERS

Aspects of this section have been submitted as abstracts and full text for publication in the XIII Vaccinium conference proceedings.

Anku, K. E., Percival, D. C., Rajasekaran, L. R., Heung, B., & Vankoughnett, M. (2024). Remote estimation of leaf nitrogen content, leaf area, and berry yield in wild blueberries. Frontiers in Remote Sensing. (Submitted)

3.1 ABSTRACT

Nitrogen (N) fertilization is a major management requirement for wild blueberry fields. While low and high N are obvious in plants, its estimation can be difficult given the perennial heterogeneous nature of the plant with residual N effects, leading to the over-application of the agrochemical. Despite this, efforts to substantially reduce N use in commercial fields to lower greenhouse gas emissions have been a major concern, coupled with the spatial variability of plant coverage. Therefore, the objective of this study was to assess the impact of N on VIs and estimate its content in wild blueberry leaves using remote sensing approaches. The study was also conducted to assess the impact of nitrogen on different growth parameters. Four trials over two years were set up in three commercial fields with nitrogen application rates of 0, 20, 40, 60, and 100 kg N ha^{-1} of soil-applied granular fertilizer treatments being used. Aerial measurements were done using a multispectral and a Zenmuse X5 camera, mounted on a DJI Matrice Pro 300 UAV and flown at 30 m to collect aerial images. Several field measurements including leaf nitrogen content (LNC), leaf area, floral and vegetative numbers, and stage, stem height, and yield were conducted. Several vegetative indices were computed for each plot, and correlation and regression analyses were conducted. Results indicated that despite the wild blueberry plant being a perennial plant with considerable residual nutrient reserves, treatments with high nitrogen application rates resulted in canopies with high field LAI values. Furthermore, using visible light VIs [green leaf index (GLI), green red vegetative index (GRVI), and visible atmospheric red index (VARI)], LNC, LAI, and

berry yield had significant R^2 estimations of 0.43, 0.48, and 0.30 respectively. It was found that using near-infrared VIs was the most effective method for estimating differences in nitrogen rates. Therefore, the use of VIs in creating prescription maps for N fertilization application is justified. Furthermore, results from this study have illustrated the potential of the multispectral sensor to estimate LNC, LAI, and berry yield parameters.

Keywords: Wild blueberry, nitrogen fertilizers, remote sensing, leaf nitrogen content, vegetative indices

3.2 INTRODUCTION

The wild blueberry plant, also called lowbush blueberry, is an economically important shrub that thrives in major areas of the world, particularly in North America (Drummond, 2019; Farooque et al., 2012; Zaman et al., 2008). Including the species *Vaccinium angustifolium* (the predominate species found in the fields) and *Vaccinium myrtilloides*, the plant grows naturally as it is managed through regular management practices (Agriculture, Aquaculture, and Fisheries, 2013). The plant has a unique structure, growth, and development, and can thrive in harsh conditions (Abbey et al., 2018; Thyssen et al., 2006). The lowbush plant is stress-tolerating and resilient, lending itself to periodic pruning, and can thrive in a range of soil types, particularly acidic soils (Glass et al., 2005; Percival & Sanderson, 2004; Thyssen et al., 2006).

Several management practices including pruning, fertilizer application, disease control, weed control, and pollination and others are used (Kinsman, 1993). Upright plant shoots are periodically pruned in alternate years; thus, fields are managed on a two-year system with a biennial production cycle of a sprout and a cropping year (Eaton & Nams, 2012a; Penman & Annis,

2005; Percival & Sanderson, 2004; Zhang et al., 2010). Thriving in low-nutrient and varied soil types, this phenomenon leads to the use of fertilizers to boost nutrient levels for plant growth and development. Although wild blueberries have low N requirements compared to other fruit crops like strawberries, concerns about their carbon footprint and resulting greenhouse gas emissions persist.

Fertilizer application is a regular practice adopted in the management and production of wild blueberries, thus, diammonium phosphates (DAP; 18-46-0) or ammonium sulfate combined with P and K are standard fertilizers used on commercial wild blueberry fields with emphasis on nitrogen utilization (Farooque et al., 2012; Gumbrewicz & Calderwood, 2022). Wild blueberry fields are low in soil nutrients (Farooque et al., 2012; Thyssen et al., 2006), and correspondingly, the plant has a generally low nutritional requirement (Saleem et al., 2013). The low nutrient status of various soil types has always demonstrated a positive plant response upon fertilizer application (Agriculture, Aquaculture, and Fisheries, 2013; Farooque et al., 2012; Maqbool et al., 2016; Percival & Sanderson, 2004; Saleem et al., 2013). Smagula & Hepler, (1978) established that the application of N (43 kg ha^{-1}) in the form of urea increased flower buds and berry yield by 22% and 25% respectively, over the unfertilized plots. Furthermore, an increase in stem length, flower buds, number of berries, and yield were observed in Maine upon application of N (20-98 kg ha^{-1}) rates (Smagula & Hepler, 1978). However, excess application of N has negative effects on yield by stimulating vegetative growth, increasing weed pressures, and causing micronutrient imbalance (Maqbool et al., 2016). Therefore, Percival & Privé (2002), proposed constant checks on lead tissue N, P, and K status as their levels are altered along the production cycle.

Several studies on the wild blueberry fields have demonstrated many effects of fertilization. Marty et al., (2019) demonstrated that inorganic fertilization increased yield by 70%, with

significant effects on weeds (Ghosh et al., 2022). Percival et al., (2003) established that multiple fertilizer applications increased stem density, leaf nitrogen content, dry weight, and harvestable yield. Eaton et al., (2009) established that N, P, and K leaf content, stem length, stem buds, blossoms per stem, and yield were higher under consecutive fertilization as compared to alternate fertilization. Conversely, a study by Saleem et al., (2013) also established that plant density, number of buds, and number of branches were non-significantly affected by fertilizer treatments and that fruit yield increased under both uniform and variable fertilizer rate applications. Despite the use of traditional approaches, producers are now moving away from the blanket application to spot application of N given the spatial variability of plant coverage and the determination of N levels using remote sensing techniques.

Research and development activities in agriculture have led to the proliferation of remote sensing techniques in plant growth monitoring and prediction (Hussain et al., 2020; Zhang et al., 2020). With the adoption of a non-destructive approach, sensors such as the red-green-blue (RGB), multispectral, hyperspectral, and thermal sensors have been utilized through the use of vegetative indices (VIs) (Maes & Steppe, 2019; Nebiker et al., 2016). Vegetative indices are important ways by which information is sourced from remote sensing data through mathematical computation using wavebands. Several studies have demonstrated the use of remote sensing techniques in estimating plant growth and development in the fields. Näsi et al., (2018) estimated biomass and nitrogen (N) content of barley and grass using an unmanned aerial vehicle (UAV). The study confirmed a high regression value of 0.89 as a good relationship between these parameters (Näsi et al., 2018). Bendig et al., (2014) also estimated the biomass of barley using crop surface models (CSMs) from a UAV-Based RGB imaging with high regression values of fresh and dry biomass being 0.81 and 0.82 respectively. This approach and technique have also been used in several crops

including wheat, rice, and soybean (Hassan et al., 2019; Souza et al., 2017; Zhou et al., 2017), however, little has been done to utilize the multispectral sensors in estimating N content and determining canopy characteristics in wild blueberry fields.

The use of multispectral sensors with VIs has been employed to monitor plant canopies. This is particularly important as most of the plant's nitrogen (N) is found in the leaves. Recent studies have demonstrated the effects of nitrogen on plant canopy in several crops using VIs. Marty et al., (2022) in a recent study on the blueberry field, investigated the sensitivity and impact of management practices on two vegetative indices, normalized difference vegetation index (NDVI) and normalized difference red edge (NDRE). The study established significant differences between VIs from different fertilizer treatments as against different management practices. However, the study did not consider the estimation of growth parameters, rather it focused on the sensitivity of NDVI and NDRE to management practices. Furthermore, the impact of N-fertilization on wild blueberry yield has been inconsistent, with some implying good outcomes (Eaton et al., 2009; Ghosh et al., 2022; Marty et al., 2019; Percival et al., 2003), with others showing either bad or no effects (Maqbool et al., 2016; Saleem et al., 2013). This is significant because the crop is a perennial plant and will have a significant pool of nutrients it will be drawing from along the production cycle. This may affect yield potential as the plant may invest either in growing tall or producing floral buds. Several limiting factors may account for some of these negative effects, which include biotic stresses (diseases and weeds), and pollination, however, considering the varying results obtained, there is a need for work to be done to confirm some major findings and estimate plant growth parameters. Therefore, from an assessment perspective, given the introduction of the non-destructive approach, there is a need to utilize remote sensing techniques to estimate the effects and impact of fertilizer application on plant growth parameters in wild

blueberry fields.

Given that the potential and application of remote sensing techniques have been demonstrated in different crops, this study was conducted using an RGB and a multispectral sensor to monitor growth parameters in wild blueberry fields. Therefore, the objective of this study was to (i) determine the effects of soil-applied N-fertilizer rates on the growth and development of wild blueberry plants; (ii) determine the N-fertilizer rate in achieving an optimum harvestable yield; (iii) determine the effect of fertilization on vegetative indices; and (iv) estimate berry yield, LAI, and LNC using predictive models.

3.3 MATERIALS AND METHODS

3.3.1 Study area

A total of four (4) experimental trials were set up in the 2020 and 2021 growing seasons. These trials were located at three geographical locations, with the first trial set up at Lemmon Hill in the 2020 growing season. In the 2021 growing season, an additional three (3) experimental trials located in Debert (DB), Lemmon Hill (LH), and Wentworth (WW), all within Nova Scotia, Canada, with their geographic coordinates (45.444445°N, -63.450472°W), (45.190360°N, -62.872721°W), and (45.642327°N, -63.611735°W) respectively, were set-up for this study (Figure 3.1.). Despite Nova Scotia being noted for Queens soil type, these three sites, DB, LH, and WW are specifically classified as orthic humo-ferric podzol, thus all three locations shared the same soil type (Nowland & MacDougall, 2013). These trials started during the vegetative growth phase of the plant and carried through the crop phase until harvest.

The locations for these trials were wide apart, thus, the distance between DB and LH was 84 km, DB to WW location was 43.5 km, and WW to LH was 111 km. These fields varied in plant density, topography, and weather conditions which introduced some uniqueness to this study. Unlike the DB and LH locations, the trial set up at the WW location was on a low-lying field with high moisture content. Generally, the trial set up at the WW location had a low plant density as compared to the trials set up in the DB and LH locations. Weeds and patches on the field varied across these three locations, with WW having the patchiest field with weeds. Disease management practices to mitigate leaf spot and floral blight diseases were used.

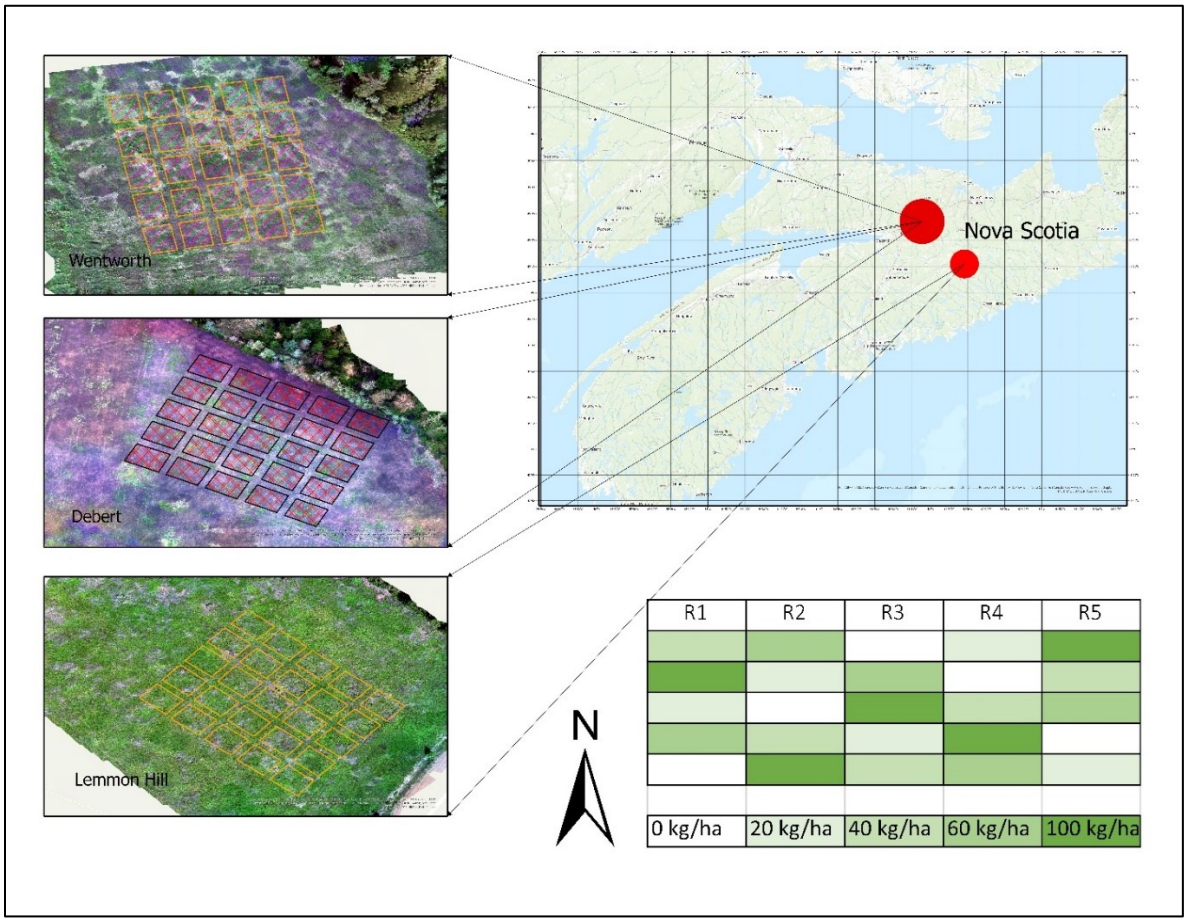

Figure 3.1. Trial sites, field plots, and the different treatment applications. R - replication

3.3.2 Experimental set-up and treatment applications

In the 2020 field season, the experimental design adopted was a randomized complete block design (RCBD) with 6 replications, 4 treatments, and a plot size of 4 × 10 m with 2 m buffers between plots. Treatments consisted of (i) untreated control (0 kg N ha^{-1}), (ii) 15 kg N ha^{-1}, (iii) 30 kg N ha^{-1}, and (iv) 60 kg N ha^{-1} using ammonium sulfate (AS) as an N source. The treatment applications were carried out using a granular fertilizer spreader (Lesco High Wheel Fertilizer Spreader), with two passes along the 4 m stretch of each plot with the deflector guard lowered to minimize application to areas outside of the plots. Across the different seasons, the application of the AS fertilizer was carried out in the vegetative (i.e., sprout phase) stage of the production.

The experimental design for the 2021 field season was a randomized complete block design (RCBD) with 5 replications, 5 treatments, and a plot size of 6 × 8 m with 2-m buffers between plots. Treatments consisted of (i) untreated control (0 kg N ha^{-1}), (ii) 20 kg N ha^{-1}, (iii) 40 kg N ha^{-1}, (iv) 60 kg N ha^{-1}, and (v) 100 kg N ha^{-1}. Treatment applications consisted of two mixed compound fertilizers; the 16-21-8 (partially wet) fertilizer was used to provide a base and then 21-0-0 (dry) fertilizer was applied to each field in spring during the sprouting phase of the plants at a rate of 10 kg of N per hectare. These granular fertilizers were applied two weeks apart (12th and 26th of June 2021) using a fertilizer spreader (Lesco high wheel fertilizer spreader). Three passes along the 6 m stretches were made on each treatment plot.

3.3.3 Field data collection

Field assessment of stem density was conducted on 5th August 2021 by collecting 4 quadrants of blueberry stems per plot using a 30 x 30 cm quadrant. Leaf area index (LAI) was determined for each plot using the LiCor 3100C leaf area meter. An SS1 Sunscan canopy analysis system (Delta

T Devices) was also used to collect LAI measurements from each plot. This was done by measuring light interception within the plant canopy using the probe. This was conducted in early October following the quadrant measurements. Physical plant characteristics such as stem length, vegetative buds, and floral bud numbers were collected. Leaf tissue N content from each plot was determined using the protocol of Maqbool et al., (2012). However, due to insufficient differences observed between treatments of the 2020 trial (Table 3.2; Appendix 2-Table A1 & A2), the trial was discontinued with several parameters not collected.

3.3.4 Plant sampling and nitrogen content analysis

Fresh leaf samples were collected from each treatment plot on 5th August 2021. The leaf tissue samples were oven-dried for 36 h at 60°C. The dry leaf tissues were ground into a fine powdery sample using the mortar and pestle. The ground leaf samples were stored in dry labeled falcon tubes and analyzed for N content using the LECO CNS-1000 elemental auto-analyzer (LECO Corp., St. Joseph, MI). Analysis of the LNC followed the procedure of Rutherford et al., (2007).

3.3.5 Aerial image acquisition and sensory platform

Across the 2 growing seasons, the DJI Matrice Pro 600 UAV and the UAV Matrice 300 were equipped with a 3-band Zenmuse X5, a 16-Mega-Pixel (MP) digital camera, and a 5-band Micasense RedEdge™ 3 multispectral camera to collect the reflected portions of light. Reflected lights from the RGB camera were collected at blue (448nm), green (548 nm), and red (650 nm) wavelengths while that of the Micasense was collected at blue (475 nm), green (560 nm), red (668 nm), red edge (717 nm), and near-infrared (840 nm) wavelength (Figure 3.2.). The Matrice Pro 300 was flown at 30 m height with a frontal image overlap of 75% and a side image overlap of 70%.

Flights on all 3 sites on the 2021 trial were conducted on 29th July 2021 and 4th August 2021, about two months after treatments were applied to plots. Images were acquired between 10 am – 2 pm under clear conditions to minimize the effects of clouds, wind, and rain. Calibration, corrections, and adjustments were carried out to minimize the effects of distortion on the quality of the imagery obtained. Depending on whether the camera is an RGB, or multispectral, aerial images were acquired at approximately 0.7 or 2.2 cm/px spatial resolution, respectively.

Figure 3.2. UAV remote sensing tools. (A) Calibration panel, (B) DJI Matrice 300 UAV fitted with a camera, and (C) A Real-time kinematic receiver.

3.3.5.1 Image processing

The raw images were processed using the Solvi platform (https://solvi.ag/features) and this consisted of (i) upload of raw images and ground control points (GCPs); (ii) stitching images into a composite orthomosaic images; (iii) digitizing individual plots; (iv) computation and extraction of vegetation indices; and (v) export of data file for analysis. Using the zonal and custom function

on Solvi, the individual plots were digitized. From the zonal function, all vegetative indices (VIs) were computed for all plots. Several VIs were determined for each plot and the values were exported for analysis. The extracted file was exported as a comma-separated-value (CSV) file into SAS software for statistical analysis. ArcGIS (version 10.5) was further used to process and digitize the images.

3.3.6 Vegetative indices

In this study, several VIs were considered (Table 3.1.), however, depending on the camera type, some vegetative indices can be computed while others cannot. This was because the computation of VI was performed based on light bands available from those cameras.

Table 3.1. Vegetative indices used in this study

Vegetation indices	**Bands[a]**	**Equation[b]**	**Reference**
Green Leaf Index (GLI)	R, G, B	$(2 \cdot R_g - R_r - R_b)/ (2 \cdot R_g + R_r + R_b)$	Louhaichi et al., (2001)
Green, Red Vegetation Index (GRVI)	R, G	$(R_g - R_r)/ (R_g + R_r)$	Sripada et al., (2006)
Normalized Difference Vegetation Index (NDVI)	R, NIR	$(R_n - R_r)/ (R_n + R_r)$	Rouse et al., (1974)
Enhanced Normalized Difference Vegetation index (ENDVI)	B, G, NIR	$(R_n + R_g)$ - $(2*R_b)/ (R_n + R_g) + (2*R_b)$	Strong et al., (2017)
Normalized Difference Red Edge (NDRE)	NIR RE	$(R_n - R_{re})/ (R_n + R_{re})$	Gitelson & Merzlyak, (1994)
Visible atmospheric red index (VARI)	G, R	$(1 + 0.5) (R_n - R_r)/ (R_n + R_r + 0.5)$	Huete, (1988)

a Indices are grouped based on the major wavelengths of the multispectral sensor: NIR (n, 840 nm), red edge of chlorophyll absorption (RE, 717 nm), red (R, 668 nm), green (G, 560 nm), blue (B, 475 nm),

b R is the reflectance at wavelength; R_n, R_{re}, R_r, R_g, and R_b are the reflectance for NIR, RE, red, green, and blue bands, respectively.

3.3.7 Statistical analysis

To determine which of the treatment applications had the highest concentration of N content in leaves, yield, vegetative buds, and plant density, analysis of variance (ANOVA) was used, and a multiple means comparison conducted to differentiate between treatments for significant effects. All conditions for statistical testing were performed, thus normality test, constant variance and independence of the error terms were conducted. Furthermore, to establish significant relationships, correlation, and regression analysis on aerial data, LAI, LNC, vegetative and productive yield components, and harvestable berry yield were conducted. A correlation analysis was carried out using all parameters, VIs, LAI, LNC, floral buds, vegetative buds, productive yield component, and the harvestable berry yield followed by a regression analysis. Linear regression is a model that describes the relationship between one dependent (Y) variable and one independent (X) variable using a straight line (Bangdiwala, et al., 2018). The model is represented by this simple equation (Eqn. 1),

$$Y = \beta_0 + \beta_1 X \ldots \text{(Eqn. 1)}$$

where β_0 is called the intercept, which defines the point on the y-axis that is intercepted by the straight line. The β_1 is called the slope which determines the change in the y-axis when a 1-unit change is observed on the x-axis (Bangdiwala, et al., 2018).

Therefore, a simple linear regression (SLR) analysis was conducted, where VIs were used as dependent variables with the other parameters set as independent variables. Where nonlinear relationships are established, other regression methods were adopted. SAS (version 9.4), Minitab

(version 19, Minitab Inc.), R-Studio (version 4.2.3), and Excel software were used to perform all statistical analyses and graphical designs. For statistical testing, Minitab was used to test all assumptions. Thus, residuals fulfilled the assumptions of normality, constant variance, and independence of error terms. SAS was used mainly for ANOVA analysis using the PROC GLIMMIX procedure. R-Studio was used for correlation and regression analysis, with Excel used for graph designs.

3.4 RESULTS

3.4.1 Effects of different nitrogen rates on vegetative indices

The initial assessment performed on the 2020 data among VIs revealed no significant difference between treatments (Table 3.2; Appendix A1 & A2), thus, nitrogen did not have an impact on vegetative indices.

Table 3.2. Analysis of variance on the impact of nitrogen rates on aerial vegetative indices observed from Lemmon Hill on 7th August 2020 during the vegetative growth phase.

Treatment	GLI	GRVI	VARI	NDVI	NDRE	ENDVI	SAVI
0 kg N/ha	0.473	0.422	0.530	0.891	0.490	0.864	0.668
15 kg N/ha	0.421	0.363	0.460	0.854	0.472	0.829	0.633
30 kg N/ha	0.476	0.428	0.540	0.893	0.498	0.865	0.672
60 kg N/ha	0.459	0.410	0.519	0.884	0.499	0.856	0.669
ANOVA Results[1]	**NS**	**NS**	**NS**	**NS**	**NS**	**NS**	**NS**

[1] Analysis of variance (ANOVA) results refer to treatment effects that were either not significant (NS) or significant at $p<0.05$. Mean separation was completed using Fisher's multiple means comparison test procedure ($\alpha=0.05$). Standard Error (S.E) = between 0.003 to 0.009

Coupled with other compounding effects, assessment on this trial was discontinued. However, data on harvestable yield were collected during harvest in 2021 (Table 3.6.) in addition to some physiological data. Conversely, the 2021 trial showed some significant differences between the various vegetative indices, thus the different nitrogen rates influenced vegetative indices (Table 3.3; Appendix A3 & A4).

Table 3.3. Analysis of variance on the effects of nitrogen rates on vegetative indices from the Wentworth location [7th October 2021]

Treatment	GLI	GRVI	VARI	NDVI	NDRE	ENDVI	SAVI
0 kg N/ha	0.049b	0.017b	0.021b	0.229c	0.097	0.207c	0.344c
20 kg N/ha	0.058b	0.023b	0.033b	0.244c	0.089	0.224c	0.365c
40 kg N/ha	0.074b	0.038b	0.060b	0.278bc	0.103	0.252bc	0.417bc
60 kg N/ha	0.087b	0.049b	0.075b	0.317ab	0.117	0.285ab	0.474ab
100 kg N/ha	0.144a	0.115a	0.179a	0.372a	0.120	0.331a	0.549a
ANOVA Results[1]	**p<0.007**	**p<0.010**	**p<0.018**	**p<0.002**	**NS**	**p<0.001**	**p<0.002**

[1] Analysis of variance (ANOVA) results refer to treatment effects that were either not significant (NS) or significant at $p<0.05$. Mean separation was completed using Fisher's multiple means comparison test procedure ($\alpha=0.05$). Standard Error (S.E) = between 0.007 to 0.015

It was observed that the highest nitrogen rate, 100 kg N/ha, was significantly different from the other treatment rates across all seven VIs. It was observed that there was significant variation between the different rates of the near-infrared (NIR) VIs as compared to the visible (VIS) light

VIs. Therefore, 100 and 60 kg N/ha were significantly different from the other treatments, unlike the VIS-VIs where treatments 1 to 4 were not significantly different (Table 3.3.).

3.4.2 Leaf nitrogen content

Results on the 2021 data have shown that there was no significant difference between treatment trials from two locations, Debert and Wentworth, whereas a significant effect ($p<0.05$) was observed between treatments at the Lemmon Hill location (Table 3.4.).

Table 3.4. Analysis of variance (ANOVA) on LNC in blueberry leaf tissues treated with 5 rates of mixed compound fertilizers at three (3) experimental sites.

Treatment	Debert (DB)	Wentworth (WW)	Lemmon Hill (LH)
1 (0 kg N/ha)	1.461	1.204	2.108 c
2 (20 kg N/ha)	1.478	1.194	2.445 b
3 (40 kg N/ha)	1.452	1.287	2.305 bc
4 (60 kg N/ha)	1.512	1.242	2.350 b
5 (100 kg N/ha)	1.618	1.367	2.729 a
ANOVA Results[1]	**NS**	**NS**	**p<0.0001**

[1]Analysis of variance (ANOVA) results refer to treatment effects that were either not significant (NS) or significant at $p<0.05$. Mean separation was completed using Fisher's multiple means comparison test procedure ($\alpha=0.05$). Standard error (SE) = DB (0.04), WW (0.05), and LH (0.25)

Treatment effects in both DB and WW locations showed no significant difference. Treatment 5 (100 kg N/ha) showed the highest mean LNC value compared to all the other treatments in all

three locations (Table 3.4.). At the LH location, it was observed that treatment 5 (100 kg N/ha) was significantly different from all the other treatments. Despite no significance from some locations, there were mean differences in the LNC values. It was observed that LNC values from the LH location were almost twice what was contained in the leaf tissues of plants from both DB and WW. The mean LNC values between WW and DB were similar.

3.4.3 Canopy and physiological characteristics

3.4.3.1 Plant density (PD) and leaf area index (LAI) using the quadrant method

Results on plant density and LAI have given some indications of happenings in the field (Table 3.5.). There was a significant difference between treatments at the DB location, with partial significance at the LH location, and no significance was observed at the WW location for the two measured parameters (Table 3.5.).

PD results at the DB location indicate that there were significant differences between treatments (Table 3.5.). Under stem length, treatments 2 and 3, were significantly different from the other treatments, with a 33.06% difference compared to the control treatment. Similar results and trends from PD were reflected in the LAI results (Table 3.5.).

At the LH location, there was no significant difference between treatments on PD with a marginally significant difference between LAI treatments (Table 3.5.). The mean difference between treatments 3 and 1 gave a 31.32% difference in stem numbers. Though marginally significant, treatments 2 to 5 observed high LAI compared to treatment 1. Compared to the control, treatments 2 to 5 were higher with about 41.19% difference. LAI results reflect a similar observation as that of PD.

Table 3.5. Analysis of variance (ANOVA) on LAI and plant density using the quadrant method at the three commercial wild blueberry fields [Collected: 5th August 2021].

Treatment	Debert		Lemmon Hill		Wentworth	
	PD (stems/m^2)	LAI	PD (stems/m^2)	LAI	PD (stems/m^2)	LAI
1 (0 kg N/ha)	1361.67bc	2.48b	844.44	3.52c	795.56	2.31
2 (20 kg N/ha)	1563.33ab	3.25a	1062.22	4.97a	906.67	2.51
3 (40 kg N/ha)	1592.78a	3.30a	1108.89	4.28abc	975.55	3.15
4 (60 kg N/ha)	1189.45c	2.68b	966.66	3.89bc	1171.11	4.19
5 (100 kg N/ha)	1314.44c	2.82ab	1051.11	4.75ab	1035.55	4.08
ANOVA Results[1]	**p<0.016**	**p<0.042**	**NS**	**p=0.059**	**NS**	**NS**

[1] Analysis of variance (ANOVA) results refer to treatment effects that were either not significant (NS) or significant at $p<0.05$. Mean separation was completed using Fisher's multiple means comparison test procedure ($\alpha=0.05$). SE (PD/LAI) = DB (42.7/0.10), LH (31.2/0.16), and WW (52.4/0.30)

At location WW, no significant difference was observed between treatments of the two parameters (Table 3.5.). Despite the no significant difference, similar variations were observed between the mean values of both parameters. Compared to the control treatment, treatment 4 had more stem numbers of about 38.19% (Table 3.5.). Therefore, the response parameters showed a direct relationship between stem density and leaf area index (LAI) (Table 3.5.). Therefore, treatments with high stem densities across the three locations observed high LAI values.

Results have shown significant effects between stem length and vegetative bud numbers, with no significant effects observed between treatments under floral buds (Table 3.6.). It was

obvious that the highest treatment rate (60 kg N/ha) resulted in the tallest stem length and vegetative bud numbers. Although the other parameters were not consistent, the control (0 kg N/ha) treatment observed a high stem length and vegetative bud numbers.

Table 3.6. Analysis of variance (ANOVA) on stem length, floral and vegetative bud numbers from treatment plots at the Lemmon Hill trial site [Collected: 16th September 2020].

Treatment	Lemmon Hill		
	Stem length (cm)	Floral bud numbers	Vegetative bud numbers
1 (0 kg N/ha)	21.35 b	5.87	18.67 b
2 (15 kg N/ha)	19.36 c	6.06	13.40 c
3 (30 kg N/ha)	22.14 ab	6.78	12.63 c
4 (60 kg N/ha)	22.57 a	6.78	21.39 a
ANOVA Results[1]	**p<0.0001**	**NS**	**p<0.0001**

[1] Analysis of variance (ANOVA) results refer to treatment effects that were either not significant (NS) or significant at $p<0.05$. Mean separation was completed using Fisher's multiple means comparison test procedure ($\alpha=0.05$). SE = SL (0.30), FBN (0.39), and VBN (0.90)

In assessing stem length at the DB location, it was observed that treatment 4 was significantly different from the other treatments. There were similar observations under both stem length and vegetative buds. The lowest performing treatments in both parameters observed about 40.95% difference compared to treatment 4 (Table 3.7.).

Table 3.7. Analysis of variance (ANOVA) on stem length and vegetative buds from treatment plots using the quadrant method at the three (3) commercial wild blueberry fields [Collected: 5th August 2021].

Treatment	Debert		Lemmon Hill		Wentworth	
	Stem length (cm)	Vegetative bud num.	Stem length (cm)	Vegetative bud num.	Stem length (cm)	Vegetative bud num.
1 (0 kg N/ha)	13.15c	18.67b	19.31a	21.04	14.45b	18.04
2 (20 kg N/ha)	10.22d	13.40c	18.49ab	19.80	16.04ab	18.16
3 (40 kg N/ha)	9.21d	12.63c	17.75ab	19.08	15.45ab	18.32
4 (60 kg N/ha)	17.21a	21.39a	15.58c	18.08	16.89a	19.40
5 (100 kg N/ha)	14.83b	18.76b	17.29b	19.16	15.90ab	18.76
ANOVA Results[1]	**p<0.0001**	**p<0.0001**	**p<0.0001**	**NS**	**p<0.026**	**NS**

[1] Analysis of variance (ANOVA) results refer to treatment effects that were either not significant (NS) or significant at $p<0.05$. Mean separation was completed using Fisher's multiple means comparison test procedure ($\alpha=0.05$). SE = DB (0.21/0.30), WW (0.26/0.30), and LH (0.27/0.35)

Significant differences ($p<0.05$) in treatments were observed under stem length but not vegetative buds at the LH location. The control treatment was significantly different from the other treatments. Treatment 4 was significantly different from all the other treatments with a reduced stem length of about 23.94% compared to the control treatment. Similar outcomes in stem length were observed under vegetative buds (Table 3.7.).

At the WW location (Table 3.7.), a significant difference was observed under stem length with no significance observed under vegetative buds. Treatment 4 was significantly different from

all other treatments with about a 16.89% difference compared to the control treatment. Similar trends in stem length were observed under vegetative buds (Table 3.7.).

Treatments from all locations indicated that there was a relationship between stem length and vegetative bud numbers. It was observed that treatments with higher stem lengths observed high vegetative bud numbers (Table 3.7.). This implied that the longer the stem, the higher the number of vegetative buds.

3.4.3.2 Leaf area index (LAI) using an aerial device

Results on LAI using the Sunscan canopy analysis system (LAI^S) showed differences between some treatments (Figure 3.3.). Results from the Debert (DB) location showed that treatments 2, 3, 4, and 5 were significantly different from the control. However, treatments 4 and 5 were significantly different from treatments 2, and 3. Compared to the highest treatment, the control treatment observed a difference of about 25.21% (Figure 3.3.).

At the LH location, results indicated significant differences between treatments (Figure 3.3.). Treatments 2, 3, 4, and 5 were significantly different from the control (treatment 1). However, treatments 4 and 5 were significantly different from treatments 1, 2, and 3. Compared to treatment 4, the control treatment observed a difference of about 27.92% (Figure 3.3.).

Results from the Wentworth location (WW) showed that treatment 5 was significantly different from the other treatments (Figure 3.3.). The control treatment showed a LAI difference of 38.29% compared to treatment 5. Treatment 3 had a difference of 41.06% compared to treatment 5.

Across the three sites, a general trend was observed. The two highest treatments, 60 and 100 kg N/ha, observed the highest leaf coverage. However, comparing all three locations it was observed that the LAI values for the LH location were about 4 times the values obtained from both DB and WW locations. Though the control treatment was the least across all three locations, the WW location showed a slightly different outcome (Figure 3.3.).

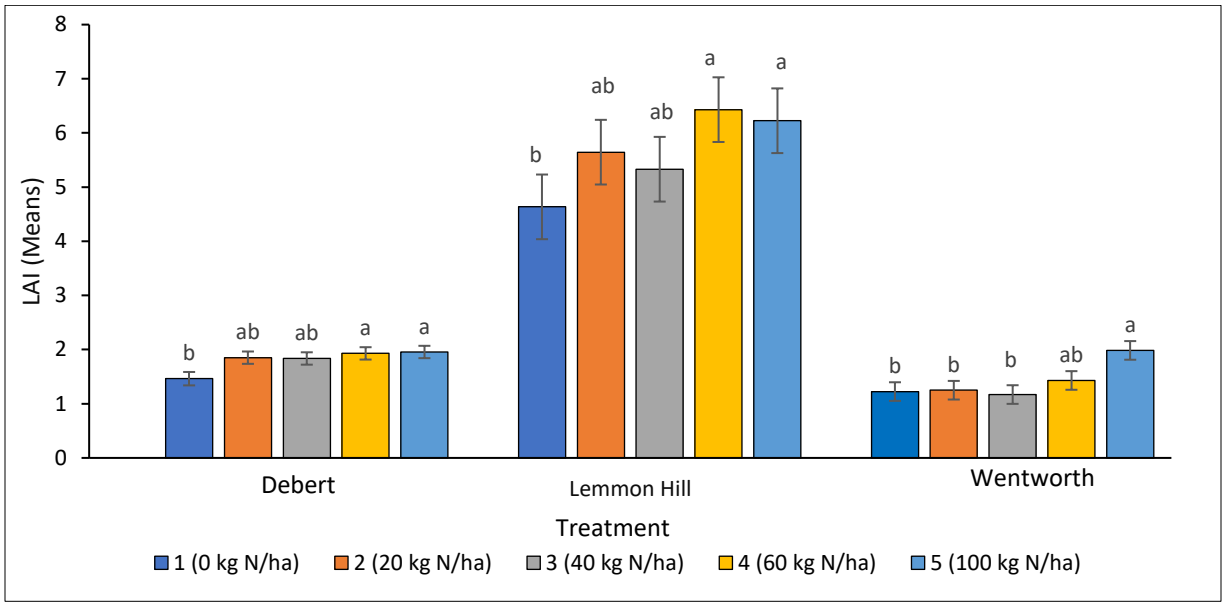

Figure 3.3. The effect of different rates of nitrogen on the leaf area index (LAI^s) of wild blueberry plants at three sites using the Sunscan canopy analysis system taken in October 2021.

3.4.4 Harvestable berry yield assessment

There were no significant effects between treatments from the 2020 trial on harvestable yield, however, mean values showed treatment differences (Table 3.8.). Compared to the highest nitrogen rate, the control treatment had the highest yield. Comparing the 2020 trial and the 2021 trials, it was observed that the 2020 trial observed over 85% increase in yields, except for the LH location which had similar yield values (Table 3.8. and 3.9.). Identifying an optimum rate of nitrogen application to a wild blueberry field is relevant to achieving higher yield. Therefore, assessing the

impact of five nitrogen treatments (0, 20, 40, 60, and 100 kg N/ha) on harvestable berry yield in the 2021 trial revealed some interesting findings. Results indicated that there were significant differences between treatments at different locations. Across the three locations, LH observed the highest harvestable berry yield compared to both DB and WW locations. Although there was no significant difference between treatments at LH, the control treatment had the least harvestable yield with a 13.4% decrease compared to treatment 3 (Table 3.9.).

Table 3.8. Analysis of variance (ANOVA) on harvestable berry yield (n = 120) treated with 4 rates of ammonium sulphate fertilizer at the Lemmon Hill site for the 2020 trial.

Treatment	Lemmon Hill (g/m^2)
1 (0 kg N/ha)	1211.73
2 (15 kg N/ha)	1151.67
3 (30 kg N/ha)	1121.87
4 (60 kg N/ha)	1034.83
ANOVA Results	**NS**

Analysis of variance (ANOVA) results refer to treatment effects that were not significant at $p<0.05$. Mean separation was completed using Fisher's multiple means comparison test procedure. The standard error (SE) = 74.53.

Significant effects were observed between treatments at WW location. Treatments 4 and 5 were significantly different from treatments 1, 2, and 3, with about a 37.9% difference in yield between treatment 4 and the control treatment. Similar yield differences of 28.1% and 43.5% were observed between treatment 4 compared to treatments 2 and 3 respectively (Table 3.9.).

Table 3.9. Analysis of variance (ANOVA) on harvestable berry yield (n = 150/location) treated with 5 rates of mixed compound fertilizers at three (3) experimental sites for the 2021 trial.

Treatment	Debert (DB)	Wentworth (WW)	Lemmon Hill (LH)
	(g/m^2)	**(g/m^2)**	**(g/m^2)**
1 (0 kg N/ha)	513.5 b	460.7 b	1043.3
2 (20 kg N/ha)	534.7 b	533.2 b	1148.0
3 (40 kg N/ha)	611.5 ab	419.2 b	1204.3
4 (60 kg N/ha)	738.1 a	741.7 a	1098.2
5 (100 kg N/ha)	546.1 b	726.7 a	1078.9
ANOVA Results[1]	**p<0.0006**	**p<0.0001**	**NS**

[1] Analysis of variance (ANOVA) results refer to treatment effects that were either not significant (NS) or significant at $p<0.05$. Mean separation was completed using Fisher's multiple means comparison test procedure ($\alpha=0.05$). SE = DB (39.7), WW (47.3), and LH (59.3)

A similar phenomenon was observed at DB, where treatment 4 was significantly different from all the treatments. Comparing treatment 4 to the control, it was observed that a 30.4% difference in yield was observed. Similar yield differences of 27.6%, 17.1%, and 25.6% were observed between treatment 4 as against treatments 2, 3, and 5 respectively (Table 3.9).

3.4.5 Relationship between aerial and field data (Growth parameters)

3.4.5.1 Correlation analysis

Pearson's correlation between the various parameters of the 2021 data showed levels of significance between specific parameters which were consistent for all three locations (Table 3.10.). Across all the 3 locations, significant correlations were established between PD and LAI, and LNC and GLI. In DB and WW locations, a significant correlation was observed between LAI and GLI. At the WW location, yield showed a significant correlation with LNC and GLI, while PD showed a significant correlation with GLI. Therefore, a positive relationship was established between PD and LAI, and this translates to an increase in GLI. These results showed that there is the possibility for some predictions to be achieved; thus, PD can be used in predicting LAI, GLI can be used in predicting LNC and finally GLI can be used in predicting LAI (Table 3.10.). At the WW location, yield showed a significant correlation with all the three VIs.

In the 2020 analysis, significantly high correlation values were observed between the various VIs and two growth parameters [Stem length (SL), floral bud numbers (FBN), and vegetative bud numbers (VBN)] (Table 3.11.). However, VBN as against the various VIs were low with no significant correlations. Aside from the other VIs, NDRE observed a low correlation effect with floral bud number and stem length.

A second assessment conducted later within the year on all 3 trials (Table 3.12.) showed that stem length had positively strong correlations with various VIs, with floral bud number showing significantly low correlation values. Despite the relatively low correlation values, floral bud number had good correlations with stem length (Table 3.12.). It was observed that high stem length correlations were observed at the WW and DB locations with almost no significant stem length correlation occurring at the LH location.

3.4.5.2 Relationship between yield, LNC, PD, and LAI

The impact of plant density, leaf area index (LAI), and LNC among other parameters can contribute to a potential prediction of yield. LH and DB locations showed weak but positive and negative relationships between LAI and yield respectively. Yield against LNC at the WW location showed a moderately strong positive relationship (Figure 3.4., b). The relationship between yield and LAI across all three locations showed no significant relationships (Figure 3.4., d-f). A poor relationship between the two parameters was observed at the three locations. Plant density and yield showed a positive but weak relationship between the two parameters (Figure 3.4., g-i). All three locations showed no significant ($p > 0.05$) relationship between those parameters.

3.4.5.3 Relationship between vegetative indices and growth parameters

Assessing the relationship between these three parameters provides some good findings. Results showed that plant density and LAI had a positively strong relationship across the three locations. All three relationships across the various locations were significant (Figure 3.5., a-c). Therefore, it implied that as plant population increases, plant leaf area also increases. The relationship between plant density and GLI showed positive relationships at both WW and DB locations with a negative relationship at LH (Figure 3.5., d-f). Among the three locations, only WW showed a significant relationship between the two parameters. Therefore, as the number of stems increases, the green leaf index value also increases. The relationship between PD and GRVI was a non-significantly weak relationship, which was across all three locations (Figure 3.5., g-i). Similar to PD and GRVI are PD and VARI, which also showed similar observations (Figure 3.5., j-l).

LNC and GLI showed a moderately strong relationship (Figure 3.6., a-b). Across all three locations, the relationships observed were significant. Both LH and DB showed a negative relationship with WW showing a positive relationship. Conforming to a negative relationship

implied that the other parameter decreases as one parameter increases (Figure 3.6., a, b). The relationship between LNC and GRVI showed a moderately strong and positive relationship at WW ($R^2 = 0.43$), with the other two locations observing low and weak relationships (Figure 3.6., d-f). The same or similar relationship to GRVI was observed between VARI and LNC (Figure 3.6., g-i).

A moderately low but positive relationship was observed between LAI and GLI at both WW and DB locations, with LH showing a negative relationship (Figure 3.7., a-c). The relationships observed were significant ($p < 0.05$) at both WW and DB locations, with LH not showing any significant difference. This implied that an increase in plant leaf area increases the green leaf index value. The relationship between GRVI and LAI was significant ($p < 0.017$) and showed a moderately strong and positive relationship at the WW location, with DB and LH locations showing very weak relationships (Figure 3.7., d-f). The relationship between VARI and LAI was similar to the relationship between GRVI and LAI (Figure 3.7., g-i).

Again, significantly ($p < 0.05$) strong relationships were established between yield and the three VIs (GLI, GRVI, and VARI) (Figure 3.8., b, e, h) at the WW location whereas DB and LH locations observed a very low outcome. Except for slight changes in the R^2 values and their probability values, the relationship dynamics between GRVI, VARI, and yield have all been the same across the 3 locations.

Table 3.10. Pearson's correlation between yield, plant density (PD), leaf area index (LAI), leaf nitrogen content (LNC), and vegetative indices (GLI, GRVI, and VARI)

2021	LEMMON HILL				WENTWORTH				DEBERT			
	Yield	**PD**	**LAI**	**LNC**	**Yield**	**PD**	**LAI**	**LNC**	**Yield**	**PD**	**LAI**	**LNC**
PD	0.186				0.039				0.321			
LAI	-0.160	0.589*			0.109	0.829*			0.276	0.695*		
LNC	0.138	0.280	0.246		0.510*	-0.017	0.158		-0.077	-0.028	0.113	
GLI	0.048	-0.216	-0.150	-0.593*	0.694*	0.405*	0.552*	0.606*	0.131	0.228	0.407*	-0.501*
GRVI	0.047	-0.116	-0.051	-0.307	0.548*	0.282	0.471*	0.653*	-0.355	-0.037	0.275	-0.089
VARI	0.043	-0.115	-0.050	-0.305	0.577*	0.312	0.502*	0.641*	-0.364	-0.051	0.272	-0.055

*Significant at $p < 0.05$

Table 3.11. Correlation analysis on stem length and floral bud numbers at Lemmon Hill [Data collected: 16th September 2020].

	Lemmon Hill						
	NDVI	**ENDVI**	**NDRE**	**SAVI**	**GLI**	**GRVI**	**VARI**
SL	0.562*	0.509*	0.472*	0.567*	0.591*	0.593*	0.502*
FBN	-0.566*	-0.528*	-0.183	-0.566*	-0.582*	-0.551*	-0.430*
VBN	0.039	0.077	0.165	0.047	0.124	0.108	0.067

*Significant at $p < 0.05$

Table 3.12. Correlation analysis on stem length and floral bud numbers from all three (3) locations of the wild blueberry fields [Data collected on December 21, 2021].

	Lemmon Hill		Wentworth		Debert	
	Floral bud No.	**Stem length**	**Floral bud No.**	**Stem length**	**Floral bud No.**	**Stem length**
NDVI	-0.179	-0.016	0.239	0.659*	-0.185	0.556*
ENDVI	-0.212	-0.101	0.197	0.601*	0.064	0.642*
NDRE	0.334	0.429*	-0.014	0.346	-0.171	0.411*
SAVI	-0.200	0.003	0.241	0.670*	-0.184	0.556*
GLI	-0.358	-0.288	0.182	0.484*	0.114	-0.294
GRVI	-0.347	-0.254	0.203	0.503*	0.044	-0.425*
VARI	-0.325	-0.220	0.185	0.493*	0.064	-0.359
Stem length	0.453*		0.722*		0.314	

***** Significant at p>0.05

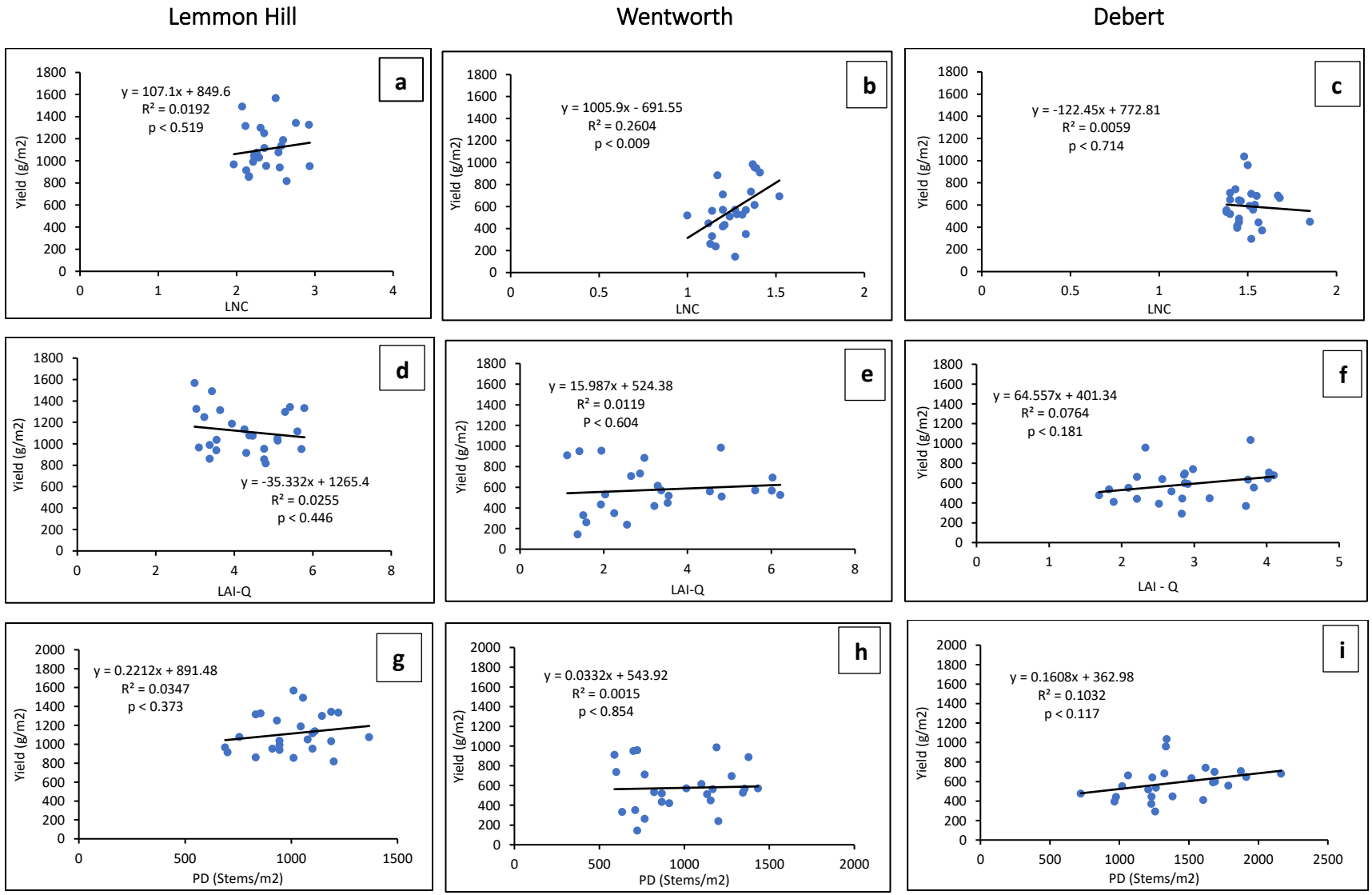

Figure 3.4. Linear regression analysis on yield using Nitrogen content, leaf area index (LAI), and plant density from the three trial sites Lemmon Hill, Wentworth, and Debert.

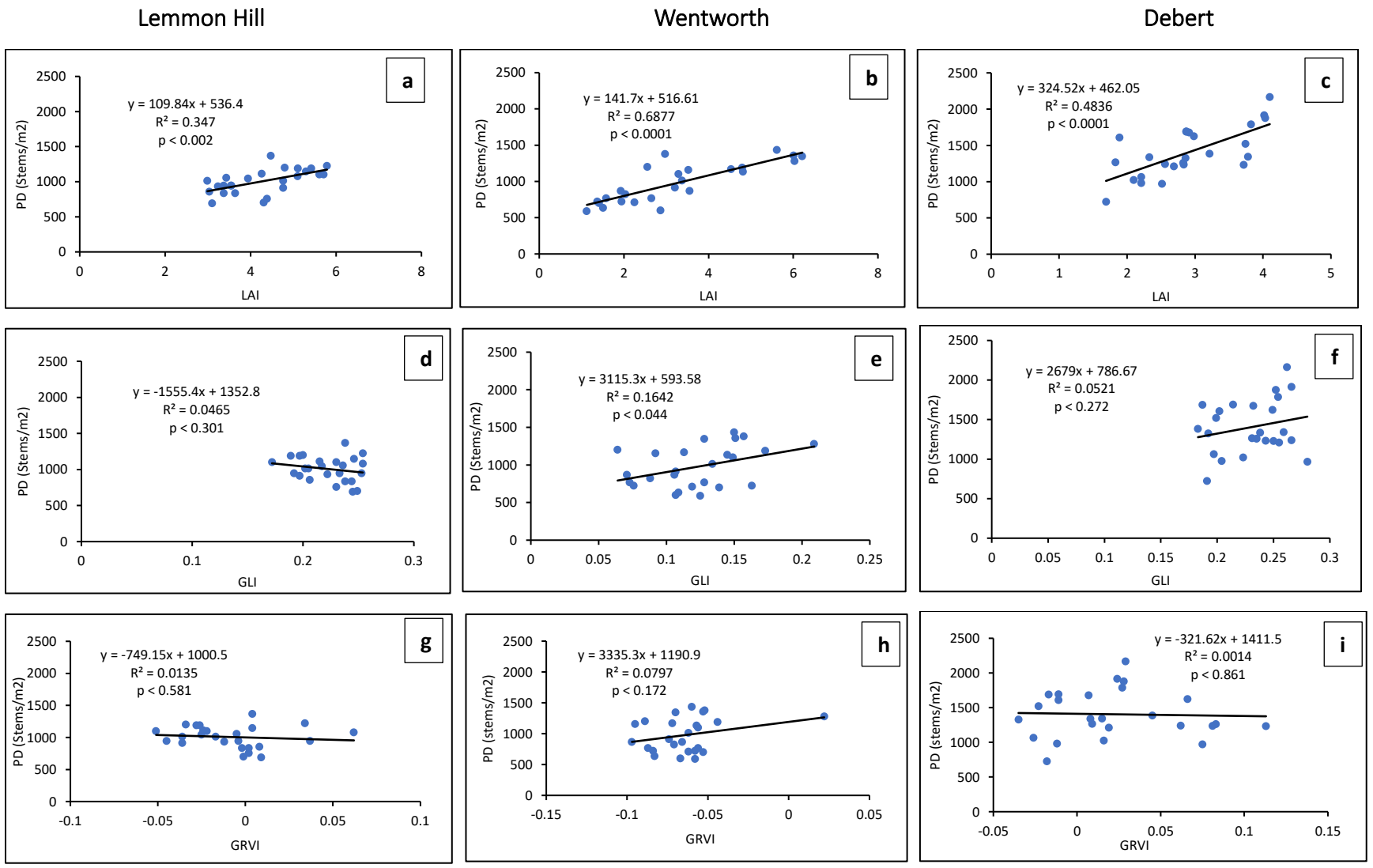
Lemmon Hill
Wentworth
Debert
a
y = 109.84x + 536.4
R² = 0.347
p < 0.002
PD (Stems/m2)
LAI
b
y = 141.7x + 516.61
R² = 0.6877
p < 0.0001
PD (Stems/m2)
LAI
c
y = 324.52x + 462.05
R² = 0.4836
p < 0.0001
PD (Stems/m2)
LAI
d
y = -1555.4x + 1352.8
R² = 0.0465
p < 0.301
PD (Stems/m2)
GLI
e
y = 3115.3x + 593.58
R² = 0.1642
p < 0.044
PD (Stems/m2)
GLI
f
y = 2679x + 786.67
R² = 0.0521
p < 0.272
PD (Stems/m2)
GLI
g
y = -749.15x + 1000.5
R² = 0.0135
p < 0.581
PD (Stems/m2)
GRVI
h
y = 3335.3x + 1190.9
R² = 0.0797
p < 0.172
PD (stems/m2)
GRVI
i
y = -321.62x + 1411.5
R² = 0.0014
p < 0.861
PD (stems/m2)
GRVI

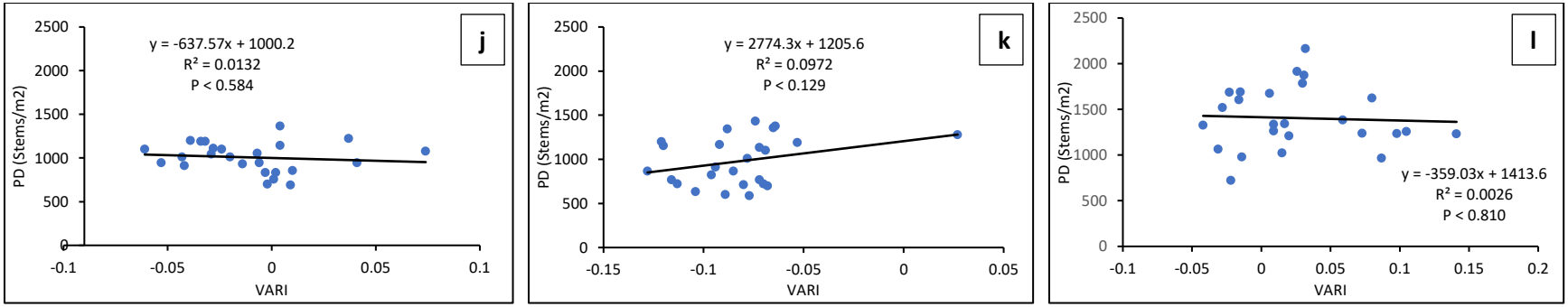

Figure 3.5. Relationship between wild blueberry growth parameters and GLI using the coefficient of determination values at three trial sites Lemmon Hill, Wentworth, and Debert. Plant density (PD) and leaf area index (LAI) (a-c), PD and GLI (d-f), PD and GRVI (g-i), and PD and VARI (j-l) define the different graphs. The relevance of a relationship was assessed using a 5% or $p < 0.05$ significance level.

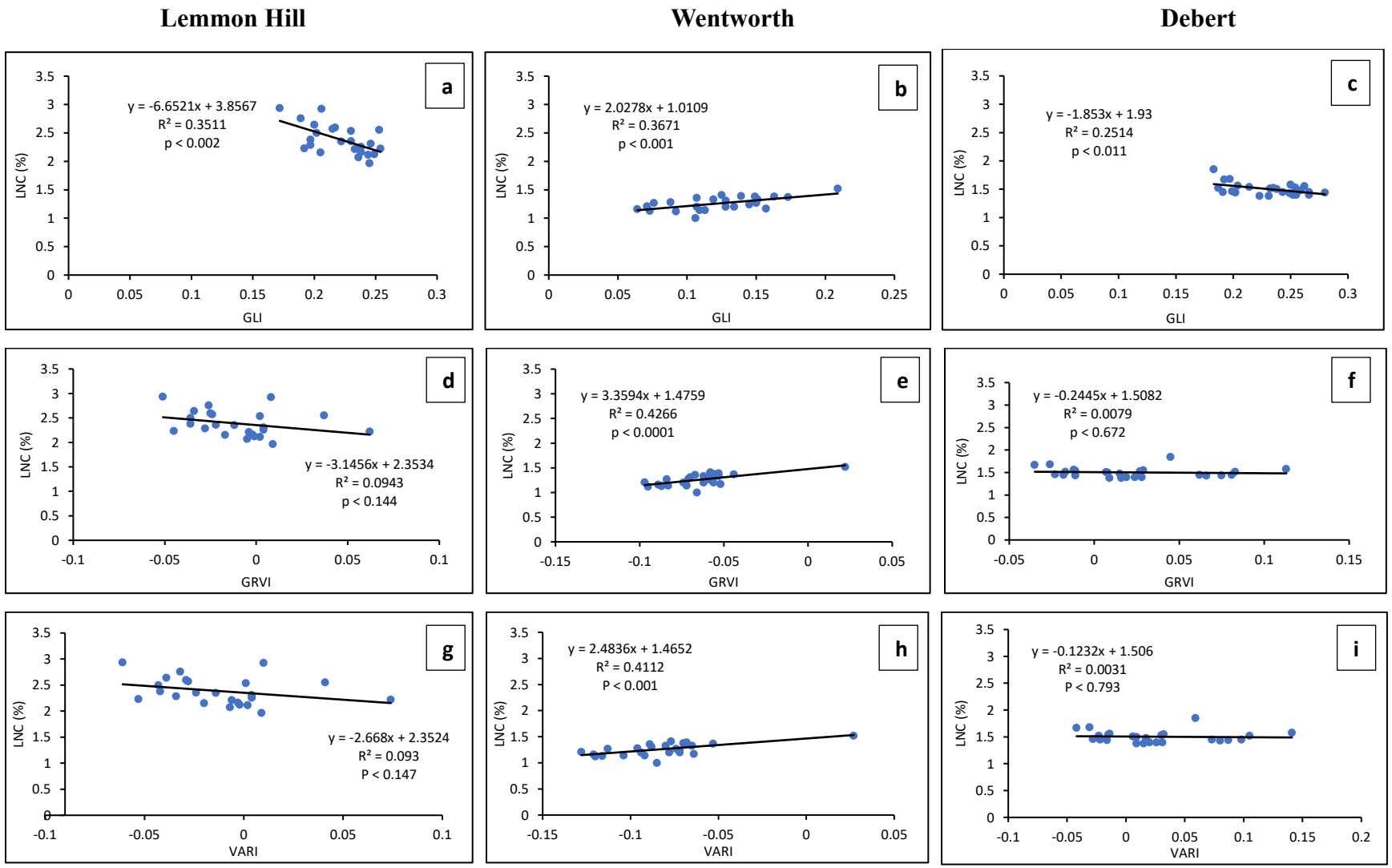

Figure 3.6. Relationship between Leaf Nitrogen Content (LNC) and vegetative indices using the coefficient of determination values at three trial sites Lemmon Hill, Wentworth, and Debert. LNC and GLI (a-c), LNC and GRVI (d-f), and LNC and VARI (g-i) define the different graphs. The relevance of a relationship was assessed using a 5% or $p < 0.05$ significance level.

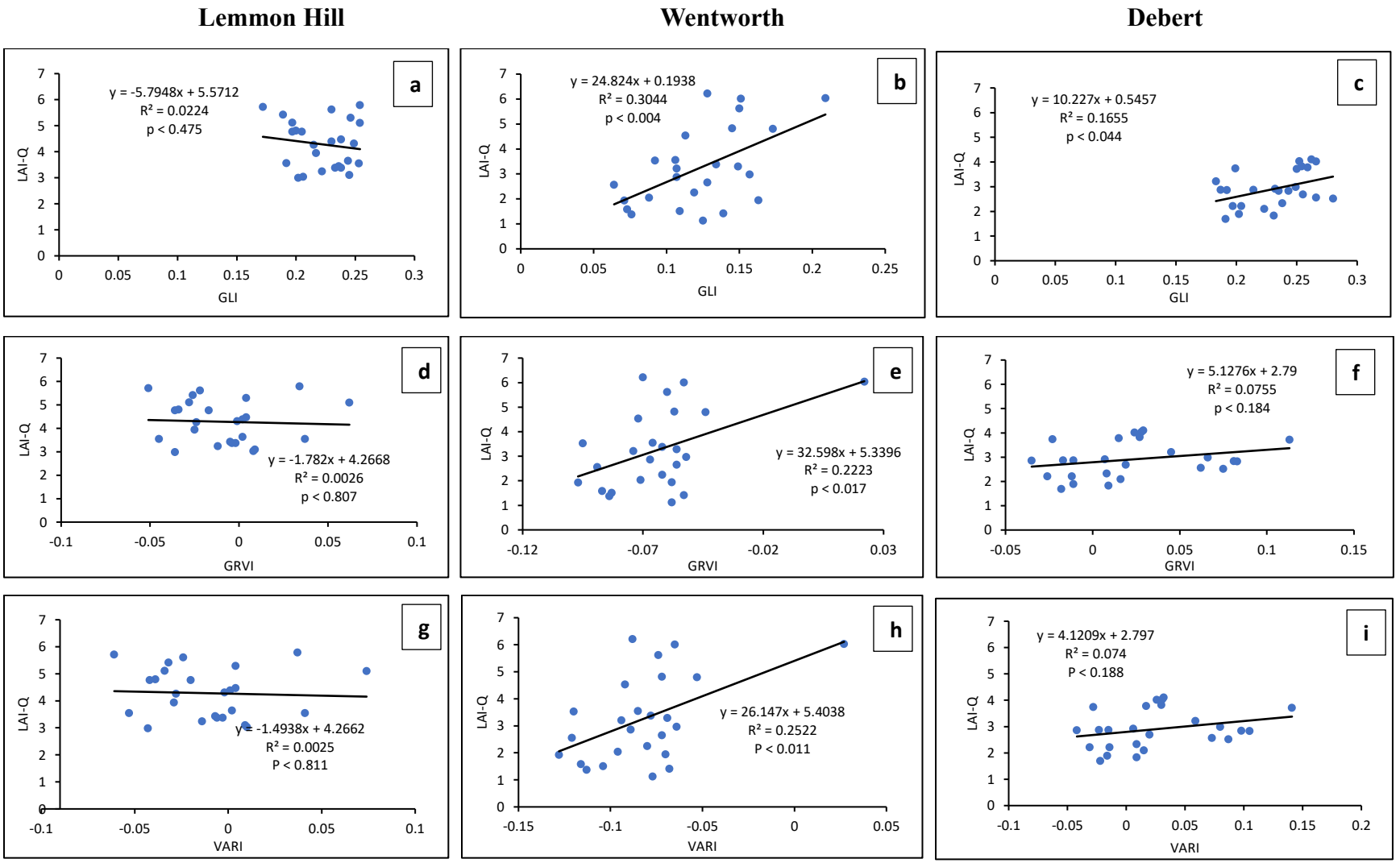

Figure 3.7. Relationship between Leaf area index (LAI) and vegetative indices using the coefficient of determination values at three trial sites Lemmon Hill, Wentworth, and Debert. LAI and GLI (a-c), LAI and GRVI (d-f), and LAI and VARI (g-i) define the different graphs. The relevance of a relationship was assessed using a 5% or $p < 0.05$ significance level.

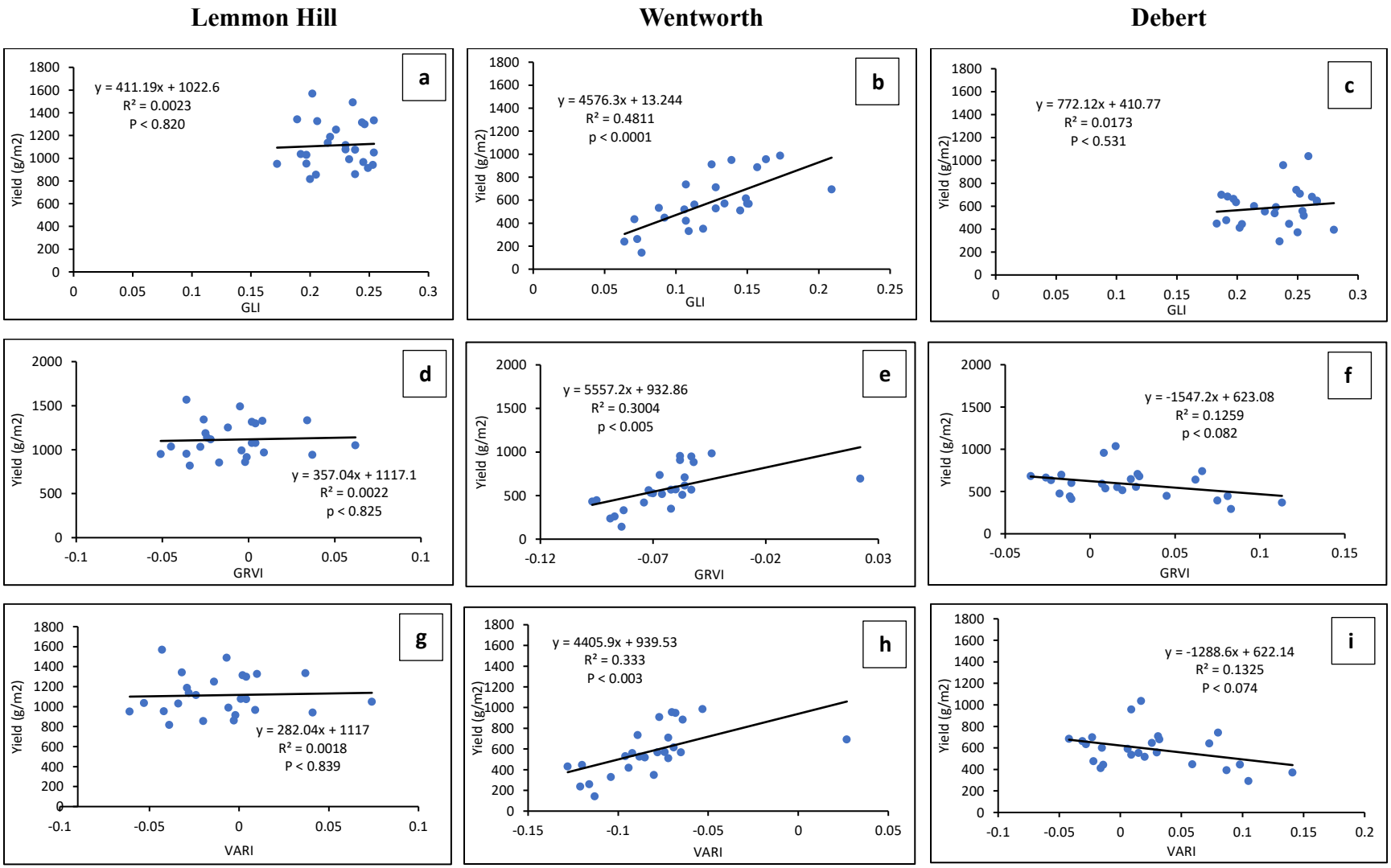

Figure 3.8. Relationship between wild blueberry yield and 3 vegetative indices GLI, GRVI, and VARI using the coefficient of determination values at three trial sites Lemmon Hill, Wentworth, and Debert. Yield and GLI (a-c), yield and GRVI (d-f), and yield and VARI (g-i), define the different graphs. The relevance of a relationship was assessed using a 5% or $p < 0.05$ significance level.

3.5 DISCUSSION

The results of this study have provided significant insights into the effect of nitrogen on vegetative indices and canopy characteristics in the wild blueberry field. Indications from these results suggest that consistent treatment effects were achieved across all three locations with few variations. Despite these findings, it was determined that variation existed between the different locations, which Marty et al., (2019) terms as the "population effect", and this would include, differences in soil and weather conditions. Since the focus of the study was targeted at understanding the direct effect of N on VIs, a preliminary assessment of the soil was not conducted, thus, there was no need to use the soil as a benchmark or standard for comparison.

3.5.1 Impact of nitrogen fertilization on growth parameters

The wild blueberry plant naturally grows in soils with low organic matter, therefore, the fields by nature are low in nitrogen (Agriculture, Aquaculture, and Fisheries, 2013; Thyssen et al., 2006). Therefore, an application of fertilizers should keep these nutrient elements at optimum levels for plant utilization. The study revealed that, despite the non-significance among the various treatments of LNC in two locations, these values fall within the accepted levels and their mean values depict some differences that were consistent for these locations (Eaton et al., 2009; Trevett, 1972). Mean differences between treatments were consistent for almost all locations with the higher treatment rates observing high levels of LNC. These results were similar in magnitude to the findings of Percival & Privé, (2002) who established treatment differences between LNC in wild lowbush blueberry plants, despite the slight difference in the number of times and levels of fertilizers applied in that study. Interestingly, the LNC obtained at the LH location was almost twice observed at the DB and WW locations. Although these values were higher than the other locations, they were slightly above the acceptable nitrogen concentration levels according to

Trevett, (1972), Eaton et al., (2009), and Agriculture, Aquaculture, and Fisheries, (2013). It can be suggested that the leaves contained very high N levels, and thus, the assimilated compounds had not yet been sequestered or utilized, however, because a prior soil analysis was not conducted, little can be provided on the soil nitrogen content and its impact on the LNC. Instead, a prior image assessment of the canopy provided a baseline to assess the independent effect of the added N, giving the soil assessment an alternative. Other reports suggest that the bulk of the blueberry plant (about 75%) lies with the rhizomes and these store mineral nutrients for growth and development. Nevertheless, because the plant is perennial, there is a possible carry-over of nutrients at varying levels which may affect nutrient determination. Therefore, this may have posed a difficulty in assessing the true nitrogen levels of plants (Percival & Privé, 2002), however, assessing issues of crop removal and competitive pressures like weeds can have a serious impact on N. This study further agrees with the work of Eaton et al., (2009) that LNC increases with nitrogen addition.

The impact of the various treatments on growth and development was consistent for both DB and WW locations. The early application of N – fertilizer enhanced stem length and vegetative buds in plants, across DB and WW locations; however, this phenomenon varied at LH. This result agrees with the findings of Eaton et al., (2009) whose work compared consecutive and alternate fertilizer applications in wild blueberry fields. The study indicated that stem height and floral bud numbers were generally high for fertilizer treatments, thus, the plant utilizes nitrogen as structural building blocks in the early developmental phase (Eaton et al., 2009). This way the plant forms its canopy within the shortest possible time and diverts resources into the following year's crop development. Stem length and vegetative buds move hand in hand; thus, they have a strong relationship (Fournier et al., 2020). Therefore, a tall plant will have several vegetative buds, and

vice versa. Converse to the findings of Percival & Privé, (2002), our results were inconsistent on vegetative bud numbers but showed significant differences in stem height (Table 3.6.).

3.5.2 Determination of an optimum nitrogen rate

Yield is a significant aspect when it comes to the wild blueberry industry, thus cost-effective practices and measures aimed at increasing berry yield are considered. The N-fertilization treatment effects on yield were obvious, thus it points to specific treatment rates being considered as better choices for high yields. Compared to the control, all other treatments led to an increase in yield. This study agreed with the findings of Percival & Privé, (2002) who examined multiple nitrogen applications over a two-year production cycle. Given that the perennial nature of the plant allows for nutrient carry-over potential, therefore an increase in N as demonstrated in the different treatments caused significant growth improvements. Harvestable yield from 60 kg N/ha was consistent in two trial locations, while it showed as the second highest in the third location. The inconsistency in treatment 4 (60 kg N/ha) at the LH location can be explained based on the plant density within those fields. The plant density in treatment 4 was low, and this probably affected the amount of yield from that treatment (Table 3.4.). Therefore, population effect and field-level variability at the different locations contributed to the differences observed, similar to the findings of Marty et al., (2019). In a similar study that compared different nitrogen fertilizer rates, no significant differences in yield, however, treated plots observed about 36% more in yield than the control treatments (Percival & Sanderson, 2004). From this study, yields from 40 kg N/ha^{1} and 100 kg N/ha^{1} also showed possibilities of selection as optimum nitrogen fertilization rates, however, the inconsistencies observed do not support their selection in this study.

Generally, an excess application of nitrogen has deleterious effects on the growth and development of wild blueberry plants (Agriculture, Aquaculture, and Fisheries, 2013). Though

toxicity was not observed, plants from treatment 5 (100 kg N/ha) may have had excess nitrogen which accounts for the relatively low growth parameters. Significantly high volatilization of ammonia, weed pressures, lack of pollination, and other winter injuries potentially reduced the amount of N and other elements like K and P available to the plant; thus, this phenomenon may be responsible for the low impact of some nitrogen treatments at some locations (Coleto et al., 2023; Thyssen et al., 2006). This concept of volatilization, however, has a low rate on the N applied in wild blueberry fields is location-specific, and can be influenced by several factors, including rainfall, temperature, and organic matter among other factors (Thyssen et al., 2006). Furthermore, results from a similar study suggest that the long-term fertilizer effect application in the first year of production has residual effects on harvestable berry yield (Eaton et al., 2009). This implied that a single, but optimum application of fertilizers greatly improves yield. This finding agreed with Percival & Privé, (2002), whose work on multiple fertilizer applications on lowbush blueberry provides a basis for this claim. Their study highlights the point that no significant difference was observed between multiple-treatment plots and single-treated plots (Percival & Privé, 2002). Furthermore, Marty et al., (2022) state that mineral fertilization has about 2 years of effect on the wild blueberry plants which also affects VIs, thus implying that a single application of fertilization may be effective in improving yield. However, after 12 days of application, Thyssen et al., (2006) also state that the greatest loss of soil-applied N was less than 4.2% indicating that the majority of fertilizers applied were still contained in the soil. Therefore, rather than applying multiple fertilizers at different stages of the growth cycle, a single fertilizer application can be done to achieve similar results. This is significant to the producer, as it serves as an economic benefit to farmers as they spend less on fertilizers.

3.5.3 Effects of nitrogen fertilization on vegetation indices

The effect of nitrogen fertilization on vegetative indices seemed inconsistent in the 2020 trial, however, significant differences established at the WW location and the other two locations (Appendix A3 & A4) showed that there was a considerable effect of nitrogen fertilization on VIs in the 2021 trial. This result agreed with the findings of Caturegli et al., (2016) who stated that colour intensity has a significant correlation with nitrogen fertilization which further correlates with vegetative indices, specifically NDVI. Nitrogen contributes significantly to plant growth as it constitutes the chlorophyll molecule content reflecting the green pigments of the plant (do Amaral et al., 2019). It is therefore expected that the higher the nitrogen content contained in a plant the greener the plant, and this should translate to a high VI value. Furthermore, this result agreed with Caturegli et al. (2016) that good correlations between LNC and VIs can be established. However, some inconsistencies observed at the two other locations are attributed to locational differences like the wetness conditions of those areas. Granular fertilizers achieve maximum effects when granules are dissolved in moisture to maximize their absorption and effects on the plant. Therefore, considering the 3 locations WW location was a low-lying field with a relatively high moisture content, allowing an easy breakdown of the granular fertilizers compared to both DB and LH locations which experienced drier conditions on an uphill field. Furthermore, the sensitivity of the red, blue, and green (RGB) reflectance values may have contributed to the indifference between treatments, thus the NIR-VIs reflected the difference in nitrogen rates (Table 3.3). The relative difference between an RGB light camera as compared to a multispectral camera may influence the data collected (Kokhan & Vostokov, 2020; Lu et al., 2021). From previous works with both data sets, it was evident that VIs computed using multispectral images are usually sensitive and have higher index values compared to an RGB image. Therefore, their ability to

determine areas of a field with high nitrogen levels can be utilized in the development of prescription maps for nitrogen application.

3.5.4 Remote estimations of plant growth parameters and yield

UAVs have been used for different purposes and have contributed immensely to the estimation of growth parameters in several crops, including wild blueberry, rice, barley, cotton, soybeans, sunflower, and grass among others (Kaivosoja et al., 2021; Kokhan & Vostokov, 2020; Li et al., 2020; Marty et al., 2019). Therefore, research advancements in remote sensing can introduce some interesting perspectives into wild blueberry management and production, through its non-destructive approach. In this study, several field parameters were estimated using VIs. This study focused on the green leaf index (GLI), Green red vegetative index (GRVI), and Visible atmospheric red index (VARI), nevertheless, conclusions were drawn regarding NDVI as well. According to Yamamoto et al., (2005), visible light VIs are strongly correlated with NDVI, therefore conclusions were drawn based on this information. UAV's predictability of yield using LNC seemed variable and inconsistent as negative correlations were observed in two locations with the other showing a positive correlation. The estimation of LNC using VIs seemed positive, however, according to the work of Bourguignon, (2007), NDVI performed poorly in quantifying N levels. This may be possible due to the environmental condition and the colouration of leaf tissues may have contributed to this challenge. Invariably, it may suggest a difficulty in using VIs in nutrient level estimations in wild blueberry tissues. Conversely, a study by Maqbool et al., (2012), established relationships using spectral reflectance bands whose approach differs from this study.

Though VIs consist of spectral data (wavelength regions), there are limitations as to the visible light bands included in the computational process. Using spectral data, Maqbool et al., (2012) established the green peak region as the best for estimating foliar N. Therefore, this suggests

the ability of these VIs (GLI, GRVI, and VARI) from the visible light regions to estimate LNC. The moderately high coefficient of determination (R^2) values observed at the WW location explains about 36.71%, 42.66%, and 41.12% variability of the data. Though better estimations can be achieved, this difficulty can be attributed to several reasons including the level of variability of the field, image resolution, and the non-homogenous nature of the canopy (Daughtry, 2000). This finding also agreed with the work of Lu et al., (2021), who showed that LNC was accurately estimated in maize ($R^2 = 0.76$) using VIs. Whereas good correlations have been found between VIs and LNC in other crops (Caturegli et al., 2016; Lu et al., 2021), variability in the plant canopy, crop features and developmental stage, background noise, topographic effects, vegetation density, and other intrinsic factors account for the difficulty to estimate nitrogen levels (Daughtry, 2000; Kokhan & Vostokov, 2020). This study further agreed with Bourguignon, (2007), whose work focused on the ability to estimate N, P, and K levels in wild blueberry leaf tissues using specific hyperspectral technologies. It was observed that the possibility of estimating N and P levels using hyperspectral technology was high yet varied for some instruments (Bourguignon, 2007).

It could be determined that as the stem number increases, plant leaf area increases, and this should directly impact the vegetative index values. Therefore, the relationship established between LAI and GLI may suggest this claim (Figure 3.7., b). Variability in leaf pigment and colour intensity becomes a significant contributor to this phenomenal difference. This is because the absorption and reflectance peak for the different pigments vary, thus making it difficult for estimated values to be determined (Sims & Gamon, 2002). The wild blueberry field is not an ever-green shrub but has a mosaic of colours that impacts the vegetative index values. Leaf colour variation affects the portion of light by either being highly absorbed or highly reflected, and this affects the vegetative indices (Marty et al., 2022). However, there is great potential for the

predictability of LAI using GLI or a near-infrared vegetative index, as these indices are not directly affected by changes in leaf colour. Percival & Beaton, (2012) established that LAI had a strong correlation with NIR bands, thus NIR vegetative indices may generate better relationships compared to VIS vegetative indices. Furthermore, Breda (2003) explains that, whereas LAI can be complex and difficult to determine, spatial and temporal variability in the field may account for these differences.

As the number of stems increases, GLI was expected to increase, giving a strong positive relationship. However, the highest R^2 value of the three locations explains only about 16.42% of the data, which was relatively low compared to other studies (Lu et al., 2021). However, PD showed a good correlation ($R = 0.83$) and regression ($R^2 = 0.69$) with LAI. Unlike row crops, plant density is highly variable across the wild blueberry field, and this impacts LAI and possibly vegetative index values. This confirms the variability levels observed in the wild blueberry fields in terms of population and clonal differences which affect leaf area (Kinsman, 1993). The findings from this study agreed with Lu et al., (2021) that LAI can be estimated by VIs, despite their description of LAI as canopy cover.

Yield estimations using vegetative indices have proved challenging on the wild blueberry field, despite the successes reported in other crops (Hussain et al., 2020; Li et al., 2020; Zhang et al., 2020). This finding agreed with the study of Barai et al., (2021) who assessed the effects of drought on wild blueberry production. The study reports that it is difficult and variable to predict harvestable yield in a wild blueberry field using VIs. This was because several variables constantly change along the production cycle making it difficult to use VIs in determining harvestable berry yield. For example, some factors such as pollination, pathogens, weeds, and insect pests contribute significantly to yield, and these vary across the field and season. However, Maqbool et al., (2010)

used optimum multiple narrow reflectance data in the prediction of harvestable yield, with very high regression values (R^2 = 0.79). Considering the slight difference in the approaches used, consideration should be given to the specific bands used and sensor resolution which affects the levels of detail to be gotten from the field. Despite the inconsistency in yield prediction, correlation values from this study (Table 3.9) have proven positive and have shown potential in yield predictions.

3.6 CONCLUSION

This study was conducted to examine the effect of different nitrogen rates on different growth parameters (LNC, yield, plant density, and LAI) and vegetative indices. Furthermore, the study examined the potential to estimate growth parameters using vegetative indices. We have demonstrated that vegetative indices computed from an RGB sensor can estimate several growth parameters on the wild blueberry fields specifically, LNC, and LAI. Whereas the estimation of PD and yield looks variable, there is a need for further studies into this aspect. Furthermore, the perennial nature of the plant introduces complexities in determining and measuring N effects, however, this study generally showed that the application of fertilizers enhanced berry yield. Interestingly, findings from the WW location in this study strongly point to a future application and adoption of liquid fertilizers on wild blueberry fields. The vegetation indices, GLI, GRVI, and VARI, obtained from an RGB sensor showed good potential in estimating growth parameters, however, it is estimated that NIR-VIs should outperform visible light VIs. This allowed the NIR-VIs to establish differences between the different nitrogen rates, unlike the VIS-VIs. Thus, further work can be conducted to consider predictions and estimations using a multispectral sensor.

CHAPTER 4: REMOTE ASSESSMENT OF WILD BLUEBERRY PHENOLOGY

Anku, K.E., Percival, D.C., Rajasekaran, L.R., Heung, B. and Vankoughnett, M. (2023). Phenological assessment of the wild blueberry field using an unmanned aerial vehicle. Acta Hortic. 1357, 35-42. DOI: 10.17660/ActaHortic.2023.1357.6 https://doi.org/10.17660/ActaHortic.2023.1357.63.1

Anku, K. E., Percival, D. C., Rajasekaran, L. R., Heung, B., & Vankoughnett, M. (2024). Phenological assessment of the wild blueberry field using an unmanned aerial vehicle. MDPI Remote Sensing (In prep)

4.1 ABSTRACT

The objective of this study was to determine the potential for using multi- and hyperspectral sensors to monitor and predict growth and development in the wild blueberry field. The study used a hand-held FieldSpec®3 hyperspectral sensor and a DJI Matrice 600 Pro unmanned aerial vehicle, which was equipped with a 5-band multispectral micasense camera. These trials were conducted in several commercial fields from 2019 to 2022. Data were sampled over the four seasons, and orthomosaic maps were generated using the Solvi platform. Plant growth and development were assessed using vegetative indices; NDVI, ENDVI, NDRE GLI, GRVI, and VARI. Correlation results for all VIs computed indicate that similar trends were observed in all sensors at the different phenological stages. The early/late bud stage (F4/F5) and bloom stage (F6/F7) showed significantly high correlation values among all growth stages. LAI, floral, and vegetative bud stages can be estimated at the tight cluster (F4/F5) and bloom (F6/F7) stages with R^2/CCC values of 0.90 / 0.84. The variable importance showed that NDVI, ENDVI, GLI, VARI, and GRVI contributed significantly to achieving these predicted values, with NDRE showing low effects. This implies that F4/F5 and F6/F7 stages are good phenological stages for making phenological predictions and estimations about plants in the wild blueberry field.

4.2 INTRODUCTION

Wild blueberries are important plants that are native to northern America and occupy large numbers of hectares for production. Recent reports from the International Blueberry Organization, (2023) and Beijing, (2023) USDA indicates that China is the largest producer and importer of blueberry followed by the United States (U.S.), Peru, Chile, and Canada. Blueberries in Canada are cultivated with over 80,657 ha of land, generating 195,892 tons of berries, valued at about $363.948 million in 2022 (Eaton & Nams, 2012b; Statistics Canada, 2023).

The phenology of the plant is critical in the management and production practices in the wild blueberry field. Thus, the plant's phenological stage commands internal and external changes. For instance, the risk for Monilinia blight infection increases once the floral and vegetative buds on the stem reach the F2 and V2 (vegetative stage 2) stages where buds expose about 2 – 5 mm of green tissue (Delbridge & Hildebrand, 1997a). Conversely, the risk of Botrytis blight infection occurs later when the floral buds are at the F6 – F7 stage when corollas are fully opened (Langdon, 2008; Percival & Beaton, 2012). Despite this phenomenon, there are variations in floral and vegetative bud growth leading to a varying pattern of disease damage, resulting from phenotypes' phenological differences. Therefore, *V. myrtilloides* phenotypes observe a delayed growth pattern, reproductive budburst, and flowering by a week as compared to *V. angustifolium* (Fournier et al., 2020). The methods for carrying out field assessments have always depended on physical monitoring which adopts a destructive approach. Therefore, to determine plant density among other growth parameters, the plants will have to be harvested and this affects the plant population. Different methods and approaches have been adopted in monitoring the phenology of wild blueberries using weather data and monitoring the biophysical traits of the plant (Krebs et al., 2009). However, this approach still poses challenges, as they leave out factors such as slope and

the variability of the field. These factors coupled with the cost of requesting the services of experienced personnel in these large commercial fields make the process difficult. Therefore, alternative approaches to monitoring growth and development in the field are required. The advancement in the use of remote sensing in agriculture has allowed for predictions and determinations to be made using VIs. These VIs are mathematical computations or ratios of the different light wavelengths reflected from vegetation (Hassan et al., 2019; Jones et al., 2007). Several studies adopting VIs have been utilized to make phenology determinations and predictions on crops including cotton, rice, and wheat (Hassan et al., 2019; Souza et al., 2017). Therefore, the physiological changes being observed in the wild blueberry field as a result of growth and development can be monitored aerially using remote sensing approaches. This allows for early field evaluation and possible predictions or estimations of growth parameters.

The use of remote sensing technologies and machine learning (ML) approaches is now becoming a routine activity for early field-scale evaluations to support management and production practices. The use of ML is tied to the application of computational algorithms designed to mimic human intelligence through learning from its surroundings (El Naqa et al., 2015; Susmita, 2019). Therefore, in understanding remote sensing data, several applications of ML have been adapted, including support vector machine (SVM), random forest (RF), K-means, and principal component analysis (Mahesh, 2020) among other hosts of algorithms to perform functions such as pattern recognition and classification (El Naqa et al., 2015). Unmanned aerial vehicles (UAVs) and hyperspectral platforms are used to acquire imagery and spectral readings (Stagakis et al., 2012), which leads to several outcomes including the computation of VIs. Vegetative indices (VIs) are important methods used to extract information from remotely sensed data. These are derived from ratios or normalized differences between two or three wavebands (Hunt et al., 2013; Tilly et al.,

2015). Thus, VIs have been adapted to monitor phenology and determine other growth parameters such as leaf area, stem branches, nitrogen content, and plant height among other parameters of the plant (Forsström et al., 2019). Recent developments in the monitoring of phenology using remote sensing have employed the use of vegetative indices (VIs) to determine, monitor, and estimate growth parameters (Hussain et al., 2020; Zhang et al., 2020). VIs, most commonly, the normalized difference vegetative index (NDVI), have been used in several studies to monitor plant growth and development in several crops with significant outcomes. A study conducted by Li et al., (2020), indicated a high correlation (R) between several VIs and above-ground biomass and yield in potato crops. Several studies have also demonstrated the possibility of using VIs to monitor plant growth and development in many crops including sunflower (Vega et al., 2015), rice (Liu et al., 2018; Zhou et al., 2017), rapeseed (Hussain et al., 2020; Zhang et al., 2020), wheat (Hassan et al., 2019), and cotton (Souza et al., 2017). Other studies on blueberries have adopted the use of the spectroradiometer, where either individual wavelength regions (Maqbool et al., 2010) or computed VIs (Forsström et al., 2019) were used to monitor or estimate growth parameters in the field. In addition, other VIs including, maximum chlorophyll index (MCI), green index (GI), green leaf index (GLI), visible atmospheric red index (VARI), and normalized difference red edge index (NDRE), have all been used to monitor growth and development in some crops (Anku et al., 2023). Outcomes from these studies, using their correlation and coefficient of determination values have demonstrated accuracy in monitoring and estimating growth and development parameters in the field. Furthermore, since the significance of the plants is derived from their yield, efforts are channeled into increasing their production. However, the phenological stages of the plant contribute significantly to processes increasing yield. Over the past 6 years, remote sensing activities on wild blueberry fields have received attention for management and production

practices in increasing plant yield. However, remote sensing technology in phenology monitoring is yet to be adopted in the wild blueberry fields.

Considering the relevance and utilization of these precision agricultural techniques as described in literature on crop production, there could be the potential of applying these remote sensing approaches in monitoring plant growth and development in wild blueberry fields. Given this, the study was conducted using the multispectral sensor and the hand-held hyperspectral radiometer to (i) determine the potential of using machine learning approaches to predict plant height, floral and vegetative buds, LAI, and harvestable yield, and (ii) to determine the best phenological stage where predictions can be made.

4.3 MATERIALS AND METHODS

4.3.1. Study area

Five trials were set up for this experiment across four growing seasons (2019, 2020, 2021, and 2022) in four commercial fields located at Farmington, Lemmon Hill, Kemptown, and Benvie Hill, NS. These trials were all conducted during the production cropping phase with substantial variability among vegetation.

The two study areas, Lemmon Hill, and Kemptown were adopted as trial sites in the 2020 growing season. These sites are among the main blueberry production sites located in Colchester County, Canada, with the geographic coordinates: 45.188587°N, 62.874343°W for Lemmon Hill, and 45.498936°N, 63.100716°W for Kemptown. These areas can be prone to wet conditions that can be encountered for an extended period. This condition increases the devasting effects of Monilinia and Botrytis blight disease on the field which affects yield (Percival & Beaton, 2012).

In the 2021 and 2022 growing season, these trials were set up in Benvie Hill and Kemptown with the geographic coordinates, 45.156832°N, 63.013834°W and 45.500938°N, 63.107150°W respectively. These trials were conducted following the same experimental treatments and designs as the 2020 trials.

4.3.2 Experimental design

The experimental design for these trials was a randomized complete block design (RCBD) with six replications, four treatments, and a plot size of 6 × 8 m with 2-m buffers between plots. At each corner, a 0.5 x 0.5 m white marker card was placed outside the stake and georeferenced with an SX Blue Platinum GPS device. Treatments consisted of 1) MB control and BB control 2) MB but no BB control, 3) no MB control but BB control, and 4) untreated control (i.e., no Monilinia or Botrytis blight prevention treatments). In addition, clusters of phenotypes were also identified and their phenological growth and development stages were carefully monitored.

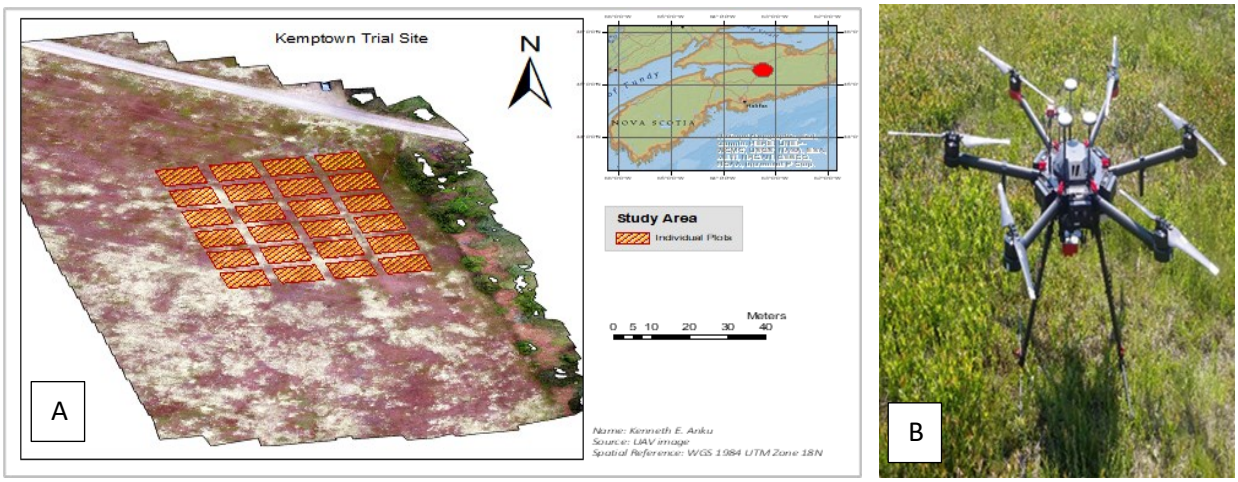

Figure 4.1. (A) Kemptown Trial Site showing individual plots at the study area, and (B) The DJI Matrice Pro 600 UAV equipped with a 5-banded mica sense camera.

4.3.3 Fungicide application

The first fungicide application of Proline® against Monilinia was done at the F2 – F3 stage while Lunar tranquility (Botrytis control) was applied at the F5 – F6 stage (10% bloom) before visual symptoms of the two diseases. The second fungicide application was between 7 to 10 days after the first application. Fungicides were applied using a Bell spray Inc. hand-held carbon dioxide propelled research sprayer equipped with a 2 m boom with 4 Tee Jet Visiflow 8002VS nozzles at 32 PSI (220 kPa) (Percival & Beaton, 2012). Treatment applications were carried out following label directions. These consist of Proline® [prothioconazole – 315 ml/ha (0.15 kg a.i./ha)] for MB and Luna Tranquility® (fluopyram and pyrimethanil – 600 g/ha at 1.2 L/ha) for BB control. Disease management is a constant practice in the field, therefore the experimental design was not intended to study the effects of fungal control products on MB and BB, but rather to stimulate variation for analysis.

4.3.4 Data acquisition

4.3.4.1 Field data collection on growth parameters

Fifteen (15) stems per plot were randomly collected using a line transect at the same time aerial imagery was acquired. These collections were conducted from the F0/F1 stage until the F8 stage (fruit set; Table 4.1). The stems were cut diagonally at 20 cm intervals along a 4 m line transect, cutting the stem as close to the base as possible (Percival & Beaton, 2012). Growth parameters taken from each plot included stem length, vegetative node, floral node, leaf area index (LAI; measured with an SS1 Sunscan Canopy Analysis System, Delta T Devices), and harvestable yield. Harvestable yield was collected with a forty-tine commercial wild blueberry hand rake from six randomly selected 1 m^2 quadrats in each plot (Percival & Beaton, 2012).

4.3.4.2 Multispectral platform and aerial image acquisition

Over the 4 years, the same UAV systems along with the same sensors, Zenmuse X5 and Micasense MX, were used as described in Section 3.3.5 of Chapter 3.

At a 30 m altitude, imagery was acquired within an interval of 12 to 16 days, depending on weather conditions for a total of 5 flights (Table 4.1). Image collection was conducted between 10 am to 2 pm under clear conditions to minimize the effects of clouds, wind, and rain. Calibration and adjustments were carried out to minimize the effects of distortion on the quality of imagery obtained.

Table 4.1. Flight details conducted in 2020, 2021, and 2022 at Lemmon Hill and Kemptown, Benvie Hill, and Kemptown, respectively, at the different Phenological stages.

Flight date	Plant stage	Sensor type	Flight height (m)	Spatial Resolution (px/cm)
Year 2020				
20th May 2020	F1 (Bud break)	Multispectral	30	2.2
2nd June 2020	F2/F3 (Tight cluster)	Multispectral	30	2.2
10th June 2020	F4/F5 (Early/late bud)	Multispectral	30	2.2
18th June 2020	F6/F7 (Bloom)	Multispectral	30	2.2
26th June 2020	F8 (Fruit set)	Multispectral	30	2.2
Year 2021				
21st May 2021	F1 (Bud break)	RGB	30	0.7
7th June 2021	F2/F3 (Tight cluster)	Multispectral	30	2.2
21st June 2021	F4/F5 (Early/late bud)	RGB	30	0.7
7th July 2021	F6/F7 (Bloom)	RGB	30	0.7

Year 2022				
5th May 2022	F1 (Bud break)	Multispectral	30	2.3
19th May 2022	F2/F3 (Tight cluster)	Multispectral	30	2.5
26th May 2022	F4/F5 (Early/late bud)	Multispectral	30	2.6
2nd June 2022	F6/F7 (Bloom)	Multispectral	30	2.3
22nd June 2022	F8 (Fruit set)	Multispectral	30	2.5

4.3.4.3 Post-processing and extraction of vegetation indices

Imagery acquired from the multispectral camera was carried through different processing stages (Figure 4.2) but followed the same description under Section 3.3.5.1 of Chapter 3.

4.3.5 Data acquisition from hyperspectral platform

A FieldSpec®3 hand-held hyperspectral radiometer (Analytical Spectral Devices, ASD, Inc. Boulder CO) was used to complement and verify data obtained from the UAV system, by collecting accurate and high-resolution spectral signatures of blueberry tissue. The device measures between 350 to 2500 nm in a 1 nm interval, producing 2,151 individual wavebands. The instrument was calibrated by taking both dark and white measurements from the spectralon (BaSO4). The final reflectance obtained was determined by a ratio of the data sample compared to the standard data from the white measurements. Therefore, the data represents an average of 50 reflectance spectra. The 10° field-of-view optical lens was held at nadir, at a height of 65 cm above the plant canopy. This reflectance measurement produced a diameter of 11.4 cm circular field of view, large enough

to cover a cluster of plants and reduce the effect of background (soil). All measurements were conducted at the same time when aerial imagery was collected.

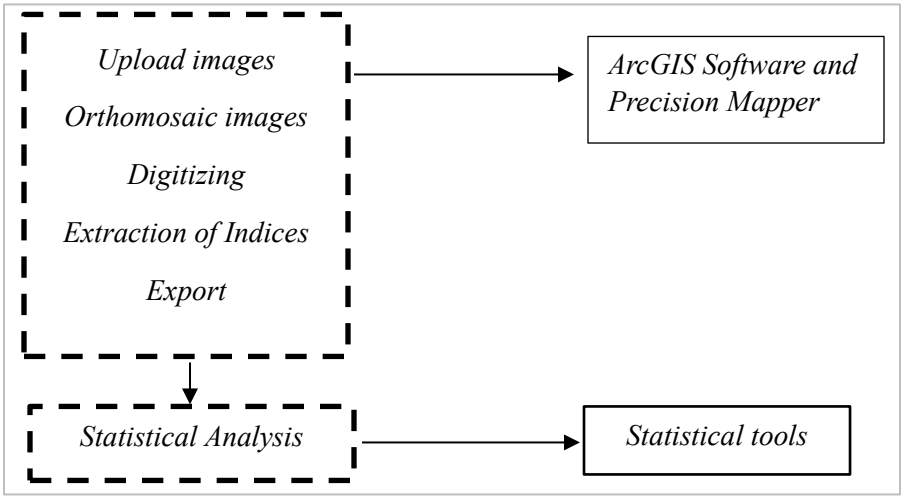

Figure 4.2. General overview of the workflow for the postprocessing of aerial images

4.3.5.1 Spectral reflectance measurement

Accurate and high-resolution spectral signatures of blueberry tissues were taken at different phenological stages using the ASD spectroradiometer. Ten spectral readings were randomly taken and averaged into a single spectrum for each plot. Therefore, to reduce bias, random sampling points were generated across each plot, where spectral readings were sampled. In total, 360 spectral readings were taken and averaged into 24 single spectrums. VIs were computed from every spectrum for analysis. The focus was given to differences observed in the visible light (400 – 690 nm) and near-infrared (700 – 1050 nm) regions as these regions are focused points for agricultural applications.

4.3.6 Vegetative indices

The computation of vegetative indices uses wavebands from the electromagnetic spectrum, thus instead of using the whole wavelength region, sections of the spectrum are considered relevant for agricultural purposes (Mahlein et al., 2013). Whereas several VIs can be obtained from the hyperspectral sensor, the multispectral sensor is limited to VIs which fall within the blue, green, red, red-edge, and near-infrared bands. Several indices have been computed from different sensors and these may range into 100's of vegetative indices (Tilly et al., 2015; Xue & Su, 2017b).

VIs used in this study were: the normalized difference vegetative index (NDVI), enhanced normalized difference vegetative index (ENDVI), normalized difference red edge (NDRE), green leaf index (GLI), green, red vegetative index (GRVI), and visible atmospheric reflectance index (VARI) (Table 3.1, chapter 3). All these can be used to monitor vegetation, and their effects play specific roles in enhancing the biophysical, biochemical, and environmental traits in its computation. Three of these VIs, NDVI, ENDVI, and NDRE, use the near-infrared (NIR) band with the other three restricted to the visible light region (VIS). Vegetative indices used in this study are the same as those represented **in Chapter 3, Table 3.1**.

4.3.7 Statistical analysis

Correlation and regression analysis were used to establish the relationship between VIs and the different growth parameters. The correlation method focused on establishing the strength of the relationship between the two quantitative (dependent and independent) variables. The regression method then described the relationship between the variables (Liang & Zeger, 1993; Ranganathan et al., 2019). Therefore, machine learning, using a supervised regression approach was utilized. The supervised machine learning regression method allowed the system to model the relationship

between the response and dependent variables after the machine had been trained. This gave the machine learning method a predictive ability. Despite the use of the coefficient of determination value (R^2), recent studies have also adopted Lin's concordance correlation coefficient (CCC) as a higher measure of accuracy and precision. CCC measures how far the linear relationship of the two variables deviates from the concordance line (Akoglu, 2018; Crawford et al., 2007; Kwiecien et al., 2011; Neuendorf, 2022). The correlation, regression analysis, and Lin's concordance correlation coefficient (CCC) analysis were performed using R software version 4.2.0.

In addition, this study modified Yu et al., (2022) approach by conducting these analyses using five (5) machine learning classifiers; stepwise multilinear regression (SMLR), K-Nearest Neighbour (KNN), random forest (RF), support vector machine (SVM), and the Cubist method (CB) to identify which method constructs the best regression relationship. These classifiers were set up using a 10-fold cross-validation approach and were repeated five times. Furthermore, a variable importance chart was produced, and this determined the overall impact of each VI, thus the most significant VI would have the most predictive power. A distinction between which VI group (VIS and NIR vegetation indices) had the most predictive power was determined by sampling the first 3 highest VIs of all regression analyses performed.

4.4 RESULTS

4.4.1 Assessment of UAV platform for data accuracy

Correlation coefficients (R), and coefficient of determination (R^2) values were used to evaluate the data accuracy from the UAV multispectral platform as assessed using the ground truthing data (Hassan et al., 2019). Significantly high R and R^2 values were observed between VIs from both the UAV and the ground truth data, with NDVI (Tight cluster) giving the highest correlation. From

the two measuring platforms, all VIs correlated positively with a range from 0.447 to 0.830. R^2 values ranged from 0.20 to 0.69 (Table 4.2). Therefore, the UAV platform was scrutinized as a high-accuracy platform for collecting data on vegetative indices. The NIR vegetative indices gave higher values compared to the VIS vegetative indices. Whereas there were some inconsistencies between the phenological stages, data measurement between the two instruments was consistent at the different phenological stages.

Table 4.2. Four selected correlative analyses between the ground and multispectral sensor

VIs	**Bud break**	**Tight cluster**	**Bloom**	**Fruit set**
	R/R²	**R/R²**	**R/R²**	**R/R²**
NDVI	0.781/0.61	0.906/0.82	0.735/0.54	0.790/0.62
NDRE	0.830/0.69	0.826/0.68	0.716/0.51	0.783/0.61
GLI	0.447/0.20	0.576/0.33	0.595/0.35	0.634/0.40
GRVI	0.560/0.31	0.784/0.62	0.603/0.36	0.650/0.42

Some indices showed stronger correlation values when compared to others in all phenological stages. Comparative analysis showed that the NDVI vegetative index gave the strongest correlation index between the spectroradiometer and Multispectral sensor. The NIR-VIs showed stronger relationships between the two sensors as compared to VIS vegetative indices. Though the other two vegetative indices were significantly different ($p < 0.05$), they varied in their correlation strength at all phenological stages. These results have shown that though these VIs can

be used to establish relationships, VI information from either of the two sensors can be used in predictions.

4.4.2 Correlations between VIs and growth parameters

Correlation analysis between VIs and growth parameters for the 2020 field season showed moderately high significant values (Figure 4.3). However, these values were inconsistent among the different parameters and phenological stages using the two instruments. Generally, results from the 3 seasons have indicated that VIs can be used to determine and potentially make predictions on different plant growth parameters in the wild blueberry fields.

Among the different phenological stages, correlation values were generally low at the bud break (F1) and the fruit set stages (F8) (Figure 4.3, A and E). However, LAI and vegetative bud numbers (VN) gave high correlation values using the NIR indices. At the tight cluster stage, high correlations were observed between VIs, plant height (PH), and LAI (Figure 4.3B). Whereas the NIR-VIs showed a high correlation with yield, VIS indices showed a good correlation with VS (Figure 4.3B). The tight cluster stage showed high correlation values between PH, floral bud stage (FS), vegetative bud stage (VS), yield and VIs (Figure 4.3C). Among these values, ENDVI was inconsistent with FS, VS, and yield. The bloom stage was characterized with high correlation values occurring at PH, FS, VN, and LAI (Figure 3C). LAI observed very high values across the different index types, with PH and VN correlating with VIS indices while FS correlated with the NIR indices. NDVI showed a high correlation with yield and VN (Figure 4.3D). The fruit set stage was characterized with the lowest correlation among the different phenological stages. Only ENDVI showed a high correlation with yield (Figure 4.3E). Generally, the tight cluster, early/late bud, and fruit set stages observed significant correlation values ($r > 0.40$) between growth

parameters and VIs. GLI, GRVI, and VARI were consistent in generating moderately high r values for the tight cluster, early/late bud, and flowering stages, whereas NDVI, ENDVI, and NDRE were consistent among some parameters at the tight cluster, and early/late bud stages. This trend points to the relevance of some visible light generated VIs which performed slightly better in some parameters as compared to the near-infrared VIs.

Similar results were observed using the hyperspectral device (Figure 4.4). At the bud break stage, r values were low (< 0.20) among several combinations (Figure 4.4A). The highest magnitude r value was a negative correlation between yield and GLI (-0.31). VIs combined with growth parameters generated a range of r values (-0.09 to 0.47) which were moderate, with PH and yield observing the highest values. At the tight cluster stage, the performance of the three VIS vegetative indices were significant; moderately high r values were observed between VIs, PH, FS, VS, and yield (Figure 4.4C). The bloom stage was characterized by high r values across several combinations. LAI gave very high r values (0.52 – 0.72), but particularly in combination with NDVI. PH and yield performed better across all VIs showing similar values which ranged from 0.11 to 0.44. VIs at this stage correlated

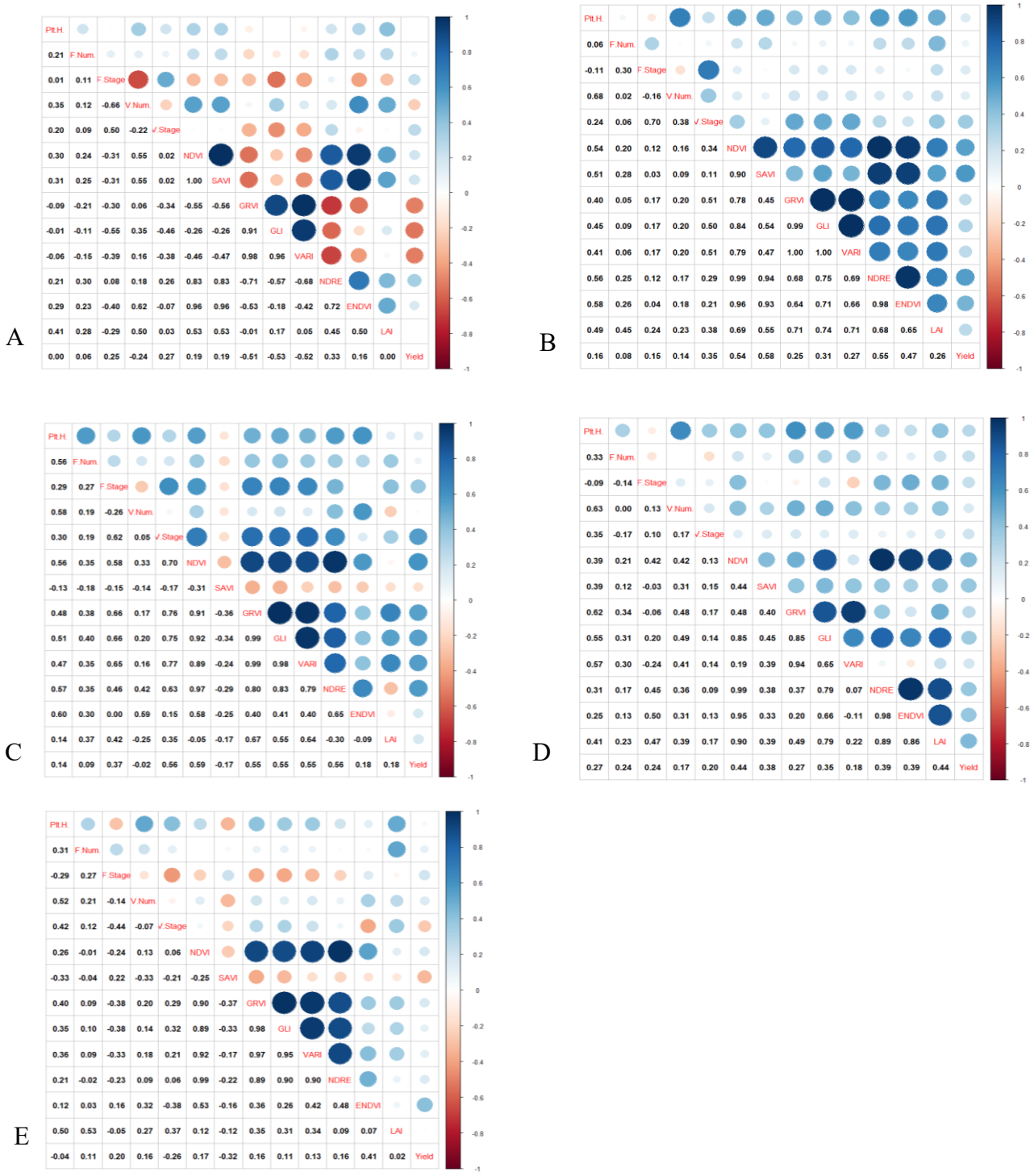

Figure 4.3. Correlation coefficients between growth parameters and VIs from Lemmon Hill and Kemptown in the 2020 growing season using the multispectral sensor at the different phenological stages. A. F1 stage (Bud break), B. F2/F3 stage (Tight cluster), C. F4/F5 stage (Early/late bud), D. F6/F7 stage (Bloom), and E. F8 stage (Fruit set). Colour intensities indicate the degree of positive (blue) and negative (red) correlation values.

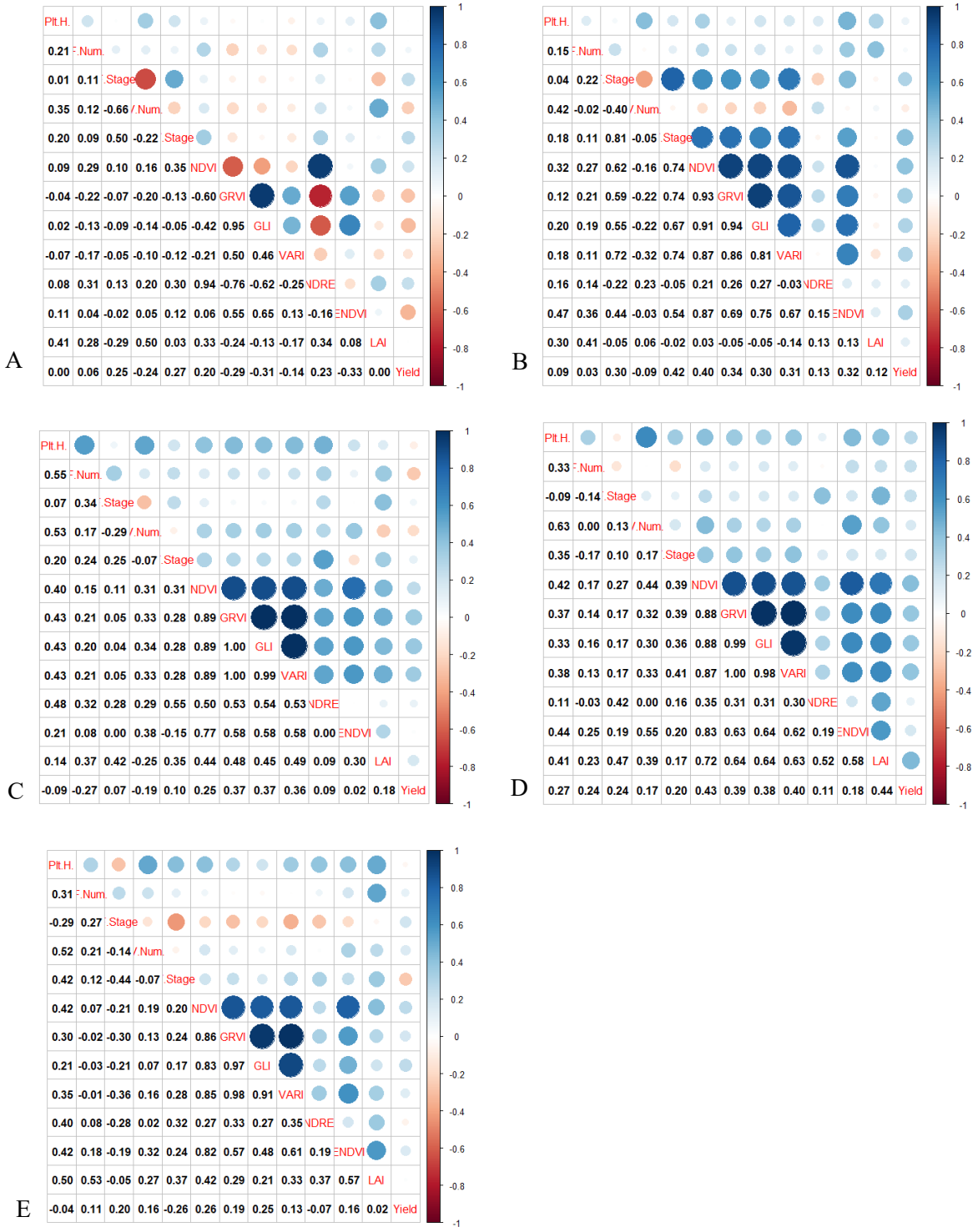

Figure 4.4. Correlation coefficients between growth parameters and VIs from Lemmon Hill and Kemptown in the 2020 growing season using the hyperspectral sensor at the different phenological stages. A. F1 stage (Bud break), B. F2/F3 stage (Tight cluster), C. F4/F5 stage (Early/late bud), D. F6/F7 stage (Bloom), and E. F8 stage (Fruit set). Colour intensities indicate the degree of positive (blue) and negative (red) correlation values.

better with growth parameters except for FN and FS (Figure 4.4D). PH also gave high r values (0.21 – 0.42) among the several VI combinations. The fruit set stage was characterized by values that were slightly above the F1 stage (Figure 4.4E).

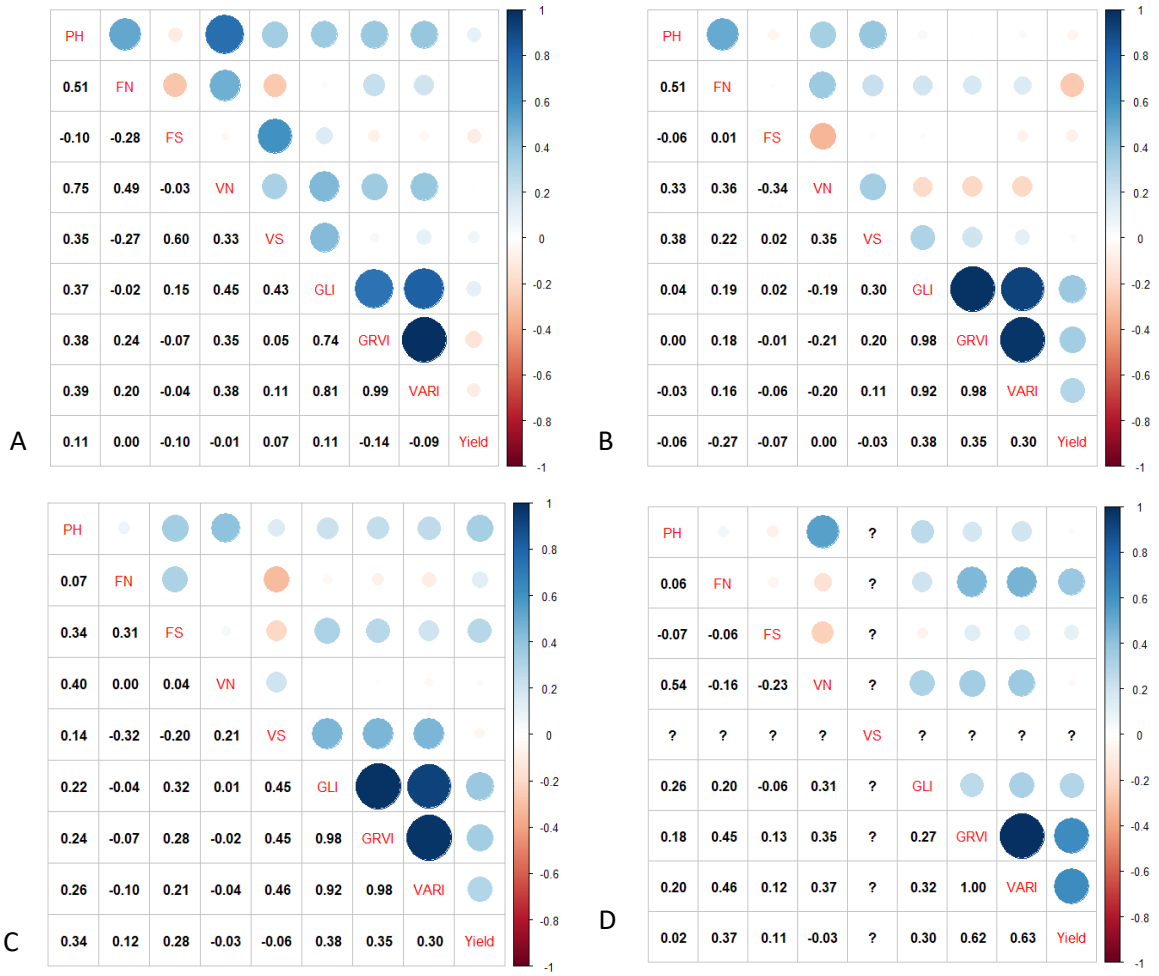

Figure 4.5. Correlation coefficients between growth parameters and VIs from Benvie Hill in the 2021 growing season using an RGB sensor at the different phenological stages. A. F1 stage (Bud break), B. F4/F5 stage (Early/late bud), C. F6/F7 stage (Bloom), and D. F8 stage (Fruit set). Colour intensities indicate the degree of positive (blue) and negative (red) correlation values.

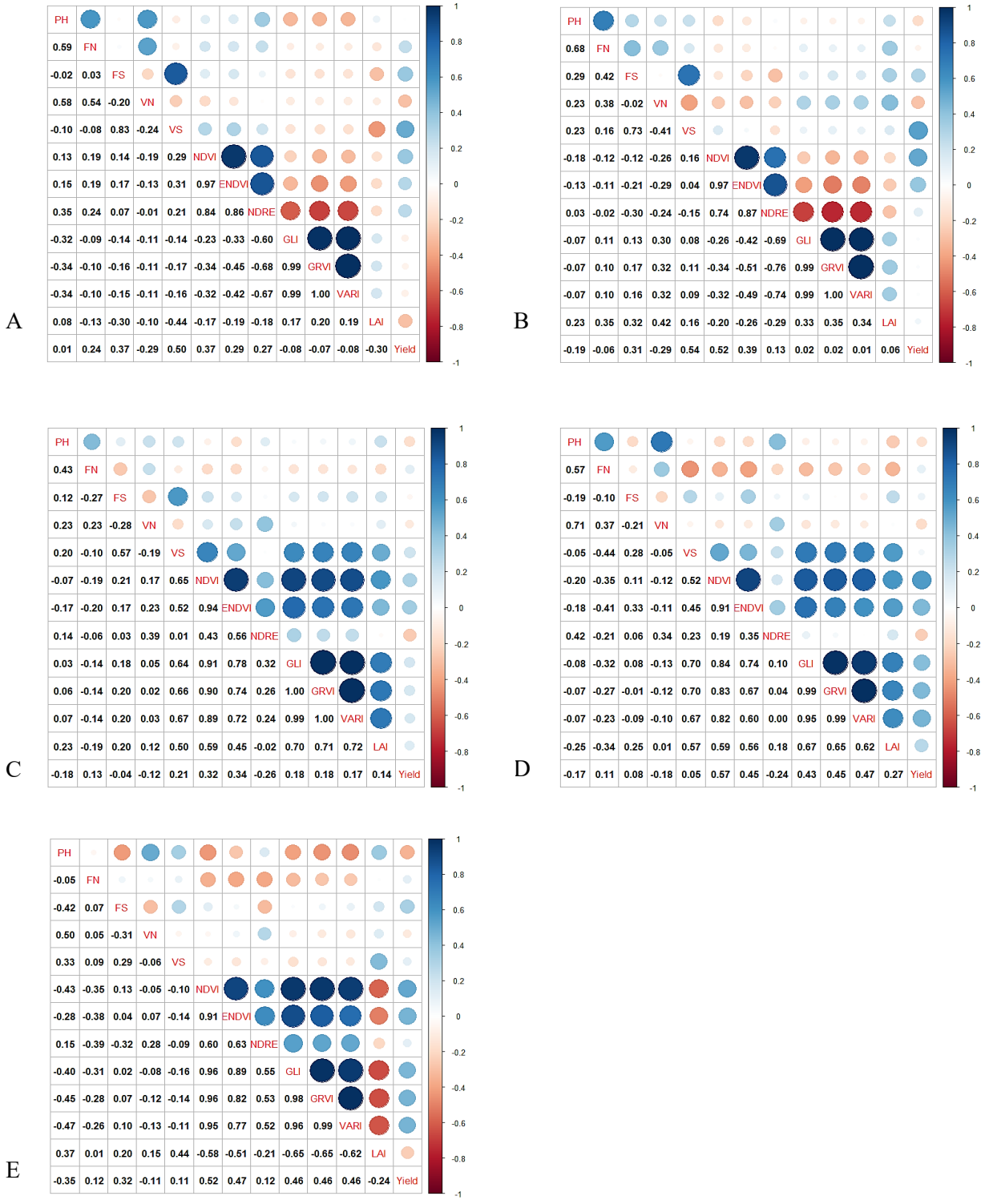

Figure 4.6. Correlation coefficients between growth parameters and VIs from Kemptown in the 2022 growing season using the multispectral sensor at the different phenological stages. A. F1 stage (Bud break), B. F2/F3 stage (Tight cluster), C. F4/F5 stage (Early/late bud), D. F6/F7 stage (Bloom), and E. F8 stage (Fruit set). Colour intensities indicate the degree of positive (blue) and negative (red) correlation values.

Correlations in the 2021 growing season between VIs and growth parameters were relatively low (Figure 4.5). The highest correlation values were observed at the tight cluster (F2/F3) and bloom (F6/F7) stages (Figure 4.5, A and C) with the other stages observing very low correlations. Generally, PH, and VN had high correlations with the various VIs at the tight cluster (F2/F3) stage with PH, VN, and VS also showing high correlations at the bloom (F6/F7) stage. Yield also had a good correlation with GLI, GRVI, and VARI at bloom (F6/F7) and fruit set (F8) stages (Figure 4.6).

Correlation analysis between VIs and growth parameters in the 2022 growing season were relatively high with some low correlations observed at some stages (Figure 4.6). Generally, LAI, and VS observed the highest correlation values at the early/late bud (F4/F5) and bloom (F6/F7) stages (Figure 4.6, C & D). The LAI and VS observed high correlation values of about 0.72 and 0.70 respectively. Despite PH showing moderately high correlation, these observations were limited to the bud break (F1) and fruit set (F8) stage, with FN being limited to the bloom (F6/F7) and fruit set (F8) stages. VIs and yield observed moderately high correlations at the bloom and fruit set stage.

4.4.3 Predicting growth parameters using the UAV platform

Variable importance enabled the determination of VIs that had the most predictive power. Therefore, variables with high importance value are drivers of the outcome, thus their value significantly affects the overall outcome (Figure 4.7). Therefore, Figure 4.7 indicates that NDVI was the dominant predictor driving the observed prediction. The 2020 data analysis revealed that the NIR -VIs contributed significantly to the outcome observed at the early/late bud and bloom stages with some predictions from the visible light vegetative indices. This observation was

consistent for all classifiers. For LAI under all phenological stages, predictions were made by NDVI, NDRE, and ENDVI. Predictions of FN and FS were made by GRVI, VARI, ENDVI, and NDRE. PH, VS, and VN were significantly predicted by VIs such as NDRE, NDVI, ENDVI, and GRVI under all phenological stages. Contributions from the individual VIs accounting for the outcomes were represented in detail (Table 4.3 - 4.6). Despite the contributions from the NIR-VIs, the VIS vegetative indices cannot be underestimated as they contributed significantly to major outcomes observed (Table 4.4 – 4.6; Appendix A5 – A7). In this document, the presentation for the different variable importance plots was considered for only four classifiers of the micasense 2020 and 2022 trials, with the best predictors selected (a minimum of 1 and a maximum of 3).

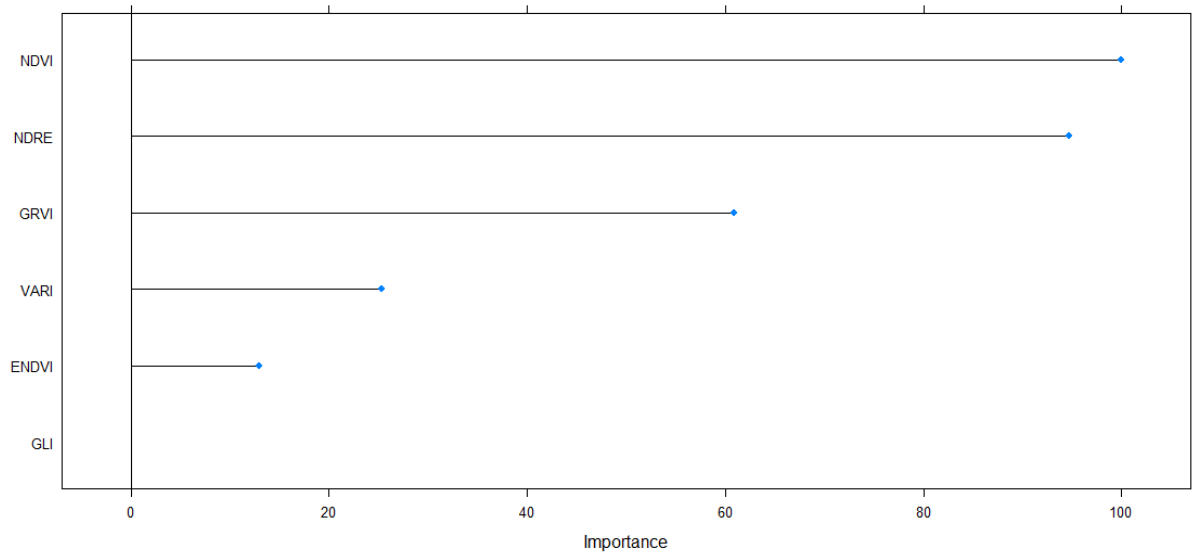

Figure 4.7. An example of a variable importance plot representing VI contributions

Among some parameters at the different phenological stages, significantly high R^2 and low RMSE values were observed (Tables 4.3, 4.7, 4.8, & 4.9). However, this observation was consistent only for LAI at all phenological stages, but FS and VS observed significantly high R^2

values only at the F4/F5 stage. Despite the relatively low values observed by LAI at the bud break, tight cluster, and early/late bud stages, LAI recorded the highest R^2 values at the bloom stage with an average of about 45 - 50% of RMSE (Table 4.3d). With the R^2, CCC, and RMSE as selective criteria, it was observed that LAI, FS, and VS stood with high chances for their estimation and prediction (Table 4.3a-e).

Compared with the multispectral sensor estimates (Table 4.3, a-e), the hand-held hyperspectral sensor (Table 4.7, a-e) produced similar outcomes. A range of R^2 values were observed between growth parameters and VIs. The LAI recorded the highest R^2 and CCC values of 0.72 and 0.70 respectively (Table 4.7d). While FS showed high estimation values at the tight cluster stage (F2/F3), VS also showed high values at both tight cluster and early/late bud stages across the different classifiers (Table 4.7, a-e).

Generally, the 2021 analyzed values obtained were low on both R^2 and CCC values, however, R^2 values were higher compared to CCC values. R^2 values ranged from below 0 to 0.60 while CCC values ranged from below 0 to 0.48 across the different parameters (Table 4.8, a - d).

The prediction of VS can best be achieved at the F2/F3 stage. Yield had very high R^2 and CCC values, however, the RMSE values were significantly high. However, it was difficult to establish the prediction stage for yield. Considering some potential in predicting the other growth parameters, it was observed that those values were relatively low. Despite the success of using the random forest (RF) classifier, it was observed that the SVM classifier was the best in achieving all the highest regression values obtained across the different parameters.

Generally, the results of the 2022 trial observed high R^2 values compared to the CCC values, which occurred across the different growth parameters and growth stages (Table 4.9, a - e).

Despite the complexities, the selection of classifiers and parameters were based on R^2, CCC, and RMSE values. There were low estimation values at the F1 stage across the different classifiers, however, some of these values increased along the growth phase of the plant.

The predictability of a parameter was dependent on the plant stage and the classifier used in the regression analysis. Therefore, among the several classifiers adopted, SVM and RF were considered best in the estimation of relationships and predictability of parameters. It was observed that SMLR, SVM, KNN, and sometimes RF generated the same variable importance plot, but consistently SVM and SMLR generated the same variable plot. Despite the several stages considered, the bloom stage (F6/F7) was best in the estimation of several parameters including LAI, floral bud stage, vegetative bud stage, and yield. Aside from the bloom stage, the early/late bud stages (F4/F5) can also be used in the estimation or prediction of these same parameters. Converse to the stated parameters, floral and vegetative bud numbers can be estimated at the bud break (F1) stage whereas plant height can be estimated at the fruit set (F8) stage.

The significant dependent variables upon which these growth parameters were selected were highlighted using the variable importance plot. Furthermore, the significance of a specific dependent variable varied from one plant stage to another, however, some VIs were consistent among the different stages. It was clear that NDVI contributes significantly to yield prediction, while NDVI, GRVI, and VARI contribute to LAI prediction. Aside from LAI and yield, the other dependent variables were not consistent in their estimation of the other parameters. The NIR indices contributed to the determination or prediction of PH, with GLI, ENDVI, and VARI contributing to the estimation of FN.

4.4.4 Assessment of phenological growth in wild blueberry plants

4.4.4.1 Assessment of phenological growth using vegetative indices (VIs)

The trend of VI measurements using the multispectral sensor as observed between the two locations and sensors looked similar but slightly different for the 2020 data. The multispectral measurements from the two locations showed that the NIR-VIs were separated from the VIS vegetative indices, except for NDRE (Figure 4.8). In both locations, NDVI and ENDVI obtained the highest VI values of a >100% and a 60.6% increase at harvest, respectively, when compared to the other indices across the different phenological stages. NDRE at Kemptown and Lemmon Hill observed a 67.9% and 51.7% increase in VI value at harvest, respectively. The VIS vegetative index from both locations progressed with an increase of over 100% in VI values for all three indices (GLI, GRVI, and VARI), with VARI being the highest. From both fields, VARI performed best among the three (3) VIS vegetative indices, followed by GLI and then GRVI at all phenological stages (Figure 4.8). Interestingly, VARI observed a continuous increase until an almost equal value with NDVI and ENDVI at the Kemptown field site. Though a similar effect of VARI was not seen at Lemmon Hill, it observed the highest increase compared to the other VIS indices. Generally, all VIs observed a varied level of decline in value at the bloom stage.

The trend of VIs using the FieldSpec® 3 radiometer in the 2020 trail was similar not only to the locations but also to the Micasense (Figure 4.9). Again, the NIR-VIs were seen above all the other VIs with NDVI (at the Kemptown location) maintaining the highest VI across all the phenological stages with an increased VI value of 83.7%. ENDVI and NDRE obtained an increase of >100% and 68.2% in VI value at the Kemptown location. The VIS vegetative index from both locations progressed with an increase of over 100% in VI values for all three indices (GLI, GRVI, and VARI). VARI obtained the highest VI value compared to the two VIS indices (Figure 4.9). The

observation at the Kemptown site was almost the same as that observed at the Lemmon Hill site (Figure 4.9). At the bloom stage for both fields, it can be observed that there were levels of inconsistencies as some VIs observed marginal decreases with others observing slight increases. In both fields, VARI, GLI, and GRVI observed an upward continuous growth throughout the different phenological stages (Figure 4.9). It can therefore be observed that NDVI and ENDVI were similar under UAV-VIs in both locations, but these two indices were greatly separated under the radiometric VIs. However, the progression of VIs across locations and sensors have been similar.

There was a great similarity between the VI trends observed between the 2020 and 2022 trials (Figures 4.9 & 4.10). However, to reduce the extent of complexity only Micasense vegetative indices were represented in these trends, thus only trends for the 2022 growing season were considered. The two apparent aspects consisted of the NIR-VIs (NDVI and ENDVI) were separated from the VIS-VIs (GLI, VARI, GRVI) while NDRE showed the same or similar trends in both years as it lurked between the two VI trends (NIR and VIS). Consistency in these trends from the different sites and years confirms the normal trend and characteristics of VIs across the growing season.

Table 4.3. Coefficient of determination (R^2) values, Lin's concordance value (CCC), and root mean square error (RMSE) values from 5 regression methods on growth parameters against VIs at the different phenological stages (a, b, c, d, & e) using the multispectral sensor for the 2020 trial. SMLR – Stepwise multilinear regression, KNN – K- nearest neighbour, RF – Random Forest, SVM – Support vector machine, and CB – Cubist. F – Floral stage

a.

	Break bud (F1)														
	SMLR			**KNN**			**RF**			**SVM**			**CB**		
Parameters	**R^2**	**CCC**	**RMSE**	**R^2**	**CCC**	**RMSE**	**R^2**	**CCC**	**RMSE**	**R^2**	**CCC**	**RMSE**	**R^2**	**CCC**	**RMSE**
Yield ($g.m^{-2}$)	0.35	0.40	225.85	0.36	0.38	223.83	0.21	0.31	249.73	0.31	0.39	240.11	0.39	0.43	223.86
LAI	0.42	0.41	0.11	0.33	0.32	0.12	0.27	0.32	0.12	0.31	0.41	0.11	0.35	0.41	0.11
Plant height (cm)	0.13	0.11	1.59	0.15	0.11	2.13	0.11	0.08	1.71	-	-	-	0.11	0.13	1.79
Floral bud no.	0.09	0.003	1.61	0.18	0.22	1.72	0.09	0.11	1.46	0.17	0.14	1.64	0.12	0.11	1.58
Floral bud stage	0.15	0.20	0.26	0.24	0.27	0.25	0.27	0.29	0.24	0.27	0.30	0.25	0.19	0.31	0.26
Veg. bud no.	0.48	0.56	3.17	0.48	0.51	3.32	0.51	0.53	3.14	0.57	0.62	2.77	0.63	0.66	2.75
Veg. bud stage	0.20	0.23	0.25	0.21	0.29	0.23	0.25	0.33	0.24	0.27	0.30	0.24	0.16	0.19	0.25

b.

	Tight cluster (F2/F3)														
	SMLR			KNN			RF			SVM			CB		
Parameters	**R^2**	**CCC**	**RMSE**	**R^2**	**CCC**	**RMSE**	**R^2**	**CCC**	**RMSE**	**R^2**	**CCC**	**RMSE**	**R^2**	**CCC**	**RMSE**
Yield ($g.m^{-2}$)	0.40	0.27	340.10	0.42	0.34	273.35	0.55	0.44	266.10	0.53	0.37	333.75	0.40	0.31	372.77
LAI	0.49	0.28	0.11	0.31	0.21	0.13	0.35	0.18	0.13	0.48	0.38	0.11	0.43	0.33	0.12
Plant height (cm)	0.33	0.18	2.12	0.37	0.31	1.94	0.28	0.24	1.90	0.45	0.19	1.85	0.36	0.19	1.86
Floral bud no.	-	-0.011	1.45	0.20	0.12	1.98	0.47	0.27	1.34	0.21	0.21	1.63	0.19	0.08	1.36
Floral bud stage	0.25	-0.03	0.69	-	0	0.53	0.19	-0.17	0.67	0.16	0.08	0.91	-	-0.06	0.56
Veg. bud no.	-	-0.18	3.08	0.38	0.23	2.59	0.34	0.06	2.64	0.40	0.32	2.37	0.38	0.29	2.23
Veg. bud stage	0.58	0.28	0.81	0.39	0.08	0.89	0.35	0.26	0.86	0.52	0.23	0.80	0.40	0.13	0.91

c.

	Early/late (F4/F5)														
	SMLR			KNN			RF			SVM			CB		
Parameters	**R^2**	**CCC**	**RMSE**	**R^2**	**CCC**	**RMSE**	**R^2**	**CCC**	**RMSE**	**R^2**	**CCC**	**RMSE**	**R^2**	**CCC**	**RMSE**
Yield ($g.m^{-2}$)	0.26	0.38	230.12	0.39	0.39	224.70	0.28	0.37	240.80	0.35	0.41	224.27	0.38	0.42	221.05
LAI	0.49	0.28	0.11	0.31	0.21	0.14	0.35	0.18	0.13	0.48	0.38	0.11	0.43	0.33	0.12
Plant height (cm)	0.38	0.44	1.88	0.25	0.31	1.99	0.31	0.40	1.94	0.46	0.52	1.76	0.34	0.41	1.99
Floral bud no.	0.12	0.21	1.50	0.11	0.11	1.59	0.19	0.13	1.55	0.16	0.22	1.48	0.15	0.16	1.57
Floral bud stage	0.57	0.61	0.52	0.66	0.68	0.47	0.66	0.67	0.46	0.67	0.67	0.47	0.59	0.63	0.49
Veg. bud no.	-	-0.18	3.08	0.38	0.23	2.59	0.34	0.06	2.64	0.40	0.32	2.37	0.38	0.29	2.23
Veg. bud stage	0.62	0.64	0.32	0.66	0.61	0.32	0.56	0.61	0.33	0.68	0.66	0.29	0.58	0.62	0.31

d.

	Bloom (F6/F7)														
	SMLR			KNN			RF			SVM			CB		
Parameters	**R^2**	**CCC**	**RMSE**	**R^2**	**CCC**	**RMSE**	**R^2**	**CCC**	**RMSE**	**R^2**	**CCC**	**RMSE**	**R^2**	**CCC**	**RMSE**
Yield ($g.m^{-2}$)	0.33	0.39	232.24	0.28	0.30	254.21	0.33	0.38	232.13	0.34	0.45	224.38	0.15	0.22	264.94
LAI	0.83	0.80	0.56	0.86	0.81	0.56	0.84	0.81	0.54	0.90	0.84	0.46	0.85	0.81	0.55
Plant height (cm)	0.41	0.48	1.45	0.52	0.58	1.41	0.50	0.54	1.37	0.51	0.55	1.32	0.47	0.54	1.38
Floral bud no.	0.10	0.08	1.08	0.11	0.07	1.03	0.07	-0.01	1.17	0.12	0.05	1.08	0.06	0.03	1.13
Floral bud stage	0.24	0.34	0.14	0.35	0.41	0.12	0.37	0.37	0.13	0.34	0.39	0.12	0.26	0.38	0.13
Veg. bud no.	0.33	0.32	1.54	0.32	0.36	1.43	0.23	0.27	1.53	0.22	0.28	1.66	0.26	0.30	1.56
Veg. bud stage	0.22	0.30	0.21	0.17	0.26	0.28	0.27	0.30	0.22	0.19	0.32	0.33	0.20	0.25	0.25

e.

	Fruit set (F8)														
	SMLR			KNN			RF			SVM			CB		
Parameters	**R^2**	**CCC**	**RMSE**	**R^2**	**CCC**	**RMSE**	**R^2**	**CCC**	**RMSE**	**R^2**	**CCC**	**RMSE**	**R^2**	**CCC**	**RMSE**
Yield ($g.m^{-2}$)	0.15	0.21	265.70	0.17	0.29	304.26	0.17	0.23	249.36	0.26	0.35	235.18	0.20	0.23	265.63
LAI	0.34	0.43	0.90	0.38	0.47	0.83	0.43	0.46	0.87	0.43	0.44	0.87	0.41	0.47	0.89
Plant height (cm)	0.19	0.24	2.05	0.14	0.16	2.00	0.14	0.15	2.14	0.15	0.23	2.88	0.18	0.16	2.19
Floral bud no.	0.16	0.06	1.05	0.09	0.11	1.00	0.13	0.00	1.08	0.11	0.19	1.11	0.17	0.19	1.05
Floral bud stage	0.16	0.24	-	0.19	0.23	-	0.26	0.34	-	0.30	0.28	-	0.29	0.28	-
Veg. bud no.	0.12	0.17	2.07	0.16	0.21	2.05	0.11	0.14	2.15	0.17	0.25	1.97	0.20	0.26	2.02
Veg. bud stage	0.15	0.21	0.17	0.17	0.29	0.20	0.17	0.23	0.17	0.26	0.35	0.17	0.20	0.23	0.18

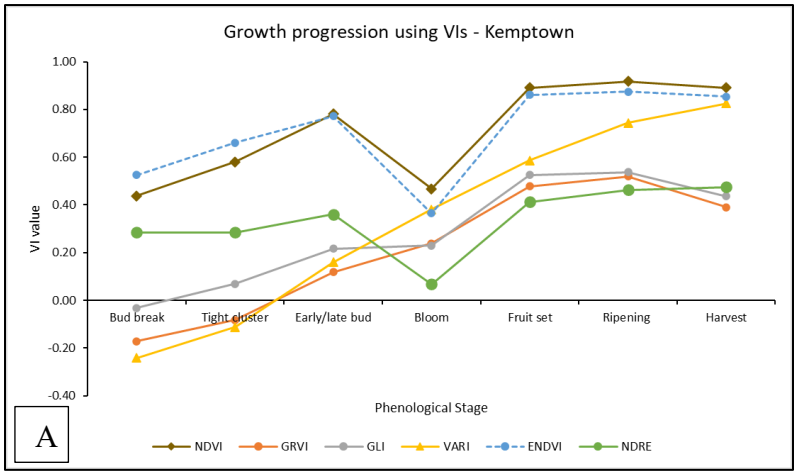

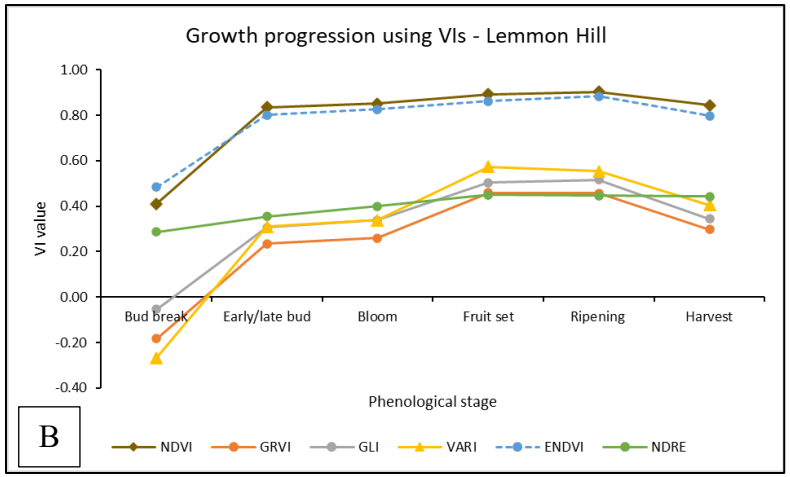

Figure 4.8. Growth progression of VIs observed in both fields at the different phenological stages using the multispectral sensor. (A) Kemptown and (B) Lemmon Hill.

Table 4.4. Rankings on an SVM classifier for the 2020 multispectral trial of best-performing indices for each phenological stage and parameter. Performance was evaluated using outputs from the variable importance chart. Percentages represent the performance of the individual vegetative indices in achieving that outcome. Indices have been arranged in order of the best index to the least performing index along with its corresponding percentage.

Bud break stage (F1)		
Parameter	**Rank**	**Percentage (%)**
Yield (g.m^{-2})	GLI, VARI, GRVI, NDRE, NDVI, ENDVI	100, 75,60, 25, 10, 0
Leaf area index	NDRE, NDVI, ENDVI, GLI, GRVI, VARI	100, 90, 80, 10, 5, 0
Plant height (cm)	NDRE, NDVI, ENDVI, GRVI, VARI, GLI	100, 95, 75, 68, 28, 0
Floral bud number	NDRE, NDVI, ENDVI, GRVI, VARI, GLI	100, 75, 70, 45, 15, 0
Floral bud stage	GLI, VARI, GRVI, NDRE, ENDVI, NDVI	100, 90, 88, 82, 30, 0
Vegetative bud number	ENDVI, NDVI, NDRE, VARI, GRVI, GLI	100, 70, 18, 3, 2, 0
Vegetative bud stage	GLI, VARI, GRVI, NDRE, ENDVI, NDVI	100, 88, 82, 30, 5, 0
Tight cluster stage (F2/F3)		
Parameter	**Rank**	**Percentage (%)**
Yield (g.m^{-2})	GRVI, NDRE, NDVI, VARI, ENDVI, GLI	100, 80,75, 70, 45, 0
Leaf area index	GRVI, VARI, GLI, ENDVI, NDRE, NDVI	100, 70, 45, 20, 14, 0
Plant height (cm)	NDRE, NDVI, ENDVI, VARI, GLI, GRVI	100, 95, 80, 5, 5, 0
Floral bud number	GRVI, VARI, NDRE, GLI, NDVI, ENDVI	100, 85, 30, 15, 10, 0
Floral bud stage	GLI, GRVI, VARI, ENDVI, NDRE, NDVI	100, 90, 78, 45, 23, 0
Vegetative bud number	ENDVI, NDRE, NDVI, GLI, VARI, GRVI	100, 68, 50, 48, 12, 0
Vegetative bud stage	GLI, VARI, GRVI, ENDVI, NDVI, NDRE	100, 92, 83, 24, 18, 0
Early/late bud stage (F4/F5)		
Parameter	**Rank**	**Percentage (%)**
Yield (g.m^{-2})	VARI, GRVI, GLI, NDVI, NDRE, ENDVI	100, 100,100, 90, 70, 0
Leaf area index	GRVI, VARI, GLI, ENDVI, NDRE, NDVI	100, 70, 45, 20, 15, 0
Plant height (cm)	ENDVI, NDVI, NDRE, GLI, GRVI, VARI	100, 78, 50, 40, 30, 0
Floral bud number	GLI, GRVI, ENDVI, NDVI, NDRE, VARI	100, 65, 55, 45, 18, 0
Floral bud stage	GRVI, VARI, GLI, NDVI, NDRE, ENDVI	100, 95, 93, 65, 45, 0
Vegetative bud number	ENDVI, NDRE, GRVI, DNVI, GLI, VARI	100, 63, 23, 22, 12, 0
Vegetative bud stage	VARI, GRVI, GLI, NDVI, NDRE, ENDVI	100, 100, 98, 80, 72, 0
Bloom stage (F6/F7)		
Parameter	**Rank**	**Percentage (%)**
Yield (g.m^{-2})	GLI, ENDVI, NDVI, GRVI, NDRE, VARI	100, 95,80, 80, 50, 0
Leaf area index	NDRE, NDVI, ENDVI, GLI, GRVI, VARI	100, 100, 90, 80, 25, 0
Plant height (cm)	GRVI, NDRE, NDVI, VARI, GLI, ENDVI	100, 85, 30, 25, 12, 0
Floral bud number	NDRE, GRVI, NDVI, GLI, VARI, ENDVI	100, 98, 82, 70, 50, 0
Floral bud stage	ENDVI, NDRE, NDVI, GLI, GRVI, VARI	100, 95, 82, 58, 25, 0
Vegetative bud number	GLI, GRVI, NDRE, NDVI, ENDVI, VARI	100, 82, 68, 50, 32, 0

Vegetative bud stage	ENDVI, GLI, GRVI, VARI, NDRE, NDVI	100, 78, 55, 38, 15, 0
	Fruit set stage (F8)	
Parameter	**Rank**	**Percentage (%)**
Yield (g.m^{-2})	ENDVI, NDRE, NDVI, GRVI, GLI, VARI	100, 90,80, 75, 50, 0
Leaf area index	GRVI, VARI, GLI, NDVI, ENDVI, NDRE	100, 95, 92, 35, 23, 0
Plant height (cm)	GRVI, VARI, GLI, ENDVI, NDRE, NDVI	100, 85, 80, 8, 4, 0
Floral bud number	NDVI, GLI, NDRE, VARI, GRVI, ENDVI	100, 75, 70, 50, 15, 0
Floral bud stage	NDRE, GRVI, VARI, NDVI, ENDVI, GLI	100, 58, 50, 40, 7, 0
Vegetative bud number	GRVI, VARI, GLI, ENDVI, NDVI, NDRE	100, 90, 88, 70, 25, 0
Vegetative bud stage	GLI, ENDVI, GRVI, NDVI, VARI, NDRE	100, 95, 45, 35, 11, 0

Table 4.5. Rankings of an RF classifier on the 2020 multispectral trial of best-performing indices for each phenological stage and parameter. Performance was evaluated using outputs from the variable importance chart. Percentages represent the performance of the individual vegetative indices in achieving that outcome. Indices have been arranged in order of the best index to the least performing index along with its corresponding percentage.

	Bud break stage (F1)	
Parameter	**Rank**	**Percentage (%)**
Yield (g.m^{-2})	GLI, VARI, ENDVI, NDVI, NDRE, GRVI	100, 55, 18, 12, 5, 0
Leaf area index	NDVI, NDRE, ENDVI, VARI, GLI, GRVI	100, 82, 50, 10, 8, 0
Plant height (cm)	NDVI, ENDVI, VARI, NDRE, GRVI, GLI	100, 88, 58, 42, 35, 0
Floral bud number	NDRE, ENDVI, NDVI, GRVI, VARI, GLI	100, 92, 80, 45, 18, 0
Floral bud stage	GLI, ENDVI, VARI, GRVI, NDRE, NDVI	100, 40, 28, 18, 13, 0
Vegetative bud number	ENDVI, GLI, NDVI, NDRE, GRVI, VARI	100, 35, 28, 10, 1, 0
Vegetative bud stage	GLI, ENDVI, VARI, GRVI, NDRE, NDVI	100, 45, 35, 28, 12, 0
	Tight cluster stage (F2/F3)	
Parameter	**Rank**	**Percentage (%)**
Yield (g.m^{-2})	ENDVI, NDRE, NDVI, VARI, GRVI, GLI	100, 72, 65, 58, 20, 0
Leaf area index	NDRE, NDVI, GRVI, GLI, ENDVI, VARI	100, 35, 25, 20, 12, 0
Plant height (cm)	NDVI, NDRE, ENDVI, VARI, GRVI, GLI	100, 75, 62, 39, 38, 0
Floral bud number	VARI, GRVI, NDRE, ENDVI, GLI, NDVI	100, 90, 15, 10, 5, 0
Floral bud stage	NDRE, GLI, VARI, NDVI, GRVI, ENDVI	100, 39, 38, 29, 8, 0
Vegetative bud number	VARI, ENDVI, NDRE, NDVI, GLI, GRVI	100, 95, 60, 52, 28, 0
Vegetative bud stage	VARI, GLI, GRVI, NDRE, NDVI, ENDVI	100, 92, 85, 30, 8, 0
	Early/late bud stage (F4/F5)	
Parameter	**Rank**	**Percentage (%)**
Yield (g.m^{-2})	VARI, GRVI, GLI, NDVI, NDRE, ENDVI	100, 90, 78, 65, 40, 0
Leaf area index	NDRE, NDVI, GRVI, GLI, ENDVI, VARI	100, 35, 25, 20, 15, 0
Plant height (cm)	ENDVI, NDVI, NDRE, GLI, VARI, GRVI	100, 75, 27, 15, 13, 0
Floral bud number	GLI, ENDVI, VARI, GRVI, NDRE, NDVI	100, 78, 50, 48, 18, 0

Floral bud stage	GRVI, VARI, GLI, ENDVI, NDVI, NDRE	100, 78, 38, 15, 12, 0
Vegetative bud number	ENDVI, NDRE, VARI, NDVI, GLI, GRVI	100, 65, 20, 19, 18, 0
Vegetative bud stage	VARI, GRVI, GLI, NDRE, ENDVI, NDVI	100, 90, 38, 23, 5, 0
Bloom stage (F6/F7)		
Parameter	**Rank**	**Percentage (%)**
Yield (g.m^{-2})	ENDVI, NDVI, NDRE, VARI, GLI, GRVI	100, 45, 23, 10, 3, 0
Leaf area index	NDVI, NDRE, ENDVI, GLI, GRVI, VARI	100, 95, 63, 60, 10, 0
Plant height (cm)	VARI, GRVI, NDRE, NDVI, ENDVI, GLI	100, 60, 35, 22, 15, 0
Floral bud number	VARI, GRVI, GLI, ENDVI, NDVI, NDRE	100, 70, 67, 50, 25, 0
Floral bud stage	NDVI, NDRE, GRVI, ENDVI, VARI, GLI	100, 48, 38, 25, 20, 0
Vegetative bud number	NDRE, GLI, NDVI, GRVI, VARI, ENDVI	100, 72, 60, 50, 43, 0
Vegetative bud stage	ENDVI, GLI, VARI, GRVI, NDRE, NDVI	100, 74, 18, 15, 8, 0
Fruit set stage (F8)		
Parameter	**Rank**	**Percentage (%)**
Yield (g.m^{-2})	ENDVI, GRVI, GLI, NDRE, VARI, NDVI	100, 85, 30, 28, 25, 0
Leaf area index	VARI, GLI, GRVI, NDVI, NDRE, ENDVI	100, 95,80, 18, 10, 0
Plant height (cm)	GLI, VARI, GRVI, ENDVI, NDVI, NDRE	100, 48, 48, 22, 3, 0
Floral bud number	GLI, GRVI, VARI, ENDVI, NDVI, NDRE	100, 58, 45, 23, 22, 0
Floral bud stage	VARI, GLI, GRVI, ENDVI, NDRE, NDVI	100, 78, 65, 60, 40, 0
Vegetative bud number	GRVI, VARI, ENDVI, GLI, NDVI, NDRE	100, 95, 93, 83, 20, 0
Vegetative bud stage	GLI, ENDVI, VARI, NDRE, GRVI, NDVI	100, 75, 40, 27, 27, 0

Table 4.6. Rankings of an SMLR and KNN classifier on the 2020 multispectral trial of best-performing indices for each phenological stage and parameter. Performance was evaluated using outputs from the variable importance chart. Percentages represent the performance of the individual vegetative indices in achieving that outcome. Indices have been arranged in order of the best index to the least performing index along with its corresponding percentage.

Bud break stage (F1)		
Parameter	**Rank**	**Percentage (%)**
Yield (g.m^{-2})	GLI, VARI, GRVI, NDRE, NDVI, ENDVI	100, 72, 60, 22, 8, 0
Leaf area index	NDRE, NDVI, ENDVI, GLI, GRVI, VARI	100, 90, 82, 10, 4, 0
Plant height (cm)	NDRE, NDVI, ENDVI, GRVI, VARI, GLI	100, 95, 75, 68, 27, 0
Floral bud number	NDRE, NDVI, ENDVI, GRVI, VARI, GLI	100,75, 72, 48, 15, 0
Floral bud stage	GLI, VARI, GRVI, NDRE, ENDVI, NDVI	100, 87, 82, 30, 5, 0
Vegetative bud number	ENDVI, NDVI, NDRE, VARI, GRVI, GLI	100, 70, 15, 3, 2, 0
Vegetative bud stage	GLI, VARI, GRVI, NDRE, ENDVI, NDVI	100, 87, 82, 30, 5, 0
Tight cluster stage (F2/F3)		
Parameter	**Rank**	**Percentage (%)**
Yield (g.m^{-2})	GRVI, NDRE, NDVI, VARI, ENDVI, GLI	100, 82, 78, 72, 45, 0
Leaf area index	GRVI, VARI, GLI, ENDVI, NDRE, NDVI	100, 68, 44, 20, 15, 0

Plant height (cm)	NDRE, NDVI, ENDVI, VARI, GLI, GRVI	100, 95, 80, 5, 5, 0
Floral bud number	GRVI, VARI, NDRE, GLI, NDVI, ENDVI	100, 85, 30, 15, 10, 0
Floral bud stage	GLI, GRVI, VARI, ENDVI, NDRE, NDVI	100, 90, 78, 42, 22, 0
Vegetative bud number	ENDVI, NDRE, NDVI, GLI, VARI, GRVI	100, 68, 50, 48, 15, 0
Vegetative bud stage	GLI, GRVI, VARI, ENDVI, NDRE, NDVI	100, 90, 78, 45, 23, 0
Early/late bud stage (F4/F5)		
Parameter	**Rank**	**Percentage (%)**
Yield (g.m^{-2})	VARI, GRVI, GLI, NDVI, NDRE, ENDVI	100, 100, 100, 90, 70, 0
Leaf area index	GRVI, VARI, GLI, ENDVI, NDRE, NDVI	100, 70, 44, 20, 15, 0
Plant height (cm)	ENDVI, NDVI, NDRE, GLI, GRVI, VARI	100, 75, 50, 38, 28, 0
Floral bud number	GLI, GRVI, ENDVI, NDVI, NDRE, VARI	100, 65, 55, 45, 18, 0
Floral bud stage	GRVI, VARI, GLI, NDVI, NDRE, ENDVI	100, 95, 92, 65, 45, 0
Vegetative bud number	ENDVI, NDRE, NDVI, GLI, VARI, GRVI	100, 67, 50, 48, 15, 0
Vegetative bud stage	GRVI, VARI, GLI, NDVI, NDRE, ENDVI	100, 95, 92, 65, 45, 0
Bloom stage (F6/F7)		
Parameter	**Rank**	**Percentage (%)**
Yield (g.m^{-2})	GLI, ENDVI, NDVI, GRVI, NDRE, VARI	100, 95, 80, 79, 50, 0
Leaf area index	NDRE, NDVI, ENDVI, GLI, GRVI, VARI	100, 100, 90, 78, 28, 0
Plant height (cm)	GRVI, NDRE, NDVI, VARI, GLI, ENDVI	100, 85, 30, 27, 13, 0
Floral bud number	NDRE, GRVI, NDVI, GLI, VARI, ENDVI	100, 98, 82, 70, 50, 0
Floral bud stage	ENDVI, NDRE, NDVI, GLI, GRVI, VARI	100, 95, 82, 58, 25, 0
Vegetative bud number	GLI, GRVI, NDRE, NDVI, ENDVI, VARI	100, 82, 67, 50, 32, 0
Vegetative bud stage	ENDVI, NDRE, NDVI, GLI, GRVI, VARI	100, 95, 82, 58, 25, 0
Fruit set stage (F8)		
Parameter	**Rank**	**Percentage (%)**
Yield (g.m^{-2})	ENDVI, NDRE, NDVI, GRVI, GLI, VARI	100, 90, 78, 75, 50, 0
Leaf area index	GRVI, VARI, GLI, NDVI, ENDVI, NDRE	100, 95, 92, 35, 22, 0
Plant height (cm)	GRVI, VARI, GLI, ENDVI, NDRE, NDVI	100, 85, 79, 8, 4, 0
Floral bud number	NDVI, GLI, NDRE, VARI, GRVI, ENDVI	100, 68, 50, 45, 35, 0
Floral bud stage	NDRE, GRVI, VARI, NDVI, ENDVI, GLI	100, 58, 50, 40, 10, 0
Vegetative bud number	GRVI, VARI, GLI, ENDVI, NDVI, NDRE	100, 90, 85, 75, 25, 0
Vegetative bud stage	NDRE, GRVI, VARI, NDVI, ENDVI, GLI	100, 58, 50, 40, 10, 0

Table 4.7. Coefficient of determination (R^2) values, concordance values (CCC), and root mean square error (RMSE) values from 5 regression methods on several growth parameters against VIs at the different phenological stages (a, b, c, d, & e) using the hand-held FieldSpec® 3 radiometer for the 2020 trial. SMLR – Stepwise multilinear regression, KNN – K- nearest neighbour, RF – Random Forest, SVM – Support vector machine, and CB – Cubist. F – Floral stage

a.

	Bud break (F1)														
	SMLR			**KNN**			**RF**			**SVM**			**CB**		
Parameters	**R^2**	**CCC**	**RMSE**	**R^2**	**CCC**	**RMSE**	**R^2**	**CCC**	**RMSE**	**R^2**	**CCC**	**RMSE**	**R^2**	**CCC**	**RMSE**
Yield ($g.m^{-2}$)	0.14	0.04	285.11	0.11	0.09	264.26	0.11	0.009	285.62	0.13	0.16	261.86	-	0.03	271.27
LAI	0.09	0.09	0.14	0.19	0.20	0.12	0.11	0.16	0.13	0.06	0.08	0.12	0.18	0.19	0.13
Plant height (cm)	-	-0.06	1.80	0.06	-0.02	1.69	0.15	-0.12	1.94	0.12	0.11	2.71	-	0	1.64
Floral bud no.	0.07	0.07	1.42	0.16	0.15	1.40	0.10	0.10	1.43	0.13	0.13	1.35	0.09	0.13	1.4
Floral bud stage	-	-0.15	0.40	0.07	-0.01	0.35	0.17	-0.17	0.39	0.15	-0.00	0.35	-	0	0.34
Veg. bud no.	-	-0.06	4.45	0.15	0.01	4.20	0.09	0.01	4.57	0.07	-0.00	4.45	-	-0.03	4.56
Veg. bud stage	0.12	0.03	0.28	0.16	0.10	0.25	0.07	-0.013	0.29	0.11	-0.00	0.26	0.11	0.04	0.27

b.

	Tight cluster (F2/F3)														
	SMLR			KNN			RF			SVM			CB		
Parameters	**R^2**	**CCC**	**RMSE**	**R^2**	**CCC**	**RMSE**	**R^2**	**CCC**	**RMSE**	**R^2**	**CCC**	**RMSE**	**R^2**	**CCC**	**RMSE**
Yield ($g.m^{-2}$)	0.21	0.24	252.14	0.23	0.29	256.35	0.23	0.28	247.53	0.39	0.42	215.65	0.22	0.36	247.02
LAI	0.12	0.04	0.35	0.15	0.03	0.15	0.21	0.01	0.17	0.20	0.26	0.15	0.26	0.08	0.16
Plant height (cm)	0.24	0.28	1.76	0.27	0.35	1.47	0.31	0.38	1.41	0.27	0.30	1.77	0.33	0.40	1.44
Floral bud no.	0.17	0.04	2.29	0.08	0.06	1.58	0.11	0.06	1.58	0.15	0.10	1.67	-	-	1.59
Floral bud stage	0.42	0.52	0.65	0.61	0.65	0.51	0.59	0.61	0.54	0.58	0.62	0.52	0.40	0.52	0.63
Veg. bud no.	0.09	-0.03	2.32	0.07	0.07	1.55	0.09	0.07	1.62	0.10	-0.00	1.5	0.09	0.03	1.64
Veg. bud stage	0.45	0.49	1.43	0.67	0.67	0.71	0.66	0.67	0.70	0.63	0.69	0.69	0.56	0.62	0.81

c.

	Early/late bud (F4/F5)														
	SMLR			KNN			RF			SVM			CB		
Parameters	**R^2**	**CCC**	**RMSE**	**R^2**	**CCC**	**RMSE**	**R^2**	**CCC**	**RMSE**	**R^2**	**CCC**	**RMSE**	**R^2**	**CCC**	**RMSE**
Yield ($g.m^{-2}$)	-	0.06	162.28	0.30	0.08	148.90	0.40	-0.002	153.07	0.52	0.34	133.81	0.42	-0.01	173.37
LAI	0.45	0.41	0.30	0.43	0.40	0.32	0.39	0.33	0.30	0.29	0.24	0.36	0.50	0.35	0.32
Plant height (cm)	0.19	0.17	1.78	0.28	0.24	1.56	0.30	0.20	1.70	0.31	0.20	1.60	0.43	0.30	1.64
Floral bud no.	-	-0.07	1.42	0.17	0.20	1.46	0.34	0.11	1.22	0.35	0.29	1.10	0.24	0.08	1.24
Floral bud stage	-	-0.12	0.27	0.40	0.07	0.26	0.27	0.13	0.22	0.25	0.19	0.30	0.31	0.03	0.23
Veg. bud no.	0.37	0.17	2.44	0.17	0.19	2.61	0.30	0.20	2.20	0.22	0.19	2.47	0.27	0.21	2.51
Veg. bud stage	0.45	0.35	0.22	0.36	0.29	0.23	0.36	0.12	0.23	0.49	0.30	0.23	0.42	0.26	0.23

d.

	Bloom (F6/F7)														
	SMLR			KNN			RF			SVM			CB		
Parameters	**R^2**	**CCC**	**RMSE**	**R^2**	**CCC**	**RMSE**	**R^2**	**CCC**	**RMSE**	**R^2**	**CCC**	**RMSE**	**R^2**	**CCC**	**RMSE**
Yield ($g.m^{-2}$)	0.30	0.25	268.46	0.19	0.21	255.44	0.17	0.16	261.82	0.26	0.23	328.98	0.31	0.29	238.67
LAI	0.59	0.57	1.28	0.75	0.74	0.73	0.74	0.74	0.71	0.71	0.71	0.78	0.72	0.72	0.77
Plant height (cm)	0.21	0.24	1.91	0.32	0.35	1.63	0.43	0.45	1.42	0.38	0.43	1.56	0.38	0.43	1.55
Floral bud no.	0.21	-0.004	1.10	0.24	0.16	1.27	0.10	0.11	1.09	0.27	0.34	1.05	0.09	0.10	1.19
Floral bud stage	0.27	-0.11	1.18	0.24	0.17	1.21	0.15	0.09	1.07	0.18	0.16	1.91	0.11	0.12	1.17
Veg. bud no.	0.34	0.26	1.74	0.24	0.28	1.63	0.28	0.37	1.47	0.24	0.34	1.60	0.20	0.28	1.60
Veg. bud stage	0.18	0.23	0.23	0.19	0.17	0.22	0.05	0.06	0.25	0.17	0.17	0.23	0.14	0.16	0.23

e.

	Fruit set (F8)														
	SMLR			KNN			RF			SVM			CB		
Parameters	**R^2**	**CCC**	**RMSE**	**R^2**	**CCC**	**RMSE**	**R^2**	**CCC**	**RMSE**	**R^2**	**CCC**	**RMSE**	**R^2**	**CCC**	**RMSE**
Yield ($g.m^{-2}$)	0.10	0.03	274.59	0.18	0.07	289.59	0.10	0.11	260.29	0.12	0.10	298.23	0.12	0.11	262.12
LAI	0.42	0.47	0.85	0.34	0.32	0.92	0.33	0.36	0.90	0.41	0.35	0.86	0.34	0.44	0.93
Plant height (cm)	0.19	0.28	2.0	0.15	0.13	2.10	0.28	0.22	2.01	0.25	0.31	2.02	0.14	0.21	2.25
Floral bud no.	-	-0.08	1.01	0.12	0.06	1.35	0.12	0.06	0.99	0.12	0.06	0.99	0.07	0.08	1.01
Floral bud stage	0.23	0.14	0.23	0.19	0.15	0.22	0.09	0.13	0.23	0.17	0.15	0.22	0.11	0.14	0.23
Veg. bud No.	0.19	-0.002	2.23	0.11	0.02	2.15	0.09	0.02	2.23	0.14	0.10	2.39	-	0.001	2.18
Veg. bud stage	0.11	0.13	0.20	0.20	0.28	0.19	0.12	0.15	0.21	0.16	0.20	0.20	0.16	0.18	0.24

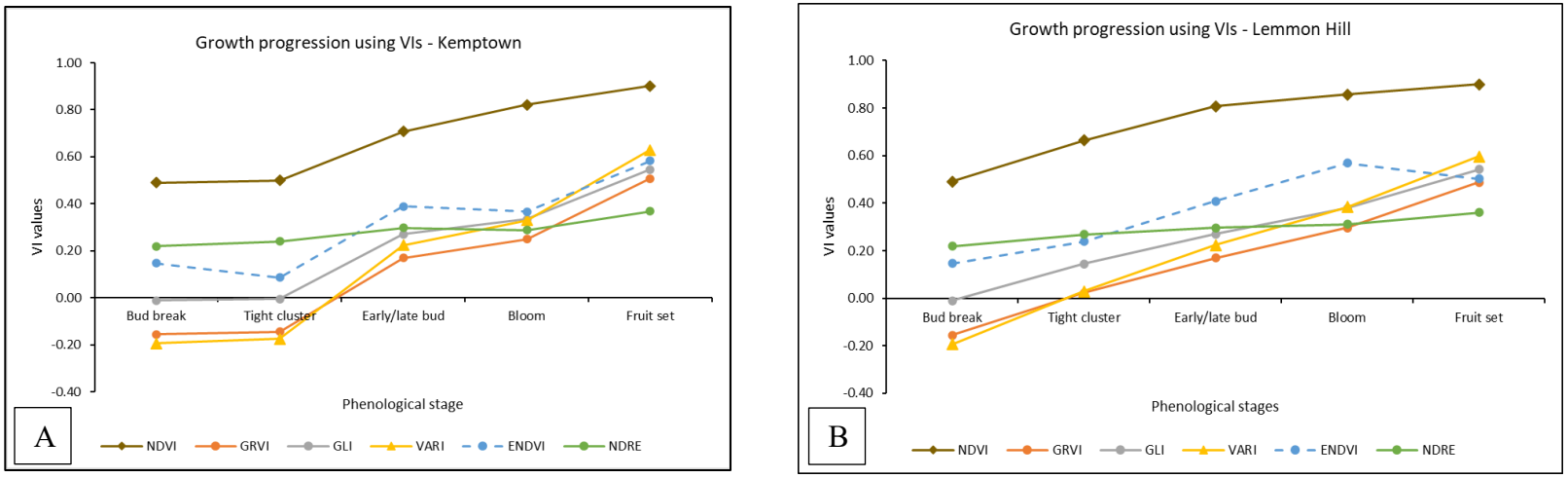

Figure 4.9. Growth progression of VIs observed on both fields at the different phenological stages using the FieldSpec® 3 hand-held radiometer. (A) Kemptown and (B) Lemmon Hill.

Table 4. 8. Coefficient of determination (R^2), Lin's concordance (CCC) values and root mean square error (RMSE) of growth parameters against several VI's (Benvie Hill, NS) using an RGB camera during the 2021 growing season. SMLR – Stepwise multilinear regression, KNN – K- nearest neighbour, RF – Random Forest, SVM – Support vector machine, and CB – Cubist. F – Floral stage

a.

	Tight cluster (F2/F3)														
	SMLR			KNN			RF			SVM			CB		
Parameters	**R^2**	**CCC**	**RMSE**	**R^2**	**CCC**	**RMSE**	**R^2**	**CCC**	**RMSE**	**R^2**	**CCC**	**RMSE**	**R^2**	**CCC**	**RMSE**
Yield ($g.m^{-2}$)	0.42	0.38	151.45	0.59	0.44	134.4	0.54	0.47	128.96	0.56	0.48	164.7	0.60	0.48	138.8
Plant height (cm)	-	-0.02	1.78	0.17	0.13	1.63	0.36	0.07	1.65	0.52	0.25	1.52	0.22	0.19	1.63
Floral bud no.	0.29	-0.02	1.09	-	0.01	0.94	0.20	-0.01	0.99	0.37	0.28	0.95	0.26	0.07	1.02
Floral bud stage	-	-0.03	0.48	0.31	0.08	0.58	0.21	0.04	0.48	0.40	0.09	0.76	0.24	0.02	0.55
Veg. bud no.	0.22	-0.06	4.20	0.13	0.11	3.84	0.39	0.02	4.22	0.32	0.04	8.07	0.15	0.01	3.98
Veg. bud stage	0.47	0.25	0.44	0.37	0.37	0.44	0.23	0.14	0.44	0.54	0.38	0.41	0.51	0.36	0.40

b.

	Early/late bud (F4/F5)														
	SMLR			KNN			RF			SVM			CB		
Parameters	**R^2**	**CCC**	**RMSE**	**R^2**	**CCC**	**RMSE**	**R^2**	**CCC**	**RMSE**	**R^2**	**CCC**	**RMSE**	**R^2**	**CCC**	**RMSE**
Yield ($g.m^{-2}$)	-	0.13	178.27	0.46	0.29	158.85	0.34	0.20	180.68	0.30	0.23	171.82	0.31	0.22	177.37
Plant height (cm)	-	0.04	3.1	0.20	0.10	3.52	0.16	-0.11	3.51	0.40	0.23	3.43	0.23	0.04	3.39
Floral bud no.	-	-0.03	1.10	0.23	0.01	1.04	0.18	-0.08	1.17	0.18	0.04	1.09	-	0.0	1.07
Floral bud stage	-	-0.05	0.42	0.20	0.13	0.43	0.19	0.02	0.45	0.41	0.27	0.47	0.34	0.06	0.38
Veg. bud no.	-	-0.02	1.71	0.24	0.11	2.07	0.19	0.01	1.85	0.27	0.08	1.70	0.25	0.15	1.66
Veg. bud stage	0.25	0.17	0.28	0.26	0.05	0.37	0.30	-0.07	0.30	0.52	0.26	0.24	0.28	0.02	0.32

c.

	Bloom (F6/F7)														
	SMLR			KNN			RF			SVM			CB		
Parameters	**R^2**	**CCC**	**RMSE**	**R^2**	**CCC**	**RMSE**	**R^2**	**CCC**	**RMSE**	**R^2**	**CCC**	**RMSE**	**R^2**	**CCC**	**RMSE**
Yield ($g.m^{-2}$)	-	-0.04	211.98	0.50	0.29	165.91	0.20	0.13	202.01	0.43	0.20	172.17	0.33	0.24	177.07
Plant height (cm)	-	0.04	3.13	0.20	0.10	3.52	0.16	-0.11	3.51	0.40	0.23	3.43	0.23	0.04	3.39
Floral bud no.	-	-0.03	1.10	-	0.01	1.02	0.18	-0.06	1.17	0.18	0.04	1.09	-	0.0	1.07
Floral bud stage	-	-0.05	0.42	0.20	0.13	0.43	0.19	0.02	0.45	0.41	0.27	0.47	0.34	0.06	0.38
Veg. bud no.	-	-0.02	1.71	0.24	0.11	2.07	0.19	0.01	1.85	0.27	0.08	1.70	0.25	0.15	1.66
Veg. bud stage	0.25	0.17	0.28	0.26	0.05	0.37	0.30	-0.07	0.30	0.52	0.26	0.24	0.28	0.03	0.32

d.

	Fruit set (F8)														
	SMLR			KNN			RF			SVM			CB		
Parameters	**R^2**	**CCC**	**RMSE**	**R^2**	**CCC**	**RMSE**	**R^2**	**CCC**	**RMSE**	**R^2**	**CCC**	**RMSE**	**R^2**	**CCC**	**RMSE**
Yield ($g.m^{-2}$)	0.48	0.40	143.42	0.53	0.44	149.26	0.61	0.46	132.91	0.56	0.42	180.36	0.50	0.38	153.57
Plant height (cm)	-	-0.10	2.54	0.15	0.01	2.29	0.34	0.02	2.48	0.30	0.09	2.84	0.26	0.02	2.47
Floral bud no.	-	0.02	1.65	0.36	0.09	1.36	0.30	0.06	1.47	0.37	0.13	1.40	0.56	0.10	1.43
Floral bud stage	0.11	-0.01	0.03	-	-	-	0.11	0.0	0.03	0.11	0.0	0.03	-	-	-
Veg. bud no.	0.30	-0.07	2.49	0.39	0.24	2.10	0.22	0.04	2.38	0.54	0.17	2.48	0.21	0.20	2.14
Veg. bud stage	0	0	-0.08	-	-	-	-	-	-	0.52	0.26	0.24	-	-	-

Table 4.9. Coefficient of determination (R^2) value, Lin's concordance (CCC) values and root mean square errors (RMSE) of growth parameters against several VI's (Kemptown) using a multispectral sensor during the 2022 growing season. SMLR – Stepwise multilinear regression, KNN – K- nearest neighbour, RF – Random Forest, SVM – Support vector machine, and CB – Cubist. F – Floral stage

	Bud break (F1)														
	SMLR			KNN			RF			SVM			CB		
Parameters	**R^2**	**CCC**	**RMSE**	**R^2**	**CCC**	**RMSE**	**R^2**	**CCC**	**RMSE**	**R^2**	**CCC**	**RMSE**	**R^2**	**CCC**	**RMSE**
Yield ($g.m^{-2}$)	0.53	0.38	293.38	0.26	0.22	351.23	0.31	0.11	294.35	0.28	0.22	299.21	0.27	0.16	324.24
LAI	-	0.0	0.07	0.29	0.03	0.07	0.12	-0.09	0.08	0.27	-0.00	0.07	-	-	-
Plant height (cm)	-	-0.02	2.64	0.35	0.16	2.65	0.25	0.02	2.43	0.22	0.00	3.24	0.30	0.12	2.55
Floral bud no.	-	-0.03	1.48	0.30	0.24	1.34	0.38	0.16	1.31	0.38	0.16	1.31	0.41	0.03	1.59
Floral bud stage	-	-0.04	0.46	0.31	0.14	0.51	0.22	-0.05	0.46	0.22	-0.05	0.46	-	-0.04	0.42
Veg. bud no.	-	-0.11	4.01	0.58	0.39	2.46	0.37	0.17	2.89	0.37	0.17	2.89	0.35	0.27	2.74
Veg. bud stage	-	-0.08	0.31	0.17	0.19	0.33	0.25	-0.02	0.28	0.19	0.11	0.28	0.35	-0.01	0.28

b.

	Tight cluster (F2/F3)														
	SMLR			KNN			RF			SVM			CB		
Parameters	**R^2**	**CCC**	**RMSE**	**R^2**	**CCC**	**RMSE**	**R^2**	**CCC**	**RMSE**	**R^2**	**CCC**	**RMSE**	**R^2**	**CCC**	**RMSE**
Yield ($g.m^{-2}$)	0.52	0.43	266.85	0.23	0.17	288.71	0.34	0.22	278.38	0.52	0.37	317.73	0.30	0.27	288.78
LAI	-	0	0.07	0.29	0.03	0.07	0.12	-0.09	0.08	0.27	-0.00	0.07	-	-	-
Plant height (cm)	-	-0.13	2.70	0.36	0.14	2.31	0.16	0.03	2.30	0.23	0.10	5.88	0.13	0.02	2.55
Floral bud no.		-0.09	1.66	0.28	0.10	1.44	0.19	0.00	1.41	0.27	0.14	2.59	0.16	0.14	1.53
Floral bud stage	0.29	0.20	0.60	0.19	0.12	0.58	0.22	-0.00	0.62	0.24	0.08	0.60	0.37	0.07	0.59
Veg. bud no.	-	-0.12	3.48	0.19	0.19	3.15	0.27	0.05	2.98	0.25	0.24	3.76	0.17	0.08	3.17
Veg. bud stage	0.39	0.13	0.78	0.29	0.08	0.77	0.19	-0.01	0.84	0.42	0.34	0.90	0.20	-0.02	0.83

c.

	Early/late bud (F4/F5)														
	SMLR			KNN			RF			SVM			CB		
Parameters	R^2	CCC	RMSE	R^2	CCC	RMSE	R^2	CCC	RMSE	R^2	CCC	RMSE	R^2	CCC	RMSE
Yield ($g.m^{-2}$)	0.49	0.44	250.52	-	0.01	310.10	0.13	0.16	309.93	0.46	0.32	252.34	0.47	0.29	279.79
LAI	0.47	0.28	0.17	0.44	0.30	0.17	0.34	0.21	0.17	0.55	0.46	0.14	-	0.31	0.14
Plant height (cm)	0.21	0.23	2.47	0.32	0.00	2.53	0.49	-0.19	2.99	0.26	0.02	2.73	0.31	-0.00	2.87
Floral bud no.	-	0.00	1.62	0.23	0.09	1.73	0.27	0.02	1.58	0.25	0.16	1.48	0.17	0.05	1.46
Floral bud stage	0.36	-0.23	0.54	0.37	0.10	0.47	0.42	0.16	0.42	0.38	0.15	0.50	0.28	0.12	0.40
Veg. bud no.	0.45	0.19	2.61	0.19	0.20	2.61	0.13	0.12	2.43	0.30	0.12	3.00	0.15	0.10	2.32
Veg. bud stage	0.60	0.40	0.30	0.56	0.44	0.32	0.55	0.43	0.29	0.40	0.24	0.34	0.55	0.39	0.30

d.

	Bloom (F6/F7)														
	SMLR			KNN			RF			SVM			CB		
Parameters	R^2	CCC	RMSE	R^2	CCC	RMSE	R^2	CCC	RMSE	R^2	CCC	RMSE	R^2	CCC	RMSE
Yield ($g.m^{-2}$)	0.44	0.30	323.36	0.47	0.34	280.23	0.42	0.27	295.83	0.49	0.36	258.37	0.35	0.30	251.81
LAI	0.48	0.20	0.46	0.57	0.31	0.40	0.51	0.30	0.37	0.57	0.40	0.38	0.49	0.34	0.39
Plant height (cm)	0.50	0.06	2.75	0.36	0.13	2.39	0.40	0.01	2.33	0.40	0.06	2.33	0.47	0.03	2.41
Floral bud no.	0.18	0.10	2.29	0.27	0.08	1.98	0.11	-0.04	2.13	0.27	0.22	3.29	0.19	0.06	2.06
Floral bud stage	0.38	0.22	0.51	0.47	0.39	0.47	0.26	0.22	0.45	0.32	0.28	0.45	0.37	0.18	0.48
Veg. bud no.	0.23	-0.10	2.76	-	0.01	2.08	0.21	0.04	2.36	0.30	0.05	2.34	-	-0.04	2.27
Veg. bud stage	0.43	0.38	0.31	0.51	0.47	0.27	0.42	0.32	0.34	0.61	0.52	0.26	0.64	0.48	0.30

e.

	Fruit set (F8)														
	SMLR			KNN			RF			SVM			CB		
Parameters	**R^2**	**CCC**	**RMSE**	**R^2**	**CCC**	**RMSE**	**R^2**	**CCC**	**RMSE**	**R^2**	**CCC**	**RMSE**	**R^2**	**CCC**	**RMSE**
Yield ($g.m^{-2}$)	0.25	0.24	324.89	0.39	0.33	284.59	0.38	0.28	292.40	0.39	0.26	258.70	0.35	0.26	291.06
LAI	0.43	0.36	0.92	0.39	0.35	1.00	0.45	0.39	0.81	0.55	0.38	0.85	0.52	0.37	0.95
Plant height (cm)	0.22	0.19	2.11	0.44	0.33	1.60	0.32	0.24	1.79	0.46	0.31	1.60	0.32	0.30	1.96
Floral bud no.	0.33	-0.13	1.69	-	0.00	1.12	0.23	-0.08	1.25	0.41	-0.00	1.13	-	0.00	1.16
Floral bud stage	0.44	0.27	0.22	0.36	0.30	0.22	0.37	0.07	0.24	0.48	0.35	0.23	0.34	0.18	0.25
Veg. bud no.	0.28	0.06	3.38	0.37	0.24	2.49	0.15	0.01	2.77	0.22	0.00	3.23	0.19	0.09	2.60
Veg. bud stage	-	-0.05	0.13	0.16	0.13	0.14	0.32	0.05	0.14	0.32	0.05	0.14	-	-0.00	0.13

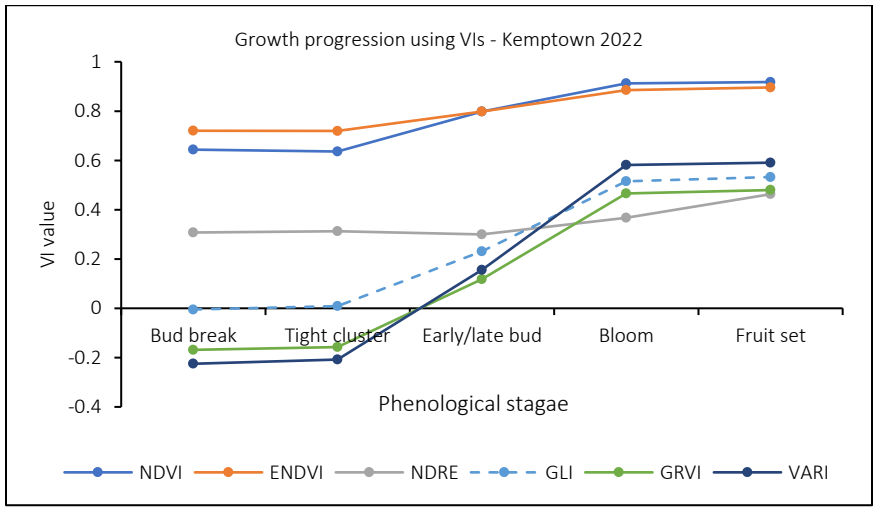

Figure 4.10. Growth progression of VIs at the different phenological stages observed at the Kemptown site in the 2022 growing season using the multispectral sensor.

4.4.4.2 Phenological growth progression of the different wild blueberry phenotypes

The general observation of the floral buds 2019, 2020, and 2022 progression of growth in the two major genotypes *Vaccinium angustifolium* and *Vaccinium myrtilloides* indicates that *V. myrtilloides* lags in floral growth. It was observed that it took between 9 to 12 days for *V. myrtilloides* to get to the stage of *V. angustifolium* (Figure 4.11, 4.12, and Appendix 3 – Figure A1), though this phenomenon varied across the development phase and the phenotypes examined. After bud break, it was observed that it took between 5 to 8 DOY for phenotypes to move from one floral stage to another, and about 38 to 45 DOY to reach full bloom. While this principle was consistent in both *V. angustifolium* and *V. myrtilloides, V. myrtilloides* still observed some lag in days until the F7 stage. It was observed that, after the F7 stage it took several days with an average of 13 to 17 days for phenotypes to reach the F8 stage. *V. angustifolium* showed a strong floral growth progression compared to *Vaccinium myrtilloides* phenotypes. *V. myrtilloides* tall and medium showed similar growth progressions.

Comparison between the 2022 observation and the others, revealed that, whereas there was an obvious delay in the start and growth progression of the *V. myrtilloides* phenotypes, the lagging period observed in 2022 result was mild. Despite this phenomenon, the different figures showed that, phenotypes behaved similar in the different locations (Figure 4.11 and Figure 4.12). However, it was observed that *V. myrtilloides* (small), showed a higher floral bud progression compared to the other phenotypes of *V. myrtilloides* (medium and tall). Generally, all the variations observed in Farmington agreed with several observations at the Lemmon Hill and Kemptown locations (Appendix 3 – Figure A1). *V. angustifolium* nigrum showed the highest growth in floral bud development with *V. myrtilloides* medium and small observing the lowest.

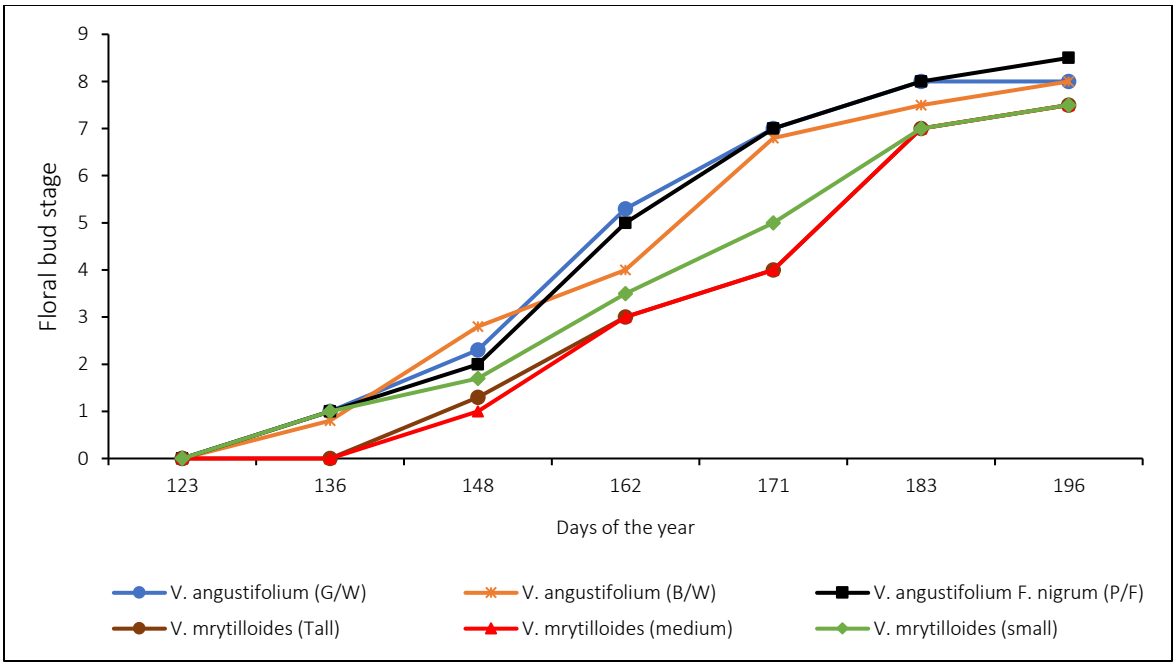

Figure 4.11. Growth progression of the different blueberry phenotypes at Farmington as monitored from May to June 2019. The different colours represent the six phenotypes.

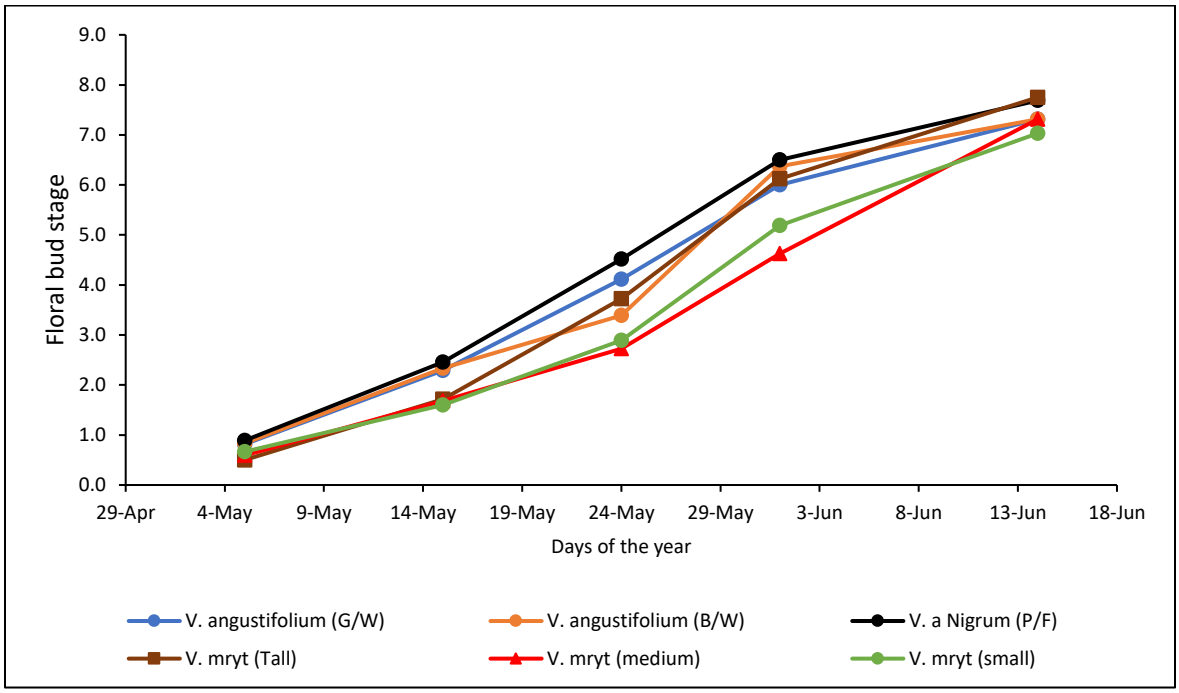

Figure 4.12. Growth progression of the different blueberry phenotypes at Kemptown as monitored from May to June 2022. The different colours represent the six phenotypes.

4.4.5 Assessment of statistical methods

Validity and precision between results necessitated a comparison between the R^2 and Lin's concordance correlation coefficient (CCC) values among several statistical classifiers. The five adopted statistical classifiers of the different parameters proved similar as the values observed were consistent among the different methods applied. Despite the slight differences in the statistical approaches of these classifiers, they were consistent in their R^2 values. The SVM generally had high R^2 values across all phenological stages, which were often consistent with the RF classifier. The SMLR classifier was also consistent with the KNN classifier, but the Cubist classifier (CB) was considered slightly different.

Comparison between R^2 and CCC values (Table 4.3a-e) showed validation and precision in CCC values as compared to R^2 values (Kwiecien et al., 2011; Neuendorf, 2022). Apart from the tight cluster stage (Table 4.3b), when R^2 values were higher than the CCC values, the remaining phenological stages observed consistently higher CCC values compared to the R^2 values (Table 4.3 a, c-e). Therefore, there is generally a good indication of high CCC values across all the phenological stages (Table 4.3, a-e).

4.5 DISCUSSION

The primary research on the wild blueberry field validates multiple discoveries concerning UAV and remote sensing techniques and presents numerous opportunities to focus on particular VIs and their application for monitoring vegetation and predicting various parameters in the wild blueberry field. From a management and operational perspective, results using both sensors indicate that a Zenmuse X5- RGB camera would achieve similar results as the Micasense, thus, the two sensors can be used to establish relationships, and make predictions.

The trends of VIs in the phenological development stages observed on the field over the period were instructive as it confirmed several other studies that show VIs can be utilized in monitoring phenology (Vega, et al., 2015; Forsström et al., 2019; Hussain et al., 2020; Tao et al., 2020). Findings from this study, confirm a major phenomenon, that, VIs have a bell-shaped (an open parabolic) representation over the field season (Forsström et al., 2019). This explains that VIs were low at the start of the crop season, but increased mid-way, and diminished at the end of the season. This phenomenon was observed due to the development of leaves over the period till the autumn-fall season when chlorophyll and other pigment degradation occurred and leaves abscised from the stem. The late summer period also corresponds to the fruit set development period which occurs in the plant. Therefore, plant leaves are major determinants of VIs and regulators of light with pigments contributing to this process (Section 2.7.3). Additionally, this observation gives insight into the phenological cycle of the wild blueberry plant, highlighting specific phenological stages for management practices. Furthermore, from the bud break stage, the increasing trend of VIs were affected at the flowering stage, where a moderate to severe decline was observed among several VIs. This observation was confirmed by the work of Hassan et al., (2019) who observed a 10% decline at the flowering stage as this was reflective in the Lemmon Hill trial, but a greater decline was observed in the Kemptown trial using the micasense. Whereas this decline was not present in the other trials and sensors, it stands to reason that this may not have been a common phenomenon. Reasons accounting for this phenomenon varied, however, variations in VIs on wild blueberry plants are notably connected to the transition between phenological stages. At the shoot area of a wild blueberry plant, there are typically more than 100 million flowers per acre, resulting in noticeable reflectance effects (Personal communication: David Percival, 2023). Leaf structure and angle impact the amount of light reflected, which affects

VI computations. Furthermore, since blueberry plants are not evergreen, the leaves at some specific phenological stages might have been affected by colouration. Thus, pink, and white flowers among other colouration of leaves create a mosaic of colours on the field (Abbey et al., 2023).

Furthermore, new vegetative growth flushes after fruit set with auxiliary buds breaking and the emergence of new flushes of leaves also contributes to this effect (Personal communication: David Percival, 2023). This occurrence was attributed to the chemical composition of leaves, weather conditions, and the varied flower petals along the different stages of development, which affects reflectance (Duy, 1999; Hall, Forsyth, et al., 1972; Wood & Barker, 1963). Other factors may include, the direction of incidence radiation, and canopy architecture, among other characteristics of the plants (Hussain et al., 2020). The variability effect is even echoed among fields, where some differences seem to be observed at the bloom stage of both Kemptown and Lemmon Hill. At the bloom stage, the trials in Kemptown observed a general decline in VIs, but the same effect was not substantially visible in the Lemmon Hill trial and the other trials in the other years. However, the major trends in VI progression remained constant for all the trials (Figure 4.8, 4.9, and 4.10). In a study by Forsström et al., (2019), spectral analysis between lingonberry and blueberry was compared. This study largely confirmed some of those findings of Forsström et al., (2019) which state that variations in the red and blue wavelength regions are responsible for the observations at the bloom and the berrying stage of the plant's development process. Therefore, since these indices are a mathematical computation of VIS and NIR light bands, this claim potentially accounts for the variations observed in our study. However, the seeming difference observed between the different trials can be accounted for by the nature and quantity of leaves, flowers, and berries developed in those fields. The number of plants and field variation at the transitioning phase affects VIs at the different phenological stages (Forsström et al., 2019).

Furthermore, in agreement with these findings, Forsström et al., (2019) showed that VIs were sensitive to blueberry shrubs observed across the field season. This indicates potential in using VIs to monitor phenology.

Predictability of growth parameters using RS techniques hinges on obtaining high R^2 or CCC and correlative values with minimal RMSE as reported in several studies (Hassan et al., 2019; Liu et al., 2018; Souza et al., 2017; Zhou et al., 2017). This study records a range of moderately high R^2 and CCC values which agrees with the findings from other crops such as wheat (Hassan et al., 2019), rapeseed (Hussain et al., 2020) and wild blueberries (Barai et al., 2021). LAI showed high predictability across the phenological stages, except for the F8 stage, whiles FS and VS were largely limited to the F4/F5 stage. This study suggests that LAI, VS, and FS are growth parameters that can be estimated at different phenological stages across the field season particularly the early/late bud and bloom stages. These findings agree with the work of Maqbool et al., (2010) who used optimum multiple narrow-band reflectance (OMNBR) indices to estimate growth parameters in the wild blueberry fields. Their study observed that across 3 phenological stages, LAI was accurately estimated at the bloom stage. This accurately confirms our result of the bloom stage (F6/F7) being the best phenological stage to estimate LAI. Even though the other parameters had relatively good R^2 values, the high RMSE values obtained posed reliability questions on the predictability of those parameters. Converse to the assertion on yield, the findings of Maqbool et al., (2010) supports the claim of some parameters like yield to be predicted using reflectance data. Despite the seemingly different approach adopted by Maqbool et al., (2010), the use of VIs may support yield predictability if measures are taken to rectify some issues on resolution, in addition to a specific harvest time. Maqbool et al., (2010) argued that the polyphenolic compounds contained in flowers and berries affected spectral resolution and accurate estimations. According

to Kinsman, (1993), the level of variability on the wild blueberry field can be very high. Therefore, the inconsistencies observed with some of the results may directly point to field variability which includes plant density across the field, different phenotypes, and the chemical composition of plants, which affects VIs. Though the wild blueberry plant is different from other crops like the rapeseed and rice plant, the results from those studies were similar. Findings from those studies point to the elongation and flowering stages serving as good estimation points for plant canopy and other biophysical characteristics of the field. Like this work, the best estimation stage for LAI is the bloom stage (white tip) (F6/F7), whereas tight cluster and early/late bud stages seem to be the best estimation stages for VS, with tight cluster (F2/F3) as the best in estimating floral bud stage (FS). In the conclusion of these studies (Liu et al., 2018; Zhou et al., 2017), it was stated that VIs that showed high correlation and prediction of LAI will equally correlate and predict yield. The earlier claim stands true as good correlation values are observed on yield with VIs but not its predictability according to this study. In a more recent study, Barai et al., (2021) confirms our position on the difficulty in predicting wild blueberry yield, however, with the adoption and correction of some methods the prediction of yield should be possible.

The phenological progression of VIs gave an indication of leaf development across the growth season. It can therefore be observed that at the bud break stage, where the presence of leaves cannot be detected, VI values were substantially low. This result was consistent with several studies that generally observed low VI values at the initial crop stage, but VI values increased as plant canopy developed (Hussain et al., 2020; Tao et al., 2020; Vega et al., 2015). This was because leaf area was progressively increasing over the growing season and their development was significant to the computation of VIs, as determined from reflectance values (Breda, 2003). The development of leaves progressed or remained constant over some phenological stages until

harvest and then later declined because of leaf abscission during the fall season (Breda, 2003: as cited in Myneni et al., 2008). This was evident as the leaf area index values depicted similar trends over the season (Figure 4.8 and Figure 4.9).

In the selection of important VIs (variable importance), several vegetative indices (VIs) contributed to the varied outcomes observed (Table 4.4 – 4.6 and A5 – A7). Rather than the single linear regression method which focused on specific indices, the adopted multiple linear regression generated several VI rankings. This agreed with the work of Yue et al., (2018) who found superior the use of multiple indices rather than a single index to estimate crop parameters. Significantly, the NIR indices such as NDVI, ENDVI, and NDRE contributed across several parameters and growth stages. However, the contribution of some VIS vegetative indices cannot be underestimated, and as such this study makes a strong case for the VIS-VIs. Studies by Liu et al., (2018) and Zhou et al., (2017) have established that VARI among other visible light VIs estimates several growth parameters. It can, therefore, be explained that though plants depend on different ratios of light, the significance of NIR wavelength to provide unique estimations on plant health, in addition to external and internal characteristics of the plant cannot be underestimated.

The use of the different statistical classifiers was necessary to verify the results and determine a suitable method. The classification methods applied proved robust, however, results obtained varied slightly under the R^2 and CCC outputs. Despite the uniqueness of these classifiers, values obtained using CB and SMLR were moderately low across all parameters at the different phenological stages. This was confirmed by Penglei et al., (2020) whose findings suggest that, though the regression methods estimate similar accuracies, some are limited in performance to specific growth stages or across the different phenological stages. Therefore, RF, SVM, and KNN classifiers performed better compared to SMLR classifier. However, in most situations, SMLR and

KNN classifies generated the same outcomes. In this study, the results obtained indicate that the SVM and RF classifiers generated high but similar values with minimal deviations. Therefore, narrowing down on the two best classifiers, SVM and RF were deemed the best classifiers in this study.

Floral bud phenological growth and development for the different phenotypes signified an obvious phenomenon. *V. myrtilloides* showed a lag in their growth development processes as compared to *V. angustifolium*. This result agreed with the work of Fournier et al., (2020) whose study on the allometry of *V. angustifolium* and *V. myrtilloides* revealed a phenological difference between the two species. Their study confirmed a delay of about 8-10 DOY in the phenological development of leaves and flowers of the *V. myrtilloides* species as compared to *V. angustifolium*. Whereas there as slight differences in the DOY, our study projects a delay of between 9 – 12 DOY for *V. myrtilloides* to catch up with *V. angustifolium*. It can be explained that this delay occurred due to genetic differences and the partitioning and mobilization of stored carbohydrates through plant allometry (Fournier et al., 2020). Sugar allocation plays a significant role in bud phenology, thus, after decapitation (tip dieback) the sink strength between the apex and the lower levels reduces. This allows for lower levels of sucrose which results in a lagging phase of those buds (Fournier et al., 2020; Janes, 2005). Thus, *V. myrtilloides,* which uses these compounds produces more leaves leading to delays in their floral bud formation. Despite the success of the study, this study considered the differences between the different phenotypes of the two broad species, *V. angustifolium* and *V. myrtilloides*. Generally, it was shown that phenotypes of *V. myrtilloides* observed a lag across the different years.

4.6 CONCLUSION

In this study, the potential of using the multispectral sensor through the computation of VIs to monitor and estimate growth and development parameters in the wild blueberry field was assessed. Results have indicated that there is potential to adopt remote sensing as a major technological tool for use in wild blueberry production. Correlative assessment of VIs against all parameters showed good indication across all phenological stages. The correlative coefficients fitted more in some VIs compared to other parameters. The coefficient of determination values varied among all VIs, but the level of variable importance differed across the growth parameters and the different phenological stages. Whereas it was difficult for yield prediction to be made, it was possible to make determinations at the F4/F5 and F6/F7 stage for LAI, FS, and VS. Though values obtained were moderately low, those represented for LAI, FS, and VS are relatively high compared to the other parameters. Therefore, with the introduction of the T40 UAV system, the application of disease control products can be conducted at specific stages of the plant.

Phenological growth over the season followed similar trends with NDVI and ENDVI assuming the highest VI values with NDRE, GLI, VARI, and GRVI observing low values in across fields. The overall results from this study have indicated the potential to use vegetative indices to monitor plant growth and make predictions. Despite the challenges observed in the other parameters, further work must be done to confirm findings on harvestable yield, among other parameters.

CHAPTER 5: DETERMINATION OF WILD BLUEBERRY PHENOTYPES USING HIGH-RESOLUTION IMAGERY FROM AN UNMANNED AERIAL VEHICLE SYSTEM

5.1 ABSTRACT

Wild blueberry fields are naturally heterogeneous with distinctly different phenotypes, which causes variation in the pattern of plant growth and development, disease damage, and berry yield. To improve management techniques, this study was conducted using remote sensing approaches to identify and map the different *Vaccinium* species. A hand-held hyperspectral sensor and an unmanned aerial vehicle (UAV) equipped with a 5-banded multispectral camera were used. Trials were set up in two commercial fields; with a plot size of 150 x 100 m. Identified phenotypes were tagged and georeferenced using an SX Blue Platinum GPS device. A pixel-supervised classification using an SVM classifier was conducted to identify the different phenotypes and other field classes. The assessment results were validated, giving an overall accuracy (OA) of 85% and a kappa value of 80. The spectroradiometer also confirmed that *V. angustifolium* f. nigrum can be identified. In conclusion, leaf colour was significant in pixel phenotype identification but was not consistent between the different years. *V. angustifolium* nigrum can be identified but there is potential to also identify *V. myrtilloides*.

Keywords: Phenotype, wild blueberry, UAV, support vector machine, classification, hyperspectral

5.2 INTRODUCTION

The wild blueberry plant popularly referred to as the lowbush blueberry, is an economically important crop in the United States (US) and Canada (Drummond, 2019; Statistics Canada, 2020). The predominant species occurring in commercial fields are *Vaccinium angustifolium* and

Vaccinium myrtilloides (Abbey et al., 2018; Drummond, 2019; Kinsman, 1993). The calcifuge plant is unique in its structure and development, with the ability to thrive under harsh conditions (Zhang et al. 2010; Abbey et al. 2018). The wild blueberry field, which is naturally heterogeneous with distinctly different species and phenotypes, is characterized by a mosaic of colours, but this colouration is dominant during the crop phase (Penman and Annis 2005; Abbey et al. 2020) of the plant. In the vegetative phase, colour variation is evident, but more prominent during the autumn season after the chlorophyll pigments dissipate (Duy, 1999). This phenomenon is also evident in the varying pattern of disease damage observed throughout commercial wild blueberry fields; pointing to the potential to identify specific clones, thus reducing fungicide application on disease tolerant phenotypes with a focus on increasing yield (Abbey et al. 2018). The plants are growing naturally but are managed using several management practices (Eaton & Nams, 2012a), therefore, site-specific management practices have become an important aspect of the production of wild blueberries.

Wild blueberry management practices such as pruning, spraying, fertilizer application, pollination, and phenology monitoring, among others, are major production practices (Kinsman, 1993). Over the years, the practice of a blanket application of fungicides on commercial wild blueberry fields has existed, and this has increased the overall production cost. A recent study by Abbey et al. (2018), showed that susceptibility or tolerance to disease varies between lowbush phenotypes, thus a varying pattern of disease spread is observed. This development in the wild blueberry industry has focused attention on the need to adopt spot application rather than a blanket application of fungicides, thus, focusing attention on the susceptible phenotype like *V. angustifolium* f. nigrum, and excluding the more tolerant species, *V. myrtilloides* (Abbey et al., 2018). This way fungicide application is reduced, leading to a significant reduction in the overall

production cost. Efforts are also being made to monitor the vegetative and floral tissue growth and development, the status of the fungal pathogens (i.e. is sporulation occurring), and environmental conditions conducive for an infection to occur. Therefore, from a pest management perspective, the advancement of remote sensing techniques integrated into the management practices of a variety of fruit crops like strawberries, grapes, mango, and banana, among others (Peña et al., 2017; Usha & Singh, 2013) directs attention to possible and improved developments in disease management practices in lowbush fruits.

Digital transformation in field management practices using artificial intelligence networks has gradually revolutionized agriculture by making use of the increasing data generated from several remote sensing sources (Benos et al., 2021). Machine learning (ML) as a significant aspect in the modernization of farming uses computational algorithms to analyze and interpret large data (Benos et al., 2021; Liakos et al., 2018). Remote sensing in precision agriculture leads to the generation of large and complex data. However, data from these sources are processed using specific algorithms and software to recognize patterns, classify, predict, cluster, and make known the unseen information in data (Carleo et al., 2019; Liakos et al., 2018). In utilizing these methods, few studies on remote sensing in fruits have mainly focused attention on the use of spectral indices to improve tree crop classification (Panda et al., 2009; Peña et al., 2017; Usha & Singh, 2013), yield improvement (Rouse et al., 1974; Zhang et al., 2020), water-stress determination in oranges (Stagakis et al., 2012), and phenotype determination using high-throughput approaches (Han et al., 2018). Some major classification works conducted on blueberry have adopted the use of hyperspectral imagery that enables differentiation, thus, separating field classes using colour patterns (Panda et al., 2009, 2016; Peltoniemi et al., 2005). Panda, et al., (2009) successfully performed classification accuracies on two images from the wild blueberry field. While the earlier

classification was low with an overall accuracy (OA) of 57.9% and a kappa of 0.24, the second image had a high OA of 94.7% with a kappa value of 0.65, where Kappa defines the degree of agreement between the observed and measured data. This study identified only field classes such as vegetation, forest, and roads among other classes without consideration for clonal differences. The clonal differences observed in wild blueberries are significant as they affect yield potential, and disease spread (Abbey et al., 2018; Kinsman, 1993). Thus, a varying pattern of disease damage can be observed with varying levels of yield. In a similar study on a blueberry orchard, Panda, et al., (2016) classified three fields with OA's of 84%, 88%, and 95%. It can be observed that colours and features form an important aspect of field sensor identification; thus, vegetation colour can be used in phenotype classification (Bruzzone & Demir, 2014; Lehmann et al., 2018).

Over the past few years, remote sensing activities on site-specific management and production practices in the wild blueberry field have received some attention. Several remote sensing works focused on management practices have been conducted in wild blueberries; pesticide delivery using aerial scans (Marc-André Michaud et al., 2006), bare spot detection and estimations using digital photography (Zhang et al., 2010), yield estimation using reflectance measurements (Maqbool et al., 2010), weed detection and management (Hennessy et al., 2022), detection of management practices using a multispectral sensors (Marty et al., 2022), drought assessment (Chan et al., 2021) and phenology assessment using remote sensing (Barai et al., 2021). Despite the gains made, remote sensing techniques on phenotype differentiation or identification of disease susceptible phenotypes remain a major concern in wild blueberry production as this impacts yield and disease spread. Therefore, there is a need to improve the sustainability of the production system by focusing on susceptible and tolerant phenotypes in the field.

Given the significance and application of these precision agricultural techniques as described in several classification studies, there is potential in applying these remote sensing approaches in site-specific management in the wild blueberry field. Considering that several machine learning techniques including support vector machine (SVM), random forest (RF), and decision tree (DTs) when applied to images have performed well in classifying crop types (Peña et al., 2017), these approaches can be adopted. Therefore, the objective of this study was to determine if it is possible to examine the population structure and distinguish between, and possibly within the two predominate wild blueberry species using an SVM classification technique.

5.3 MATERIALS AND METHODS

5.3.1 Study area

Lowbush plants from two commercial fields located at Meadowvale (MV) and East Village (EV) were used for this study conducted in the 2019/2020 and 2020/2021 growing seasons, respectively. Meadowvale is one of the prime locations for wild blueberry cultivation, and this location comprises both new and old fields located within Nova Scotia, Canada, with the geographic coordinate (45.164799°N, 63.012645°W). The second trial located at East Village was conducted on a relatively small commercial wild blueberry field located within Colchester County in Nova Scotia, Canada, with the geographic coordinate (45.440486°N, 63.542147°W). These fields were sparsely dense with wild blueberry plant stands and were subject to all the management practices on a blueberry field. For this experiment, new fields are usually preferred because these fields mostly contain all the different wild blueberry phenotypes specifically *V. myrtilloides* (Kinsman 1993; personal communication, 2019).

These areas are prone to wet conditions that can be encountered for an extended period. This condition increases the devasting effects of diseases on the field which affects plant yield (D. Percival & Beaton, 2012). Therefore, fungicide treatments are applied to control Monilinia and Botrytis blight in the field.

5.3.2 Experimental setup and determination of phenotypes

Wild blueberries are not planted or cultivated like other row crops, like, maize, and tomato, therefore, twelve patches of each clone were identified across a plot size of 150 m x 100 m. Each identified patch of phenotype (Table 2.1) was tagged, and their geographic locations were acquired using an SX Blue Platinum GPS device. The identified phenotypes are listed in Table 2.1 of Chapter two.

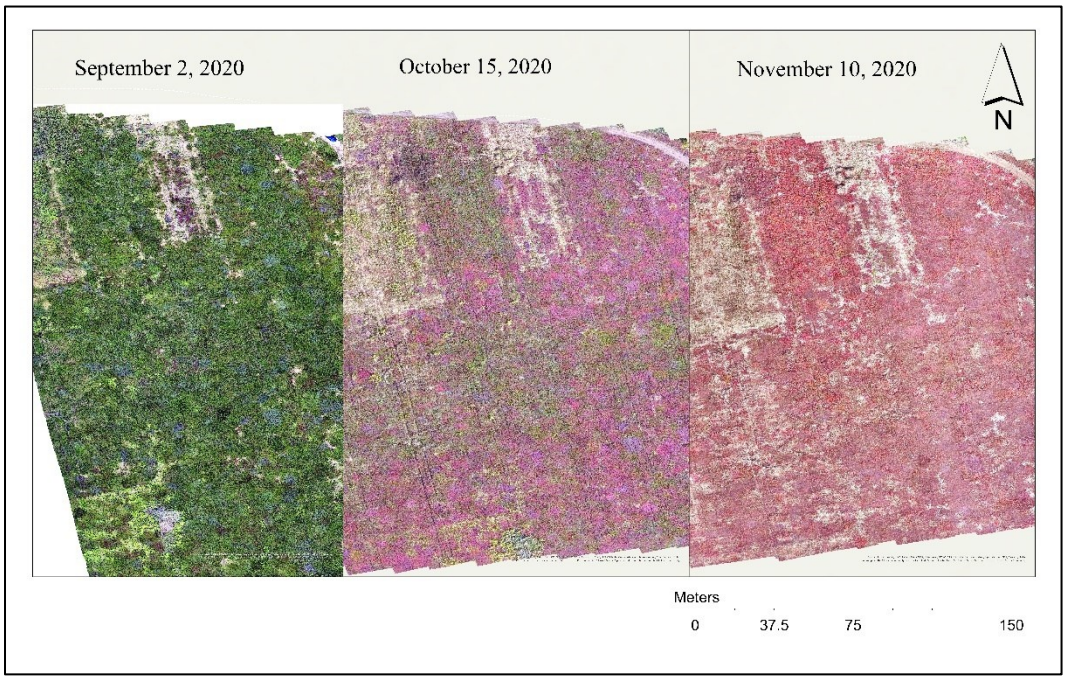

Figure 5.1. Changes in leaf colour observed on the wild blueberry field (East Village)

5.3.3 Multispectral platform and aerial image acquisition

The DJI Matrice Pro 600 along with the same camera sensors were used as described in Section 3.3.5 of Chapter three.

Table 5.1. Flight conducted during the 2019/2020 and 2020/2021 growing seasons using the RGB and multispectral cameras.

2019/2020			2020/2021		
Date	**Height**	**Resolution (cm/px)***	**Date**	**Height**	**Resolution (cm/px)***
10th Aug. 2019	60 m	4.0	2nd Sept. 2020	30 m	2.1
20th Sept. 2019	60 m	3.9	15th Sept. 2020	30 m	2.2
3rd Oct. 2019	60 m	3.8	28th Sept. 2020	30 m	2.2
16th Oct. 2019	60 m	3.9	15th Oct. 2020	30 m	2.2
22nd Oct. 2019	60 m	3.9	26th Oct. 2020	30 m	1.9
4th June 2020	30 m	0.7	10th Nov. 2020	30 m	2.2
17th June 2020	60 m	3.8	20th May 2021	30 m	2.1
7th July 2020	30 m	2.0	3rd June 2021	30 m	2.3
30th July 2020	30 m	2.0	17th June 2021	30 m	2.1
			8th July 2021	30 m	0.7
			8th Aug. 2021	30 m	0.7

* Multispectral image - Resolution above 1.8 cm/px

Flights were conducted at different time points (Table 5.1) along with the growing phase of the plant, particularly towards the end of its vegetative phase (June to November), to identify the different phenotypes through changes in leaf pigments. Flights were conducted under an open

sky condition (near noon) and in minimal winds to reduce the effects of distortions and shadows. Calibration and adjustments were carried out to minimize the effects of distortion on the quality of the imagery obtained.

5.3.4 Post-processing of aerial imagery

The development of an orthomosaics image followed the same approach as described in Section 3.3.5.1 in Chapter three. Subsequent processes were carried out in ArcGIS, and this was the classification aspect of the image processing. Therefore, the composite image was exported into ArcGIS Pro for the classification and identification of phenotypes. ArcGIS Pro version 10.5 was used for digitizing and further processing of images as shown (Figure 5.3).

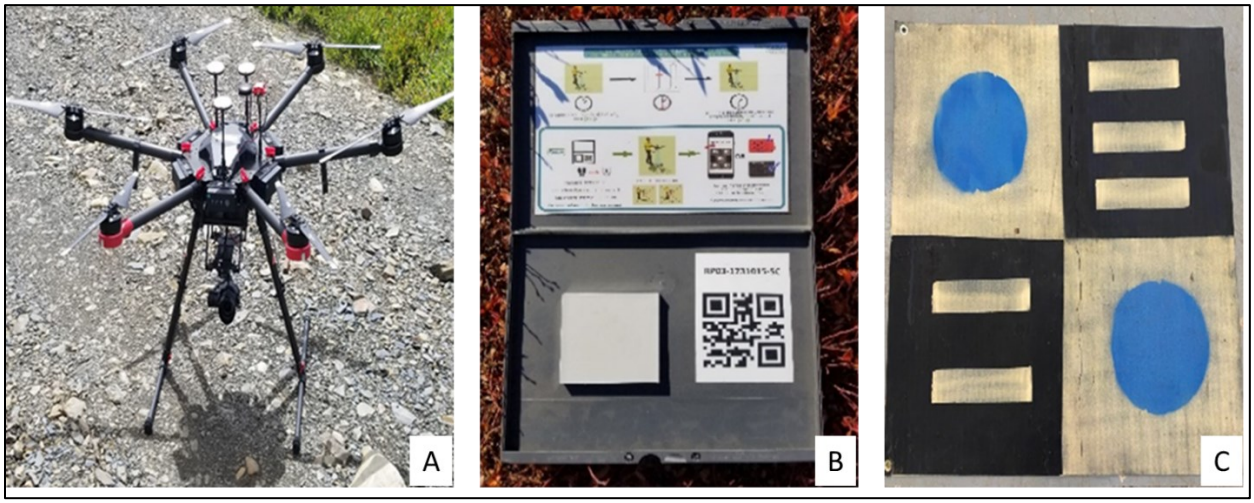

Figure 5.2. Images of some tools used in conducting a UAV flight. (A) DJI Matrice Pro 600 equipped with a Zenmuse X5 camera, (B) Calibration reflectance panel, and (C) Ground control mat.

Orthomosaic images from the different dates were analyzed to identify images that had pronounced differences in phenotypes. After image sampling, it was observed that images taken after early October had challenges (no colour pattern) (Figure 1) with phenotype identification,

with similar challenges to imagery taken from early season to July. Therefore, images taken between August and early October were settled upon for classification with their vegetative stage mainly at the V6 stage. Furthermore, despite using the two cameras, the multispectral images were considered for classification while the RGB orthomosaic imagery served as complementary data.

5.3.5 Image classification of phenotypes

A supervised pixel classification was conducted on the multispectral image by digitization using polygons to develop classes for the training samples. In this classification process, random accuracy points were generated by the create assessment points tool and this was updated by the updated accuracy assessment points tool. The combination of these tools ensured that points had valid class values for the classified and ground truth fields. This process generated the user accuracy and producer accuracy for each class as well as the overall accuracy and the kappa index. The user's accuracy indicates a false positive classification, where pixels are incorrectly classified when they should have been classified as something else. Conversely, the producer's accuracy indicates false negatively classified pixels, where some pixels are misclassified (ArcGIS Pro 2.8, ESRI Resources 2020).

Accuracy assessment is significant in classification studies; thus, the workflow provided the needed steps and processes to generate a confusion matrix table for the various classifications conducted. In the study, ArcGIS Pro software was the main platform used in this process. Accuracy evaluation in ArcGIS Pro worked well and is similar to "extract points" as adopted in other procedures like ArcMap. In this study, a workflow (Figure 3) was adopted for the accuracy evaluation in our classifications conducted using ground truth points. All major steps and processes have been highlighted (Figure 5.3). ArcGIS was utilized to establish training classes for the pixel

classification method through a Support Vector Machine (SVM) tool (Lewis & Brown, 2001). An accuracy assessment was conducted using the training samples manager and classification tools. A confusion matrix was later generated for the classification (Deindorfer, 2016; ESRI Resource, 2023; ESRI Resources, 2020).

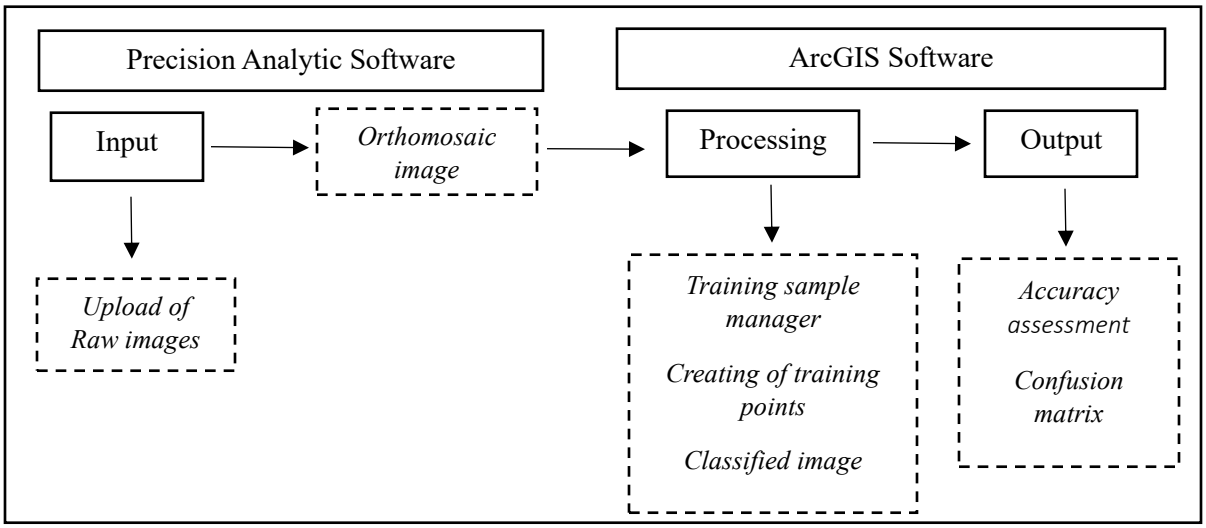

Figure 5.3. General workflow adopted in the phenotype classification process.

5.3.6 Support vector machine (SVM), training samples, and validation

The SVM is a supervised classification method that was adopted in this study. It is one of the most widely used classifiers because it provides some advantages compared to examples like the maximum likelihood classification method. Unlike other classifiers, SVM needs only a few samples that are not required to be normally distributed. Additionally, it handles noise, correlated bands, and uneven numbers or sizes of training samples within each class (ESRI Resources 2020). In this study, about 40 training sample pixels were selected per class. Of this number, about 75% of the samples were used as training sets with the remaining 25% used as validation sets during the cross-validation process. Validation of the results was conducted using GPS points of identified phenotype locations on the field.

5.3.7 Hyperspectral platform

The hyperspectral platform adopted was the same as described in Section 4.3.5 in Chapter four. In this study, both ground and aerial measurements were simultaneously conducted.

The twelve patches of each phenotype were identified and tagged. Ten spectral readings were collected from each patch, amounting to 720 spectral readings. For analysis, spectral readings were averaged into a single spectrum for each patch. Since there was complexity and the constraint of time in analyzing high dimensional data, the high dimensional data was reduced by the selection of optimal bands. Therefore, the reduction process was done using factor 5 due to the high correlation between adjacent wavelengths (Figure 4). In consequence, only 300 wavelengths were considered for analysis (AL-Saddik et al., 2017; Heim et al., 2019). These wavelength bands fell between 349 nm to 1601 nm, with the other section of the wavelength spectrum (1601nm to 2500nm) characterized with noise and was thus excluded in the analysis. However, for analysis only wavebands from 350 nm to 1000 nm were considered.

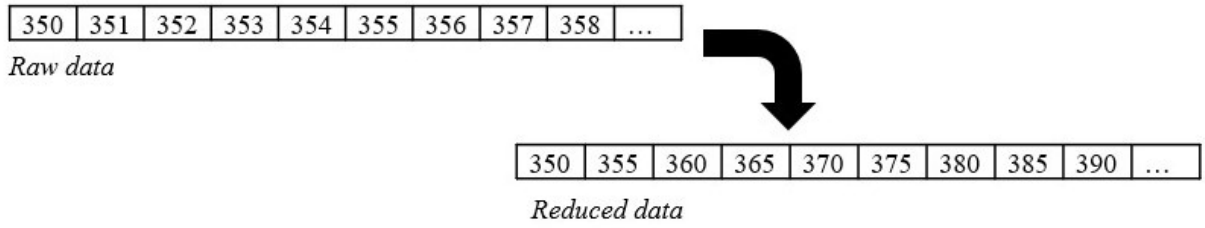

Figure 5.4. Process for wavelength data reduction of a hyperspectral radiometer

5.3.8 Accuracy for image classification

Analysis of the classification was done based on the ground-truthing from the site. All the randomly selected pixels from the classified images were compared with corresponding land use

classes on the ground to verify and determine the classification accuracy of the supervised pixel classification technique of the identified phenotypes. Accuracy assessment forms the last step of every classification process as this quantitatively assesses the correct selection of pixels to their land cover classes (Rwanga & Ndambuki, 2017). Using ArcGIS Pro (software version 2.8, ESRI Resources 2020), an accuracy assessment was developed for the classification conducted.

Evaluation on the identification of phenotypes was done based on four criteria for the performance of the classification process. These included the producer's accuracy (Eqn. 1), user's accuracy (Eqn. 2), overall accuracy (Eqn. 3), and the kappa index (Eqn. 4). Higher accuracies imply better performance of the image classification process (Abd-Elrahman et al., 2021; Panda et al., 2009). The equations for the following accuracy parameters are as follows:

Producer accuracy

$$= \frac{\text{Number of correctly classified point in a class}}{\text{Total number of points within a class}} \text{ x } 100 \quad (1)$$

User accuracy

$$= \frac{\text{Number of correctly classified point in a class}}{\text{Total number of classified points in a group out of the entire points selected}} \text{ x } 100 \quad (2)$$

Overall accuracy

$$= \frac{\text{Total number of correctly classified points}}{\text{Total numner of reference samples chosen}} \text{ x } 100 \quad (3)$$

Kappa index

$$= \frac{N \sum_{i,j=1}^{r} x_{ij} - \sum_{i,j=1}^{r} (x_{i+} x_{j+})}{N^2 - \sum_{i,j=1}^{r} (x_{i+} x_{j+})} \quad (4)$$

Aside from the three accuracy methods, Kappa analysis, which is a discrete multivariate analysis that measures the levels of agreement or accuracy, was used in this study. It measures the level of agreement between two raters with an independent criterion of assessing a condition (Abd-Elrahman et al., 2021; Panda et al., 2009).

Where;

r = the number of rows in error matrix, N = total number of observations (pixels), X_n = total observations in row i and column j, X_i+ and X_j+ are the totals of row I and column j, respectively.

5.3.9 Spectral analysis

Linear Discriminant Analysis (LDA) is popularly known as a discrimination or classification method and is used based on the theory of separation or characterization of samples into groups. Therefore, outputs from the cross-validation discriminant analysis were used to compute an accurate assessment result on spectral data taken from the respective imagery dates. Minitab software (version 19, Minitab Inc.) was used to perform the discriminant analysis on spectral readings between the different phenotypes of the wild blueberry field as adopted by (Peña et al., 2017) and (Zheng et al., 2018). This approach also led to the generation of the user, producer, and overall accuracies, which enabled verification of the performance of the classification process.

5.4 RESULTS

Classification analysis on multispectral images and spectral data was conducted to determine the potential for identifying phenotypes in wild blueberry fields. Despite the challenges encountered in the field, results from these two methods suggest a potential to identify specific phenotypes in the field.

Spectral reflectance measurement on all six phenotypes proved similar, however, some slight differences were observed (Figure 5.5). Across both the visible light region (VIS) and the near-infrared region (NIR), similar reflectance was observed. However, it was observed that *V. angustifolium* species generally observed a higher reflectance at the NIR (700nm to 1400nm) compared to the *V. myrtilloides* species.

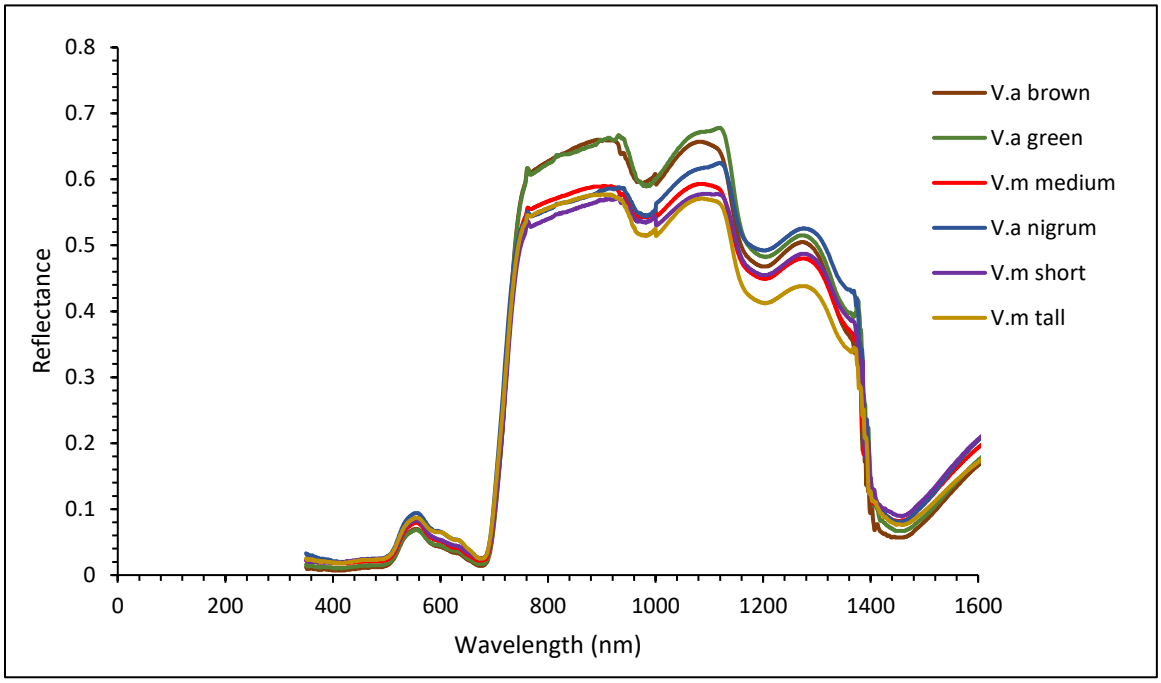

Figure 5.5. Spectral reflectance from all 6 phenotypes

Furthermore, in the visible light region, no clear patterns were observed. Other water-absorbing regions caused noisy portions, thus the exclusion of those sections (1601nm to 2500nm). However, it was observed that between the 999 nm and 1003 nm range, some spectral variations

were determined. All three *V. myrtilloides* (short, medium, and tall) species observed similar progressions whereas *V. angustifolium* nigrum observed a sharp but upward progression from 998 nm to 1002 nm (Figure 5.5). *V. angustifolium* green observed no changes in that region. However, upon sampling 720 spectral readings, it turns out that these variations were not consistent among the various phenotypes, but they only signified water-absorbing regions.

Table 5.2. Accuracy assessment on spectral readings for detecting species of *Vaccinium angustifolium* (VA) and *Vaccinium myrtilloides* (VM) at East Village (2020/2021 field season).

Phenotypes	**VA green**	**VA brown**	**VA nigrum**	**VM short**	**VM medium**	**VM tall**	**Total**	**U. Accuracy (%)**
VA green	2	2	2	1	2	1	10	1.18
VA brown	15	6	8	9	7	4	49	5.79
VA nigrum	57	69	77	63	63	44	373	44.09
VM short	2	1	4	1	2	2	12	1.42
VM medium	7	9	12	7	6	5	46	5.44
VM tall	58	54	38	60	61	85	356	42.08
Total	141	141	141	141	141	141	846	
P. Accuracy (%)	1.42	4.26	54.61	0.71	4.26	60.28		20.92%

VA – *Vaccinium angustifolium* and VM – *Vaccinium myrtilloides*

Discriminant analysis of the spectral data points to a potential in the identification of some clones. *V. myrtilloides* (VM tall) and *V. angustifolium* f. nigrum were the two outstanding clones among the others, that showed high user and producer values (Table 5.2). Though a slightly lower value is observed under nigrum it confirms the outcome from the orthomosaic imageries (Table 5.3); that nigrum can be picked out on the field.

Accuracy and precision are important aspects of aerial data analysis; thus, the computation of accurate assessment results became relevant for its reliability. The high kappa value observed indicated the reliability of the results obtained (Table 5.3). The initial classifications of the 2020/2021 imagery (Figure 5.6A) were aimed at identifying all six phenotypes, which led to the generation of an output (mixels), making it difficult to differentiate between all six phenotypes. However, *V. a.* f, nigrum stood out among all the other phenotypes (Figure 5.6B and 5.7[A&B]) indicating that phenotype separation can be achieved between August and September of each growing season. Based on that finding, identification was narrowed down to nigrum since it was easier to differentiate nigrum compared to the other phenotypes (Figures 5.6A & B).

Table 5.3. Confusion matrix and accuracy assessment on image classification for the identification of *Vaccinium angustifolium* nigrum at East Village in the 2020/2021 field season (Image taken on 15th September 2020)

Classification	V. nigrum	Vegetation	Red leaves	Bare area	Total	U. Accuracy (%)	Kappa (%)
V. nigrum	15	11	3	0	29	52	
Vegetation	1	33	0	0	34	97	
Red leaves	0	0	10	0	10	100	
Bare ground	0	0	0	30	30	100	
Total	16	44	13	30	103	0	
P. Accuracy (%)	94	75	77	100	0	85	
Kappa (%)							80

Similar classifications were conducted on the 2019 image data from Meadowvale; however, the classification output was moderately low with similar mixels and misclassifications encountered (Figure 5.8).

Classification results on East Village (Figure 5.7 and Table 5.3) have shown that bare area and nigrum had high producer's accuracy of 100% and 94% respectively, with vegetation and red leaves obtaining 75% and 77% respectively. At the user accuracy level, bare ground and red leaves had the highest percentage, with nigrum being the least. An overall accuracy value of 85% indicated high chances of identifying the phenotype, nigrum, and other field classes.

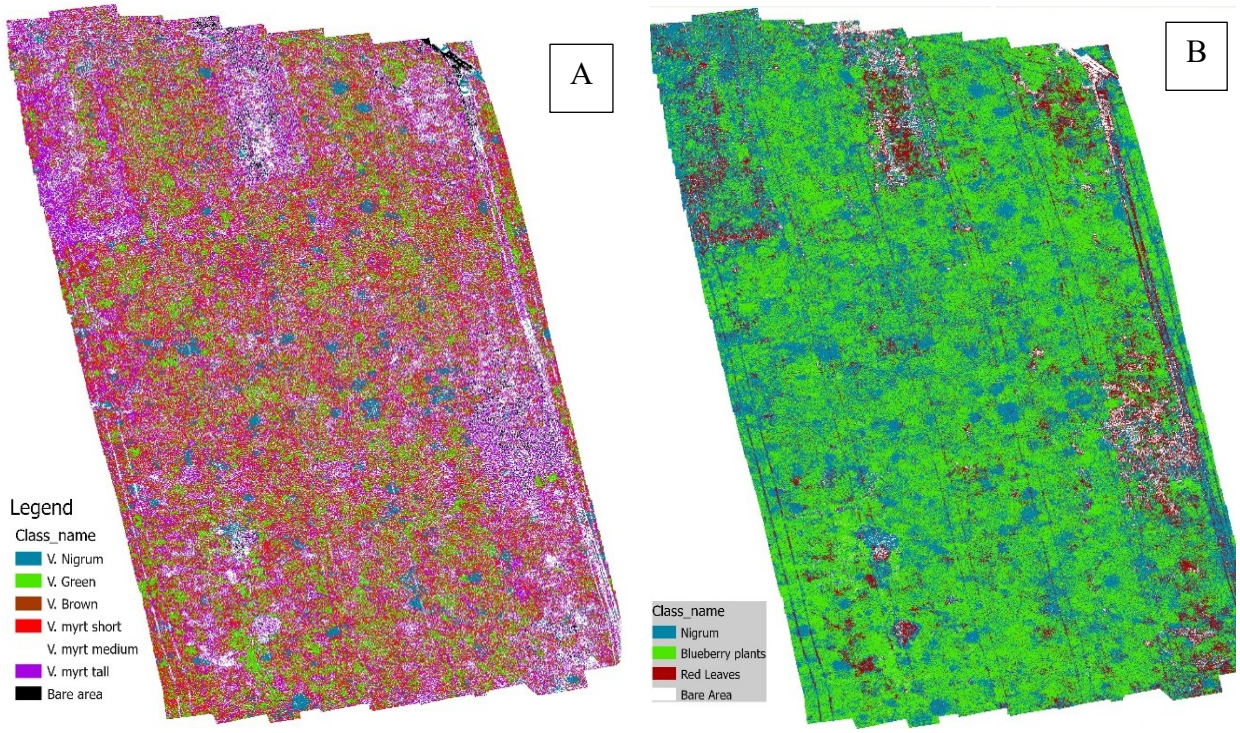

Figure 5.6. Classified images of wild blueberry phenotypes and other classes on the East Village. (A) Identification of all phenotypes and (B) Identification of VA nigrum and other field classes.

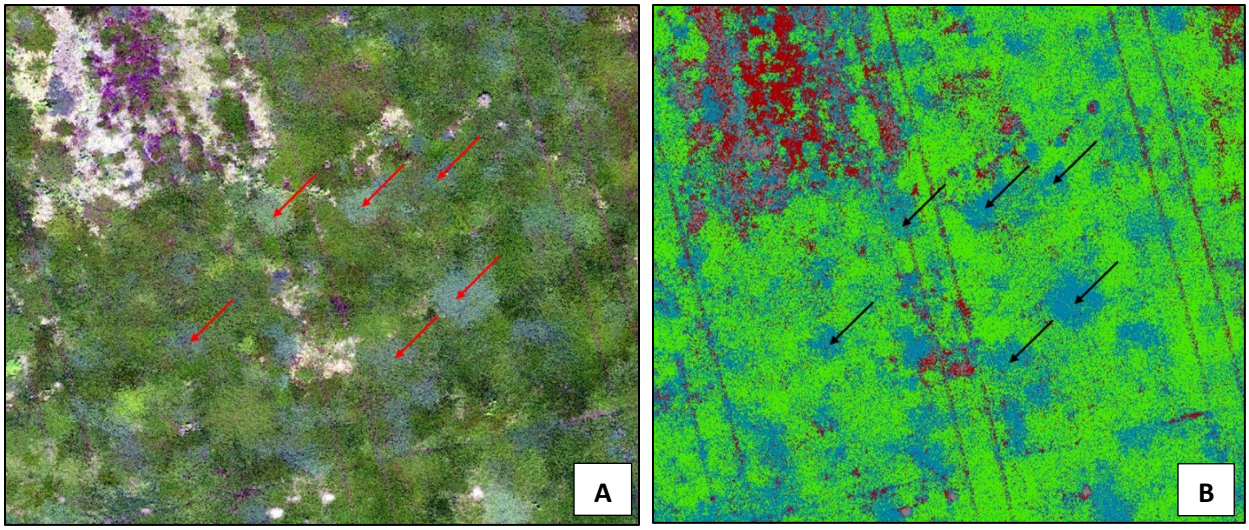

Figure 5.7. Identified *V. angustifolium* nigrum on the wild blueberry field. (A) Raw orthomosaics image and (B) Classified image identifying nigrum locations on the field (arrows indicating nigrum location).

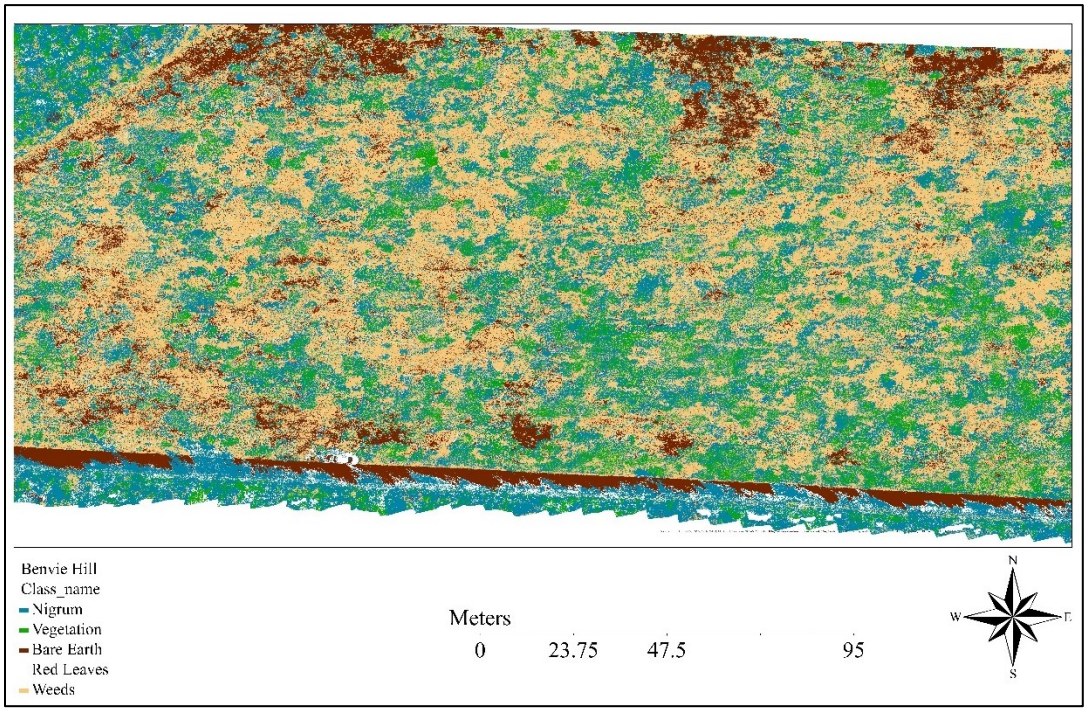

Figure 5.8. Classified images of wild blueberry plants and other field classes from Meadowvale in the 2019/2020 field season (Image taken on 3rd October 2019).

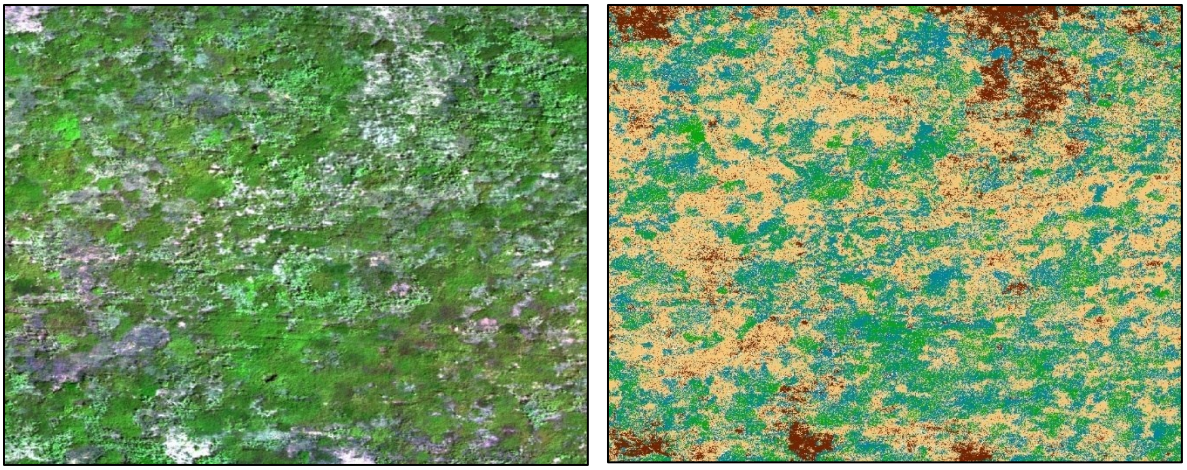

Figure 5.9. Identified field classes from the 2019/2020 field season at the Meadowvale location.

Table 5.4. Confusion matrix and accuracy assessment on image classification for the identification of *Vaccinium angustifolium* nigrum at Meadowvale in the 2019/2020 field season.

Class	Nigrum	Vegetation	Bare earth	Red leaves	Weeds	Total	U. Accuracy (%)	Kappa (%)
Nigrum	7	0	0	0	0	7	100	
Vegetation	24	12	2	22	19	79	15	
Bare earth	2	0	7	0	0	9	78	
Red leaves	0	0	0	0	0	0	0	
Weeds	8	2	1	6	38	55	69	
Total	41	14	10	28	57	150	0	
P. Accuracy (%)	17	86	70	0	67	0	43	
Kappa								28

Though phenotype identification was low (Figures 5.8 and 5.9), the classification process identified major field classes. The same plant variation observed at the East Village trial was not

observed in the Meadowvale trial, thus phenotype classification from the Meadowvale location did not yield the same outcome as that of East Village. Furthermore, output values from the confusion matrix showed that it was difficult to achieve a good classification from the imagery taken at the Meadowvale location (Table 5.4).

It can be observed that the overall classification (43%) conducted on the Meadowvale imagery was moderately low (Table 5.4). Though misclassifications were observed, it was more under the vegetation class. This assessment provides a low kappa value of 28% which implies a poor classification model.

5.5 DISCUSSION

Having achieved relevant outcomes from the preliminary assessment of wild blueberry coverage and disease assessments between phenotypes on the field, this study was aimed at determining the possibility of examining the population structure and distinguishing between, and possibly within the two predominate wild blueberry species. The remote sensing equipment, UAV, and the Field Spectroradiometer have shown potential and capability in identifying mixed vegetation, forest, woodland, and grassland, as have been demonstrated in several studies using advanced processing techniques (Peltoniemi et al. 2005; Panda, et al., 2009; Usha and Singh 2013; Panda, Hoogenboom, and Paz 2016; Peña, et al., 2017). Despite challenges faced in the wild blueberry field, this study went a step further by showing the possibility of differentiating between phenotypes on the field

using these remote techniques coupled with an advanced machine learning technique like the support vector machine (SVM).

A supervised pixel classification method was performed on the orthomosaic images with a discriminate method applied to the spectral data. Though both methods target phenotypes, the supervised pixel classification method distinguished other classes on the field while the discriminate method focused only on phenotypes. Classification outputs have shown that the blueberry plant can be delineated and distinguished on the field (Table 5.2 and 5.3). Thus, the accuracy assessment (Table 5.2 and 5.3) using the user accuracy, producer accuracy, overall accuracy, and kappa value proved that point. These findings agree with that of Panda, et al., (2009) who used satellite imagery to distinguish blueberry vegetation from mixed vegetation, with overall accuracy and kappa statistics of 94.7% and 65% respectively. In that study two classifications from two images were conducted, however, the authors settled on the better classification. Despite this similarity, our classification work proved superior based on overall accuracy. It was obvious that variability on the blueberry field was a major challenge, but this is the first time a study like this has been conducted in wild blueberry plants. In this study, the initial classification which was aimed at identifying all six phenotypes among other field classes like weeds and bare earth proved challenging, coupled with the elevated level of variability observed on the field. The output (mixels) made it challenging to clearly identify some phenotypes while other phenotype populations were either under or overestimated in the identification process. This level of variability in the field (Drummond, 2019) made it necessary for the study to focus on an outstanding phenotype i.e., *V. angustifolium* f. nigrum. Compared with the 2019 classification work, it can be observed that nigrum was not as outstanding as the classification performed on the image obtained from the trial at the East Village location, thus, that classification work did not

meet the target. This is largely explained by the prevailing conditions of a field and the time a flight is taken. Time is key in visibly identifying the differences between phenotypes as this impacts the leaf pigment (Duy, 1999).

The wild blueberry field is heterogeneous and thus consists of different phenotypes (Duy, 1999). However, the natural form of the field introduces levels of complexity in the identification process as phenotypes are scattered on the field (Penman & Annis, 2005). Though the classification method identified nigrum, with a 52% user's accuracy, this implies that the identified phenotype had a 48% misclassification. Rwanga and Ndambuki (2017) states that the user's accuracy gives reliability to the user, thus, this classification accuracy is more relevant to its utilization on the field. Therefore, a 52% user's accuracy for nigrum is moderately high, but can be improved upon. However, this observation can be attributed to a few factors including variability (crosses among plants) and the reflectance and scattering properties of the other vegetation classes. This agrees with Panda, et al., (2016), whose work on blueberry orchards was similar to a previous study they conducted in 2009 (Panda et al., 2009). The high variability observed on the field can arise from possible crosses that exist between the different phenotypes. Despite the non-compatibility between diploids (*V. myrtilloides*) and tetraploids (*V. angustifolium*), studies by Griffiths, Pegler, and Tonguthaisri (1971) and Vander Kloet (1978) established that, *V. angustifolium* and *V. myrtilloides* can hybridize but with low percentages of success. Therefore, the possibility of germinated phenotypes adding up to the levels of variation observed on the field is high. Since identification was done based on specific leaf colour types using pixels, then the possibility of identifying similar leaf colour types that do not reflect a specific phenotype class may be high. This point is well explained by Kinsman (1993) who expounds that there is so much variability in the field. This situation may give rise to a spectrum of colours displayed on the field. It is possible

some species over time can fade out on the field leaving specifically the dominant ones. Therefore, though the *V. angustifolium* f nigrum value observed under the user's accuracy was relatively low, it buttresses the point that variability may account for these situations. Despite the use of the support vector machine (SVM) in the identification process, the leaf colour range posed a major challenge, but findings from both the UAV and Field Spectroradiometer points that *V. angustifolium* f. nigrum can potentially be identified.

The field spectroradiometer which focused solely on phenotypes complemented the UAV in its identification and classification. With a moderately low overall accuracy level of 20.92% (Table 5.2), it explains that *V. angustifolium* f. nigrum and *V. myrtilloides* (tall) can potentially be identified in the field. Considering the user accuracies for VA f. nigrum (44.09%) and VM tall (42.08%), which is relevant for their utilization on the field, this poses a significant challenge. Despite this clarity, it focuses attention on the fact that there were lots of misclassification of phenotypes, and this can best be explained as phenotype variability, as already highlighted by Kinsman (1993). This may further shift focus to the similarities between these phenotypes rather than focusing attention on their spatial differences, because these phenotypes keep changing all the time. Therefore, though there are striking differences in stem colour, flower colour, pubescence on some stems and leaves, and fruit colour (Ashley, 2020; Jamieson, 2008), these phytomorphological differences may command little to no spectral differences in the plant.

Time is of the essence in the identification of these phenotypes, thus, leaf colour differentiation (Duy, 1999) between August and September of every growing season is ideal in picking out VA f. nigrum. Whereas it is easy to pick out *V. angustifolium* f. nigrum and *V. myrtilloides* on the field by eye, it is very difficult to pick them out at the early stages of the season using the UAV. This is because the pubescence on the stems of *V. myrtilloides* plant (Wood et al.,

2013) gives it a greyish-white colour which is similar to plant debris on the field, making the classification of images taken during the early growing phase very difficult if not impossible. It becomes more challenging when plant leaves assume an all-green leaf colour around June – July of both the vegetative and cropping phases, though some mixed colouration (tinges of red) can still be observed. After this phase, leaf colour differentiation begins to set in with a more normal form taking place at the vegetative phase. Berry yield harvest as a significant aspect of the production process inflicts levels of stress on the plant at the cropping phase, which leads to changes in leaf colour. Though in some cases differentiation can be observed before harvest, fruit colour and the harvesting process interfere with this phenomenon. Colouration from this point becomes more prominent in all phenotypes with no exception and pattern. Over time, plant leaves assume different shades of red through to blue colour and fall off the plant (Duy, 1999; Raven et al., 1992).

Though the identification of phenotypes in the wild blueberry field is faced with challenges, developments from this study have identified *V. angustifolium* f. nigrum. This study impacts disease management through the development of prescription maps for the spot application of fungicides on susceptible phenotypes rather than a blanket application in the field. This implies better returns and cost savings on the overall production with a reduction in the amount of chemicals applied to the environment. Additionally, variable rate application of agrochemical products such as fertilizers, can be adopted and applied to plants on the field. Further investigations can be considered on phenotypic variability in yield. This is necessary because differences in phenotypes (Agriculture, Aquaculture, and Fisheries, 2014) contribute largely to the overall yield variation observed on the field, even more as commercial fields are dominated by these two species.

5.6 CONCLUSION

This study aimed to potentially identify phenotypes on the wild blueberry fields using remote sensing techniques, and our outcome was affirmative. There was potential in identifying *V. angustifolium* f. nigrum and the differentiation of other classes on the wild blueberry field. Though there were significant challenges in identifying *V. myrtilloides*, the time of the season and the plant's developmental stage were key in their determination. Identification of phenotypes at the early stages of growth using the UAV was challenging. However, there was potential in phenotype identification between August and October when autumn begins to set in, and colour differentiation becomes prominent in the matured leaves (at vegetative stage 6) of the plant. Therefore, phenotypes as important as they are, over an extensive acreage of land, yield phenotypic differences may have a direct and significant bearing on the quantities of berries harvested from a field. Therefore, identifying disease-susceptible and tolerant phenotypes, and high-yielding phenotypes coupled with centered and good management practices can lead to potentially high-yield generation from the field.

The image classification method proved highly effective with high accuracy values as compared to the field spectroradiometer which targeted only phenotypes. Considering some slight differences observed, the spectroradiometer confirms the identification of nigrum and a determination of *V. myrtilloides* tall. However, the process is marred with challenges that are common to wild blueberry fields. Despite these challenges, further studies that explore other techniques can be undertaken in the identification of *Vaccinium myrtilloides*.

CHAPTER 6: REMOTE ASSESSMENT OF MONILINIA AND BOTRYTIS FLORAL DISEASES IN WILD BLUEBERRY FIELDS

6.1 ABSTRACT

Monilinia blight and Botrytis blossom blight diseases are endemic to most wild blueberry fields, affecting foliage and flowers respectively. Destructive techniques have long been used for disease assessment; however, this can be improved by using remote sensing techniques. Therefore, this study aimed to assess the potential of using multi- and hyperspectral sensors to detect and evaluate the impact of Monilinia and Botrytis blight disease on the wild blueberry field. Two approaches were used, (i) plot, and (ii) patch assessment using a 5-band Micasense camera and a hyperspectral radiometer respectively. Two commercial fields located at Lemmon Hill and Farmington were used, and at each site a randomized complete block experimental design with six replications, four treatments, and a plot size of 6 x 8 m, with a 2 m buffer between plots. Treatments consisted of (i) untreated control, (ii) Monilinia control, (iii) Botrytis control, and (iv) Monilinia and Botrytis control. Furthermore, 3 patches each of Monilinia blight, Botrytis blight, and healthy plant were also identified, and spectral readings were taken. Plant health assessments were conducted using vegetative indices (VIs) and field methods. Classification and correlation analyses were conducted on disease parameters. Results showed that there were no significant treatment differences in high values of VIs compared with non-treated plots. Correlation analysis showed that the light vegetative indices especially VARI, had good correlations (-0.41 – 0.58) with MB leave disease and BB floral disease. Results using the patch assessment have shown that there are significant differences in the spectral response of healthy and diseased tissues, especially in the near-infrared regions (715 nm – 1050 nm). This difference had a direct correlation with disease severity and identified specific wavebands of interest. The three classifiers behaved similarly, but SVM and RF

performed better than KNN with an overall classification of 96.6%. Aside from BB, the classification of the levels of disease severity was successful under all three classifiers. Overall, results have illustrated the potential of using visible light vegetative indices to differentiate and assess MB and BB disease pressures.

Keywords: Remote sensing, multispectral, Monilinia blight, Botrytis blight, wild blueberry, classification

6.2 INTRODUCTION

Wild blueberry plants are challenged with several diseases, but prominent among them are the floral diseases consisting of Monilinia blight and Botrytis blossom blight disease (Hildebrand & Braun, 1991; Lambert, 1990; Penman & Annis, 2005). Monilinia blight disease caused by *Monilini vaccinii-corymbosi* (Reade) Honey (*M.vc*) and Botrytis blossom blight disease caused by *Botrytis cinerea* Pers.:Fr are yield-limiting diseases that affect both foliage and flowers of the plant (Hildebrand & Braun, 1991; McArt et al., 2016). In Nova Scotia, Botrytis blight disease has led to about 30 – 35% loss of wild blueberries (Delbridge & Hildebrand, 1995). The loss of blueberries because of Monilinia and Botrytis blight may vary in severity depending on the prevailing conditions on the field (Thompson & Annis, 2014). Disease severity varies on the field; thus, it depends on the temperature and wetness of the field, the inoculum levels, and the history of the field (Delbridge & Hildebrand, 1997b; Oudemans et al., 2018). However, assessment of disease pressures on the field has been done through a traditional intensive sampling using line transects, and visual scouting of diseases which can be laborious, time-consuming, expensive, and requires a high level of expertise (Abdulridha et al., 2020). Therefore, shifting from this traditional approach will require some advanced techniques.

Advancements in the use of remote sensing techniques have allowed for a shift from the destructive approach to a non-destructive assessment of diseases in the field (Jones et al., 2007; Khaled et al., 2018; Tao et al., 2020). Developments in research have shown the capability of remote techniques in detecting disease and their development in several crops (Khaled et al., 2018). A study conducted by Mahlein et al., (2013) developed a spectral disease index (SDI) to differentiate between three diseases (Cercospora leaf spot, sugar beet rust, and powdery mildew). With several other techniques, diseases have been determined in crops (Calderón et al., 2013; Heim et al., 2019; Huang et al., 2012; Mirandilla et al., 2023; Zheng et al., 2018). Abdulridha et al., (2019) used a multispectral sensor to detect laurel wilt disease in avocados. These techniques have been used to observe changes and detect pests and diseases in several crops; *Cnaphalocrocis medinalis* in rice (Huang et al., 2012), *Schizaphis graminum* in wheat (Yang et al., 2005), and yellow rust disease in wheat (Zheng et al., 2018) among others. With an added potential in detecting or discriminating diseases, VIs such as the normalized difference vegetative index (NDVI), green leaf index (GLI), green, red vegetative index (GRVI), enhanced NDVI (ENDVI), and chlorophyll index (Cl) among several indices have been used in the detection process (Mahlein et al., 2013; Tilly et al., 2015; Xue & Su, 2017a). Therefore, depending on the disease severity, VIs can discriminate between healthy and diseased plants on the field. This process is influenced by the pigment composition of the plant leading to some unique spectral signatures. Despite the success of these techniques, these methods have not been explored in the wild blueberry fields for disease assessment. Remote detection of Botrytis blight has been conducted in strawberries (Siedliska et al., 2018), and eggplant leaves (Wu, Feng, & He, 2008), and recently in cavities using ultrasonic imager (Liu et al., 2021). However, little is known about both Monilinia blight and Botrytis blossom blight using remote detection in wild blueberries. Since major studies conducted

on wild blueberry fields focus on other assessments, much consideration is needed in disease assessment.

The significance of disease and its management is paramount in every agricultural enterprise including wild blueberries. Though major investments in research and development point to the destructive approach (Percival & Beaton, 2012), there is a need to potentially explore the non-destructive approaches. Rather than laboratory assessments which is the popular method, field assessment can be explored using rapid automated remote sensing techniques. Therefore, the ability to detect or identify diseases can be realized using sensors such as multispectral and hyperspectral sensors. This study was aimed at exploring the use of both multispectral and hyperspectral sensors in disease detection. Therefore, the objective of this study was to assess the potential of using vegetative indices to differentiate and determine between healthy and diseased plants in wild blueberry fields.

6.3 MATERIALS AND METHODS

6.3.1 Disease assessment by plots

6.3.1.1 Study area

Across five growing seasons (2019, 2020, 2021, 2022), seven trials were set up in different commercial fields for this study. These sites consist of Farmington (FT), Lemmon Hill (LH), Kemptown (KT), Mount Thom (MT), Web Mountain (WM) and Fox Point (FP). These sites are considered among some of the main blueberry production sites located in Nova Scotia, with geographic coordinates (45.573652°N, 63.894130°W - FT), (45.188587°N, 62.874343°W - LH), (45.498936°N, 63.100716°W - KT), (45.492214°N, 62.992821°W - MT), (45.567471°N,

63.693730°W - WM) and (45.395997°N, 64.505709°W - FP) respectively. These areas are prone to wet conditions that can be encountered for an extended period. This condition increases the devasting effect of diseases on the field which affects plant yield (Percival & Beaton, 2012).

6.3.1.2 Experimental design and fungicide application

The same experimental design and fungicide application as discussed in Sections 4.3.2 and 4.3.3 of Chapter four was adopted.

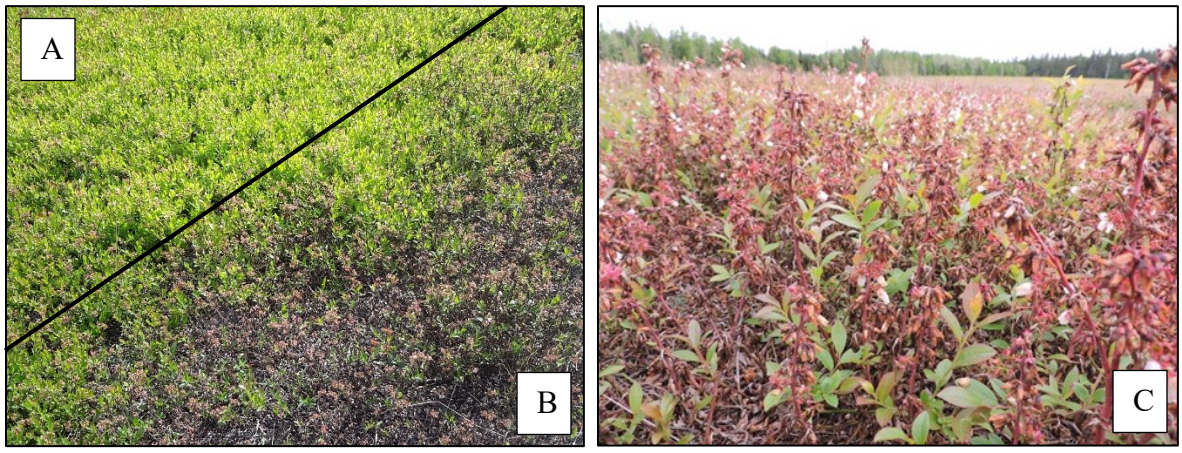

Figure 6.1. Disease spread on the wild blueberry field. (A) A healthy blueberry patch, (B) Monilinia blight disease-infested patch, and (C) a Botrytis blight disease-infested field

6.3.1.3 Disease assessment, yield component, and berry yield

This study adopted the methods of Percival & Beaton, (2012) as described in Section 4.3.4.1 of Chapter four. Stem collection was done seven to ten days after the initial fungicide application and at weekly intervals until fruit set. The stem samples were kept in plastic bags, placed on ice, and then taken back to the laboratory for further examination of Monilinia and Botrytis blight disease developments (incidence and severity). Disease incidence was determined as the proportion of

floral buds or leaf buds with visual symptoms of disease within a stem (**A**). Severity was estimated by proportion tissue area of each flower with visual symptoms of Monilinia and Botrytis blight on a stem. Disease severity was assessed as the percentage of floral tissue area or leaf tissue area infected with visual symptoms of the disease on the stem (**B**). Other parameters to be recorded include stem length, number of vegetative nodes, number of floral nodes per stem, and number of flowers per stem of buds and bud stages.

A. Disease incidence% (E.g., Floral/Leaf basis):

$$= \frac{\text{Number of floral nodes/tissue or vegetative nodes/tissue affect with at least a lesion}}{\text{Total number of floral or vegetative nodes}} \text{ x } 100$$

B. Disease Severity (E.g., Surface Area Basis) 0 to 100% rating scale where 0 = no disease and 100% = entire surface of each blossom/ leaf tissue area affected (average of the overall percentage of blossom/ leaf surface area affected)

Berries were harvested in August with a forty-tine commercial wild blueberry hand rake from six randomly selected 1 m^2 quadrat in each plot. Harvested berries from each plot were weighed with an Avery Mettler PE 6000 digital balance, and data was recorded.

6.3.2 Data collection

6.3.2.1 Remote assessment by plot using the micasense camera

The process described and used in Sections 3.3.5 and 3.3.5.1 of Chapter three was adopted. However, imagery was acquired within an interval of seven to twelve days.

6.3.2.2 Disease assessment by patch using the hyperspectral sensor

Three patches of each treatment, MB, BB, and healthy (control), were identified separately and tagged. Field assessments of the diseased patch were calculated as a percentage area of plant tissue infected with the disease (Percival & Beaton, 2012). Therefore, spectral readings were taken at the 3 disease severities: low (1 – 30%), moderate (30 – 70%), and high (70 – 100%) disease damage.

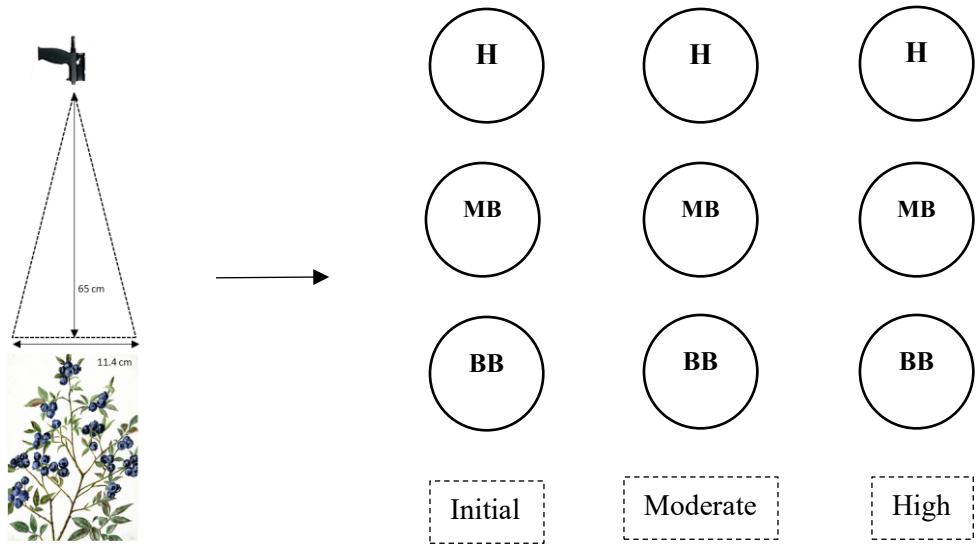

Figure 6.2. Treatment layout for data collection using the handheld hyperspectral radiometer. H – Healthy patch, MB – Monilinia blight patch, and BB – Botrytis blight patch. Initial, moderate, and high represent disease severity levels.

6.3.2.3 Data acquisition from hyperspectral platform

The same hyperspectral platform used in Section 4.3.5 of chapter four was utilized. Similarly, the same vegetative indices listed in Table 3.1 of Chapter three were also used, but with an addition of SAVI, which is described under Table 2.5 of Chapter two.

6.3.2.4 Statistical analysis (parameter and aerial analysis)

As adopted by Devadas et al., (2015), an analysis of variance (ANOVA) was performed to determine which treatments; healthy, MB, and BB disease were significantly different at the different severity levels. Healthy, MB, and BB treatments were compared at three severity levels (low, moderate, and severe) for all vegetative indices as adopted by Zheng et al., (2018) and Calderón et al., (2013). Therefore, where differences are observed, the least significant difference (LSD) was used for multiple means comparison at $\alpha = 0.05$. For statistical testing, the error terms fulfill all model assumptions, thus the assumptions of normality (Anderson-Darling test at $\alpha = 0.1$), constant variance, and independence of the error terms were fulfilled. The ANOVA was conducted using the Statistical Analysis System (SAS) (version 9.4, SAS Institute, Inc., Cary, NC).

Spectral data were explored to distinguish between diseased and healthy plant treatments at the different stages using three parameters (i) spectral difference value, (ii) sensitivity values, and (iii) correlation values which established the strength of the relationship between spectral bands.

Spectral difference value = (Mean reflectance value of healthy plants - mean reflectance of diseased plants)

Sensitivity Value $= \frac{(\text{Mean reflectanc of diseased plant [MB or BB]})}{(\text{Mean reflectance of healthy plants})}$ of each wavelength

Classification analysis was further performed on the hyperspectral data using 3 classifiers namely, the K - nearest neighbour (KNN), random forest (RF), and support vector machine (SVM) as have been conducted in other studies (Huang et al., 2012; Mirandilla et al., 2023). A dataset of 270 spectral readings was computed into 90 VIs which were subjected to classification with 0.75 and 0.25 of the data set used as test and training samples respectively. This approach was subjected

to a 10-fold cross-validation and the process repeated 20 times. In addition, the variable inflation factor (VIF) (Figure) analysis was conducted, as this measured the degree of multicollinearity of the independent variables. Therefore, the number of independent variables in this multiple regression model was reduced because there was high correlation between some variables. These methods were used in this supervised classification to ultimately generate a variable importance chart and the accumulated local effect (ALE) plots. Therefore, predictors were represented as vegetative indices which allowed a VI value to determine which treatment group they belonged to. In addition, the probability histogram function which defines the likelihood of a series of random variable outcomes predicting a discrete variable or a continuous variable was assessed. Thus, this function is a statistical measure used to determine the ability of a VI to discriminate between diseases (Su et al., 2018). These statistical analyses were all conducted in R software version 4.2.3 (R Core Team, 2023).

6.4 RESULTS

6.4.1 Patch assessment

For each treatment class shown (Figure 6.3a), spectral signatures were averaged into a single class. It was obvious that disease treatments as compared to healthy plants have a significant spectral difference as severity increases. These spectral differences are seen both in the visible and near-infrared light regions. The disease spectrum observes a low absorption of light in the blue and red regions coupled with a low level of reflectance in the green and near-infrared regions. The healthy vegetation observed a strong absorption of blue and red light with a strong reflectance of green

and near-infrared light. These differences can be associated with pigment changes in leaves which are mostly seen in the visible light region (455 – 770 nm) (Figure 2.3).

Progression in disease severity had significant impact on the different treatment signatures. Therefore, it was observed (Figure 6.3) that low severity stage showed almost the same spectral curve for all treatments except for MB. A clear difference is realized as severity progresses, therefore, dissociation becomes prominent between the different severity levels.

The spectral signature of the healthy plant was consistent with high photosynthetic activity around the visible (VIS) region, thus a high reflectance peak of the photosynthetic pigments around the green regions were observed, coupled with a high reflectance at the near infrared (NIR) regions (Figure 6.3a). This observation was consistent with the spectral signatures of the healthy plant; thus, the healthy signatures were used as standards for comparison with the spectral signatures of diseased tissues. The reflectance graph indicates an average of spectral signatures of healthy, MB and BB diseases at their different severity levels. Some differences were observed between the healthy and diseased signatures both at the visible (350 – 700 nm) and the near-infrared (701-1050 nm) regions. According to the degree of Monilinia blight disease severity, the reflectance was either high or low, thus, high severity observed low reflectance while healthy showed a high reflectance both at the VIS and NIR regions.

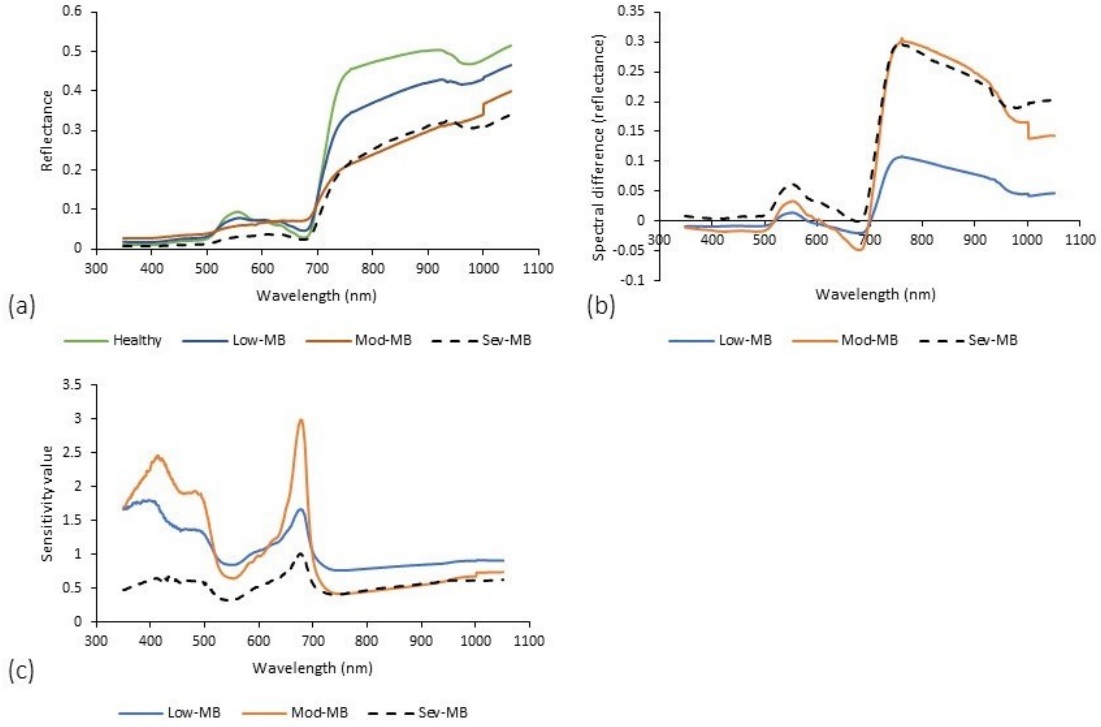

Figure 6.3. Reflectance data on Monilinia blight (MB) disease:(a) Mean reflectance values, (b) Spectral difference and (c) Sensitivity values.

Spectral differences between the healthy and the various MB severities revealed specific points of interest. All three severities (high, moderate, and low) showed similar patterns, thus 555, 681, and 761 nm are considered the highest points of interest (Figure 6.3b). Whereas low severity observed the lowest spectral difference, high and moderate severities observed a high spectral difference. Sensitivity values slightly differed but were largely similar across the three severities. In all three severities, these wavelengths 745, 680, 554, 484, and 415 nm were the highest sensitivity points and were consistent for all three conditions (Figure 6.3c).

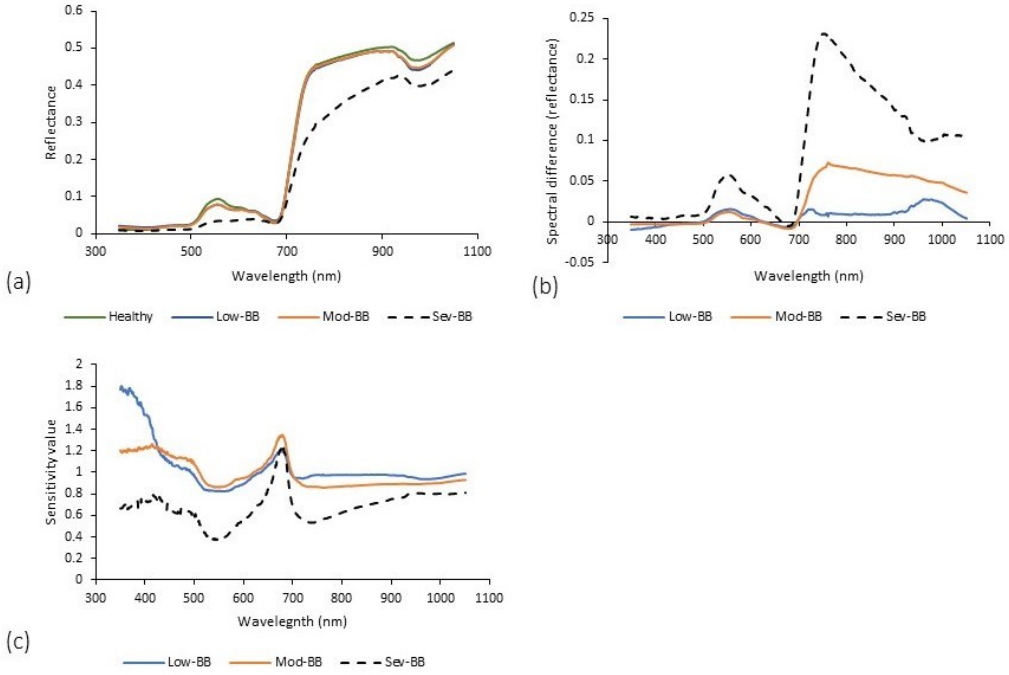

Figure 6.4. Reflectance data on Botrytis blight (BB) disease:(a) Mean reflectance values, (b) Spectral difference and (c) Sensitivity values.

Spectral reflectance for the healthy and diseased signatures was consistent with established principles, thus, high absorbance was observed at the blue and red regions with high reflectance at the green and near-infrared regions of the healthy tissues. This occurrence is consistent with the healthiness and photosynthetic activity of the plant, thus, a deviation from the norm may reflect either biotic or abiotic interference. The graph indicates an average of spectral signatures of healthy and diseased tissues at different severity levels (Figure 6.4a). Spectral differences between the different treatments were observed at the visible (350-700 nm) and near-infrared (701-1050 nm) portions of the light spectrum. Unlike the healthy treatment, the spectral signature of the diseased tissues observed a low reflectance at the spectrum's VIS and NIR regions. However, similar

spectral patterns were observed for the diseased signatures except for the high severity that observed a low reflectance in the VIS regions.

The difference in reflectance values varied depending on the disease severity level, thus, high severity observed a significant change in value compared to moderate and low Botrytis blight disease (Figure 6.4b). Between 500 to 680 nm wavelength, differences were established between the high, moderate, and low severity, however, there was no difference between the low and the moderate severity at the VIS region (Figure 6.4b). From 710 nm to 1000 nm wavelength, significant variations were observed between the different severities.

Botrytis blight sensitivity differences occurred at the VIS and NIR regions, thus, the three severities can be differentiated between 350-680 nm and 700-900 nm (Figure 6.4c). The high severity observed a clear difference in both the visible and the near-infrared regions as compared to the low and moderate severities. Across the spectrum length, low and moderate severity performed similarly while high severity maintained a similar pattern but with a significant difference in sensitivity value.

6.4.1.1 Analysis of variance on spectral signatures using vegetative indices

Furthermore, an analysis of variance using vegetative indices showed that there was significant differences between treatments (Table 6.1). At the 3 severity levels, significant differences were established across all treatments. Consistently, MB was significantly different from the healthy treatment with some significant differences from BB treatment. The BB treatment was not consistent under both moderate and severe disease levels; however, low BB showed some consistency across all 6 VIs. Therefore, it indicates that there is possibility in identifying or classifying these broad treatment groups.

Table 6.1. Analysis of disease assessment on healthy patch, Monilinia diseased patch, and Botrytis disease patch at the different severities using vegetative indices (VIs).

Treatments	**NDVI^{L}**	**NDVI^{M}**	**NDVI^{S}**	**ENDVI^{L}**	**ENDVI^{M}**	**ENDVI^{S}**
Healthy	0.879 a	0.903 a	0.903 a	0.548 a	0.610 a	0.610 a
MB	0.771 b	0.571 c	0.621 b	0.412 b	0.170 c	0.019 c
BB	0.830 ab	0.652 b	0.652 b	0.590 ab	0.219 b	0.219 b
ANOVA	**p < 0.004**	**p < 0.001**	**p < 0.001**	**p < 0.001**	**p < 0.001**	**p < 0.001**
	GLI^{L}	**GLI^{M}**	**GLI^{S}**	**GRVI^{L}**	**GRVI^{M}**	**GRVI^{S}**
Healthy	0.565 a	0.590 a	0.590 a	0.501 a	0.538 a	0.538 a
MB	0.345 b	0.056 c	0.105 c	0.229 b	-0.08 c	-0.004 b
BB	0.428 b	0.199 b	0.194 b	0.327 b	0.028 b	0.028 b
ANOVA	**p < 0.001**	**p < 0.001**	**p < 0.001**	**p < 0.001**	**p < 0.001**	**p < 0.001**
	NDRE^{L}	**NDRE^{M}**	**NDRE^{S}**	**SAVI^{L}**	**SAVI^{M}**	**SAVI^{S}**
Healthy	0.288 a	0.299 b	0.299 a	0.670 a	0.720 a	0.720 a
MB	0.269 c	0.245 c	0.241 b	0.545 b	0.345 b	0.281 c
BB	0.302 b	0.315 a	0.315 a	0.621 a	0.377 b	0.377 b
ANOVA	**p < 0.001**	**p < 0.008**	**p < 0.001**	**p < 0.007**	**p < 0.001**	**p < 0.001**
	VARI^{L}	**VARI^{M}**	**VARI^{S}**			
Healthy	0.600a	0.645 a	0.645 a			

MB	0.292b	-0.112 b	-0.007 b
BB	0.404b	0.035 b	0.035 b
ANOVA	**p < 0.001**	**p < 0.001**	**p < 0.001**

[1] Analysis of variance (ANOVA) with significance at $p<0.05$. Mean separation was completed using Fisher's multiple means comparison test procedure ($\alpha=0.05$). L, M, and S represent low, moderate, and severe disease damage.

6.4.1.2 Classification of diseases using KNN, RF, and SVM classifiers

Classification using vegetative indices under the different classifiers revealed similarities and differences between some of these classifiers. Results have shown that discrimination or classification into the three broad groups achieved very good results with the highest overall accuracy (OA) value of 96.6% (Table 6.2). Across the entire table, between the producer and user accuracy, the highest accuracy achieved was 100%, and this occurred under Botrytis blight disease using the RF classifier. Classification of Botrytis blight received high percentages under both user's and producer's accuracy of RF and SVM classifiers. However, comparing the 3 classifiers and their disease treatments, results have shown that the SVM classifier generated the best outcome among the three classifiers. In addition, some relatively low accuracy values obtained for Monilinia indicate some levels of misclassification (Table 6.2). The classification of Monilinia blight under both RF and SVM classifiers of the user's and producer's accuracy received the lowest values under both SVM and RF classifiers. Generally, these results have shown that broadly identifying these major classes is possible using VIs, with the highest possibility of identifying Botrytis blight conditions (Table 6.2).

Table 6.2. Confusion matrix on disease conditions using KNN, RF, and SVM classifiers.

Classifier		Botrytis	Healthy	Monilinia	U. accuracy (%)
K – Nearest Neighbour	Botrytis	31.8	1.2	1.9	91.1
	Healthy	1.1	32.2	0.9	94.2
	Monilinia	0.4	0.0	30.5	98.7
	P. accuracy (%)	95.5	96.5	91.5	94.7
Random Forest	Botrytis	33.3	0.0	0.1	99.8
	Healthy	0.0	31.1	1.3	96.1
	Monilinia	0.0	2.2	32.0	93.5
	P. accuracy (%)	100	93.3	96.0	96.5
Support Vector Machine (SVM)	Botrytis	32.2	0.0	0.1	99.8
	Healthy	0.0	32.2	1.2	96.5
	Monilinia	1.1	1.1	32.1	93.5
	P. accuracy (%)	96.7	96.7	96.3	96.6

Conversely, the classification of the three disease severity levels highlights different levels of misclassification both under the user's and producer's accuracy (Table 6.3). However, results using the OA, showed that the SVM classifier among the three classifiers was the best, with a value of 76.83%, followed by KNN (70.8%) and then RF (70.67%) classifier. Furthermore, results from all three classifiers have shown that determination of BB at low severity was consistently high under both user's and producer's accuracy with the highest value of 95.27%. Determination of both moderate and severe BB condition was very poor under all 3 classifiers. Conversely, MB low, moderate, and severe conditions were highly classified under all 3 classifiers.

Table 6.3. Confusion matrix of the different disease severities using KNN, RF, and SVM classifiers.

Classifier		Low - BB	Mod. - BB	Sev. - BB	Healthy	Low - MB	Mod. - MB	Sev. - MB	U. accuracy (%)
K – Nearest Neighbour (KNN)	**Low – BB**	7.89	1.00	1.00	1.11	0	0.50	0	68.6
	Mod – BB	1.06	0.44	9.67	0	0	0.33	0	3.9
	Sev – BB	1.17	9.50	0.28	0	0	0.28	0	2.5
	Healthy	1.00	0	0	32.11	1.11	0	0	93.8
	Low – MB	0	0.17	0.17	0.11	10.00	0	0	95.8
	Mod – MB	0	0	0	0	0	10.00	1.00	90.9
	Sev - MB	0	0	0	0	0	0	10.11	100
	P. accuracy (%)	71	4	2.5	96.3	90	90	91	70.8
Random Forest (RF)	**Low – BB**	8.72	1.56	1.83	0	0	0	0	72.02
	Mod – BB	1.94	0.78	9.22	0	0	0	0	6.51
	Sev – BB	0.28	8.78	0.06	0	0	0	0	0.61
	Healthy	0.17	0	0	31.11	1.11	0	0	96.05
	Low – MB	0	0	0	2.22	10	0	0	81.82
	Mod – MB	0	0	0	0	0	10	1.11	90
	Sev - MB	0	0	0	0	0	1.11	10	90
	P. accuracy (%)	78.5	7	0.5	93.33	90	90	90	70.67
Support Vector Machine (SVM)	**Low – BB**	7.83	0.17	0.22	0	0	0	0	95.27
	Mod – BB	1.11	2.28	8.56	0	0	0	0	19.07
	Sev – BB	1.11	8.67	2.33	0	0	0.06	0	19.18
	Healthy	0.00	0	0	32.22	1.11	0	0	96.67
	Low – MB	1.06	0	0	1.11	10.00	0	0	82.19
	Mod – MB	0.00	0	0	0	0	11.06	0	100
	Sev - MB	0.00	0	0	0	0	0	11.11	100
	P. accuracy (%)	70.5	20.5	21	96.6	90	99.5	100	76.83

The healthy treatments were highly classified under all 3 classifiers with SVM and RF generating the two highest classification values of 96.67% and 96.05% respectively (Table 6.3). Generally, SVM performed best compared to KNN and RF classifiers, with a consistent outcome across the three disease levels of both MB and BB. Therefore, it can be stated that all three severity levels of MB disease can be determined, however, only the low severity of Botrytis blight disease can be determined. Moderate and low severity conditions of BB have shown difficulty in their classification thus, alternative approaches can be utilized.

6.4.1.3 Variable importance chart

The effect of multicollinearity was resolved using the variable inflation factor (VIF) analysis. Therefore, out of the 7 independent variables, only three (ENDVI, NDRE, and VARI) were used in the classification process, thus, their individual contributions can be observed in their variable importance chart and accumulated local effect (ALE) plots under the different classifiers. Therefore, the classifications conducted identified predictors (VIs) that contributed significantly to the results observed.

Comparing all 3 classifiers, the contribution of VARI in classifying BB, Healthy, and MB was significant under KNN and RF (Figures 6.5 and A2) but was second under the SVM classifier. NDRE was significant under only SVM, but second under RF in classifying BB, Healthy, and MB treatments. The contribution of ENDVI was low as it was represented second under only KNN, but last in both SVM and RF classifiers which is further explained by the ALE plot (Figure 6.6). The same output was observed under the disease severity levels, except that VARI was significantly high in all 3 classifiers.

The broad classification under disease severity also followed similar patterns of contribution from VARI, NDRE, and ENDVI, thus, the ALE plot highlights in detail the individual contributions in achieving the established classifications from the different classifiers (Figure 6.7). Conversely, the Probability density function (PDF) establishes the likelihood of these variables predicting or classifying any of these treatments. Results have shown that the visible light vegetative indices (VIS) contributed significantly (Figures 6.8 and A5).

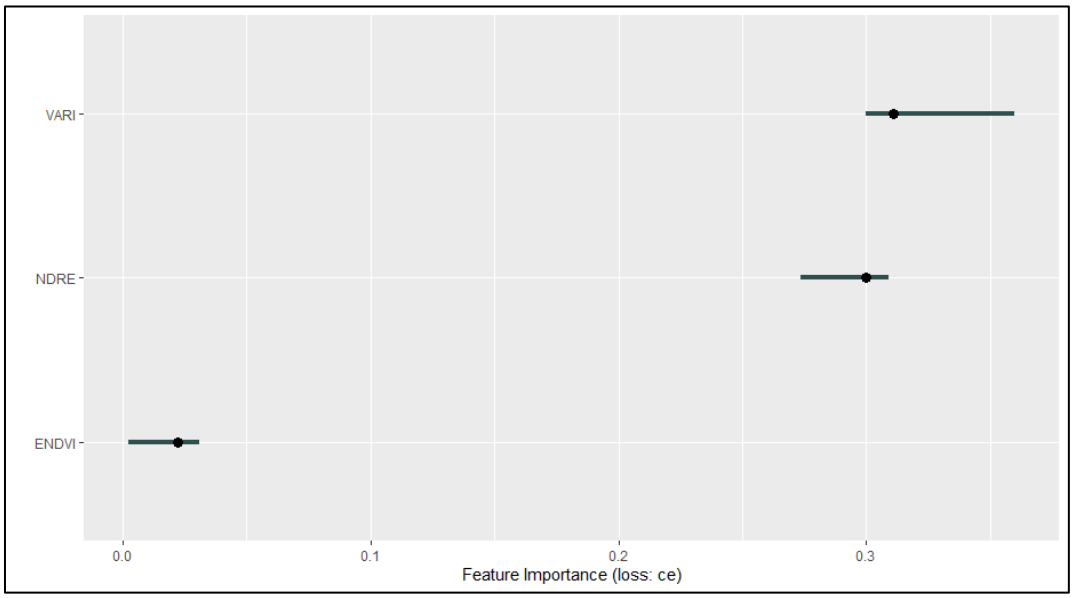

Figure 6.5. A variable importance chart on the three selected VIs (VARI, NDRE, and ENDVI) using an RF classifier to determine the 3 conditions, BB, Healthy, and MB treatments.

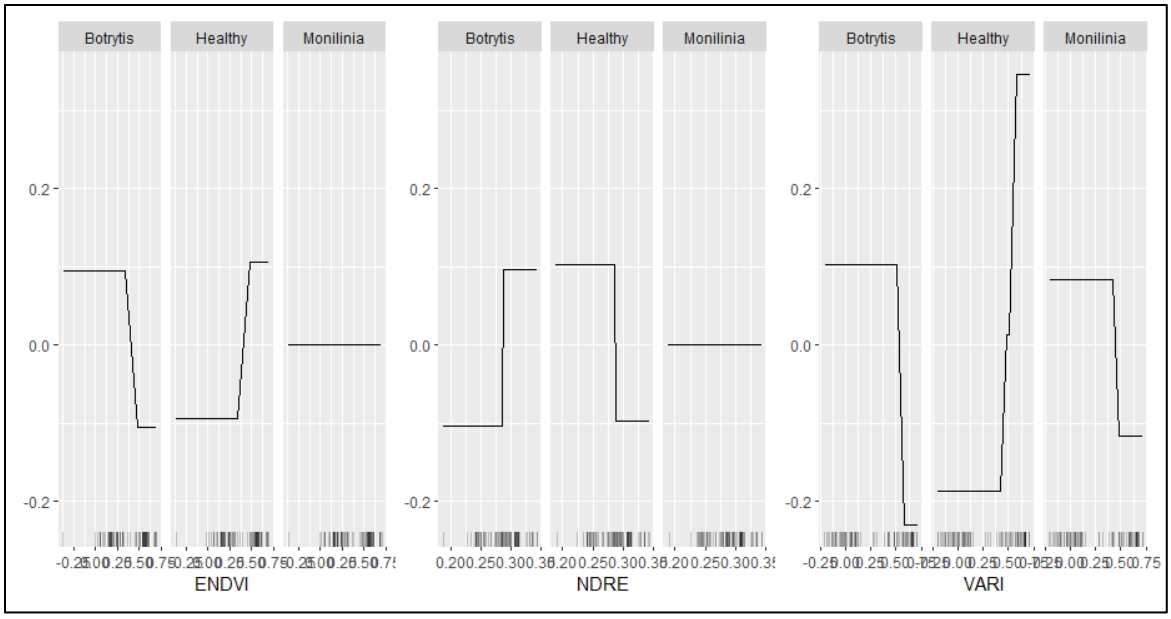

Figure 6.6. ALE plots on the broad treatment classifications of contributions from the three selected variables (ENDVI, NDRE, and VARI) under the RF classifier.

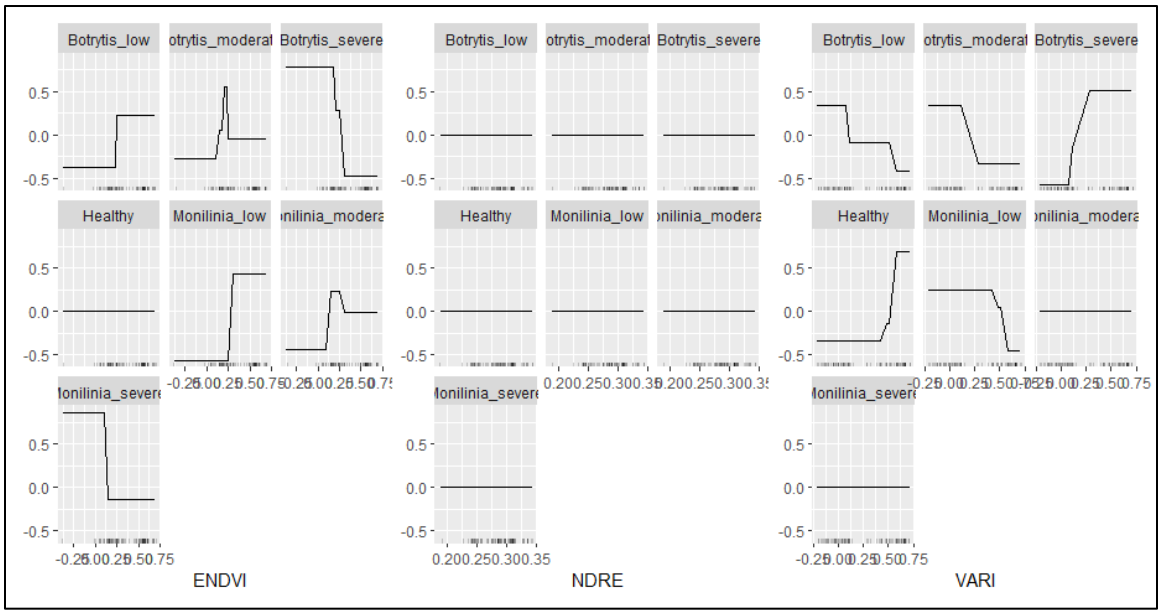

Figure 6.7. ALE plots on the different disease severity classifications of ENDVI, NDRE, and VARI using the RF classifier.

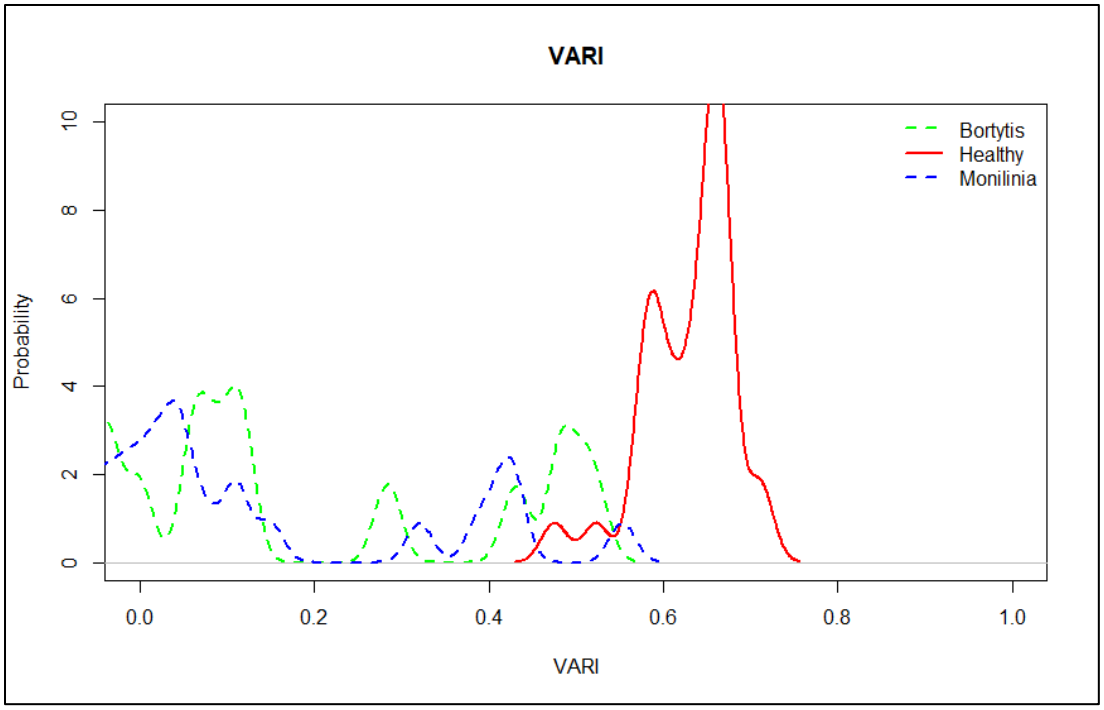

Figure 6.8. The probability density function of VARI measured on the three treatment conditions.

6.4.2 Plot assessments

On the plot assessment aspects, the general comparison between aerial and ground data revealed that there was a moderately low correlation, thus, VIs did not perform as expected in determining disease from an aerial perspective. Though there were relatively no significant differences between the field treatments (Tables 6.6 and 6.8), analysis using VIs (Tables 6.7 and 6.9) also revealed similar results. Since VIs reflected what was obtained from the various plots, it stands to explain the nonsignificant differences observed in the disease trials (Tables 6.6 and 6.8). Furthermore, the difficulty in establishing differences between field treatments were confirmed by their reflectance values (Figure 6.9). Therefore, at the blue, green, and red bands of the light regions, no significant differences were established.

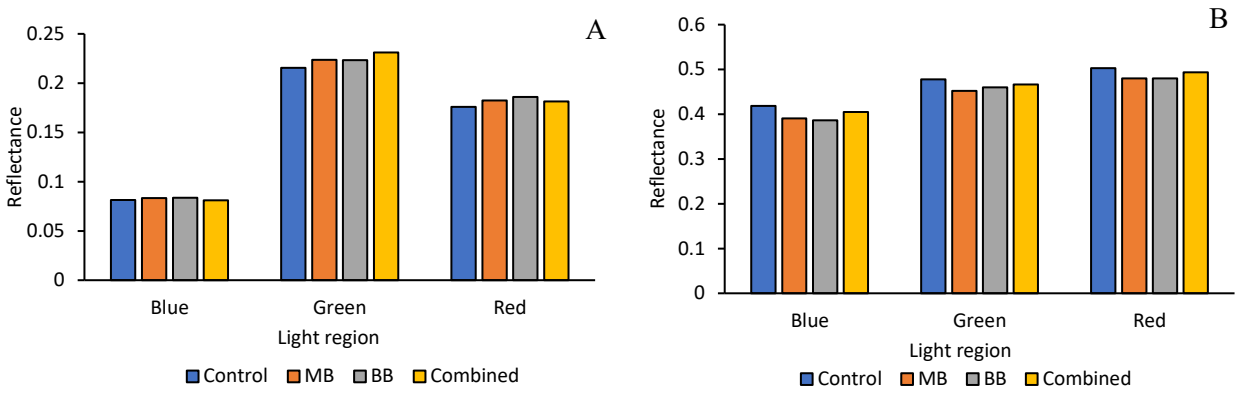

Figure 6.9. Mean reflectance data from 2 flights showing 3 specific light bands under the four disease treatments from the Farmington trial; (A) 19th June 2019 and (B) 10th June 2019.

Despite the non-significance observed between treatments, it was observed that mean values from the control treatments (Tables 6.5 and 6.7) were consistently low for all sampled dates for the light VIs, except for the NIR indices. For the NIR indices, the Botrytis control treatment obtained the lowest mean values with the combined treatments showing generally high mean values for some indices across the two tables (Tables 6.5 and 6.7). Notwithstanding, the non-significance of VIs between the different treatments, differences in mean values reflecting treatment differences can be inferred. Therefore, the combined treatments across the different VIs observed the highest values, indicating some marginal differences between treatments (Tables 6.5 and 6.7;). Differences using reflectance values confirm the outcome of the treatment differences **Appendix Table 1A – 19A** between VIs. Results have shown little to no differences between the light bands of the various treatments (Figure 6.9). Since VIs are computed using reflectance values from these light regions, thus the non-significance observed between these reflectance values translates into a nonsignificant difference between VIs.

Table 6.4. Incidence and severity of Monilinia and *Botrytis* blight disease observed from Kemptown after the 2nd fungicide application. Plant samples for this observation were collected on [4th June 2020, 3rd collection].

Treatment	*Monilinia* incidence of floral nodes (%)[1]	*Monilinia* incidence of vegetative nodes (%)[2]	Monilinia severity of floral node[3]	Monilinia severity of Vegetative node[4]	*Botrytis* incidence of floral nodes (%)[5]	*Botrytis* incidence of vegetative nodes (%)[6]	Botrytis severity of floral node[7]	Botrytis severity of vegetative node[8]
Untreated Control	0	0.01	0	0.06	0	0	0	0
Monilinia Control	0	0	0	0	0	0	0	0
Botrytis Control	0	0	0	0	0	0	0	0
Monilinia & Botrytis Control	0	0	0	0	0	0	0	0
ANOVA Results[9]	**NS**	**NS**	**NS**	**NS**	**NS**	**NS**	**NS**	**NS**

[1,2,5,6] % Incidence = 0 to 100% where 0 = no blossoms/leaves affected and 100 = all blooms/leaves are affected with at least one lesion. [3,4,7,8] Severity = 0 to 9 rating scale where 0 = no disease and 9 >= 90% of each blossom/leaf tissue is affected. [9] Analysis of variance (ANOVA) represented treatments that were significant or otherwise. Mean separation was completed using Fisher's multiple means comparison test procedure (ά=0.05).

Table 6.5. Aerial vegetative indices (VIs) were observed from Kemptown after the 2nd fungicide application.

Treatment	GLI	GRVI	VARI	NDVI	NDRE	ENDVI	SAVI
Untreated Control	0.044	-0.109	-0.147	0.559	0.281	0.645	0.810
Monilinia Control	0.070	-0.084	-0.113	0.601	0.291	0.678	0.844
Botrytis Control	0.080	-0.067	-0.093	0.556	0.275	0.640	0.768
Monilinia & Botrytis Control	0.082	-0.070	-0.095	0.605	0.289	0.680	0.847
ANOVA Results[1]	**NS**	**NS**	**NS**	**NS**	**NS**	**NS**	**NS**

[1] Analysis of variance (ANOVA) results refer to treatment effects that were either not significant (NS) or significant at $p<0.05$. Mean separation was completed using Fisher's multiple means comparison test procedure (ά=0.05).

Table 6.6. Incidence and severity of Monilinia and *Botrytis* blight disease observed from Kemptown after the 3rd fungicide application. Plant samples for this observation were collected on [17th June 2020, 4th collection].

Treatment	*Monilinia* incidence of floral nodes (%)[1]	*Monilinia* incidence of vegetative nodes (%)[2]	Monilinia severity of floral node[3]	Monilinia severity of Vegetative node[4]	*Botrytis* incidence of floral nodes (%)[5]	*Botrytis* incidence of vegetative nodes (%)[6]	Botrytis severity of floral node[7]	Botrytis severity of vegetative node[8]
Untreated Control	0.01	0.19	0.11	0.76	0.17a	0	1.33a	0
Monilinia Control	0	0.21	0	0.53	0.02b	0	0.11b	0
Botrytis Control	0.01	0.01	0.09	0.11	0b	0	0b	0
Monilinia & Botrytis Control	0.02	0.03	0.33	0.11	0b	0	0b	0
ANOVA Results[9]	**NS**	**NS**	**NS**	**NS**	**Sig. (p<0.0016)**	**NS**	**Sig. (p<0.0080)**	**NS**

1,2,5,6 % Incidence = 0 to 100% where 0 = no blossoms/leaves affected and 100 = all blooms/leaves are affected with at least one lesion.
3,4,7,8 Severity = 0 to 9 rating scale where 0 = no disease and 9 >= 90% of each blossom/leaf tissue is affected.
9 Analysis of variance (ANOVA) results refer to treatment effects that were either not significant (NS) or significant at p<0.05. Mean separation was completed using Fisher's multiple means comparison test procedure (ά=0.05).

Table 6.7. Aerial vegetative indices (VIs) observed from Kemptown after the 3rd fungicide application.

Treatment	GLI	GRVI	VARI	NDVI	NDRE	ENDVI	SAVI
Untreated Control	0.195	0.196	0.318	0.426	0.056	0.334	0.634
Monilinia Control	0.241	0.254	0.408	0.501	0.078	0.385	0.734
Botrytis Control	0.222	0.229	0.362	0.434	0.056	0.345	0.592
Monilinia & Botrytis Control	0.261	0.278	0.436	0.510	0.084	0.396	0.727
ANOVA Results[1]	**NS**	**NS**	**NS**	**NS**	**NS**	**NS**	**NS**

1 Analysis of variance (ANOVA) results refer to treatment effects that were either not significant (NS) or significant at p<0.05. Mean separation was completed using Fisher's multiple means comparison test procedure (ά=0.05).

6.4.2.1 Correlation and regression analysis

The overall strength and direction of correlation between MB and BB incidence and severity varied across the different years (Tables 6.10.1 to 6.10.7). Correlation values were generally low with a blend of both positive and negative correlation strengths across the different years. A significantly high correlation strength occurred between VIs (GLI, VARI, GRVI, NDVI, SAVI) and BB incidence and severity components, with values ranging between 0.41 to 0.58. Observation shows that both the near-infrared VIs and the light VIs had a good correlation with MB leave incidence and severity and both MB and BB floral incidence and severity. However, these observations were not consistent across the different years.

Table 6.8. Relationship between ground observations and VIs. A correlation between Monilinia blight (MB) and Botrytis blight (BB) severity on floral buds (Fb) and leaves (L) compared to vegetative indices obtained on the 10th and 19th of June 2019 at Farmington.

	10th June 2019		**19th June 2019**		
Vegetative indices	MB/Fb severity	MB/L severity	MB/Fb severity	MB/L severity	BB/Fb severity
GLI	0.17	0.06	0.11	0.38*	-0.08
GRVI	0.07	0.19	0.13	0.34	-0.07
VARI	0.09	0.09	0.14	0.33	-0.06

*Significant at $p < 0.05$.

Table 6.9. Correlation of different VIs with Monilinia blight (MB) and Botrytis blight (BB) incidence and severity on floral buds (Fb) and leaves (L) obtained from trial plots at Kemptown on the 28th of May and 17th of June 2020.

Vegetative indices	28th May 2020		17th June 2020					
	MB/L Incidence	MB/L severity	MB/Fb Incidence	MB/Fb Severity	MB/L Incidence	MB/L severity	BB/Fb Incidence	BB/Fb Severity
GLI	-0.06	0.02	0.26	0.31	0.37	0.31	-0.24	-0.26
GRVI	-0.03	0.04	0.27	0.32	0.38	0.31	-0.24	-0.26
VARI	-0.04	0.04	0.27	0.31	0.39*	0.32	-0.25	-0.27
NDVI	-0.17	-0.06	0.21	0.29	0.32	0.25	-0.25	-0.23
ENDVI	-0.19	-0.08	0.21	0.29	0.29	0.23	-0.24	-0.24
NDRE	-0.18	-0.09	0.08	0.15	0.04	0.02	-0.19	-0.14
SAVI	-0.26	-0.14	0.20	0.28	0.40*	0.33	-0.25	-0.24

*Significant at $p<0.05$

Table 6.10. Correlation of different VIs with Monilinia blight (MB) and Botrytis blight (BB) incidence and severity on floral buds (Fb) and leaves (L) obtained from trial plots at Lemmon Hill on the 28th of May and 4th of June 2020.

Vegetative indices	28th May 2020				4th June 2020			
	MB/Fb Incidence	MB/Fb severity	MB/L Incidence	MB/L severity	MB/Fb Incidence	MB/Fb Severity	MB/L Incidence	MB/L severity
GLI	0.37	0.37	0.36	0.30	-0.33	-0.33	-0.11	-0.12
GRVI	0.33	0.33	0.36	0.29	-0.34	-0.34	-0.078	-0.12
VARI	-0.02	-0.02	0.48*	0.41*	-0.31	-0.31	-0.01	-0.05
NDVI	0.20	0.20	0.33	0.29	-0.10	-0.10	-0.41*	-0.34

ENDVI	0.18	0.18	0.25	0.23	-0.04	-0.04	-0.39*	-0.30
NDRE	-0.04	-0.04	0.25	0.23	-0.01	-0.01	-0.35	-0.29
SAVI	-0.55*	-0.55*	0.19	0.22	0.12	0.12	0.09	0.11

*Significant at $p<0.05$

Table 6.11. Correlation of different VIs with Monilinia blight (MB) and Botrytis blight (BB) incidence and severity on floral buds (Fb) obtained from trial plots at Mount Thom on the 12th of June 2021.

Vegetative indices	MB/Fb Incidence	MB/Fb severity	BB/Fb Incidence	BB/Fb severity
GLI	0.080	0.080	-0.375	-0.375
GRVI	0.022	0.022	-0.067	-0.067
VARI	0.031	0.031	-0.105	-0.105

*Significant at $p<0.05$

Table 6.12. Correlation of different VIs with Monilinia blight (MB) and Botrytis blight (BB) incidence and severity on floral buds (Fb) and leaves (L) obtained from trial plots at Farmington on 26th May 2022.

Vegetative indices	MB/Fb Incidence	MB/Fb severity	MB/L Incidence	MB/L severity	BB/Fb Incidence	BB/Fb Severity	BB/L Incidence	BB/L severity
GLI	0.02	0.02	-0.18	-0.18	0.39	0.39	-0.13	-0.16
GRVI	0.04	0.04	-0.16	-0.16	0.37	0.37	-0.16	-0.19
VARI	0.04	0.04	-0.16	-0.16	0.37	0.37	-0.15	-0.18
NDVI	0.09	0.09	-0.13	-0.22	0.35	0.35	-0.05	-0.06
ENDVI	0.07	0.07	-0.15	-0.25	0.37	0.37	-0.01	-0.02
NDRE	0.10	0.10	-0.06	-0.22	0.25	0.25	-0.33	0.32
SAVI	0.10	0.10	-0.13	-0.15	0.35	0.35	-0.16	-0.19

*Significant at p<0.05

Table 6.13. Correlation of different VIs with Monilinia blight (MB) and Botrytis blight (BB) incidence and severity on floral buds (Fb) and leaves (L) obtained from trial plots at Farmington on 2nd June 2022.

Vegetative indices	MB/Fb Incidence	MB/Fb severity	MB/L Incidence	MB/L severity	BB/Fb Incidence	BB/Fb Severity	BB/L Incidence	BB/L severity
GLI	0.22	0.07	-0.23	-0.27	0.54*	0.43*	-0.04	-0.04
GRVI	0.20	0.04	-0.24	-0.28	0.57*	0.47*	-0.06	-0.06
VARI	0.18	0.02	-0.25	-0.28	0.58*	0.47*	-0.07	-0.07
NDVI	0.16	0.11	-0.26	-0.24	0.41*	0.29	-0.08	-0.08
ENDVI	0.21	0.17	-0.23	-0.20	0.33	0.22	-0.06	-0.06
NDRE	0.14	0.12	-0.01	-0.02	0.22	0.20	0.22	0.22
SAVI	0.13	0.03	-0.23	-0.26	0.48*	0.36	-0.14	-0.14

*Significant at p<0.05

Though the harvestable yield results do not have a direct bearing on the focus of this study, it does illustrate the need and implication of disease management in the production system. Therefore, across the various years, the effect of the combined treatment (MB + BB) caused a significant increase in yield except in 2019 and 2023 at LH and FP respectively. Yields from LH and FP observed a reduction of about 7.5% and 21% when compared to the control treatment. In both locations, this situation occurred because the treatment plots had lots of bare or weedy areas which affected the plant population, thus leading to low yields from those plots. Across the different years, the combined treatment was different from the control by a yield difference of between 14.6% to 95.1%. This implies that in almost all situations, the MB + BB control treatment performed better than the control, thus, the control treatments observed significantly low yields across the different years. However, results under Monilinia control also showed consistently high

yield values across several fields. This may reflect the significance of leaves in the photosynthetic mechanism of the plant as MB affects plant foliage.

Despite the generally low disease severity from the year 2020 to 2023, treatment effects were reflected in the yield results (Table 6.11). The 2019 results observed the highest disease severity which reflected the yield differences between the control and the combined treatments. From 2019 at LH, MB control treatments have had the highest yield. These results may explain why plant foliage is significant to yield or fruit production. However, other factors like the number of flowers and pollination also contribute significantly to harvestable yield.

Table 6.14. Analysis of variance (ANOVA) on the harvestable berry yield of Monilinia and Botrytis blight disease trials from 2019 to 2023

Treatment	FT (2019) ($g.m^2$)	LH (2019) ($g.m^2$)	LH (2020) ($g.m^2$)	KT (2020) ($g.m^2$)	MT (2021) ($g.m^2$)	FT (2022) ($g.m^2$)	FP (2023) ($g.m^2$)	WM (2023) ($g.m^2$)
Untreated control	660.71d	635.65b	926.72	552.61c	699.28b	575.19b	375.50 bc	418.20 b
MB control	990.61b	833.69a	921.58	1101.86a	863.39a	862.81a	430.47 b	460.47 b
BB control	792.14c	691.28b	907.75	654.84c	688.31b	700.36ab	568.87 a	416.90 b
MB + BB control	1288.89a	588.19b	1025.83	798.36b	836.17a	833.50a	310.33 c	578.80 a
ANOVA Results[1]	**p<0.0001**	**p<0.0028**	**NS**	**p<0.0001**	**p<0.0040**	**p<0.0022**	**p<0.0001**	**p<0.0001**

[1] Analysis of variance (ANOVA) results refer to treatment effects that were either not significant (NS) or significant at $p<0.05$. Mean separation was completed using Fisher's multiple means comparison test procedure ($\alpha=0.05$).

6.5 DISCUSSION

This study was conducted using two approaches, (i) plot assessment (UAV: Micasense) and (ii) patch assessment (hand-held hyperspectral radiometer), to ascertain whether vegetative indices can be used to determine disease severity and incidence on the wild blueberry field. Results from this study have given a good indication of utilizing both sensors. The study established that disease determination in the wild blueberry field is possible using the hyperspectral radiometer. However, determination of disease severity levels using VIs was possible but challenging at the plot level. The study has shown great potential of the light VIs to determine or identify diseases in fields. This study agrees with several studies on disease determination using VIs (Abdulridha et al., 2019; Pourazar et al., 2019; Siedliska et al., 2018; Wu, et al., 2008).

6.5.1 Plot assessments of Monilinia and Botrytis blight diseases using the micasense

Field conditions are major determinants of the degree of disease incidence and severity (Jose et al., 2021). The disease incidence and severity of MB and BB diseases were not observed and, in some situations, occurred sparsely (Table 6.4 and 6.6). Despite the pockets of infections on the field, disease spread and severity were substantially low, and this can be attributed to the unfavourable weather conditions, and the differences in phenotypic resistance (Abbey et al., 2023; Jose et al., 2021). Thus, until conditions are fulfilled, and large patches of plants show symptoms of disease damage, aerial identification, and determination of disease on the wild blueberry field can be difficult to assess. Monilinia and Botrytis blight disease symptoms affect the plant's physiology causing leaves to appear dark brown or dense grey (Abbey et al., 2023; Jose et al., 2021). As indicated (Figures 6.3 and 6.4), this disease phenomenon caused an increase in reflectance at the VIS region but a decrease in both red-edge and the NIR regions of the

electromagnetic spectrum when compared to the healthy plants. This principle is significant in most situations and agrees with the findings of Mahlein et al., (2013) and Zheng et al., (2018). In addition, Yue et al., (2019) suggest that the visible and near-infrared regions of the spectrum are the most important in stimulating biochemical and biophysical processes in plants explaining why differences in reflectance were observed around these regions (Figures 6.3 and 6.4). Therefore, the changes observed in the VIS and NIR regions can be associated with a decrease in pigmentation (chloroplast) and changes associated with leaf structure and water content (Mahlein et al., 2013; Zheng et al., 2018). Furthermore, the changes in the spectral reflectance at the shortwave infrared (SWIR) regions can be associated with lignin and protein content in the leaves (Zheng et al., 2018).

Generally, a significant difference in VIs was not established, however, mean differences between treatments were established using VIs. Conversely, the destructive assessment method (line transect method) established some significant differences between treatments (Table 6.4). These findings agree with the work of Devadas et al., (2015) who established that canopy analysis using VIs on a large scale have proven ineffective in quantifying or identifying disease. Their initial work which focused on identifying stripe rust disease on individual leaves in the laboratory using VIs (Devadas et al., 2009) proved successful with significant differences between VIs, but translating that onto the field showed a sharp contrast between the two findings. Thus, there is a challenge that makes it difficult to obtain similar lab results when translated to the field. However, the nature of some plants can make these transitions difficult if not impossible. The wild blueberry plant is characteristically a low-growing shrub, with non-evergreen leaves, and high canopy density, with small visible structures. This presents a challenge as diseases growing within the plant canopy cannot easily be detected aerially. Due to the effects of diseases, the plant's leaf area and other developing structures shrink, and this reduces the area affected by the disease as

compared to the total leaf area of the plot. Coupled with this, the collective assessment of the entire plot reduces the significance of disease effect because of the confounding effect of the healthy plant population within the plot. At the individual plant or patch level, significant differences can be achieved (Table 6.1), but at the canopy or plot level, several factors may come into play making it difficult to achieve the needed results (Table 6.4 and 6.7). This result further agrees with the work of Di Gennaro et al., (2016) who monitored leaf strip disease in grapevines affected by the esca disease complex. Their findings made positive strides in treatment differentiation but also unlocked challenges with VIs assessments at the plot level. Results from this study agreed with the work of Huang et al., (2012), who monitored rice at the canopy level using hyperspectral imaging. Conversely, the work of Vélez et al., (2023) partially disagreed with this study as they established differences between BB and healthy grape vines using a Wilcoxon test. At the plot level, their variable importance plot supported our result as NDVI was the least important variable in that determination.

Correlation (r) analysis of VIs with the incidences and severities of MB and BB showed a few significantly good results, however, these results were not consistent across the different years. GLI, VARI, GRVI, NDVI, and SAVI produced some moderately high r values. Despite not being specific to MB and BB diseases, these results were similar to the works of Devadas et al., (2009, 2015) and Di Gennaro et al., (2016) who correlated results between aerial measurements using the multispectral sensor as against ground disease measurements. Results varied, however, r values across the different growth seasons showed moderately high significant results between aerial and ground measurements which were similar to those studies. Several factors in effect may account for these observations, including leaf colouration, stress tolerance of the plant, the influence of weeds and other growing plants (Pinto et al., 2020). At the field level, disease determination is

possible but the challenge of differentiating between severities can be difficult. It is often expected that diseases will be detected at an early stage before destroying plants, however, most of these detections or determinations happen after disease destruction has occurred. Disease infections progress until the development of necrotic leaves which makes them easy to identify and discriminate, but the challenge occurs when diseased tissues are buried within the canopy. Therefore, considering the high plant density rate of the field, this creates a minimal or negligible effect in spectral reflectance leading to a statistically non-significant effect. Therefore, until the disease effect is substantial, or its occurrence is on the canopy surface, significant differences between VIs may not be established. However, some of these challenges can be attributed to flush growth (Fang et al., 2017) that also occur around these regions, serving as a compensatory mechanism, aiding the plants recovery from diseased situations.

6.5.2 Patch assessment of Monilinia and Botrytis blight diseases using the hyperspectral radiometer

This study revealed that there was a significant treatment difference between healthy, MB and BB patches of wild blueberry plants at different severity levels (Figure 6.1). This result was similar and agrees with the findings of Vaštakaitė-Kairienė et al., (2021) who established significant differences between *Botrytis cinerea,* and healthy plant tissues collected at different time points. Though the majority of the regressions established were moderately low, they proved the potential of VIs in achieving some of these results. This study also agrees to the work of Devadas et al., (2015) and Di Gennaro et al., (2016) as discussed previously. Furthermore, the findings from this study also agree with the work of Abdulridha et al., (2020) who discriminated between disease severities using VIs and identified target spots in tomatoes using the hyperspectral technique.

Focusing on the spectral reflectance diagrams (Figures 6.3 and 6.4), indication shows that similar trends or patterns were observed between healthy and BB infested plants with slight differences at the NIR regions (Vaštakaitė-Kairienė et al., 2021). BB disease affects mainly flowers (Abbey et al., 2023) which are a fraction compared to the total biomass of the plant. However, the other consideration was to focus on the related biochemicals and biophysical portions of the spectrum.

Despite these developments, the reflectance from these plants compared to a healthy plant looked similar with very slight differences. This is because the gross effect of the affected floral tissue compared to foliage may be insignificant, thus accounting for the similarity between spectral readings from the healthy and BB patches. Unlike MB which affects the plant foliage, thus should command a significant spectral difference when compared to the healthy treatment. These results have indicated that the VIS and NIR regions contribute significantly to the identification of disease severity. In this study, 8 wavelength bands, 415, 484, 554, 555, 680, 681, 745, and 761 nm have shown to be sensitive in the determination of MB disease, whereas 3 bands, 457, 665, and 694 nm were sensitive to BB disease. Identification and detection of *Botrytis cinerea* disease in this study have shown great similarity to several studies despite the differences in the crop types (Chaerle et al., 2007; Vaštakaitė-Kairienė et al., 2021; Vélez et al., 2023a; Wu, Feng, Zhang, et al., 2008). Findings from this study strongly agree with the work of Polder et al., (2013) and Wu, et al., (2008) who identified selected bands of interest in the identification of BB disease. The 3 sensitive bands identified in this study closely relate to the work of Polder et al., (2013), despite some slight variations. Apart from pathological determinations of the MB disease, there is little to no study on specific remote sensing work conducted in other crops or in wild blueberries. Therefore, this study provides a basis and grounds for further research in remote sensing in MB disease.

Despite the success in using other VIs, results highlighted the ability of VARI, GLI, and GRVI to discriminate healthy plants from diseased plants with minimal overlap. Therefore, the probability graph has shown the discriminating abilities of the different VIs (Figure 6.8 and 6.5A) with VARI performing best among all VIs. This result partially agrees with the work of Su et al., (2018) who identified the abilities of NDVI, SAVI, GLI, and NDRE, in their order of importance as being able to discriminate between diseases. Although both studies highlight some of these VIs, the order of importance was different. Thus, this study suggests the light vegetative indices (VARI, GLI) ahead of the other near-infrared VIs (ENDVI, NDVI). Further confirmation is derived from the variable importance plots which also puts VARI ahead of the near-infrared VIs. Since a high correlation exists between VARI, GLI, and GRVI, it can therefore be assumed that these VIs have a great impact in discriminating diseases.

Clearly, results have shown that healthy tissues can be discriminated from diseased tissues but with significant challenges in discriminating between BB severity levels. This result agrees with the findings of Mirandilla et al., (2023) who detected three major diseases in rice using spectral reflectance. Aside from establishing good classification at a more progressed diseased severity level, their work highlighted the significance of RF and SVM classifier. In another related study, Abdulridha et al., (2019) detected the laurel wilt disease and discriminated between healthy and non-healthy plants in avocado using KNN and the neural network multiplayer perceptron (MLP). Despite some challenges with KNN classifying BB, this study has shown levels of accuracy of the KNN classifier that is promising to use in estimating diseases. Estimations of the low, moderate, and severe BB disease were consistent between the different classifiers. Consistently, all the 3 classifiers generated very good accuracies on disease severities. Generally, moderate, and severe BB were poorly determined across the 3 classifiers. This may imply a

systemic difficulty in identifying BB at the moderate and severe levels. Again, it can be observed that SVM performed better than RF and KNN classifiers with an overall accuracy of 76.83% as against 70.8% and 70.67% for KNN and RF respectively. The machine learning (ML) classifiers adopted in this study proved robust as the overall accuracy of the 3 classifiers were 94.7%, 96.5%, and 96.6% for KNN, RF, and SVM respectively.

The significance of the two techniques cannot be underplayed but results point to the use of the hyperspectral as a superior sensor over the Micasense multispectral sensor. Therefore, whereas a spectrum list of VIs can be generated using the hyperspectral device, the multispectral sensor limits the number of VIs (Zahiri et al., 2022). Therefore, in agreement with Huang et al., (2012), we conclude that the hyperspectral reflectance device can achieve great results over the multispectral sensor, however, both devices could not perform early or prior detection to the onset of visible and economically damaging effects of diseases in wild blueberries. Despite this, both tools have demonstrated strong potential in estimating post disease effects on the field.

6.6 CONCLUSION

Vegetative indices have played a significant role in disease determination, and this study has established that potential. However, determining Monilinia and Botrytis blight incidence and severity was achieved using the hyperspectral approach. Results narrowed down by identifying 415, 484, 554, 555, 680, 681, 745, 761 nm and 457, 665, 694 nm as significant wavelength bands for the determination of MB and BB diseases. Interestingly, direction points to the use of the visible light vegetation (VIS) indices (VARI) as they have proven capable in the disease determination process. Despite the success achieved using the hyperspectral sensor, VIs at the plot level could not establish treatment differences. However, it can be said that the confounding effect from the

healthy plants within the plots affects the overall disease effect and reduces the significance of the disease, thus the inability of VIs at the plot level to differentiate diseases. Furthermore, it was difficult to determine a single VI that dominantly correlated with disease incidence and severity. However, results point to the use of the light vegetative indices (VARI, GLI, and GRVI) which showed a correlation of BB incidence and severity on floral buds with these indices. MB incidence and severity also correlated with the visible light vegetation indices, specifically VARI.

The general assessment between the two techniques showed that the classifications using the hyperspectral sensor generated results when compared to those from the Micasense, however, VIs have the potential to determine diseases. Despite the similarities observed in using different classifiers, RF and SVM proved superior in their classification process with an overall accuracy of 96.6%.

CHAPTER 7: GENERAL DISCUSSION

7.1 DISCUSSION

The wild blueberry plant (woody calcifuge plant) is unique with a massive root/rhizome system. Most fields rely on pre-existing stands of 2 species with slightly different genetics and morphological characteristics. The plant is unique as it is not planted, no tillage practices adopted and has the resilience to withstand harsh conditions. Therefore, the cultivation of the plant focuses on management practices that control issues of diseases and nutrient management of the field. Embedded in these broad challenges lies the issue of phenological growth and phenotypic variations which causes a heterogenous pattern of disease spread on the field. Monilinia blight and Botrytis blight disease are two yield-limiting diseases of the crop that affect the plant at different stages of its growth and development. However, the plant population in the field consists of both tolerant and susceptible disease phenotypes, which vary the spread and pattern of disease damage. Therefore, a key component of the study was to see if the variability in these two key areas (phenology and phenotype) could be defined/characterized with remote sensing technologies and integrated into better management practices. The major techniques in assessing these components and other nutrient estimations have always depended on traditional destructive approaches, which come with their limitations. Given the interconnectedness of these components (fertilization, phenology, and phenotype) and the associated challenges, there is a need for an introduction of other methods for assessment in the wild blueberry field.

This research aimed to address challenges with site-specific management practices by improving yield, sustaining production, and environmental protection by reducing the amount of agrochemicals used, which reduces the overall cost of production, through partly understanding the potential and effectiveness of using vegetative indices for assessments on the field. Therefore,

the objectives of this thesis were to (i) assess and understand the use of remote sensing techniques to monitor growth and development, (ii) identify the disease-tolerant phenotypes, (iii) assess the floral blight diseases in the field, and (iv) examine the impact of nitrogen on canopy characteristics and estimations, vegetative indices, and on growth parameters.

The production system of wild blueberries requires fertilization as a necessary management practice to enhance the growth and development of plants. Therefore, forming the basis to start this discussion, **Chapter 3** of this study focused on the remote estimation of canopy LNC and the impact of N on VIs and growth parameters. This chapter provides new knowledge and significant insight and understanding into the use of vegetation indices (VIs) to make predictions and estimations in the field. Impacts and estimations of this nature have been established in several crops including the wild blueberry plant, but with varying outcomes. Ultimately, this study established significant performance from the N treatments, indicating that an increase in N causes significant growth and development effects. Of all measured parameters, yield, leaf area index (LAI), leaf nitrogen content (LNC), plant density (PD), floral, and vegetative buds were important considerations in this determination. In most cases, the N rate (60 kg ha^{-1}) achieved significantly high values across all measured parameters. These findings were similar in magnitude to the findings of Percival & Sanderson, (2004). Furthermore, a study conducted by Percival & Privé, (2002) showed no significant differences between multiple treatments and single treatments of nitrogen. It, therefore, stands to agree with this study that, a single application of nitrogen can be adopted because of the residual N effects (Marty et al., 2022). However, adopting that approach hinges on factors like the nature of soil which may contribute to that effect and help in cost savings to the farmer. Most importantly, their study highlighted some challenges that were encountered with granular fertilization on the wild blueberry plant which have previously been discussed in

Chapter 3 (Percival & Privé, 2002). In addition, it was established that an increase in soil nitrogen affects positively LNC and vegetative index values. This is because nitrogen forms the building blocks of the chlorophyll pigment in plant cells, thus, an increase in N has a resultant effect on VIs which measures the reflectance effects from plant leaves. Therefore, colour intensity and increase in VIs have a direct bearing on nitrogen content (Caturegli et al., 2016). This allows for easy assessment of the yield potential of the field by monitoring the canopy characteristics and floral bud developments allowing sufficient growing time of buds for next year's crop.

The estimation of parameters such as LNC, PD, yield, and LAI generated some interesting results with varying outcomes. Significant, but moderate regression values were achieved for these parameters at the Wentworth location using the 3 visible light vegetative indices (GLI, VARI, and GRVI). Similar results have been achieved in several crops including rice, blueberries, cotton, and sunflower, among others (Kaivosoja et al., 2021; Kokhan & Vostokov, 2020; Li et al., 2020; Marty et al., 2019). Aside from highlighting the relevance of VIs, this study also indicates the potential for other variables to be used as predictors in the estimation of other growth parameters. Generally, stem length and floral buds, and PD and LAI all demonstrated positively strong linear relationships between those variables. This may partly be explained by focusing on the relationships between these variables. The number of plant stands and their leaf spread directly relates to leaf area. Also, since the growth and development of floral buds and vegetative buds occur on the same stem, it therefore does not come as a surprise the relationship between the two parameters. Despite our inability to use the near-infrared VIs in all estimations, results using the visible light vegetative indices have demonstrated potential in estimating growth parameters.

Furthermore, based on trial assessments, it is worth noting that the granular fertilizer used may not have been adequately available to the plant since the pellets may not have been dissolved,

thus making nutrients unavailable to the plant. Out of the 3 sites, the Wentworth site was characterized by moist soils which possibly enabled nutrients to be readily available to the plants. There is, therefore, a gradual shift from the use of granular fertilizers to an adoption of liquid fertilizers which makes nutrients readily available to the plants. However, both granular and liquid fertilizers may have their advantages and disadvantages.

The resultant effect of applying nitrogen to the field is to enhance growth and development, thus, focusing on this aspect becomes the next important step in the management practice of the wild blueberry production system. Therefore, monitoring plant phenology is a significant consideration as it influences majorly disease control, pollination, and harvestable yield. Therefore, serving as basis, this introduces the discussion into Chapter 4 of the study.

Chapter 4 of this study provided new knowledge and understanding of the use of vegetative indices to make predictions or estimations of the wild blueberry field. This work presents both new and confirmatory information on estimating the growth and development of the plant for advocating timely agricultural management practices. This study serves as a starting point in understanding field estimations of the growth and development of the plant using vegetative indices. Vegetative indices have been used in several studies in the estimation of growth parameters (Hussain et al., 2020; Maqbool et al., 2010; Stagakis et al., 2012; Vega et al., 2015). Several outcomes have been determined in most crops: some VIs observed either a high or low correlation and regression estimates with growth parameters (Hussain et al., 2020; Maqbool et al., 2010). The study of the wild blueberry plant showed similar outcomes with low to high regression values (r^2). Overall, leaf area index (LAI) was the constant estimated growth parameter across the different phenological stages with high regression values. The highest estimation of this parameter occurred at the bloom stage (F6/F7) (Maqbool et al., 2010) with NDVI among other VIs contributing to that

effect. Aside from the LAI, the other parameters with good estimations on the field were the floral bud stage (FS) and vegetative bud stage (VS), which observed medium to high correlation and regression values. It was obvious and not surprising that plant leaves contributed to the index values obtained. The bulk of what was observed from an aerial perspective is plant canopy, of which plant leaves are the significant majority. Therefore, the bulk of the reflectance activity from an aerial perspective depicts the characteristics of plant leaves (Forsström et al., 2019). Despite the importance of estimating LAI, the growth stage where this significant determination can be achieved matters. The highest estimations occurred at the bloom (F6/F7) stage. However, good regression models were also established at the early/late bud stage (F4/F5) for some other parameters, like floral bud stage (FS) and vegetative bud stage (VS). Generally, the estimation of other parameters was constantly varying. Harvestable yield was a typical example of a varying parameter that was difficult to estimate using VIs. This study also confirms the challenge of not being able to successfully estimate harvestable yield from the blueberry field, because the variability in yield is also associated with how deep the crop is in the canopy. This observation led to high RSME values, which was not peculiar to only this study but also to MacEachern et al., (2023), who achieved yield estimations using deep learning approaches. A study by Barai et al., (2021) stated the difficulty of using VIs to make predictions on harvestable yield in the wild blueberry field, and this supports the position of this study. It is important to highlight that several factors contribute to yield, and these factors vary across the production system. Worthy of mention is pollination and the number of flower buds. However, the colour mosaic observed on the wild blueberry field may directly influence the computation of vegetative indices (Forsström et al., 2019). Therefore, though VIs can be used in some of these estimations, significant limitations may require alternative approaches. In the assessment of the different classifiers, it became apparent

that the SVM and RF classifiers were the best regression methods to be adopted in these estimations. The basis for adopting these practical measures like field estimations was to enhance production. Successful adoption and implementation of routine activities are tied to monitoring the growth and development of the plant, thus, significant activities like fungicide application and pollination using bees can be carried out effectively. Therefore, the study has established that LAI can be estimated at the F6/F7 stage with floral and vegetative buds being estimated at the F4/F5 stage.

Identifying the different species that make up the wild blueberry population structure is important as monitoring the growth and development of the plant on wild blueberry fields. *Vaccinium angustifolium*, *Vaccinium myrtilloides,* and some hybrids are generally the main plant species constituting the population structure of most commercial fields (Table 5.1) (Abbey et al., 2023). The variation observed at the phenotypic level contributes to the phenological variation observed on the field. Therefore, understanding the growth and development of these phenotypes along with their characteristics would enhance better management practices and decisions.

Based on this background, **Chapter 5** of this study provided new knowledge by way of identifying the different phenotypes in the wild blueberry field using remote sensing. Considering the physical characteristics of these phenotypes, it was assumed that identifying them on the field would be easier using these techniques. In this study, it was clear that only *Vaccinium angustifolium* f. nigrum was successfully identified using pixel analysis. A unique bluish leaf colour characterized *Vaccinium angustifolium* f. nigrum, which made it easy to identify field patches of this phenotype. Generally, there was great difficulty identifying all 6 phenotypes (Table 5.1). Panda et al., (2009) conducted a similar study in differentiating blueberry shrubs from mixed vegetation; that is forest, tall trees, wild blueberry shrubs, and other field classes. However, the present study went a step

further in trying to differentiate between blueberry species in the field to identify the disease tolerant species. The challenges encountered were not anticipated. The initial thoughts were that brick-red leaf colour only occurs in *V. angustifolium* species, as a means for discrimination. However, that assumption was not accurate, as the brick-red colour occurs in both *V. angustifolium* and *V. myrtilloides* species. The initial trial did not yield the needed outcome but provided the basis for the subsequent trial conducted. The effects of mixed pixels go a long way to indicate the similarities that exist between the different phenotypes. Among these mixed pixels, *V. angustifolium* f. nigrum stood out among the rest and, therefore, directed our focus in this classification work.

Aside from the major findings, it also established possibilities and difficulties in this campaign. Identifying *V. myrtilloides* species by the eye in early spring was a very easy task but practically impossible from an aerial perspective. Orthomosaics around this period had a whitish or pale background which assumed the nature of the pubescent structures on the stems and leaves. Another difficulty had to do with the differentiation between *V. angustifolium* green and brown. At the flower and stem level, the differing levels of anthocyanin in these species cause their stems and fruits to differ in colour (Hall, Aalders, et al., 1972; Wood & Barker, 1963). Therefore, differentiation using plant leaves can be challenging. It is often important to note that this level of classification cannot be conducted at any time of the year but should be limited to late September or early October. Furthermore, differentiation between the three *V. myrtilloides* phenotypes also holds a similar effect to that of *V. angustifolium* brown and green, except that stem height was the only distinguishing factor. The final classification analysis identified nigrum with about 80% overall accuracy. This implied that the possibility of identifying nigrum on the field was very high. The original aim was to identify *V. myrtilloides* but identifying nigrum was a fortunate stroke of

serendipity as *V. angustifolium* f. nigrum phenotypes are very susceptible to Monilinia blight and Botrytis blight diseases. This development fits into the broader aim of utilizing the target or spot application method which would identify and focus attention on just the *V. angustifolium* f. nigrum phenotypes. Therefore, this objective has identified *V. angustifolium* f. nigrum phenotypes on the wild blueberry field.

The sensors have been excellent at defining where wild blueberries are geospatially located in fields and also their phenological growth and development stages. Despite the challenge of the phenotypic aspects, the study identified *V. angustifolium* f. nigrum phenotypes within the field. A significant characteristic of *V. myrtilloides* is their tolerance or avoidance mechanism to both Monilinia and Botrytis blight disease (Abbey et al., 2018; Lambert, 1990; Penman & Annis, 2005). Therefore, identifying *V. myrtilloides* allows the use of a spot method for applying disease control products instead of a uniform broadcast application. Furthermore, identifying *Vaccinium angustifolium* f. nigrum also allows for spot application of disease control products. Therefore, the implications of diseases on the field can be diverse and vary among the population structure with the phenological stage of the plant determining their susceptibility to diseases or otherwise. This reinforces the connectedness between phenology and phenotype being crucial to the spread and pattern of disease development in the production system. As important as disease management is to the production system, its determination, monitoring, and measurement have employed traditional destructive approaches using the line and transect method. Therefore, implementing modern techniques in these aspects was adopted, serving as the basis for Chapter 6 of this thesis.

Chapter 6 provided new knowledge and understanding of the remote sensing assessment of Monilinia and Botrytis blight disease in wild blueberry fields. This study provided knowledge on Monilinia and Botrytis blight incidence and severity assessment using vegetative indices (VIs)

on the field. Six and three wavelength bands that have shown sensitivity in the identification of MB and BB diseases have been identified in wild blueberries. The system adopted for this study was intended for early disease detection of MB and BB diseases, but that was not successful. What the present system could do was to provide a reasonably active estimate of growth and development stages on a geospatial basis that may be used in integrated disease management predictive models and geospatially applying disease control products when the critical value (e.g. F2 for MB) has been attained. Therefore, the use of VIs is a common part of field assessment in the determination of different parameters including diseases (Franke et al., 2005; Mahlein et al., 2013; Zhang et al., 2019). Generally, diseases may behave similarly or differently, depending on the pathogen-host interactions (AL-Saddik et al., 2017). It was observed that Monilinia blight (MB) and Botrytis blight (BB) disease effects followed the generally known spectral pattern of disease deterioration in plants (Figures 6.3 and 6.4).

Little is known about remote determinations in MB; however, studies point to some determinations of BB disease (Polder et al., 2013; Vaštakaitė-Kairienė et al., 2021; Wu, Feng, Zhang, et al., 2008). The gray mold disease caused by the fungus, *Botrytis cinerea,* has been researched using remote sensing and detected in several crops including *Phaseolus vulgaris* (Chaerle et al., 2007), egg plant (Wu, et al., 2008), lettuce (Vaštakaitė-Kairienė et al., 2021) and grapevines (Vélez et al., 2023b). These works have focused on different aspects of Botrytis detection with significant results, thus findings from this work agree with these studies. In addition, this study has provided great insight and background into the determination of Monilinia blight disease. The estimation of MB and BB incidence and severity using correlation analysis was moderately successful across the four years with a non-significant VI effect. On different fronts, this study partially agreed with other field studies as have been indicated in chapter 6. However, it

must be pointed out that the majority of field studies emphasized the difficulty in establishing significant differences between VIs (Devadas et al., 2009; Di Gennaro et al., 2016).

Classification assessments at the patch level showed that healthy tissues can be differentiated from MB and BB tissues with high accuracy. Therefore, this can be used to assess disease damage after infection has occurred. This is useful in predicting yield and also if estimations of damage for crop insurance purposes are required. However, under all 3 classifiers, there were challenges with disease determination at specifically 2 levels of severity of BB disease. It is important to note that the cumulative effect of a disease may be non-significant compared to the leaf surface area of healthy tissues on the field. This situation nullifies the disease effects and renders it as negligible which possibly accounts for the non-significance observed at the field level. Highlighting the significance of VIs, the variable importance plot (VIP) singles out VARI as the most important VI in the regression analysis under all 3 classifiers. Therefore, a significant statement from this study, emphasizes the need to utilize the visible light vegetation indices (VARI, GLI, and GRVI) in disease-related studies on the wild blueberry field. Several studies suggest that the near-infrared vegetation indices (NDVI, NDRE, ENDVI) are considered better than the visible light VIs in most of these determinations, but these VIS-VIs performed slightly better than the NIR indices in this classification work.

In hindsight, it was observed that the wild blueberry plant exhibited “a recovery ability” and flushes of growth after MB infected the plants. This implies that diseased plants that abscise their leaves have the potential to develop new leaves. Over a considerable length of time, this phenomenon sometimes masks the disease effects introducing some challenges in VI computations. The high correlative VIs can further be explored using regression models to make some predictions on either the incidence or severity of a disease. Therefore, several possibilities

can be explored in the future, and further work on disease determination of MB and BB diseases. In summary, this objective has identified 8 and 3 wavelength bands of MB and BB diseases respectively using remote sensing.

7.2 CHALLENGES AND LIMITATIONS

Notwithstanding the progress made in this study, several challenges were encountered, but the major ones include, (i) low disease pressures as a result of weather conditions, (ii) equipment breakdown, and (iii) Covid-19 lab access and field access restrictions. As observed from the tables, disease pressures were generally low across the different years, except in 2019 where high disease pressures were observed. This can be attributed to the changes observed in climatic conditions over the past years. The effect of these weather conditions caused low disease pressures that did not reflect treatment effects. Furthermore, a breakdown of our DJI M600 drone, malfunctioning of the Micasense camera, non-available drone pilot, and issues with the Sunscan cables among other tools and processes hampered the progress of this work, and for this reason, work could not proceed or alterations to the methods occurred in some situations. Alternative approaches like renting a drone and flying them were adopted but that could not salvage the situation. The last point Covid-19 was a global crisis that came with different strings of restrictions depending on your location. There were times when I could not access my leaf samples to measure in time and that led to me losing some samples. Travel restrictions and access to facilities were the main challenges as federal, provincial, university, and departmental regulations were all set in force.

7.3 CONCLUSION

This study assessed the potential of an unmanned aerial vehicle (UAV) equipped with different sensors and the hyperspectral radiometer to make field determinations of diseases, phenology

monitoring, phenotype identification and nitrogen estimations. Several outcomes were reflective with respect to each of these components, thus demonstrating the potential in using these remote techniques. This study provides evidence in nitrogen estimation and the determination of other growth parameters. Despite the challenge in estimating yield, considerable success was achieved in the estimation of leaf area index and plant density using VIs. The significance of VIs in these estimations were important but limited to the light vegetative indices, however, evidence from this study points to a consideration in the use of the near-infrared VI for estimations.

Monitoring plant growth and development was equally achieved through the estimation of growth parameters including floral and vegetative bud numbers and their stages, LAI, and yield. However, LAI was the best estimated parameter occurring at the bloom stage (F6/F7) with floral and vegetative bud stages occurring at the early/late anthesis stage (F4/F5). Considerably, the estimation of yield was a major challenge in this study, however, alternative approaches should be considered.

Identifying *V. angustifolium* f. nigrum as a susceptible phenotype to Monilinia and Botrytis bight disease became the major focus and outcome from this study. There were significant challenges (mixed pixels) in the determination of the other phenotypes which can be attributed to the phenotype variation on the field. Success was achieved using the pixel level classification between late-September and early-October of which leaf colour differentiation was prominent allowing the determination of nigrum.

This study provided evidence that Monilinia and Botrytis blight disease can be identified by focusing on specific wavelength bands and vegetative indices using the hyperspectral radiometer. However, there were significant challenges with field disease determination using VIs. Therefore, the estimation of MB and BB disease incidence and severity using VIs was moderately

successful with the visible light vegetation indices playing a pivotal role. Therefore, a significant statement from this study emphasized the need for some consideration in the utilization of visible light vegetation indices (VARI, GLI, and GRVI) in these analyses. Therefore, the broad classifications conducted indicate the ability to differentiate Monilinia severities from healthy plants, but not moderate and severe Botrytis blight disease.

In summary, it is significant to state that many studies have focused on and generalized the effects of specific VIs, but this does not nullify their potential effects. In most situations where those VIs were not impactful; it implied that other VIs may play those significant roles. The use of VIs holds true in the determination of major parameters in wild blueberry fields. Therefore, this study which focused on wild blueberries has; (i) discovered the ability to detect *V. angustifolium* f. nigrum using an SVM classification technique; (ii) identified selected wavebands significant in the identification of MB and BB diseases; (iii) differentiated healthy tissues from Monilinia and Botrytis blight diseased tissues; (iv) identified F6/F7 as the best phenological stage for field estimation of LAI; (v) established that nitrogen has a significant effect on VIs, and (vi) established that LNC can be estimated using VIs.

7.3.1 Recommendations and future research

This work has been successful in generating new and complementary knowledge on the wild blueberry field, however, there are still some unearthed aspects that can potentially be conducted in future research.

There were some challenges with the study, and this related to the uncertain nature of disease presence in the field. The low presence of disease observed from 2020 to 2023 could have

been complimented with alternative approaches like inoculation. Therefore, for future considerations and advancements in this study, some changes can be adopted. Two significant introductions that could enhance future research in this study are: (i) implementing controlled research as an initial stage connected to field research, and (ii) utilizing a hyperspectral imaging system for disease assessment and analysis. Exploring laboratory work provides significant control of variables and provides a step-by-step monitoring of disease development, unlike uncertain field situations. Furthermore, despite the success of using the RGB, multispectral sensors, and the handheld Spectroradiometer, future field research can adopt the hyperspectral imaging system in its disease assessments. This system provides a larger field-of-view (fov) and easy data form as compared to the spectroradiometer with a small fov and a complex data form. This approach should help create a faster, easier, and step-by-step process to analyze disease development and work with data which has become paramount in many circles. These two changes when adopted would serve as an initial basis for determining and transitioning into the field assessments.

Furthermore, it is recommended that a future study should investigate or explore the development of unique vegetative indices (VIs) and approaches for the prediction of yield and disease determination of MB and BB diseases. The unique nature of the wild blueberry field requires unique VIs in some of its determinations. Also, regression models can be developed to help predict MB and BB diseases in the field. Other recommendations include (i) significant adjustments to flight height, and (ii) the use of liquid fertilizers rather than granular fertilizers. Despite the inability to implement some of these recommendations, ongoing studies in the Wild Blueberry Research Program are utilizing some of these measures. Therefore, these recommendations when adopted will greatly improve future research of this study.

REFERENCES

Aalders, L. E., & Hall, I. V. (1961). Pollen incompatibility and fruit set in lowbush blueberries. *Canadian Journal of Genetics and Cytology*, *3*(3), 300–307. https://doi.org/10.1139/g61-034

Aalders, L. E., Stark, R., Hall, I. V., Jackson, L. P., Penney, B. G., & Rayment, A. F. (1972). Selection of an "optimum" time to harvest lowbush blueberry fruit. *Canadian Journal of Plant Science*, *52*(5), 701–705. https://doi.org/10.4141/cjps72-115

Aasen, H., Burkart, A., Bolten, A., & Bareth, G. (2015). Generating 3D hyperspectral information with lightweight UAV snapshot cameras for vegetation monitoring: From camera calibration to quality assurance. *ISPRS Journal of Photogrammetry and Remote Sensing*, *108*, 245–259. https://doi.org/10.1016/j.isprsjprs.2015.08.002

Abbey, J. A., Percival, D., Asiedu, S. K., Prithiviraj, B., & Schilder, A. (2020). Management of Botrytis blossom blight in wild blueberries by biological control agents under field conditions. *Crop Protection*, *131*, 105078. https://doi.org/10.1016/j.cropro.2020.105078

Abbey, J., Jose, S., Percival, D., Jaakola, L., & Asiedu, S. K. (2023). Modulation of defense genes and phenolic compounds in wild blueberry in response to Botrytis cinerea under field conditions. *BMC Plant Biology*, *23*(1), 117. https://doi.org/10.1186/s12870-023-04090-5

Abbey, J., Percival, D., Asiedu, S. K., & Schilder, A. (2018). Susceptibility to Botrytis blight at different floral stages of wild blueberry phenotypes.

Abd-Elrahman, A., Britt, K., & Liu, T. (2021). Deep Learning Classification of High-Resolution Drone Images Using the ArcGIS Pro Software: FOR374/FR444, 10/2021. *EDIS*, *2021*(5). https://doi.org/10.32473/edis-fr444-2021

Abdulridha, J., Ampatzidis, Y., Kakarla, S. C., & Roberts, P. (2020). Detection of target spot and bacterial spot diseases in tomato using UAV-based and benchtop-based hyperspectral imaging techniques. *Precision Agriculture*, *21*(5), 955–978. https://doi.org/10.1007/s11119-019-09703-4

Abdulridha, J., Ehsani, R., Abd-Elrahman, A., & Ampatzidis, Y. (2019). A remote sensing technique for detecting laurel wilt disease in avocado in presence of other biotic and abiotic stresses. *Computers and Electronics in Agriculture*, *156*, 549–557. https://doi.org/10.1016/j.compag.2018.12.018

Advancements on the wild blueberry fields. (2021). [Personal communication].

Agriculture and Agri-Food Canada. (2022). Statistical overview of the Canadian fruit industry 2021. Horticulture Section Crops and Horticulture Division. https://agriculture.canada.ca/sites/default/files/documents/2022-12/Fruit%20Report_2021_ENG.pdf

Agriculture, Aquaculture, and Fisheries. (2010). Growth and development of the wild blueberry. Wild Blueberry Factsheet (A.2.0). https://www2.gnb.ca/content/dam/gnb/Departments/10/pdf/Agriculture/WildBlueberries-BleuetsSauvages/a20e.pdf

Agriculture, Aquaculture, and Fisheries. (2013). Soil fertility and fertilizers for wild blueberry production. New Brunswick Canada. https://www2.gnb.ca/content/dam/gnb/Departments/10/pdf/Agriculture/WildBlueberries-BleuetsSauvages/D20-e.pdf

Agriculture, Aquaculture, and Fisheries. (2014). Growth and development of the wild blueberry. https://www2.gnb.ca/content/dam/gnb/Departments/10/pdf/Agriculture/WildBlueberries-BleuetsSauvages/a20e.pdf

Akoglu, H. (2018). User's guide to correlation coefficients. *Turkish Journal of Emergency Medicine*, *18*(3), 91–93. https://doi.org/10.1016/j.tjem.2018.08.001

Alkema, J., & Seager, S. L. (1982). The chemical pigments of plants. *Journal of Chemical Education*, *59*(3), 183. https://doi.org/10.1021/ed059p183

AL-Saddik, H., Simon, J.-C., & Cointault, F. (2017). Development of spectral disease indices for '*Flavescence dorée'* grapevine disease identification. *Sensors*, *17*(12), 2772. https://doi.org/10.3390/s17122772

Anadon-Rosell, A., Rixen, C., Cherubini, P., Wipf, S., Hagedorn, F., & Dawes, M. A. (2014). Growth and phenology of three dwarf shrub species in a six-year soil warming experiment at the alpine treeline. *PLoS ONE*, *9*(6), e100577. https://doi.org/10.1371/journal.pone.0100577

Anku, K. E., Percival, D. C., Rajasekaran, L. R., Heung, B., & Vankoughnett, M. (2023). Phenological assessment of the wild blueberry field using an unmanned aerial vehicle. *Acta Horticulturae*, *1357*, 35–42. https://doi.org/10.17660/ActaHortic.2023.1357.6

Ashley, K. A. (2020). Population Structure and Reproductive Biology of *Monilinia vaccinii-corymbosi* (Reade) Honey in Lowbush Blueberry in Maine. Electronic Theses and Dissertations 3242. https://digitalcommons.library.umaine.edu/etd/3242

Barai, K., Tasnim, R., Hall, B., Rahimzadeh-Bajgiran, P., & Zhang, Y.-J. (2021). Is Drought Increasing in Maine and Hurting Wild Blueberry Production? *Climate*, *9*(12), 178. https://doi.org/10.3390/cli9120178

Barker, W. G., & Collins, W. B. (1963). Growth and development of the lowbush blueberry: apical abortion. *Canadian Journal of Botany*, *41*(9), 1319–1324. https://doi.org/10.1139/b63-112

Beijing, A. (2023, April 12). Blueberry Annual Voluntary 2023 [Review of *Blueberry Annual Voluntary 2023*, by L. Mcleod]. United States Department of Agriculture (USDA)- Foreign Agricultural Service. https://apps.fas.usda.gov/newgainapi/api/Report/DownloadReportByFileName?fileName=Blueberry%20Annual%20Voluntary%202023_Beijing%20ATO_China%20-%20People%27s%20Republic%20of_CH2023-0046.pdf

Bell, H. P. (1950). Determinate growth in the blueberry. *Canadian Journal of Research*, *28c*(6), 637–644. https://doi.org/10.1139/cjr50c-039

Bell, H. P. (1957). The development of the blueberry seed. *Canadian Journal of Botany*, *35*(2), 139–153. https://doi.org/10.1139/b57-015

Bendig, J., Bolten, A., Bennertz, S., Broscheit, J., Eichfuss, S., & Bareth, G. (2014). Estimating biomass of barley using crop surface models (CSMS) derived from UAV-based RGB imaging. *Remote Sensing*, *6*(11), Article 11. https://doi.org/10.3390/rs61110395

Bendig, J., Yu, K., Aasen, H., Bolten, A., Bennertz, S., Broscheit, J., Gnyp, M. L., & Bareth, G. (2015). Combining UAV-based plant height from crop surface models, visible, and near infrared vegetation indices for biomass monitoring in barley. *International Journal of Applied Earth Observation and Geoinformation*, *39*, 79–87. https://doi.org/10.1016/j.jag.2015.02.012

Benos, L., Tagarakis, A. C., Dolias, G., Berruto, R., Kateris, D., & Bochtis, D. (2021). Machine Learning in Agriculture: A Comprehensive Updated Review. *Sensors*, *21*(11), 3758. https://doi.org/10.3390/s21113758

Blackburn, G. A. (1998). Quantifying chlorophylls and carotenoids at leaf and canopy scales. *Remote Sensing of Environment*, *66*(3), 273–285. https://doi.org/10.1016/S0034-4257(98)00059-5

Bourguignon, C. (2007). *The feasibility of determining foliar nitrogen, phosphorus and potassium contents using existing hyperspectral technologies in wild blueberry fields*. Dalhousie University and Nova Scotia Agricultural College. https://central.bac-lac.gc.ca/.item?id=MR26866&op=pdf&app=Library&is_thesis=1&oclc_number=445209792

Boyd, N. S., & White, S. (2010). PRE and POST Herbicides for Management of Goldenrods (*Solidago spp.*) and Black Bulrush (*Scirpus atrovirens*) in Wild Blueberry. Weed Technology, 24(4), 446–452. https://doi.org/10.1614/WT-09-068.1

Breda, N. J. J. (2003). Ground-based measurements of leaf area index: A review of methods, instruments and current controversies. *Journal of Experimental Botany*, *54*(392), 2403–2417. https://doi.org/10.1093/jxb/erg263

Brewer, C. A., Smith, W. K., & Vogelmann, T. C. (1991). Functional interaction between leaf trichomes, leaf wettability and the optical properties of water droplets. *Plant, Cell and Environment*, *14*(9), 955–962. https://doi.org/10.1111/j.1365-3040.1991.tb00965.x

Broge, N. H., & Leblanc, E. (2001). Comparing prediction power and stability of broadband and hyperspectral vegetation indices for estimation of green leaf area index and canopy chlorophyll density. *Remote Sensing of Environment*, *76*(2), 156–172. https://doi.org/10.1016/S0034-4257(00)00197-8

Bruzzone, L., & Demir, B. (2014). A Review of Modern Approaches to Classification of Remote Sensing Data. In I. Manakos & M. Braun (Eds.), *Land Use and Land Cover Mapping in Europe* (Vol. 18, pp. 127–143). Springer Netherlands. https://doi.org/10.1007/978-94-007-7969-3_9

Bush, E. R., Mitchard, E. T. A., Silva, T. S. F., Dimoto, E., Dimbonda, P., Makaga, L., & Abernethy, K. (2020). Monitoring mega-crown leaf turnover from space. *Remote Sensing*, *12*(3), 429. https://doi.org/10.3390/rs12030429

Calderón, R., Navas-Cortés, J. A., Lucena, C., & Zarco-Tejada, P. J. (2013). High-resolution airborne hyperspectral and thermal imagery for early detection of Verticillium wilt of olive using fluorescence, temperature and narrow-band spectral indices. *Remote Sensing of Environment*, *139*, 231–245. https://doi.org/10.1016/j.rse.2013.07.031

Calderón, R., Navas-Cortés, J., & Zarco-Tejada, P. (2015). Early detection and quantification of *Verticillium wilt* in olive using hyperspectral and thermal imagery over large areas. *Remote Sensing*, *7*(5), 5584–5610. https://doi.org/10.3390/rs70505584

Calderwood, L., Yarborough, D. E., & Smagula, J. M. (2020). 223-Interpreting your leaf analysis results - cooperative extension: Maine wild blueberries - University of Maine Cooperative Extension [The University of Maine]. *Cooperative Extension: Maine Wild Blueberries*. https://extension.umaine.edu/blueberries/factsheets/production/interpreting-your-leaf-analysis-results/

Cárdenas, S. J. L., Romero, N. C., Pizaña, J. M. G., Hernández, J. M. N., & Gómez, J. M. M. (2015). Geospatial technologies to support coniferous forests research and conservation efforts in Mexico. *Ecology, Habitat and Conservation*, 67–123.

Carleo, G., Cirac, I., Cranmer, K., Daudet, L., Schuld, M., Tishby, N., Vogt-Maranto, L., & Zdeborová, L. (2019). Machine learning and the physical sciences. *Reviews of Modern Physics*, *91*(4), 045002. https://doi.org/10.1103/RevModPhys.91.045002

Carvalho, R. F., Takaki, M., & Azevedo, R. A. (2011). Plant pigments: The many faces of light perception. *Acta Physiologiae Plantarum*, *33*(2), 241–248. https://doi.org/10.1007/s11738-010-0533-7

Caturegli, L., Corniglia, M., Gaetani, M., Grossi, N., Magni, S., Migliazzi, M., Angelini, L., Mazzoncini, M., Silvestri, N., Fontanelli, M., Raffaelli, M., Peruzzi, A., & Volterrani, M. (2016). Unmanned Aerial Vehicle to Estimate Nitrogen Status of Turfgrasses. *PLOS ONE*, *11*(6), e0158268. https://doi.org/10.1371/journal.pone.0158268

Chaerle, L., Hagenbeek, D., Vanrobaeys, X., & Van Der Straeten, D. (2007). Early detection of nutrient and biotic stress in *Phaseolus vulgaris*. *International Journal of Remote Sensing*, *28*(16), 3479–3492. https://doi.org/10.1080/01431160601024259

Chan, C., Nelson, P. R., Hayes, D. J., Zhang, Y.-J., & Hall, B. (2021). Predicting water stress in wild blueberry fields using airborne visible and near-infrared imaging spectroscopy. *Remote Sensing*, *13*(8), 1425. https://doi.org/10.3390/rs13081425

Chappelle, E. W., Kim, M. S., & McMurtrey, J. E. (1992). Ratio analysis of reflectance spectra (RARS): An algorithm for the remote estimation of the concentrations of chlorophyll A, chlorophyll B, and carotenoids in soybean leaves. *Remote Sensing of Environment*, *39*(3), 239–247. https://doi.org/10.1016/0034-4257(92)90089-3

Chen, J. M. (1996). Evaluation of vegetation indices and a modified simple ratio for boreal applications. *Canadian Journal of Remote Sensing*, *22*(3), 229–242. https://doi.org/10.1080/07038992.1996.10855178

Chen, X., Yarborough, D., & D'Appollonio, J. (2017). Wild blueberry systems approach economic and risk analysis. *Acta Horticulturae, 1180*, 143–150. https://doi.org/10.17660/ActaHortic.2017.1180.20

Chiasson, G., & Argall, J. (1996). Pollination of wild blueberries. *New Brunswick Department of Agriculture, Aquaculture, and Fisheries*.

Chiasson, G., & Morin, C. (2011). Growth and Development of the Wild Blueberry. Wild Blueberry Production Guide. https://perlebleue.ca/images/documents/amenagement/guideanglais/esection3.pdf

Coleto, I., Marín-Peña, A. J., Urbano-Gámez, J. A., González-Hernández, A. I., Shi, W., Li, G., & Marino, D. (2023). Interaction of ammonium nutrition with essential mineral cations. *Journal of Experimental Botany*, *74*(19), 6131–6144. https://doi.org/10.1093/jxb/erad215

Crawford, S. B., Kosinski, A. S., Lin, H.-M., Williamson, J. M., & Barnhart, H. X. (2007). Computer programs for the concordance correlation coefficient. *Computer Methods and Programs in Biomedicine*, *88*(1), 62–74. https://doi.org/10.1016/j.cmpb.2007.07.003

Darnell, R. L. (1991). Photoperiod, Carbon Partitioning, and Reproductive Development in Rabbiteye Blueberry. *Journal of the American Society for Horticultural Science*, *116*(5), 856–860. https://doi.org/10.21273/JASHS.116.5.856

Daughtry, C. (2000). Estimating Corn Leaf Chlorophyll Concentration from Leaf and Canopy Reflectance. *Remote Sensing of Environment*, *74*(2), 229–239. https://doi.org/10.1016/S0034-4257(00)00113-9

de Castro, A., Torres-Sánchez, J., Peña, J., Jiménez-Brenes, F., Csillik, O., & López-Granados, F. (2018). An Automatic Random Forest-OBIA Algorithm for Early Weed Mapping between and within Crop Rows Using UAV Imagery. *Remote Sensing*, *10*(3), 285. https://doi.org/10.3390/rs10020285

Debnath, S. C. (2007). Propagation of *Vaccinium* in vitro: A Review. *International Journal of Fruit Science*, *6*(2), 47–71. https://doi.org/10.1300/J492v06n02_04

Deindorfer, H. (2016). Hands-on experience with the Image Classification Wizard (ArcGIS Pro 1.3). *ArcGIS Blog*. https://www.esri.com/arcgis-blog/products/imagery/imagery/hands-on-experience-with-the-image-classification-wizard-arcgis-pro-1-3/

Delbridge, R., & Hildebrand, P. (1995). Botrytis Blight of Lowbush Blueberry. https://cdn.dal.ca/content/dam/dalhousie/images/sites/wild-blueberry/pdfs/Botrytis_Blight_%20Lowbush_Blueberry.pdf.

Delbridge, R., & Hildebrand, P. (1997a). Botrytis Blight of Lowbush Blueberry. Lowbush Blueberry Fact Sheet. Lowbush Blueberry Fact Sheet. https://cdn.dal.ca/content/dam/dalhousie/images/sites/wild-blueberry/pdfs/Botrytis_Blight_%20Lowbush_Blueberry.pdf

Delbridge, R., & Hildebrand, P. (1997b). Monilinia blight of lowbush blueberry. Lowbush Blueberry Fact Sheet. http://nsac.ca/wildblue/facts/disease/monilini.asp

Deng, L., Mao, Z., Li, X., Hu, Z., Duan, F., & Yan, Y. (2018). UAV-based multispectral remote sensing for precision agriculture: A comparison between different cameras. *ISPRS Journal of Photogrammetry and Remote Sensing*, *146*, 124–136. https://doi.org/10.1016/j.isprsjprs.2018.09.008

Devadas, R., Lamb, D. W., Backhouse, D., & Simpfendorfer, S. (2015). Sequential application of hyperspectral indices for delineation of stripe rust infection and nitrogen deficiency in wheat. *Precision Agriculture*, *16*(5), 477–491. https://doi.org/10.1007/s11119-015-9390-0

Devadas, R., Lamb, D. W., Simpfendorfer, S., & Backhouse, D. (2009). Evaluating ten spectral vegetation indices for identifying rust infection in individual wheat leaves. *Precision Agriculture*, *10*(6), 459–470. https://doi.org/10.1007/s11119-008-9100-2

Di Gennaro, S., Battiston, E., Di Marco, S., Facini, O., Matese, A., Nocentini, M., Mugnai, L., & Palliotti, A. (2016). Unmanned Aerial Vehicle (UAV)-based remote sensing to monitor grapevine leaf stripe disease within a vineyard affected by esca complex. *Phytopathologia Mediterranea*, 262–275. https://doi.org/10.14601/Phytopathol_Mediterr-18312

Digital Globe. (2014). Remote Sensing Technology Trends and Agriculture. Remote Sensing. https://dg-cms-uploads-production.s3.amazonaws.com/uploads/document/file/31/DG-RemoteSensing-WP.pdf

do Amaral, E. S., Vieira Silva, D., Dos Anjos, L., Schilling, A. C., Dalmolin, Â. C., & Mielke, M. S. (2019). Relationships between reflectance and absorbance chlorophyll indices with RGB (Red, Green, Blue) image components in seedlings of tropical tree species at nursery stage. *New Forests*, *50*(3), 377–388. https://doi.org/10.1007/s11056-018-9662-4

Drummond, F. (2019). Reproductive biology of wild blueberry (*Vaccinium angustifolium* Aiton). *Agriculture*, *9*(4), 69. https://doi.org/10.3390/agriculture9040069

Drummond, F. A., & Rowland, L. J. (2020). The ecology of autogamy in wild blueberry (*Vaccinium angustifolium* Aiton): Does the Early Clone Get the Bee? *Agronomy*, *10*(8), 1153. https://doi.org/10.3390/agronomy10081153

Drummond, F. A., & Yarborough, D. E. (2014). growing season effects on wild blueberry (*Vaccinium angustifolium*) in Maine and implications for management. *Acta Horticulturae*, *1017*, 101–107. https://doi.org/10.17660/ActaHortic.2014.1017.9

Drummond, F., Annis, S., Smagula, J. M., & Yarborough, D. E. (2009). Organic production of wild blueberries insects and diseases. *Acta Horticulturae*, *810*, 275–286. https://doi.org/10.17660/ActaHortic.2009.810.35

Duy, J. C. (1999). A survey of the quantitative intraspecific variation of anthocyanins, phenolics and antioxidant capacity in leaves and fruit of *Vaccinium angustifolium* Aiton clones in Nova Scotia. https://central.bac-lac.gc.ca/.item?id=MQ37796&op=pdf&app=Library&oclc_number=50712788

Eaton, L. J., Glen, R. W., & Wyllie, J. D. (2004). Efficient Mowing for Pruning Wild Blueberry Fields. *Small Fruits Review*, *3*(1–2), 123–131. https://doi.org/10.1300/J301v03n01_12

Eaton, L. J., & Nams, V. O. (2012a). Honey bee stocking numbers and wild blueberry production in Nova Scotia. *Canadian Journal of Plant Science*, *92*(7), 1305–1310. https://doi.org/10.4141/cjps2012-045

Eaton, L. J., & Nams, V. O. (2012b). Honey bee stocking numbers and wild blueberry production in Nova Scotia. *Canadian Journal of Plant Science*, *92*(7), 1305–1310. https://doi.org/10.4141/cjps2012-045

Eaton, L. J., Sanderson, K. R., & Fillmore, S. A. E. (2009). Comparison of consecutive and alternate fertilizer applications in wild blueberry production. *Canadian Journal of Plant Science*, *89*(1), 93–98. https://doi.org/10.4141/CJPS08068

Eitel, J. U. H., Long, D. S., Gessler, P. E., Hunt, E. R., & Brown, D. J. (2009). Sensitivity of Ground-Based Remote Sensing Estimates of Wheat Chlorophyll Content to Variation in Soil Reflectance. *Soil Science Society of America Journal*, *73*(5), 1715–1723. https://doi.org/10.2136/sssaj2008.0288

El Naqa, I., Li, R., & Murphy, M. J. (Eds.). (2015). Machine Learning in Radiation Oncology. Springer International Publishing. https://doi.org/10.1007/978-3-319-18305-3

Erdle, K., Mistele, B., & Schmidhalter, U. (2011). Comparison of active and passive spectral sensors in discriminating biomass parameters and nitrogen status in wheat cultivars. *Field Crops Research*, *124*(1), 74–84. https://doi.org/10.1016/j.fcr.2011.06.007

ESRI Resource. (2023). Performing image classification—Imagery Workflows | *Documentation* [Environmental System Research Institute (ESRI) Resource]. Imagery Workflows. https://doc.arcgis.com/en/imagery/workflows/resources/performing-image-classification.htm

ESRI Resources. (2020). Compute Confusion Matrix *(Spatial Analyst)—ArcGIS Pro* | *Documentation* [Environmental System Research Institute (ESRI) Resource]. Spatial Analyst. https://pro.arcgis.com/en/pro-app/latest/tool-reference/spatial-analyst/compute-confusion-matrix.htm

Fang, Y., Williamson, J., Darnell, R., Li, Y., & Liu, G. (2017). Nitrogen Uptake and Allocation at Different Growth Stages of Young Southern Highbush Blueberry Plants. *HortScience*, *52*(6), 905–909. https://doi.org/10.21273/HORTSCI11723-17

Farooq, M. (2018). Management of goldenrods (*Solidago spp*.) in wild blueberry (*Vaccinium angustifolium* Ait.) fields. Dalhousie University. https://dalspace.library.dal.ca/handle/10222/74162

Farooque, A. A., Zaman, Q. U., Schumann, A. W., Madani, A., & Percival, D. (2012). Delineating management zones for site specific fertilization in wild blueberry fields. *Applied Engineering in Agriculture*. http://hdl.handle.net/10222/38985

Faust, M., Erez, A., Rowland, L. J., Wang, S. Y., & Norman, H. A. (1997). Bud dormancy in perennial fruit trees: Physiological basis for dormancy induction, maintenance, and release. *HortScience*, *32*(4), 623–629. https://doi.org/10.21273/HORTSCI.32.4.623

Forsström, P., Peltoniemi, J., & Rautiainen, M. (2019). Seasonal dynamics of lingonberry and blueberry spectra. *Silva Fennica*, *53*(2). https://doi.org/10.14214/sf.10150

Fournier, M.-P., Paré, M. C., Buttò, V., Delagrange, S., Lafond, J., & Deslauriers, A. (2020). How plant allometry influences bud phenology and fruit yield in two *Vaccinium species*. *Annals of Botany*, *126*(5), 825–835. https://doi.org/10.1093/aob/mcaa083

Franke, J., Menz, G., Oerke, E.-C., & Rascher, U. (2005). Comparison of multi- and hyperspectral imaging data of leaf rust infected wheat plants (M. Owe & G. D'Urso, Eds.; p. 59761D). https://doi.org/10.1117/12.626531

Ghosh, D., Brahmachari, K., Skalický, M., Roy, D., Das, A., Sarkar, S., Moulick, D., Brestič, M., Hejnak, V., Vachova, P., Hassan, M. M., & Hossain, A. (2022). The combination of organic and inorganic fertilizers influence the weed growth, productivity and soil fertility of monsoon rice. *PLOS ONE*, *17*(1), e0262586. https://doi.org/10.1371/journal.pone.0262586

Gibson, L. D. (2011). Characterization of fruit development and ripening *of Vaccinium angustifolium Ait.* in relation to microclimate conditions. https://dalspace.library.dal.ca/bitstream/handle/10222/14407/Gibson_Lara_Dawn_MSc_AGRI_Nov_2011.pdf?sequence=5&isAllowed=y

Gitelson, A. A., Gritz †, Y., & Merzlyak, M. N. (2003). Relationships between leaf chlorophyll content and spectral reflectance and algorithms for non-destructive chlorophyll assessment in higher plant leaves. *Journal of Plant Physiology*, *160*(3), 271–282. https://doi.org/10.1078/0176-1617-00887

Gitelson, A. A., & Merzlyak, M. N. (1996). Signature analysis of leaf reflectance spectra: Algorithm development for remote sensing of chlorophyll. *Journal of Plant Physiology*, *148*(3–4), 494–500. https://doi.org/10.1016/S0176-1617(96)80284-7

Gitelson, A. A., Merzlyak, M. N., & Chivkunova, O. B. (2001). Optical Properties and Nondestructive Estimation of Anthocyanin Content in Plant Leaves. *Photochemistry and Photobiology*, *74*(1), 38–45. https://doi.org/10.1562/0031-8655(2001)0740038OPANEO2.0.CO2

Gitelson, A. A., Viña, A., Arkebauer, T. J., Rundquist, D. C., Keydan, G., & Leavitt, B. (2003). Remote estimation of leaf area index and green leaf biomass in maize canopies: Remote estimation of leaf area index. *Geophysical Research Letters*, *30*(5), n/a-n/a. https://doi.org/10.1029/2002GL016450

Gitelson, A., & Merzlyak, M. N. (1994). Spectral Reflectance Changes Associated with Autumn Senescence of Aesculus hippocastanum L. and Acer platanoides L. Leaves. Spectral Features and Relation to Chlorophyll Estimation. *Journal of Plant Physiology*, *143*(3), 286–292. https://doi.org/10.1016/S0176-1617(11)81633-0

Glass, V. M., Percival, D. C., & Proctor, J. T. A. (2005). Tolerance of lowbush blueberries (*Vaccinium angustifolium* Ait.) to drought stress. II. Leaf gas exchange, stem water potential and dry matter partitioning. *Canadian Journal of Plant Science*, *85*(4), 919–927. https://doi.org/10.4141/P03-028

Gordon, E. (2017, July 8). 5.2: The Electromagnetic Spectrum. Chemistry LibreTexts. https://chem.libretexts.org/Courses/Furman_University/CHM101%3A_Chemistry_and_Global_Awareness_(Gordon)/05%3A_Basics_of_Nuclear_Science/5.02%3A_The_Electromagnetic_Spectrum

Griffin, J. J., & Blazich, F. A. (2008). Ericaceae—Heath family *Vaccinium L.* https://citeseerx.ist.psu.edu/viewdoc/download?doi=10.1.1.297.9826&rep=rep1&type=pdf

Griffiths, D. J., Pegler, R. A. D., & Tonguthaisri, T. (1971). Cross compatibility between diploid and tetraploid perennial ryegrass (*Lolium perenne* L.). *Euphytica*, *20*(1), 102–112. https://doi.org/10.1007/BF00146780

Gumbrewicz, R., & Calderwood, L. (2022). Fertility Effects on Blueberry Gall Midge (Diptera: Cecidomyiidae) in Wild Blueberry (*Vaccinium angustifolium*; Ericales: Ericaceae). *Journal of Economic Entomology*, *115*(3), 783–791. https://doi.org/10.1093/jee/toac043

Haboudane, D. (2004). Hyperspectral vegetation indices and novel algorithms for predicting green LAI of crop canopies: Modeling and validation in the context of precision agriculture. *Remote Sensing of Environment*, *90*(3), 337–352. https://doi.org/10.1016/j.rse.2003.12.013

Haboudane, D., Miller, J. R., Tremblay, N., Zarco-Tejada, P. J., & Dextraze, L. (2002). Integrated narrow-band vegetation indices for prediction of crop chlorophyll content for application to precision agriculture. *Remote Sensing of Environment*, *81*(2–3), 416–426. https://doi.org/10.1016/S0034-4257(02)00018-4

Hall, I. V., Aalders, L. E., & Jackson, L. P. (1972). Physiology of the Lowbush Blueberry on JSTOR. https://www.jstor.org/stable/4253311

Hall, I. V., Aalders, L. E., & McRAE, K. B. (1982). Lowbush blueberry production in eastern Canada as related to certain weather data. *Canadian Journal of Plant Science*, *62*(3), 809–812. https://doi.org/10.4141/cjps82-120

Hall, I. V., Forsyth, F. R., Aalders, L. E., & Jackson, L. P. (1972). Physiology of the lowbush blueberry. http://www.jstor.org/stable/4253311

Hall, I. V., Forsyth, F. R., & Newbery, R. J. (1970). Effect of temperature on flower bud and leaf anthocyanin formation in the lowbush blueberry1. *HortScience*, *5*(4), 272–273. https://doi.org/10.21273/HORTSCI.5.4.272

Hall, I. V., & Ludwig, R. A. (1961). The effects of photoperiod, temperature, and light intensity on the growth of the lowbush blueberry (*Vaccinium angustifolium* Ait.). *Canadian Journal of Botany*, *39*(7), 1733–1739. https://doi.org/10.1139/b61-151

Han, L., Yang, G., Yang, H., Xu, B., Li, Z., & Yang, X. (2018). Clustering field-based maize phenotyping of plant-height growth and canopy spectral dynamics using a UAV remote-sensing approach. *Frontiers in Plant Science*, *9*, 1638. https://doi.org/10.3389/fpls.2018.01638

Hanson, E. J. (2006). Nitrogen fertilization of highbush blueberry. *Acta Horticulturae*, *715*, 347–352. https://doi.org/10.17660/ActaHortic.2006.715.51

Hanson, E., & Lansing, E. (n.d.). *Managing Blueberry Nutrition*.

Hassan, M. A., Yang, M., Rasheed, A., Yang, G., Reynolds, M., Xia, X., Xiao, Y., & He, Z. (2019). A rapid monitoring of NDVI across the wheat growth cycle for grain yield prediction using a multi-spectral UAV platform. *Plant Science*, *282*, 95–103. https://doi.org/10.1016/j.plantsci.2018.10.022

Heim, R. H. J., Wright, I. J., Allen, A. P., Geedicke, I., & Oldeland, J. (2019). Developing a spectral disease index for myrtle rust (*Austropuccinia psidii*). *Plant Pathology*, *68*(4), 738–745. https://doi.org/10.1111/ppa.12996

Hennessy, P. J., Esau, T. J., Schumann, A. W., Zaman, Q. U., Corscadden, K. W., & Farooque, A. A. (2022). Evaluation of cameras and image distance for CNN-based weed detection in wild blueberry. *Smart Agricultural Technology*, *2*, 100030. https://doi.org/10.1016/j.atech.2021.100030

Hicklenton, P. R., Reekie, J. Y. C., MacKenzie, K., Eaton, L. J., & Havard, P. (2002). Freeze damage and frost tolerance thresholds for flowers of the lowbush blueberry (*Vaccinium angustifolium* Ait.). *Acta Horticulturae*, *574*, 193–201. https://doi.org/10.17660/ActaHortic.2002.574.29

Hildebrand, P. D., & Braun, P. G. (1991). Factors Affecting Infection of Lowbush Blueberry by Ascospores of *Monilinia Vaccinii-Corymbosi*. *Canadian Journal of Plant Pathology*, *13*(3), 232–240. https://doi.org/10.1080/07060669109500935

Hildebrand, P. D., McRae, K. B., & Lu, X. (2001). Factors affecting flower infection and disease severity of lowbush blueberry by *Botrytis cinerea*. *Canadian Journal of Plant Pathology*, *23*(4), 364–370. https://doi.org/10.1080/07060660109506957

Huang, J., Liao, H., Zhu, Y., Sun, J., Sun, Q., & Liu, X. (2012). Hyperspectral detection of rice damaged by rice leaf folder (*Cnaphalocrocis medinalis*). *Computers and Electronics in Agriculture*, *82*, 100–107. https://doi.org/10.1016/j.compag.2012.01.002

Huché-Thélier, L., Crespel, L., Gourrierec, J. L., Morel, P., Sakr, S., & Leduc, N. (2016). Light signaling and plant responses to blue and UV radiations—Perspectives for applications in horticulture. *Environmental and Experimental Botany*, *121*, 22–38. https://doi.org/10.1016/j.envexpbot.2015.06.009

Huete, A. (1988). Huete, AR A soil-adjusted vegetation index (SAVI). Remote sensing of environment. *Remote Sensing of Environment*, *25*, 295–309.

Hunt, E. R., Doraiswamy, P. C., McMurtrey, J. E., Daughtry, C. S. T., Perry, E. M., & Akhmedov, B. (2013). A visible band index for remote sensing leaf chlorophyll content at the canopy scale. *International Journal of Applied Earth Observation and Geoinformation*, *21*, 103–112. https://doi.org/10.1016/j.jag.2012.07.020

Hunt, Honeycutt, W., Yarborough, D., & Starr, G. (2009). 631-Guide to Efficient Irrigation of the Wild Blueberry - *Cooperative Extension: Maine Wild Blueberries - University of Maine Cooperative Extension*. Maine Wild Blueberries. https://extension.umaine.edu/blueberries/factsheets/irrigation/guide-to-efficient-irrigation-of-the-wild-blueberry/

Hussain, S., Gao, K., Din, M., Gao, Y., Shi, Z., & Wang, S. (2020). Assessment of UAV-Onboard Multispectral Sensor for Non-Destructive Site-Specific Rapeseed Crop Phenotype Variable at Different Phenological Stages and Resolutions. *Remote Sensing*, *12*(3), 397. https://doi.org/10.3390/rs12030397

International Blueberry Organization (IBO). (2023, April 27). USDA Reports on Status of China's Blueberry Sector. Blueberry International Organization. https://www.internationalblueberry.org/2023/04/27/usda-reports-on-status-of-chinas-blueberry-sector/

Isaacs, R., & Kirk, A. K. (2010). Pollination services provided to small and large highbush blueberry fields by wild and managed bees. *Journal of Applied Ecology*, *47*(4), 841–849. https://doi.org/10.1111/j.1365-2664.2010.01823.x

Jamieson, A. R. (2008). Developing seed-propagated lowbush blueberry families. *HortScience*, *43*(6), 1686–1689. https://doi.org/10.21273/HORTSCI.43.6.1686

Janes, D. E. (2005). Carbohydrate dynamics of the wild blueberry floral bud *(Vaccinium angustifolium)*. https://central.bac-lac.gc.ca/.item?id=MQ94139&op=pdf&app=Library&is_thesis=1&oclc_number=61427077

Javorek, S. K., Mackenzie, K. E., & Vander Kloet, S. P. (2002). Comparative Pollination Effectiveness Among Bees (Hymenoptera: Apoidea) on Lowbush Blueberry (Ericaceae: *Vaccinium angustifolium*). *Annals of the Entomological Society of America*, *95*(3), 345–351. https://doi.org/10.1603/0013-8746(2002)095[0345:CPEABH]2.0.CO;2

Jensen, K. I. N., & Specht, E. G. (2002). Response of lowbush blueberry (*Vaccinium angustifolium*) to hexazinone applied early in the fruiting year. *Canadian Journal of Plant Science*, *82*(4), 781–783. https://doi.org/10.4141/P01-188

Jones, C. L., Maness, N. O., Stone, M. L., & Jayasekara, R. (2007). Chlorophyll Estimation Using Multispectral Reflectance and Height Sensing. *Transactions of the ASABE*, *50*(5), 1867–1872. https://doi.org/10.13031/2013.23938

Jordan, C. F. (1969). Derivation of Leaf-Area Index from Quality of Light on the Forest Floor. *Ecology*, *50*(4), 663–666. https://doi.org/10.2307/1936256

Jose, S., Abbey, J., Jaakola, L., & Percival, D. (2021). Elucidation of the molecular responses during the primary infection of wild blueberry phenotypes with *Monilinia vaccinii-corymbosi* under field conditions. *BMC Plant Biology*, *21*(1), 493. https://doi.org/10.1186/s12870-021-03281-2

Kaivosoja, J., Hautsalo, J., Heikkinen, J., Hiltunen, L., Ruuttunen, P., Näsi, R., Niemeläinen, O., Lemsalu, M., Honkavaara, E., & Salonen, J. (2021). Reference Measurements in Developing UAV Systems for Detecting Pests, Weeds, and Diseases. *Remote Sensing*, *13*(7), 1238. https://doi.org/10.3390/rs13071238

Kami, C., Lorrain, S., Hornitschek, P., & Fankhauser, C. (2010). Light-Regulated Plant Growth and Development. In *Current Topics in Developmental Biology* (Vol. 91, pp. 29–66). Elsevier. https://doi.org/10.1016/S0070-2153(10)91002-8

Kaur, J., Percival, D., Hainstock, L. J., & Privé, J.-P. (2012). Seasonal growth dynamics and carbon allocation of the wild blueberry plant (*Vaccinium angustifolium* Ait.). *Canadian Journal of Plant Science*, *92*(6), 1145–1154. https://doi.org/10.4141/cjps2011-204

Khaled, A. Y., Abd Aziz, S., Bejo, S. K., Nawi, N. M., Seman, I. A., & Onwude, D. I. (2018). Early detection of diseases in plant tissue using spectroscopy – applications and limitations. *Applied Spectroscopy Reviews*, *53*(1), 36–64. https://doi.org/10.1080/05704928.2017.1352510

Kinsman, G. B. (1993). *The history of the lowbush blueberry industry in Nova Scotia, 1950-1990*. Blueberry Producers' Association of Nova Scotia.

Kokhan, S., & Vostokov, A. (2020). Using Vegetative Indices to Quantify Agricultural Crop Characteristics. *Journal of Ecological Engineering*, *21*(4), 120–127. https://doi.org/10.12911/22998993/119808

Kovaleski, A. P., Williamson, J. G., Olmstead, J. W., & Darnell, R. L. (2015). Inflorescence Bud Initiation, Development, and Bloom in Two Southern Highbush Blueberry Cultivars. *Journal of the American Society for Horticultural Science*, *140*(1), 38–44. https://doi.org/10.21273/JASHS.140.1.38

Krebs, C. J., Boonstra, R., Cowcill, K., & Kenney, A. J. (2009). Climatic determinants of berry crops in the boreal forest of the southwestern Yukon. *Botany*, *87*(4), 401–408. https://doi.org/10.1139/B09-013

Kron, K. A., Powell, E. A., & Luteyn, J. L. (2002). Phylogenetic relationships within the blueberry tribe (Vaccinieae, Ericaceae) based on sequence data from MATK and nuclear ribosomal ITS regions, with comments on the placement of *Satyria*. *American Journal of Botany*, *89*(2), 327–336. https://doi.org/10.3732/ajb.89.2.327

Kumar, S., Kumar, S., & Mohapatra, T. (2021). Interaction Between Macro- and Micro-Nutrients in Plants. *Frontiers in Plant Science*, *12*, 665583. https://doi.org/10.3389/fpls.2021.665583

Kwiecien, R., Kopp-Schneider, A., & Blettner, M. (2011). Concordance analysis: Part 16 of a series on evaluation of scientific publications. *Deutsches Ärzteblatt International*. https://doi.org/DOI:10.3238/arztebl.2011.0515

Lambert, D. H. (1990). Effect of pruning method on the incidence of mummy berry and other lowbush diseases. *Plant Disease*, *74*(3), 199–201.

Lan, Y., Shengde, C., & Fritz, B. (2017). Current status and future trends of precision agricultural aviation technologies. *International Journal of Agricultural and Biological Engineering*, *10*(3), 1–17. https://doi.org/10.3965/j.ijabe.20171003.3088

Lang, G. A., Early, J. D., Martin, G. C., & Darnell, R. L. (1987). Endo-, Para-, and Ecodormancy: Physiological Terminology and Classification for Dormancy Research. *HortScience*, *22*(3), 371–377. https://doi.org/10.21273/HORTSCI.22.3.371

Langdon, D. H. (2008). Biological control of Monilinia and Botrytis blights in lowbush blueberries. https://atrium.lib.uoguelph.ca/xmlui/bitstream/handle/10214/23561/Langdon_DonnaH_MSc.pdf?sequence=1&isAllowed=y

Lee, W.-J., & Lee, C.-W. (2018). Forest Canopy Height Estimation Using Multiplatform Remote Sensing Dataset. *Journal of Sensors*, *2018*, 1–9. https://doi.org/10.1155/2018/1593129

Lehmann, M., Nguyen, U., Allan, M., & van der Woerd, H. (2018). Colour Classification of 1486 Lakes across a Wide Range of Optical Water Types. *Remote Sensing*, *10*(8), 1273. https://doi.org/10.3390/rs10081273

Lewis, H. G., & Brown, M. (2001). A generalized confusion matrix for assessing area estimates from remotely sensed data. *International Journal of Remote Sensing*, *22*(16), 3223–3235. https://doi.org/10.1080/01431160152558332

Li, B., Xu, X., Zhang, L., Han, J., Bian, C., Li, G., Liu, J., & Jin, L. (2020). Above-ground biomass estimation and yield prediction in potato by using UAV-based RGB and hyperspectral imaging. *ISPRS Journal of Photogrammetry and Remote Sensing*, *162*, 161–172. https://doi.org/10.1016/j.isprsjprs.2020.02.013

Liakos, K., Busato, P., Moshou, D., Pearson, S., & Bochtis, D. (2018). Machine Learning in Agriculture: A Review. *Sensors*, *18*(8), 2674. https://doi.org/10.3390/s18082674

Liang, K. Y., & Zeger, S. L. (1993). Regression Analysis for Correlated Data. *Annual Review of Public Health*, *14*(1), 43–68. https://doi.org/10.1146/annurev.pu.14.050193.000355

Liu, T., Li, R., Zhong, X., Jiang, M., Jin, X., Zhou, P., Liu, S., Sun, C., & Guo, W. (2018). Estimates of rice lodging using indices derived from UAV visible and thermal infrared images. *Agricultural and Forest Meteorology*, *252*, 144–154. https://doi.org/10.1016/j.agrformet.2018.01.021

Liu, Y., Kuo, J., Cox, K., Heuvel, J. V., Petersen, K., & Lal, A. (2021). Imaging and Detection of Botrytis Cinerea with Gigahertz Ultrasonic Imager. *2021 IEEE International Ultrasonics Symposium (IUS)*, 1–4. https://doi.org/10.1109/IUS52206.2021.9593815

Lopes, M. S., & Reynolds, M. P. (2012). Stay-green in spring wheat can be determined by spectral reflectance measurements (normalized difference vegetation index) independently from phenology. *Journal of Experimental Botany*, *63*(10), 3789–3798. https://doi.org/10.1093/jxb/ers071

Louhaichi, M., Borman, M. M., & Johnson, D. E. (2001). Spatially Located Platform and Aerial Photography for Documentation of Grazing Impacts on Wheat. *Geocarto International*, *16*(1), 65–70. https://doi.org/10.1080/10106040108542184

Lu, J., Cheng, D., Geng, C., Zhang, Z., Xiang, Y., & Hu, T. (2021). Combining plant height, canopy coverage and vegetation index from UAV-based RGB images to estimate leaf nitrogen concentration of summer maize. *Biosystems Engineering*, *202*, 42–54. https://doi.org/10.1016/j.biosystemseng.2020.11.010

Luby, J. J., Ballington, J. R., Draper, A. D., Pliszka, K., & Austin, M. E. (1991). Blueberries and cranberries (*Vaccinium*). *Acta Horticulturae*, *290*, 393–458. https://doi.org/10.17660/ActaHortic.1991.290.9

Lyu, H., McLean, N., McKenzie-Gopsill, A., & White, S. N. (2021). Weed Survey of Nova Scotia Lowbush Blueberry (*Vaccinium Angustifolium* Ait.) Fields. International Journal of Fruit Science, 21(1), 359–378. https://doi.org/10.1080/15538362.2021.1890674

MacEachern, C. B., Esau, T. J., Schumann, A. W., Hennessy, P. J., & Zaman, Q. U. (2023). Detection of fruit maturity stage and yield estimation in wild blueberry using deep learning convolutional neural networks. *Smart Agricultural Technology*, *3*, 100099. https://doi.org/10.1016/j.atech.2022.100099

Maes, W. H., & Steppe, K. (2019). Perspectives for Remote Sensing with Unmanned Aerial Vehicles in Precision Agriculture. *Trends in Plant Science*, *24*(2), 152–164. https://doi.org/10.1016/j.tplants.2018.11.007

Mahesh, B. (2020). Machine learning algorithms. https://doi.org/10.21275/ART20203995

Mahlein, A.-K., Rumpf, T., Welke, P., Dehne, H.-W., Plümer, L., Steiner, U., & Oerke, E.-C. (2013). Development of spectral indices for detecting and identifying plant diseases. *Remote Sensing of Environment*, *128*, 21–30. https://doi.org/10.1016/j.rse.2012.09.019

Manning, P., & Cutler, G. C. (2018). Ecosystem functioning is more strongly impaired by reducing dung beetle abundance than by reducing species richness. *Agriculture, Ecosystems & Environment*, *264*, 9–14. https://doi.org/10.1016/j.agee.2018.05.002

Maqbool, R., Percival, D. C., Adl, M. S., Zaman, Q. U., & Buszard, D. (2012). In situ estimation of foliar nitrogen in wild blueberry using reflectance spectra. *Canadian Journal of Plant Science*, *92*(6), 1155–1161. https://doi.org/10.4141/cjps2011-203

Maqbool, R., Percival, D., Zaman, Q., Astatkie, T., Adl, S., & Buszard, D. (2016). Improved Growth and Harvestable Yield through Optimization of Fertilizer Rates of Soil-applied Nitrogen, Phosphorus, and Potassium in Wild Blueberry (*Vaccinium angustifolium* Ait.). *HortScience*, *51*(9), 1092–1097. https://doi.org/10.21273/HORTSCI08204-16

Maqbool, R., Zaman, Q., Percival, D., & Sharpe, S. (2010). Narrow Band Reflectance Measurements Can Be Used to Estimate Leaf Area Index, Flower Number, Fruit Set, and Berry Yield of the Wild Blueberry (*Vaccinium angustifolium* Ait.). *Acta Hort. 926*, *Acta Hort. 926*. https://www.actahort.org/members/showpdf?session=2007635

Marc-André Michaud, Chris Watts, & David Percival. (2006). Precision Pesticide Delivery Based on Aerial Spectral Imaging. *2006 CSBE/SCGAB, Edmonton, AB Canada, July 16-19, 2006*. 2006 CSBE/SCGAB, Edmonton, AB Canada, July 16-19, 2006. https://doi.org/10.13031/2013.22081

Marty, C., Khare, S., Rossi, S., Lafond, J., Boivin, M., & Paré, M. C. (2022). Detection of Management Practices and Cropping Phases in Wild Lowbush Blueberry Fields Using Multispectral UAV Data. *Canadian Journal of Remote Sensing*, *48*(3), 469–480. https://doi.org/10.1080/07038992.2022.2070144

Marty, C., Lévesque, J.-A., Bradley, R. L., Lafond, J., & Paré, M. C. (2019). Lowbush blueberry fruit yield and growth response to inorganic and organic N-fertilization when competing with two common weed species. *PLOS ONE*, *14*(12), e0226619. https://doi.org/10.1371/journal.pone.0226619

Matese, A., Toscano, P., Di Gennaro, S., Genesio, L., Vaccari, F., Primicerio, J., Belli, C., Zaldei, A., Bianconi, R., & Gioli, B. (2015). Intercomparison of UAV, Aircraft and Satellite Remote Sensing Platforms for Precision Viticulture. *Remote Sensing*, *7*(3), 2971–2990. https://doi.org/10.3390/rs70302971

McArt, S. H., Miles, T. D., Rodriguez-Saona, C., Schilder, A., Adler, L. S., & Grieshop, M. J. (2016). Floral scent mimicry and vector-pathogen associations in a pseudoflower-inducing plant pathogen system. *PLOS ONE*, *11*(11), e0165761. https://doi.org/10.1371/journal.pone.0165761

McIsaac, D. (1997). Growing Wild Lowbush Blueberries in Nova Scotia. Horticulturist, Production Technology Branch, Nova Scotia Department of Agriculture and Marketing. Wild Blueberry Fact Sheet. https://cdn.dal.ca/content/dam/dalhousie/images/sites/wild-blueberry/pdfs/Growing_Wild_Lowbush_Blueberries_NS.pdf

Mirandilla, J. R. F., Yamashita, M., Yoshimura, M., & Paringit, E. C. (2023). Leaf Spectral Analysis for Detection and Differentiation of Three Major Rice Diseases in the Philippines. *Remote Sensing*, *15*(12), 3058. https://doi.org/10.3390/rs15123058

Mmbaga, M. T., Steadman, J. R., & Roberts, J. J. (1994). Interaction of bean leaf pubescence with rust urediniospore deposition and subsequent infection density. *Annals of Applied Biology*, *125*(2), 243–254. https://doi.org/10.1111/j.1744-7348.1994.tb04966.x

Moola, F. M., & Mallik, A. U. (1998). Phenology of *Vaccinium* spp. in a black spruce (*Picea mariana*) plantation in northwestern Ontario: Possible implications for the timing of forest herbicide treatments. *Canadian Journal of Forest Research*, *28*(10), 1579–1585. https://doi.org/10.1139/x98-151

Moore, J. N. (1993). The blueberry industry of North America. *V International Symposium on Vaccinium Culture*, *346*, 15–26.

Myneni, R. B., Hall, F. G., Sellers, P. J., & Marshak, A. L. (1995). The interpretation of spectral vegetation indexes. *IEEE Transactions on Geoscience and Remote Sensing*, *33*(2), 481–486. https://doi.org/10.1109/TGRS.1995.8746029

Myneni, R. B., Hoffman, S., & Knyazikhin, Y. (2008). Leaf Area Index. *Agronomie*, *20(1), 3–22*. https://appgeodb.nancy.inra.fr/biljou/pdf/LAI_Encyclopedia_of_Ecology_849.pdf

Näsi, R., Viljanen, N., Kaivosoja, J., Alhonoja, K., Hakala, T., Markelin, L., & Honkavaara, E. (2018). Estimating Biomass and Nitrogen Amount of Barley and Grass Using UAV and Aircraft Based Spectral and Photogrammetric 3D Features. *Remote Sensing*, *10*(7), Article 7. https://doi.org/10.3390/rs10071082

Nebiker, S., Lack, N., Abächerli, M., & Läderach, S. (2016). Light-weight multispectral UAV sensors and their capabilities for predicting grain yield and detecting plant diseases. *ISPRS - International Archives of the Photogrammetry, Remote Sensing and Spatial Information Sciences*, *XLI-B1*, 963–970. https://doi.org/10.5194/isprsarchives-XLI-B1-963-2016

Neuendorf. (2022). The Pearson correlation (r) vs. Lin's Concordance coefficient. https://academic.csuohio.edu/kneuendorf/c63310/CorrsCompared10.pdf

Noormets, M., & Olson, A. R. (2006). Bud-autogamy in the velvet-leaf blueberry, *Vaccinium myrtilloides* Michx. *Canadian Journal of Plant Science*, *86*(1), 245–250. https://doi.org/10.4141/P04-118

Nowland, J. L., & MacDougall, J. I. (2013). Soils of Cumberland county Nova Scotia. *Nova Scotia Soils Survey*, *Report No. 17*. https://sis.agr.gc.ca/cansis/publications/surveys/ns/index.html

Oerke, E.-C. (2020). Remote Sensing of Diseases. *Annual Review of Phytopathology*, *58*(1), 225–252. https://doi.org/10.1146/annurev-phyto-010820-012832

Ollinger, S. V. (2011). Sources of variability in canopy reflectance and the convergent properties of plants. *New Phytologist*, *189*(2), 375–394. https://doi.org/10.1111/j.1469-8137.2010.03536.x

Oudemans, P., Besancon, T., Pavlis, G., & Rodriguez-Saona, C. (2018). 2018 Commercial Blueberry Pest Control Recommendations for New Jersey (e265). file:///C:/Users/staff/Downloads/e265.pdf

Pajares, G. (2015). Overview and Current Status of Remote Sensing Applications Based on Unmanned Aerial Vehicles (UAVs). *Photogrammetric Engineering & Remote Sensing*, *81*(4), 281–330. https://doi.org/10.14358/PERS.81.4.281

Panda, S. S., Hoogenboom, G., & Paz, J. (2009). Distinguishing blueberry bushes from mixed vegetation land use using high resolution satellite imagery and geospatial techniques. *Computers and Electronics in Agriculture*, *67*(1–2), 51–58. https://doi.org/10.1016/j.compag.2009.02.007

Panda, S. S., Hoogenboom, G., & Paz, J. (2016). Blueberry orchard delineation with high-resolution imagery and self-organizing map neural image classification. *Agricultural Research & Technology:Open Access Journal*, *3*(1). https://doi.org/10.19080/ARTOAJ.2016.03.555602

Parmentier, C. M., Rowland, L. J., & Linc, M. J. (1998). Water status in relation to maintenance and release from dormancy in blueberry flower buds. *Journal of the American Society for Horticultural Science*, *123*(5), 762–769. https://doi.org/10.21273/JASHS.123.5.762

Peltoniemi, J. I., Kaasalainen, S., Näränen, J., Rautiainen, M., Stenberg, P., Smolander, H., Smolander, S., & Voipio, P. (2005). BRDF measurement of understory vegetation in pine forests: Dwarf shrubs, lichen, and moss. *Remote Sensing of Environment*, *94*(3), 343–354. https://doi.org/10.1016/j.rse.2004.10.009

Peña, M. A., Liao, R., & Brenning, A. (2017). Using spectrotemporal indices to improve the fruit-tree crop classification accuracy. *ISPRS Journal of Photogrammetry and Remote Sensing*, *128*, 158–169. https://doi.org/10.1016/j.isprsjprs.2017.03.019

Penglei, L., Zhang, X., Wang, W., & Zheng, H. (2020). Estimating aboveground and organ biomass of plant canopies across the entire season of rice growth with terrestrial laser scanning. https://doi.org/10.1016/j.jag.2020.102132

Penman, L. N., & Annis, S. L. (2005). Leaf and Flower Blight Caused by *Monilinia vaccinii-corymbosi* on Lowbush Blueberry: Effects on Yield and Relationship to Bud Phenology. *Phytopathology®*, *95*(10), 1174–1182. https://doi.org/10.1094/PHYTO-95-1174

Penuelas, J., Bareth, F., & Filella, I. (1995). Semi-empirical indices to assess carotenoids/chlorophyll a ratio from leaf spectral reflectance. *Photosynthetica*, *31*(2), 221–230.

Penuelas, J., Llusia, J., Pinol, J., & Filella, I. (1997). Photochemical reflectance index and leaf photosynthetic radiation-use-efficiency assessment in Mediterranean trees. *International Journal of Remote Sensing*, *18*(13), 2863–2868. https://doi.org/10.1080/014311697217387

Penuelas, J., Pinol, J., Ogaya, R., & Filella, I. (1997). Estimation of plant water concentration by the reflectance Water Index WI (R900/R970). *International Journal of Remote Sensing*, *18*(13), 2869–2875. https://doi.org/10.1080/014311697217396

Percival, D., & Beaton, E. (2012). Suppression of *Monilinia* Blight: Strategies for Today and Potential Fungicide Options for Tomorrow. *International Journal of Fruit Science*, *12*(1–3), 124–134. https://doi.org/10.1080/15538362.2011.619357

Percival, D. C., Janes, D. E., Stevens, D. E., & Sanderson, K. (2003). Impact of multiple fertilizer applications on plant growth, development, and yield of wild lowbush blueberry (*Vaccinium angustifolium* Aiton). *Acta Horticulturae*, *626*, 415–421. https://doi.org/10.17660/ActaHortic.2003.626.57

Percival, D. C., & Privé, J. P. (2002). Nitrogen formulation influences plant nutrition and yield components of lowbush blueberry (*Vaccinium angustifolium* Ait.). *Acta Horticulturae*, *574*, 347–353. https://doi.org/10.17660/ActaHortic.2002.574.52

Percival, D., Jose, S., Guo, L., Schilder, A., & Olson, R. A. (2018). *Monilinia vaccinii-corymbosi* sensitivity to demethylation inhibitor fungicides and its effect on Monilinia blight control in wild blueberry fields. *North American Blueberry Research Extension Workers Conference, Proceeding Papers*. https://digitalcommons.library.umaine.edu/cgi/viewcontent.cgi?article=1004&context=nabrew2018

Percival, D., & Sanderson, K. (2004). Main and Interactive Effects of Vegetative-Year Applications of Nitrogen, Phosphorus, and Potassium Fertilizers on the Wild Blueberry. *Small Fruits Review*, *3*(1–2), 105–121. https://doi.org/10.1300/J301v03n01_11

Pinto, F., Celesti, M., Acebron, K., Alberti, G., Cogliati, S., Colombo, R., Juszczak, R., Matsubara, S., Miglietta, F., Palombo, A., Panigada, C., Pignatti, S., Rossini, M., Sakowska, K., Schickling, A., Schüttemeyer, D., Stróżecki, M., Tudoroiu, M., & Rascher, U. (2020). Dynamics of sun-induced chlorophyll fluorescence and reflectance to detect stress-induced variations in canopy photosynthesis. *Plant, Cell & Environment*, *43*(7), 1637–1654. https://doi.org/10.1111/pce.13754

Polder, G., Pekkeriet, E., Snikkers, M., & Ur, W. (2013). A Spectral Imaging System for Detection of Botrytis in Greenhouses. *EFITA-WCCA-CIGR Conference, "Sustainable Agriculture through ICT Innovation,"* 8.

Pourazar, H., Samadzadegan, F., & Dadrass Javan, F. (2019). Aerial multispectral imagery for plant disease detection: Radiometric calibration necessity assessment. *European Journal of Remote Sensing*, *52*(sup3), 17–31. https://doi.org/10.1080/22797254.2019.1642143

R Core Team. (2023). R: A language and environment for statistical computing (4.2.3) [Computer software]. R Foundation for Statistical Computing. https://www.R-project.org/

Ranganathan, S., Gribskov, M. R., Nakai, K., & Schönbach, C. (Eds.). (2019). Encyclopedia of bioinformatics and computational biology. Elsevier.

Raven, P. H., Evert, F. R., & Eichhorn, E. S. (1992). *The Biology of Plants*. https://archive.org/stream/raven-biology-of-plants-8th-edition/Raven%20Biology%20of%20Plants%208th%20Edition_djvu.txt

Reeh, K. W. (2012). Commercial Bumble Bees as Vectors of the Microbial Antagonist Clonostachys for Management of Botrytis Blight in Wild Blueberry (Vaccinium angustifolium). *Unpublished Masters Dissertation at Dalhousie University*. https://dalspace.library.dal.ca/bitstream/handle/10222/15008/Reeh_Kevin_MSc_AGRI_June_2012.pdf?sequence=1&isAllowed=y

Reeh, K. W., & Cutler, G. C. (2013). Laboratory efficacy and fungicide compatibility of *Clonostachys rosea* against *Botrytis* blight on lowbush blueberry. *Canadian Journal of Plant Science*, *93*(4), 639–642. https://doi.org/10.4141/cjps2012-306

Riddick, E. W., & Simmons, A. M. (2014). Do plant trichomes cause more harm than good to predatory insects?: Plant trichomes and predators. *Pest Management Science*, *70*(11), 1655–1665. https://doi.org/10.1002/ps.3772

Ritchie, R. J., & Runcie, J. W. (2014). A portable reflectance-absorptance-transmittance meter for photosynthetic work on vascular plant leaves. *Photosynthetica*, *52*(4), 614–626. https://doi.org/10.1007/s11099-014-0069-y

Rouse, J. W., Haas, R. H., Schell, J. A., & Deering, D. W. (1974). Monitoring vegetation systems in the Great Plains with ERTS. *NASA Special Publication*, *351(1974), 309*. https://ntrs.nasa.gov/api/citations/19730017588/downloads/19730017588.pdf

Rutherford, P. M., McGill, W. B., Arocena, J. M., & Figueiredo, C. T. (2007). Soil sampling and methods of analysis: Total Nitrogen (M. R. Carter & E. G. Gregorich, Eds.). CRC press.

Rwanga, S. S., & Ndambuki, J. M. (2017). Accuracy Assessment of Land Use/Land Cover Classification Using Remote Sensing and GIS. *International Journal of Geosciences*, *08*(04), 611–622. https://doi.org/10.4236/ijg.2017.84033

Saleem, S. R., Zaman, Q. U., Schumann, A. W., Madani, A., Farooque, A. A., & Percival, D. C. (2013). Impact of variable rate fertilization on subsurface water contamination in wild blueberry cropping system. *Applied Engineering in Agriculture*, *29(2), 225–232*, 8.

Santiago, J. P. (2011). Improving Lowbush Blueberry (*Vaccinium angustifolium* Ait.) Growth and Development through Optimal Mineral Nutrition. *Electronic Theses and Dissertations*. https://digitalcommons.library.umaine.edu/etd/728/

Santiago, J. P., & Smagula, J. M. (2013). Effects of nitrogen form and ratio on in vitro shoot multiplication and growth of lowbush blueberry (*Vaccinium angustifolium* Ait.). *Acta Horticulturae*, *988*, 129–135. https://doi.org/10.17660/ActaHortic.2013.988.14

Sharpe, S. (2008). *Potential for Hyperspectral Technology in Wild Blueberry (Vaccinium angustifolium Ait.) Production*. *47*(3). https://www.collectionscanada.gc.ca/obj/thesescanada/vol2/002/MR43524.PDF?is_thesis=1&oclc_number=693657324

Siedliska, A., Baranowski, P., Zubik, M., Mazurek, W., & Sosnowska, B. (2018). Detection of fungal infections in strawberry fruit by VNIR/SWIR hyperspectral imaging. *Postharvest Biology and Technology*, *139*, 115–126. https://doi.org/10.1016/j.postharvbio.2018.01.018

Sims, D. A., & Gamon, J. A. (2002). Relationships between leaf pigment content and spectral reflectance across a wide range of species, leaf structures and developmental stages. *Remote Sensing of Environment*, *81*(2–3), 337–354. https://doi.org/10.1016/S0034-4257(02)00010-X

Smagula, J. M., & Hepler, P. R. (1978). Comparison of Urea and Sulfur-coated Urea as Nitrogen Sources for Lowbush Blueberries Growing on a Colton Gravelly Loamy Sand1. *Journal of the American Society for Horticultural Science*, *103*(6), 818–820. https://doi.org/10.21273/JASHS.103.6.818

Smagula, J. M., & Litten, W. (2002). Correcting lowbush blueberry boron deficiency with soil or foliar application. *Acta Horticulturae*, *574*, 363–371. https://doi.org/10.17660/ActaHortic.2002.574.54

Souza, H. B., Baio, F. H. R., & Neves, D. C. (2017). Using passive and active multispectral sensors on the correlation with the phenological indices of cotton. *Engenharia Agrícola*, *37*(4), 782–789. https://doi.org/10.1590/1809-4430-eng.agric.v37n4p782-789/2017

Spann, T. M., Williamson, J. G., & Darnell, R. L. (2004). Photoperiod and Temperature Effects on Growth and Carbohydrate Storage in Southern Highbush Blueberry Interspecific Hybrid. *Journal of the American Society for Horticultural Science*, *129*(3), 294–298. https://doi.org/10.21273/JASHS.129.3.0294

Sripada, R. P., Heiniger, R. W., White, J. G., & Meijer, A. D. (2006). Aerial Color Infrared Photography for Determining Early In-Season Nitrogen Requirements in Corn. *Agronomy Journal*, *98*(4), 968–977. https://doi.org/10.2134/agronj2005.0200

Stagakis, S., González-Dugo, V., Cid, P., Guillén-Climent, M. L., & Zarco-Tejada, P. J. (2012). Monitoring water stress and fruit quality in an orange orchard under regulated deficit irrigation using narrow-band structural and physiological remote sensing indices. *ISPRS Journal of Photogrammetry and Remote Sensing*, *71*, 47–61. https://doi.org/10.1016/j.isprsjprs.2012.05.003

Starast, M., Karp, K., & Vool, E. (2007). Effect of NPK fertilization and elemental sulphur on growth and yield of lowbush blueberry. *Agricultural and Food Science*, *16*(1), Article 1. https://doi.org/10.2137/145960607781635859

Statistics Canada. (2020). *Estimates, production and farm gate value of fresh and processed fruits* [Dataset]. Government of Canada. https://doi.org/10.25318/3210036401-ENG

Statistics Canada. (2023). *Estimates, production and farm gate value of fresh and processed fruits* [Dataset]. Government of Canada. https://doi.org/10.25318/3210036401-ENG

Stephens, D. T., Levesque, D. E., & Davis, A. R. (2012). Pollen-ovule ratios in seven species of *Vaccinium* (Ericaceae) and stamen structure in *Vaccinium myrtilloides* and *Vaccinium vitis-idaea*. This article is part of a Special Issue entitled “Pollination biology research in Canada: Perspectives on a mutualism at different scales”. *Botany*, *90*(7), 599–614. https://doi.org/10.1139/b2012-061

Strehler, B. L., & Arnold, W. (1951). Ligh Production by Green Plants. *The Journal of General Physiology*, 809–820.

Strong, C. J., Burnside, N. G., & Llewellyn, D. (2017). The potential of small-Unmanned Aircraft Systems for the rapid detection of threatened unimproved grassland communities using an Enhanced Normalized Difference Vegetation Index. *PLOS ONE*, *12*(10), e0186193. https://doi.org/10.1371/journal.pone.0186193

Su, J., Liu, C., Coombes, M., Hu, X., Wang, C., Xu, X., Li, Q., Guo, L., & Chen, W.-H. (2018). Wheat yellow rust monitoring by learning from multispectral UAV aerial imagery. *Computers and Electronics in Agriculture*, *155*, 157–166. https://doi.org/10.1016/j.compag.2018.10.017

Susmita, R. (2019). *Proceedings of the International Conference on Machine Learning, Big Data, Cloud and Parallel Computing: Trends, perspectives and prospects: COMITCON-2019: 14th-16th February, 2019*. IEEE. https://ieeexplore.ieee.org/stamp/stamp.jsp?tp=&arnumber=8862451

Tao, H., Feng, H., Xu, L., Miao, M., Yang, G., Yang, X., & Fan, L. (2020). Estimation of the Yield and Plant Height of Winter Wheat Using UAV-Based Hyperspectral Images. *Sensors*, *20*(4), 1231. https://doi.org/10.3390/s20041231

Thompson, A. A., & Annis, S. L. (2014). Fungicide Sensitivity Assessed in *Monilinia vaccinii-corymbosi* Isolates from Lowbush Blueberry Fields in Maine. *Plant Health Progress*, *15*(3), 141–144. https://doi.org/10.1094/PHP-RS-13-0127

Thyssen, G., Percival, D., Burton, D., & Sanderson, K. (2006). Effect of nitrogen fertilizers on ammonia volatilization in wild blueberry production. *Canadian Journal of Plant Science*, *86*(Special Issue), 1383–1386. https://doi.org/10.4141/P06-121

Tilly, N., Aasen, H., & Bareth, G. (2015). Fusion of Plant Height and Vegetation Indices for the Estimation of Barley Biomass. *Remote Sensing*, *7*(9), 11449–11480. https://doi.org/10.3390/rs70911449

Tirmenstein, D. (1990). *Vaccinium myrtilloides. In: Fire Effects Information System* [U.S. Department of Agriculture, Forest Service, Rocky Mountain Research Station, Fire Sciences Laboratory]. Fire Effects Information System (FEIS). https://www.fs.usda.gov/database/feis/plants/shrub/vacmyt/all.html

Tirmenstein, D. (1991). *Vaccinium angustifolium* [U.S. Department of Agriculture, Forest Service, Rocky Mountain Research Station, Fire Sciences Laboratory]. Fire Effects Information System (FEIS). https://www.fs.usda.gov/database/feis/plants/shrub/vacang/all.html

Trevett, M. F. (1972). A second approximation of leaf analysis standards for lowbush blueberry. Research in the Life Sciences. *Maine Agricultural Experiment Station*, *19*, 15–16.

Uchida, R. (2000). Essential Nutrients for Plant Growth: Nutrient Functions and Deficiency Symptoms. *Plant Nutrient Management in Hawaii's Soils*, *4*, 31–55.

USGS, L. B. T. (2013). Integrated Taxonomic Information System (ITIS). https://doi.org/10.5066/F7KH0KBK

Usha, K., & Singh, B. (2013). Potential applications of remote sensing in horticulture—A review. *Scientia Horticulturae*, *153*, 71–83. https://doi.org/10.1016/j.scienta.2013.01.008

Vander Kloet, S. P. (1978). Systematics, Distribution, and Nomenclature of the Polymorphic *Vaccinium Angustifolium*. *Rhodora*, *80*(823), 358–376.

Vander Kloet, S. P. (1988). The genus *Vaccinium* in North America. Agriculture Canada Publication. https://publications.gc.ca/collections/collection_2014/aac-aafc/agrhist/A43-1828-1988-eng.pdf

Vander Kloet, S. P., & Avery, T. S. (2010). Vaccinium on the edge. *Edinburgh Journal of Botany*, *67*(1), 7–24. https://doi.org/10.1017/S0960428609990199

Vander Kloet, S. P., & Dickinson, T. A. (2009). A subgeneric classification of the genus Vaccinium and the metamorphosis of V. section Bracteata Nakai: More terrestrial and less epiphytic in habit, more continental and less insular in distribution. *Journal of Plant Research*, *122*(3), 253–268. https://doi.org/10.1007/s10265-008-0211-7

Vaštakaitė-Kairienė, V., Rasiukevičiūtė, N., Dėnė, L., Chrapačienė, S., & Valiuškaitė, A. (2021). Determination of Specific Parameters for Early Detection of *Botrytis cinerea* in Lettuce. *Horticulturae*, *8*(1), 23. https://doi.org/10.3390/horticulturae8010023

Vega, F. A., Ramírez, F. C., Saiz, M. P., & Rosúa, F. O. (2015). Multi-temporal imaging using an unmanned aerial vehicle for monitoring a sunflower crop. *Biosystems Engineering*, *132*, 19–27. https://doi.org/10.1016/j.biosystemseng.2015.01.008

Velásquez, A. C., Castroverde, C. D. M., & He, S. Y. (2018). Plant–Pathogen Warfare under Changing Climate Conditions. *Current Biology*, *28*(10), R619–R634. https://doi.org/10.1016/j.cub.2018.03.054

Vélez, S., Ariza-Sentís, M., & Valente, J. (2023a). Dataset on unmanned aerial vehicle multispectral images acquired over a vineyard affected by *Botrytis cinerea* in northern Spain. *Data in Brief*, *46*, 108876. https://doi.org/10.1016/j.dib.2022.108876

Vélez, S., Ariza-Sentís, M., & Valente, J. (2023b). Mapping the spatial variability of Botrytis bunch rot risk in vineyards using UAV multispectral imagery. *European Journal of Agronomy*, *142*, 126691. https://doi.org/10.1016/j.eja.2022.126691

Vicente, R., Vergara-Díaz, O., Kerfal, S., López, A., Melichar, J., Bort, J., Serret, M. D., Araus, J. L., & Kefauver, S. C. (2019). Identification of traits associated with barley yield performance using contrasting nitrogen fertilizations and genotypes. *Plant Science*, *282*, 83–94. https://doi.org/10.1016/j.plantsci.2018.10.002

Vilfan, N., van der Tol, C., Muller, O., Rascher, U., & Verhoef, W. (2016). Fluspect-B: A model for leaf fluorescence, reflectance and transmittance spectra. *Remote Sensing of Environment*, *186*, 596–615. https://doi.org/10.1016/j.rse.2016.09.017

Vilhar, U., Beuker, E., Mizunuma, T., Skudnik, M., Lebourgeois, F., Soudani, K., & Wilkinson, M. (2013). Tree Phenology. In *Developments in Environmental Science* (Vol. 12, pp. 169–182). Elsevier. https://doi.org/10.1016/B978-0-08-098222-9.00009-1

Viña, A., Gitelson, A. A., Rundquist, D. C., Keydan, G., Leavitt, B., & Schepers, J. (2004). Monitoring Maize (*Zea mays* L.) Phenology with Remote Sensing. *Agronomy Journal*, *96*(4), 1139–1147. https://doi.org/10.2134/agronj2004.1139

Vincini, M., Frazzi, E., & D'Alessio, P. (2007). Narrow band vegetation indexes from hyperion and directional chris/proba data for canopy chlorophyll density estimation in maize. *In Proceedings of the Envisat Symposium*, 23–27.

Walter, A., Liebisch, F., & Hund, A. (2015). Plant phenotyping: From bean weighing to image analysis. *Plant Methods*, *11*(1), 14. https://doi.org/10.1186/s13007-015-0056-8

Wang, L., Tian, Y., Yao, X., Zhu, Y., & Cao, W. (2014). Predicting grain yield and protein content in wheat by fusing multi-sensor and multi-temporal remote-sensing images. *Field Crops Research*, *164*, 178–188. https://doi.org/10.1016/j.fcr.2014.05.001

Weingarten, E., Martin, R. E., Hughes, R. F., Vaughn, N. R., Shafron, E., & Asner, G. P. (2022). Early detection of a tree pathogen using airborne remote sensing. *Ecological Applications*, *32*(2). https://doi.org/10.1002/eap.2519

Weiss, M., Jacob, F., & Duveiller, G. (2020). Remote sensing for agricultural applications: A meta-review. *Remote Sensing of Environment*, *236*, 111402. https://doi.org/10.1016/j.rse.2019.111402

White, M. A., de BEURS, K. M., Didan, K., Inouye, D. W., Richardson, A. D., Jensen, O. P., O'Keefe, J., Zhang, G., Nemani, R. R., van LEEUWEN, W. J. D., Brown, J. F., de WIT, A., Schaepman, M., Lin, X., Dettinger, M., Bailey, A. S., Kimball, J., Schwartz, M. D., Baldocchi, D. D., … Lauenroth, W. K. (2009). Intercomparison, interpretation, and assessment of spring phenology in North America estimated from remote sensing for 1982-2006. *Global Change Biology*, *15*(10), 2335–2359. https://doi.org/10.1111/j.1365-2486.2009.01910.x

White, S. N., Boyd, N. S., & Van Acker, R. C. (2012). Growing Degree-day Models for Predicting Lowbush Blueberry (Vaccinium angustifolium Ait.) Ramet Emergence, Tip Dieback, and Flowering in Nova Scotia, Canada. *HortScience*, *47*(8), 1014–1021. https://doi.org/10.21273/HORTSCI.47.8.1014

Williamson, J. G., Maust, B. E., & NeSmith, D. S. (2001). Timing and Concentration of Hydrogen Cyanamide Affect Blueberry Bud Development and Flower Mortality. *HortScience*, *36*(5), 922–924. https://doi.org/10.21273/HORTSCI.36.5.922

Wood, F. A., & Barker, W. G. (1963). Stem Pigmentation in Lowbush Blueberry. *Plant Physiology*, *38*(2), 191–193. https://doi.org/10.1104/pp.38.2.191

Wood, G. W. (1961). The influence of honeybee pollination on fruit set of the lowbush blueberry. *Canadian Journal of Plant Science*, *41*(2), 332–335. https://doi.org/10.4141/cjps61-045

Wood, G. W. (2004). The Wild Blueberry Industry—Past. *Small Fruits Review*, *3*(1–2), 11–18. https://doi.org/10.1300/J301v03n01_03

Wood, S., Smreciu, A., & Gould, K. (2013). *Vaccinium myrtilloides:* Blueberry, velvet-leaf blueberry, Canada blueberry, velvet-leaf huckleberry. https://acrre.ualberta.ca/acrre/wp-content/uploads/sites/45/2018/04//Vaccinium_myrtilloides.pdf

Woolley, J. T. (1971). Reflectance and Transmittance of Light by Leaves. *Plant Physiology*, *47*, 656–662.

Wu, D., Feng, L., & He, Y. (2008). Early detection of Botrytis cinerea on Eggplant leaves based on visible and near-infrared spectroscopy. *51*(3), 1133–1139.

Wu, D., Feng, L., Zhang, C., & He, Y. (2008). Early Detection of Botrytis cinerea on Eggplant Leaves Based on Visible and Near-Infrared Spectroscopy. *Transactions of the ASABE*, *51*(3), 1133–1139. https://doi.org/10.13031/2013.24504

Xue, J., & Su, B. (2017a). Significant Remote Sensing Vegetation Indices: A Review of Developments and Applications. *Journal of Sensors*, *2017*, 1–17. https://doi.org/10.1155/2017/1353691

Xue, J., & Su, B. (2017b). Significant Remote Sensing Vegetation Indices: A Review of Developments and Applications. *Journal of Sensors*, *2017*, 1–17. https://doi.org/10.1155/2017/1353691

Yamamoto, H., Hashimoto, T., Seki, M., Yuda, N., Mitomi, Y., & Yoshioka, H. (2005). Evaluation of GLI reflectance and vegetation indices with MODIS products. https://apps.dtic.mil/sti/pdfs/ADA449784.pdf

Yang, C. (2020). Remote Sensing and Precision Agriculture Technologies for Crop Disease Detection and Management with a Practical Application Example. *Engineering*, *6*(5), 528–532. https://doi.org/10.1016/j.eng.2019.10.015

Yang, Z., Rao, M. N., Elliott, N. C., Kindler, S. D., & Popham, T. W. (2005). Using ground-based multispectral radiometry to detect stress in wheat caused by greenbug (Homoptera: Aphididae) infestation. *Computers and Electronics in Agriculture*, *47*(2), 121–135. https://doi.org/10.1016/j.compag.2004.11.018

Yarborough, D., Drummond, F., Annis, S., & D'Appollonio, J. (2017). Maine wild blueberry systems analysis. *Acta Horticulturae*, *1180*, 151–160. https://doi.org/10.17660/ActaHortic.2017.1180.21

Yarborough, D. E. (2004). Factors Contributing to the Increase in Productivity in the Wild Blueberry Industry. *Small Fruits Review*, *3*(1–2), 33–43. https://doi.org/10.1300/J301v03n01_05

Yarborough, D. E. (2012). Establishment and Management of the Cultivated Lowbush Blueberry (*Vaccinium angustifolium*). *International Journal of Fruit Science*, *12*(1–3), 14–22. https://doi.org/10.1080/15538362.2011.619130

Yarborough, D. E., Hanchar, J. J., Skinner, S. P., & Ismail, A. A. (1986). Weed Response, Yield, and Economics of Hexazinone and Nitrogen use in Lowbush Blueberry Production. *Weed Science*, *34*(5), 723–729. https://doi.org/10.1017/S0043174500067758

Yu, D., Zha, Y., Sun, Z., Li, J., Jin, X., Zhu, W., Bian, J., Ma, L., Zeng, Y., & Su, Z. (2022). Deep convolutional neural networks for estimating maize above-ground biomass using multi-source UAV images: A comparison with traditional machine learning algorithms. *Precision Agriculture*. https://doi.org/10.1007/s11119-022-09932-0

Yue, J., Yang, G., Tian, Q., Feng, H., Xu, K., & Zhou, C. (2019). Estimate of winter-wheat above-ground biomass based on UAV ultrahigh-ground-resolution image textures and vegetation indices. *ISPRS Journal of Photogrammetry and Remote Sensing*, *150*, 226–244. https://doi.org/10.1016/j.isprsjprs.2019.02.022

Zahiri, Z., Laefer, D. F., Kurz, T., Buckley, S., & Gowen, A. (2022). A comparison of ground-based hyperspectral imaging and red-edge multispectral imaging for façade material classification. *Automation in Construction*, *136*, 104164. https://doi.org/10.1016/j.autcon.2022.104164

Zaman, Q. U., Schumann, A. W., Percival, D. C., & Gordon, R. J. (2008). Estimation of Wild Blueberry Fruit Yield Using Digital Color Photography. *Transactions of the ASABE*, *51*(5), 1539–1544. https://doi.org/10.13031/2013.25302

Zhang, D., Wang, Q., Lin, F., Yin, X., Gu, C., & Qiao, H. (2020). Development and Evaluation of a New Spectral Disease Index to Detect Wheat Fusarium Head Blight Using Hyperspectral Imaging. *Sensors*, *20*(8), 2260. https://doi.org/10.3390/s20082260

Zhang, F., Zaman, Q. U., Percival, D. C., & Schumann, A. W. (2010). Detecting Bare Spots in Wild Blueberry Fields Using Digital Color Photography. *Applied Engineering in Agriculture*, *26*(5), 723–728. https://doi.org/10.13031/2013.34938

Zhang, J., Huang, Y., Pu, R., Gonzalez-Moreno, P., Yuan, L., Wu, K., & Huang, W. (2019). Monitoring plant diseases and pests through remote sensing technology: A review. *Computers and Electronics in Agriculture*, *165*, 104943. https://doi.org/10.1016/j.compag.2019.104943

Zhang, J., Wang, C., Yang, C., Xie, T., Jiang, Z., Hu, T., Luo, Z., Zhou, G., & Xie, J. (2020). Assessing the Effect of Real Spatial Resolution of In Situ UAV Multispectral Images on Seedling Rapeseed Growth Monitoring. *Remote Sensing*, *12*(7), 1207. https://doi.org/10.3390/rs12071207

Zhang, X., Friedl, M. A., Schaaf, C. B., Strahler, A. H., Hodges, J. C. F., Gao, F., Reed, B. C., & Huete, A. (2003). Monitoring vegetation phenology using MODIS. *Remote Sensing of Environment*, *84*(3), 471–475. https://doi.org/10.1016/S0034-4257(02)00135-9

Zhang, X., Zhang, F., Qi, Y., Deng, L., Wang, X., & Yang, S. (2019). New research methods for vegetation information extraction based on visible light remote sensing images from an unmanned aerial vehicle (UAV). *International Journal of Applied Earth Observation and Geoinformation*, *78*, 215–226. https://doi.org/10.1016/j.jag.2019.01.001

Zheng, Q., Huang, W., Cui, X., Shi, Y., & Liu, L. (2018). New Spectral Index for Detecting Wheat Yellow Rust Using Sentinel-2 Multispectral Imagery. *Sensors*, *18*(3), 868. https://doi.org/10.3390/s18030868

Zhou, X., Zheng, H. B., Xu, X. Q., He, J. Y., Ge, X. K., Yao, X., Cheng, T., Zhu, Y., & Cao, W. X. (2017). Predicting grain yield in rice using multi-temporal vegetation indices from UAV-based multispectral and digital imagery. https://doi.org/10.1016/j.isprsjprs.2017.05.003

APPENDICES

APPENDIX 1: List of publications and conference presentations

Peer reviewed publications

Anku, K. E., Percival, D. C., Rajasekaran, L. R., Heung, B., & Vankoughnett, M. (2024). Remote estimation of Nitrogen and its impact on growth parameters in wild blueberries. Frontiers in remote sensing. (Submitted)

Anku, K. E., Percival, D. C., Rajasekaran, L. R., Heung, B., & Vankoughnett, M. (2024). Remote assessment of phenology on the wild blueberry field using multi and hyperspectral sensors. Remote sensing MDPI. (In Prep)

Conference publications

Anku, K. E., Percival, D. C., Rajasekaran, L. R., Heung, B., & Vankoughnett, M. (2023). Phenological assessment of the wild blueberry field using an unmanned aerial vehicle. Acta Horticulturae, 1357, 35–42. https://doi.org/10.17660/ActaHortic.2023.1357.6

Percival, D. C., Anku, K., & Langdon, J. (2023). Phenotypic, phenology, and disease pressure assessments in wild blueberry fields through the use of remote sensing technologies. Acta Horticulturae, 1357, 123–130. https://doi.org/10.17660/ActaHortic.2023.1381.17

Manuscripts under preparation

Anku, K. E., Percival, D. C., Rajasekaran, L. R., Heung, B., & Vankoughnett, M. (In Prep). Determination of wild blueberry phenotypes using high-resolution imagery from an unmanned aerial vehicle. Canadian Journal of Remote Sensing.

Anku, K. E., Percival, D. C., Rajasekaran, L. R., Heung, B., & Vankoughnett, M. (In Prep). Determination of Monilinia and Botrytis blight diseases using multi and hyperspectral sensors. Remote sensing MDPI

Conference and seminar presentations

Anku, K. E., Percival, D. C., Rajasekaran, L. R., Heung, B., & Vankoughnett, M. (2021). Phenological assessment of the wild blueberry field using an unmanned aerial vehicle. XII International Vaccinium Symposium. Oral Presentation; 30 August – Sept. 1, 2021.

Anku, K., (2021). Potential use of vegetative indices to detect and estimate disease severities of Monilinia and Botrytis blight on wild blueberry fields. Tri-Society Virtual Conference. Oral Presentation; 6th July 2021. Retrieved from https://trisocieties2021.ca/flipbook/?page=6

Anku, K. and Percival, D., (2019). Remote Assessment of Phenological and Phenotypical Variability in Wild Blueberry Fields. Plant Canada Conference 2019, Ontario, University of Guelph 7th - 10th July 2019. Retrieved from http://www.plantcanada.ca/proceeding/2019/Plant%20Canada%202019%20Program%20Booklet.pdf

Abbey, J., Anku, K., and Percival, D., (2019). Disease Management and Remote Sensing 2019/2020. PEI Wild Blueberry Information Day and Annual General Meeting of PEI WBGA. Florence Simmons Performing Hall on 5th April 2019. Retrieved from http://www.gov.pe.ca/af/agweb/events_calendar/displaylinks.php3?event_id=3373

Anku, K. and Percival, D., (2019). Remote Sensing and Geospatial Phenotype and Phenology Mapping in Wild Blueberry Fields. Fields Day at Spring Hill. Poster Presentation; 18th July 2019.

Anku, K., (2019). Remote Sensing and Geospatial Phenotype and Phenology Mapping. Twilight Meeting for Growers and Producers. Poster Presentation; 30th May 2019.

APPENDIX 2: Impact of nitrogen on vegetative indices

Table A 1. Analysis of Variance on the effects of nitrogen rates on vegetative indices observed from Lemmon Hill on [26th June 2020].

Treatment	GLI	GRVI	VARI	NDVI	NDRE	ENDVI	SAVI
0 kg N/ha	0.293	0.218	0.291	0.787	0.383	0.760	0.593
15 kg N/ha	0.244	0.161	0.217	0.738	0.371	0.718	0.553
30 kg N/ha	0.286	0.210	0.281	0.780	0.382	0.753	0.590
60 kg N/ha	0.279	0.202	0.271	0.772	0.381	0.746	0.584
ANOVA Results[1]	**NS**	**NS**	**NS**	**NS**	**NS**	**NS**	**NS**

[1] Analysis of variance (ANOVA) results refer to treatment effects that were either not significant (NS) or significant at $p<0.05$. Mean separation was completed using Fisher's multiple means comparison test procedure ($\alpha=0.05$).

Table A 2. Analysis of Variance on the effects of nitrogen rates on vegetative indices observed from Lemmon Hill on [16th September 2020].

Treatment	GLI	GRVI	VARI	NDVI	NDRE	ENDVI	SAVI
0 kg N/ha	0.278	0.261	0.392	0.512	0.131	0.452	0.586
15 kg N/ha	0.251	0.219	0.320	0.438	0.122	0.418	0.500
30 kg N/ha	0.276	0.252	0.372	0.498	0.129	0.452	0.569
60 kg N/ha	0.277	0.260	0.389	0.488	0.150	0.436	0.558
ANOVA Results[1]	**NS**	**NS**	**NS**	**NS**	**NS**	**NS**	**NS**

[1]Analysis of variance (ANOVA) results refer to treatment effects that were either not significant (NS) or significant at $p<0.05$. Mean separation was completed using Fisher's multiple means comparison test procedure ($\alpha=0.05$).

Table A 3. Analysis of variance on the effects of nitrogen rates on vegetative indices (n = 25) from Lemmon Hill [6th October 2021]

Treatment	GLI	GRVI	VARI	NDVI	NDRE	ENDVI	SAVI
0 kg N/ha	0.240a	0.305a	0.553a	0.535	0.139	0.339	0.773a
20 kg N/ha	0.246a	0.309a	0.549a	0.512	0.152	0.351	0.759a
40 kg N/ha	0.210ab	0.263ab	0.480ab	0.495	0.151	0.318	0.711ab
60 kg N/ha	0.219a	0.272ab	0.485ab	0.505	0.154	0.331	0.704ab
100 kg N/ha	0.159b	0.206b	0.395b	0.447	0.150	0.276	0.650b
ANOVA Results[1]	**p<0.038**	**p<0.031**	**p<0.048**	**NS**	**NS**	**NS**	**p<0.037**

[1]Analysis of variance (ANOVA) results refer to treatment effects that were either not significant (NS) or significant at p<0.05. Mean separation was completed using Fisher's multiple means comparison test procedure (α=0.05).

Table A 4. Analysis of variance on the effects of nitrogen rates on vegetative indices (n = 25) from the Debert location [22nd October 2021].

Treatment	GLI	GRVI	VARI	NDVI	NDRE	ENDVI	SAVI
0 kg N/ha	-0.100	-0.155	-0.296	-0.046	0.020	0.030c	-0.069
20 kg N/ha	-0.077	-0.142	-0.259	-0.026	0.035	0.070bc	-0.039
40 kg N/ha	-0.076	-0.148	-0.261	-0.033	0.036	0.078ab	-0.050
60 kg N/ha	-0.062	-0.137	-0.239	0.008	0.026	0.112ab	0.011
100 kg N/ha	-0.059	-0.138	-0.233	0.014	0.051	0.125a	0.021
ANOVA Results[1]	**NS**	**NS**	**NS**	**NS**	**NS**	**p<0.004**	**NS**

[1]Analysis of variance (ANOVA) results refer to treatment effects that were either not significant (NS) or significant at p<0.05. Mean separation was completed using Fisher's multiple means comparison test procedure (α=0.05).

APPENDIX 3: Growth progression of the different wild blueberry species and variable importance table

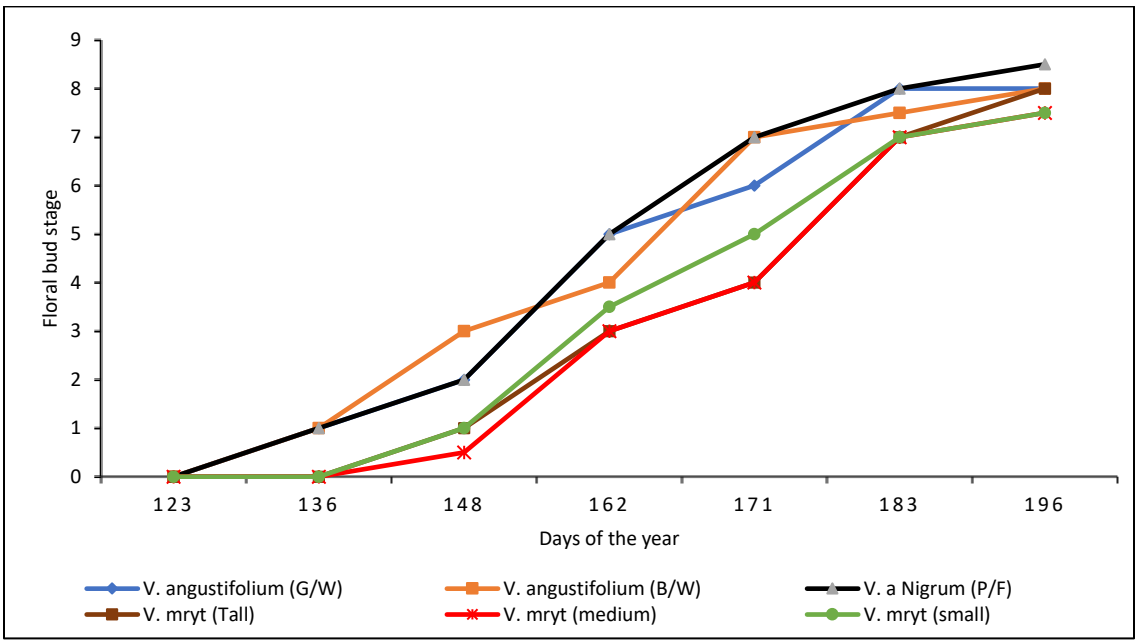

Figure A 1. Growth progression of the different blueberry phenotypes at Lemmon Hill as monitored from May to June 2020. The different colours represent the six phenotypes.

Table A 5. Rankings of an SVM classifier on the 2022 multispectral trial of best-performing indices for each phenological stage and parameter. Performance was evaluated using outputs from the variable importance chart. Percentages represent the performance of the individual vegetative indices in achieving that outcome. Indices have been arranged in order of the best index to the least performing index along with its corresponding percentage.

Bud break (F1)		
Parameter	**Rank**	**Percentage (%)**
Yield (g.m^{-2})	NDVI, GLI, VARI, ENDVI, GRVI, NDRE	100, 70, 35, 25, 20, 0
Leaf area index	NDRE, ENDVI, GLI, GRVI, NDVI, VARI	100, 58, 10, 5, 4, 0
Plant height (cm)	GLI, VARI, GRVI, ENDVI, NDVI, NDRE	100, 90, 82, 30, 12, 0
Floral bud number	NDRE, GLI, VARI, ENDVI, GRVI, NDVI	100, 90, 35, 25, 25, 0
Floral bud stage	NDVI, NDRE, GRVI, ENDVI, VARI, GLI	100, 52, 10, 8, 5, 0
Vegetative bud number	GLI, VARI, GRVI, ENDVI, NDVI, NDRE	100, 78, 70, 42, 40, 0
Vegetative bud stage	NDRE, NDVI, ENDVI, GRVI, VARI, GLI	100, 55, 40, 12, 13, 0
Tight cluster (F2/F3)		
Parameter	**Rank**	**Percentage (%)**
Yield (g.m^{-2})	NDVI, ENDVI, NDRE, GRVI, GLI, VARI	100, 55, 10, 5, 3, 0
Leaf area index	NDRE, ENDVI, GLI, GRVI, NDVI, VARI	100, 58, 10, 5, 4, 0
Plant height (cm)	NDVI, ENDVI, NDRE, VARI, GLI, GRVI	100, 93, 38, 5, 4, 0
Floral bud number	NDVI, ENDVI, GLI, VARI, GRVI, NDRE	100, 55, 47, 30, 20, 0

Floral bud stage	NDRE, ENDVI, GLI, NDVI, GRVI, VARI	100, 38, 20, 10, 5, 0
Vegetative bud number	GLI, NDVI, NDRE, ENDVI, VARI, GRVI	100, 68, 50, 40, 18, 0
Vegetative bud stage	NDRE, NDVI, GLI, ENDVI, VARI, GRVI	100, 78, 42, 22, 1, 0
	Bud break (F4/F5)	
Parameter	**Rank**	**Percentage (%)**
Yield (g.m^{-2})	NDRE, ENDVI, GRVI, GLI, VARI, NDVI	100, 65, 10, 10, 8, 0
Leaf area index	VARI, GRVI, GLI, NDVI, ENDVI, NDRE	100, 98, 95, 80, 58, 0
Plant height (cm)	NDRE, ENDVI, GLI, GRVI, VARI, NDVI	100, 58, 18, 10, 10, 0
Floral bud number	ENDVI, NDRE, NDVI, GLI, GRVI, VARI	100, 90, 63, 30, 5 0
Floral bud stage	ENDVI, NDVI, VARI, GRVI, GLI, NDRE	100, 98, 35, 30, 30, 0
Vegetative bud number	NDVI, ENDVI, NDRE, GLI, GRVI, VARI	100, 48, 30, 10, 5, 0
Vegetative bud stage	NDVI, ENDVI, GRVI, VARI, GLI, NDRE	100, 82, 80, 80, 70, 0
	Bud break (F6/F7)	
Parameter	**Rank**	**Percentage (%)**
Yield (g.m^{-2})	NDVI, ENDVI, VARI, GRVI, NDRE, GLI	100, 90, 85, 35, 27, 0
Leaf area index	NDVI, ENDVI, GLI, GRVI, VARI, NDRE	100, 90, 88, 85, 75, 0
Plant height (cm)	ENDVI, NDRE, NDVI, GRVI, VARI, GLI	100, 93, 93, 5, 2, 0
Floral bud number	GLI, GRVI, VARI, ENDVI, NDVI, NDRE	100, 85, 65, 45, 25, 0
Floral bud stage	NDRE, VARI, GRVI, ENDVI, GLI, NDVI	100, 78, 55, 53, 50, 0
Vegetative bud number	ENDVI, NDVI, NDRE, GLI, GRVI, VARI	100, 60, 55, 13, 10, 0
Vegetative bud stage	GLI, GRVI, VARI, NDVI, NDRE, ENDVI	100, 98, 90, 58, 55, 0
	Fruit set (F8)	
Parameter	**Rank**	**Percentage (%)**
Yield (g.m^{-2})	NDVI, VARI, GRVI, GLI, ENDVI, NDRE	100, 85, 83, 79, 55, 0
Leaf area index	VARI, GRVI, GLI, NDVI, ENDVI, NDRE	100, 95, 82, 78, 62, 0
Plant height (cm)	GRVI, VARI, NDVI, GLI, ENDVI, NDRE	100, 95, 92, 83, 22, 0
Floral bud number	GLI, VARI, NDRE, GRVI, NDVI, ENDVI	100, 100, 90, 88, 79, 0
Floral bud stage	NDVI, GRVI, GLI, VARI, NDRE, ENDVI	100, 95, 68, 60, 58, 0
Vegetative bud number	VARI, GRVI, NDVI, GLI, NDRE, ENDVI	100, 100, 80, 78, 57, 0
Vegetative bud stage	ENDVI, VARI, GRVI, NDRE, GLI, NDVI	100, 48, 35, 20, 15, 0

Table A 6. Rankings of an RF classifier on the 2022 multispectral trial of best-performing indices for each phenological stage and parameter. Performance was evaluated using outputs from the variable importance chart. Percentages represent the performance of the individual vegetative indices in achieving that outcome. Indices have been arranged in order of the best index to the least performing index along with its corresponding percentage.

	Bud break (F1)	
Parameter	**Rank**	**Percentage (%)**
Yield (g.m^{-2})	NDVI, GLI, GRVI, VARI, ENDVI, NDRE	100, 65, 38, 35, 25, 0
Leaf area index	VARI, GLI, GRVI, NDRE, ENDVI, NDVI	100, 90, 80, 30, 22, 0
Plant height (cm)	GLI, VARI, GRVI, ENDVI, NDVI, NDRE	100, 90, 83, 42, 23, 0
Floral bud number	VARI, GLI, NDRE, GRVI, NDVI, ENDVI	100, 95, 90, 70, 18, 0
Floral bud stage	NDVI, VARI, GRVI, GLI, ENDVI, NDRE	100,82, 75, 70, 65, 0
Vegetative bud number	GLI, GRVI, VARI, ENDVI, NDVI, NDRE	100, 85, 85, 55, 48, 0
Vegetative bud stage	VARI, GLI, GRVI, NDRE, ENDVI, NDVI	100, 68, 48, 22, 20, 0

Tight cluster (F2/F3)		
Parameter	**Rank**	**Percentage (%)**
Yield (g.m^{-2})	NDVI, ENDVI, GLI, GRVI, NDRE, VARI	100, 15, 5, 2, 1, 0
Leaf area index	VARI, GLI, GRVI, NDRE, ENDVI, NDVI	100, 90, 80, 30, 22, 0
Plant height (cm)	NDVI, ENDVI, NDRE, VARI, GRVI, GLI	100, 61, 15, 9, 4, 0
Floral bud number	ENDVI, NDVI, VARI, GLI, GRVI, NDRE	100, 90, 75, 70, 38, 0
Floral bud stage	NDRE, VARI, ENDVI, GLI, GRVI, NDVI	100, 88, 50, 42, 4, 0
Vegetative bud number	GRVI, ENDVI, GLI, VARI, NDVI, NDRE	100, 75, 70, 35, 20, 0
Vegetative bud stage	GLI, GRVI, NDRE, NDVI, VARI, ENDVI	100, 40, 35, 18, 15, 0
Bud break (F4/F5)		
Parameter	**Rank**	**Percentage (%)**
Yield (g.m^{-2})	NDRE, ENDVI, NDVI, GLI, GRVI, VARI	100, 60, 38, 4, 1, 0
Leaf area index	GRVI, GLI, VARI, ENDVI, NDVI, NDRE	100, 98, 98, 58, 58, 0
Plant height (cm)	ENDVI, NDRE, GRVI, NDVI, VARI, GLI	100, 80, 62, 40, 35, 0
Floral bud number	GLI, ENDVI, GRVI, NDRE, VARI, NDVI	100, 95, 42, 40, 25, 0
Floral bud stage	ENDVI, NDVI, GRVI, VARI, GLI, NDRE	100, 80, 58, 58, 58, 0
Vegetative bud number	NDRE, ENDVI, NDVI, VARI, GRVI, GLI	100, 90, 70, 25, 20, 0
Vegetative bud stage	GLI, GRVI, VARI, NDVI, ENDVI, NDRE	100, 90, 75, 47, 42, 0
Bud break (F6/F7)		
Parameter	**Rank**	**Percentage (%)**
Yield (g.m^{-2})	GRVI, NDVI, VARI, ENDVI, NDRE, GLI	100, 98, 55, 40, 8, 0
Leaf area index	NDVI, GLI, GRVI, ENDVI, VARI, NDRE	100, 82, 50, 35, 12, 0
Plant height (cm)	NDVI, ENDVI, GLI, NDRE, VARI, GRVI	100, 75, 35, 30, 10, 0
Floral bud number	GLI, NDVI, GRVI, NDRE, ENDVI, VARI	100, 65, 35, 32, 28, 0
Floral bud stage	NDRE, ENDVI, GLI, VARI, GRVI, NDVI	100, 45, 18, 8, 8, 0
Vegetative bud number	NDRE, VARI, GRVI, NDVI, ENDVI, GLI	100, 60, 50, 38, 28, 0
Vegetative bud stage	VARI, GRVI, GLI, NDVI, NDRE, ENDVI	100, 78, 68, 58, 35, 0
Fruit set (F8)		
Parameter	**Rank**	**Percentage (%)**
Yield (g.m^{-2})	GLI, VARI, NDVI, ENDVI, GRVI, NDRE	100, 90, 85, 82, 55, 0
Leaf area index	VARI, GRVI, ENDVI, GLI, NDVI, NDRE	100, 98, 68, 68, 38, 0
Plant height (cm)	NDVI, VARI, GLI, GRVI, NDRE, ENDVI	100, 88, 78, 75, 10, 0
Floral bud number	GRVI, NDRE, GLI, NDVI, VARI, ENDVI	100, 95, 85, 30, 4, 0
Floral bud stage	NDRE, NDVI, VARI, ENDVI, GLI, GRVI	100, 45, 30, 10, 5, 0
Vegetative bud number	VARI, GRVI, NDRE, GLI, ENDVI, NDVI	100, 80, 50, 40, 17, 0
Vegetative bud stage	ENDVI, GRVI, VARI, NDVI, NDRE, GLI	100, 90, 72. 40, 30, 0

Table A 7. Rankings of a KNN and SMLR classifier on the 2022 multispectral trial of best-performing indices for each phenological stage and parameter. Performance was evaluated using outputs from the variable importance chart. Percentages represent the performance of the individual vegetative indices in achieving that outcome. Indices have been arranged in order of the best index to the least performing index along with its corresponding percentage.

Bud break (F1)		
Parameter	**Rank**	**Percentage (%)**

Yield (g.m^{-2})	NDVI, GLI, VARI, ENDVI, GRVI, NDRE	100, 70, 35, 28, 20, 0
Leaf area index	NDRE, ENDVI, GLI, GRVI, NDVI, VARI	100, 58, 10, 4, 3, 0
Plant height (cm)	GLI, VARI, GRVI, ENDVI, NDVI, NDRE	100, 90, 82, 30, 10, 0
Floral bud number	NDRE, GLI, VARI, ENDVI, GRVI, NDVI	100, 88, 38, 28, 28, 0
Floral bud stage	NDVI, NDRE, GRVI, ENDVI, VARI, GLI	100, 53, 10, 5, 4, 0
Vegetative bud number	GLI, VARI, GRVI, ENDVI, NDVI, NDRE	100, 78, 70, 42, 40, 0
Vegetative bud stage	NDRE, NDVI, ENDVI, GRVI, VARI, GLI	100, 55, 40, 10, 12, 0
	Tight cluster (F2/F3)	
Parameter	**Rank**	**Percentage (%)**
Yield (g.m^{-2})	NDVI, ENDVI, NDRE, GRVI, GLI, VARI	100, 55, 10, 5, 3, 0
Leaf area index	NDRE, ENDVI, GLI, GRVI, NDVI, VARI	100, 58, 10, 5, 4, 0
Plant height (cm)	NDVI, ENDVI, NDRE, VARI, GLI, GRVI	100, 92, 38, 5, 4, 0
Floral bud number	NDVI, ENDVI, GLI, VARI, GRVI, NDRE	100, 55, 48, 35, 20, 0
Floral bud stage	NDRE, ENDVI, GLI, NDVI, GRVI, VARI	100, 38, 20, 10, 5, 0
Vegetative bud number	GLI, NDVI, NDRE, ENDVI, VARI, GRVI	100, 70, 50, 39, 18, 0
Vegetative bud stage	NDRE, NDVI, GLI, ENDVI, VARI, GRVI	100, 78, 42, 20, 1, 0
	Bud break (F4/F5)	
Parameter	**Rank**	**Percentage (%)**
Yield (g.m^{-2})	NDRE, ENDVI, GRVI, GLI, VARI, NDVI	100, 65, 10, 10, 8,0
Leaf area index	VARI, GRVI, GLI, NDVI, ENDVI, NDRE	100, 98, 95, 80, 55, 0
Plant height (cm)	NDRE, ENDVI, GLI, GRVI, VARI, NDVI	100, 58, 18, 10, 10, 0
Floral bud number	ENDVI, NDRE, NDVI, GLI, GRVI, VARI	100, 90, 65, 35, 3, 0
Floral bud stage	ENDVI, NDVI, VARI, GRVI, GLI, NDRE	100, 100, 35, 30, 30, 0
Vegetative bud number	NDVI, ENDVI, NDRE, GLI, GRVI, VARI	100, 48, 30, 10, 4, 0
Vegetative bud stage	NDVI, ENDVI, GRVI, VARI, GLI, NDRE	100, 85,80, 80, 72, 0
	Bud break (F6/F7)	
Parameter	**Rank**	**Percentage (%)**
Yield (g.m^{-2})	NDVI, ENDVI, VARI, GRVI, NDRE, GLI	100, 90, 85, 35, 28, 0
Leaf area index	NDVI, ENDVI, GLI, GRVI, VARI, NDRE	100, 90, 88, 85, 75, 0
Plant height (cm)	ENDVI, NDRE, NDVI, GRVI, VARI, GLI	100, 93, 93, 5, 2, 0
Floral bud number	GLI, GRVI, VARI, ENDVI, NDVI, NDRE	100, 85, 65, 45, 25, 0
Floral bud stage	NDRE, VARI, GRVI, ENDVI, GLI, NDVI	100, 78, 55, 53, 50, 0
Vegetative bud number	NDVI, ENDVI, NDRE, GLI, GRVI, VARI	100, 60, 55, 15, 12, 0
Vegetative bud stage	GLI, GRVI, VARI, NDVI, NDRE, ENDVI	100, 95, 90, 35, 32, 0
	Fruit set (F8)	
Parameter	**Rank**	**Percentage (%)**
Yield (g.m^{-2})	NDVI, VARI, GRVI, GLI, ENDVI, NDRE	100, 88, 85, 78, 55, 0
Leaf area index	VARI, GRVI, GLI, NDVI, ENDVI, NDRE	100, 95, 82, 78, 64, 0
Plant height (cm)	GRVI, VARI, NDVI, GLI, ENDVI, NDRE	100, 98, 95, 83, 22, 0
Floral bud number	GLI, VARI, NDRE, GRVI, NDVI, ENDVI	100, 100, 92, 88, 78, 0
Floral bud stage	NDVI, GRVI, GLI, VARI, NDRE, ENDVI	100, 95, 70, 60, 58, 0
Vegetative bud number	VARI, GRVI, NDVI, GLI, NDRE, ENDVI	100, 100, 80, 78, 55, 0
Vegetative bud stage	ENDVI, VARI, GRVI, NDRE, GLI, NDVI	100, 48, 37, 20, 12, 0

APPENDIX 4: Assessment tables on disease, variable importance chart, and ALE plots

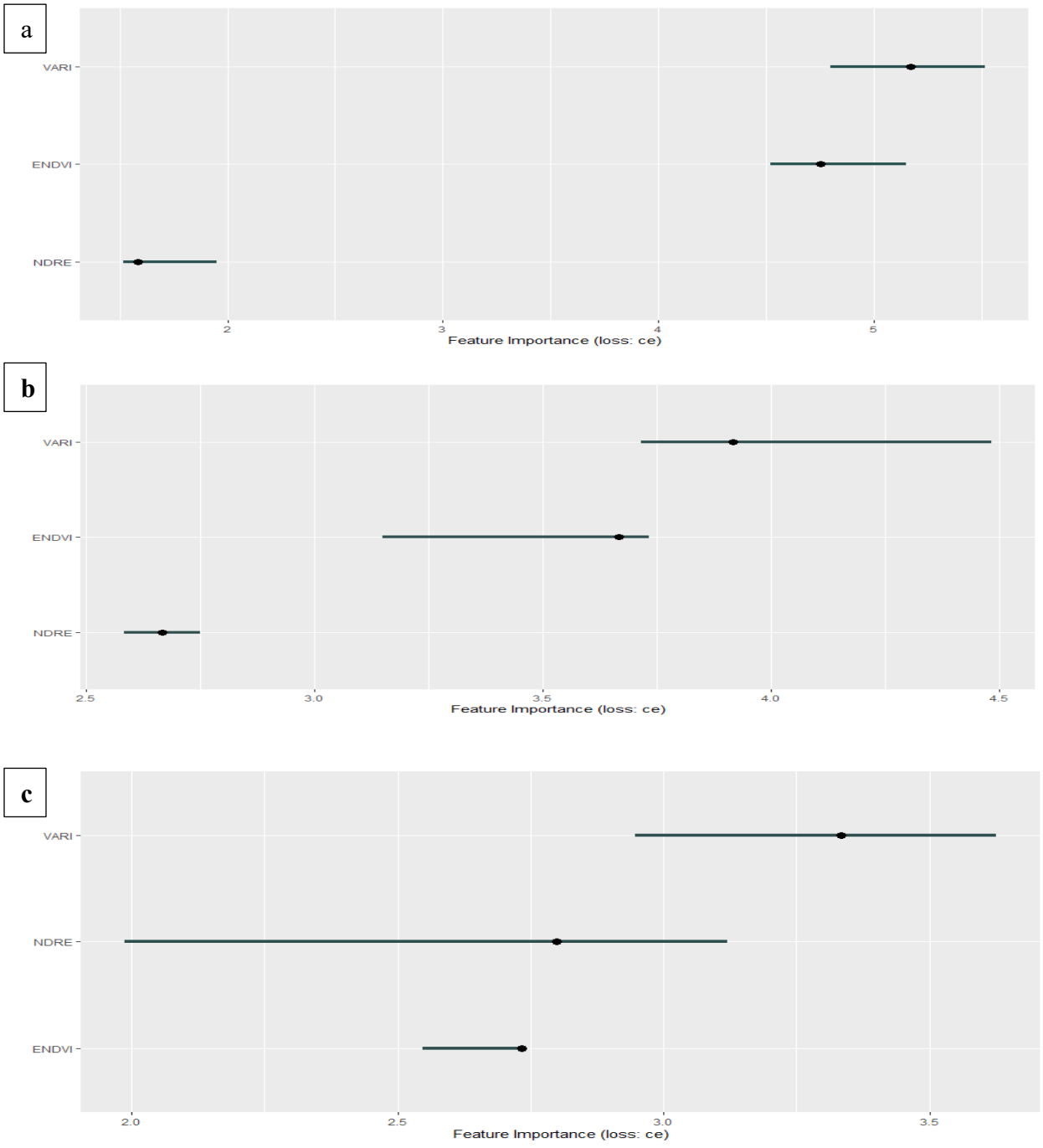

Figure A 2. Variable importance charts for the selected VIs under the combined condition (BB, Healthy, and MB) using (a) KNN, (b) RF, and (c) SVM classifiers.

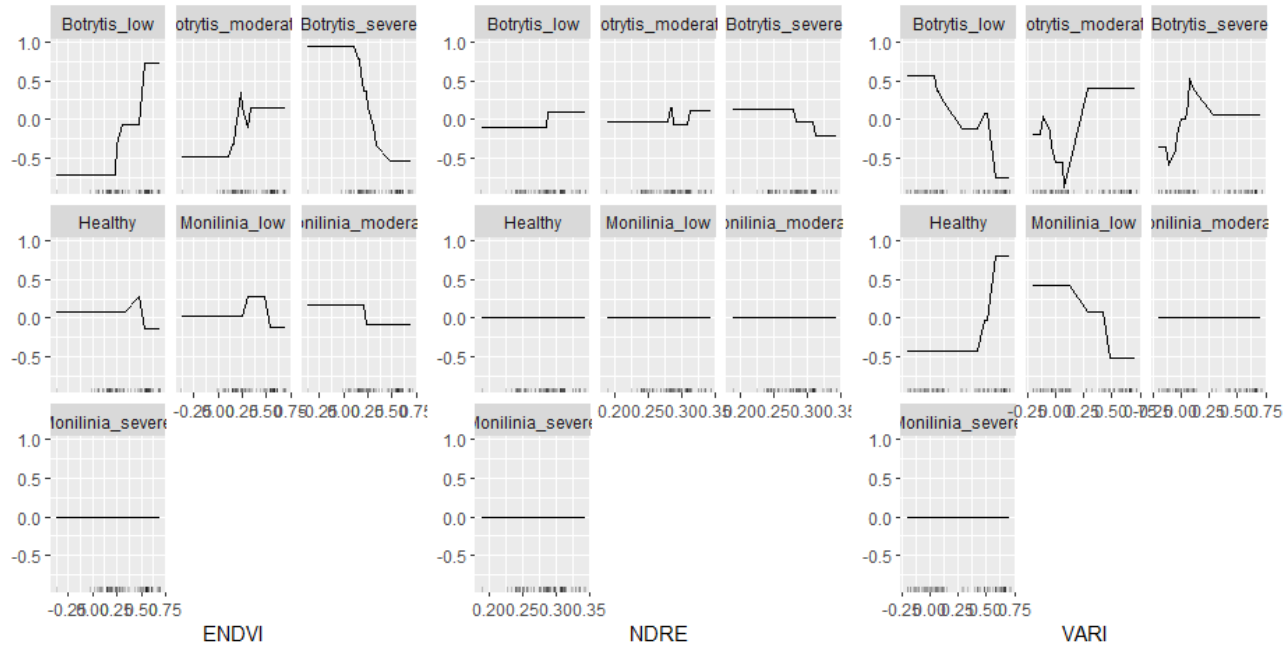

Figure A 3. ALE plot of ENVI, NDRE, and VARI under the different levels of disease severity using the KNN classifier.

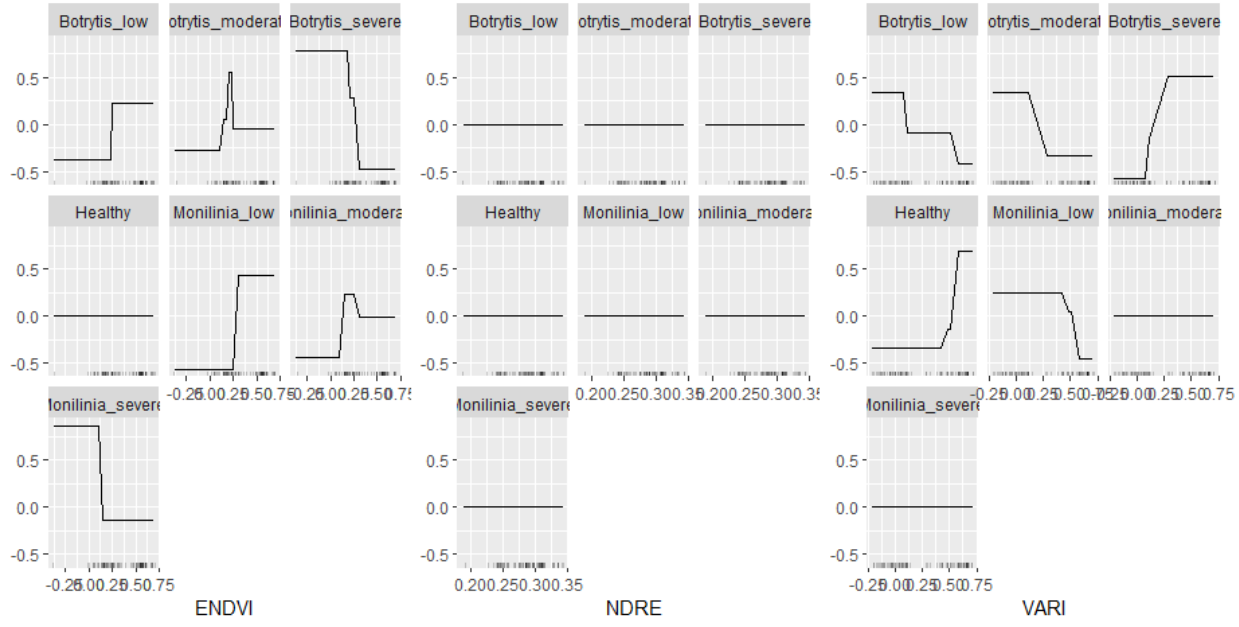

Figure A 4. ALE plots of ENVI, NDRE, and VARI under the different levels of disease severity using the RF classifier.

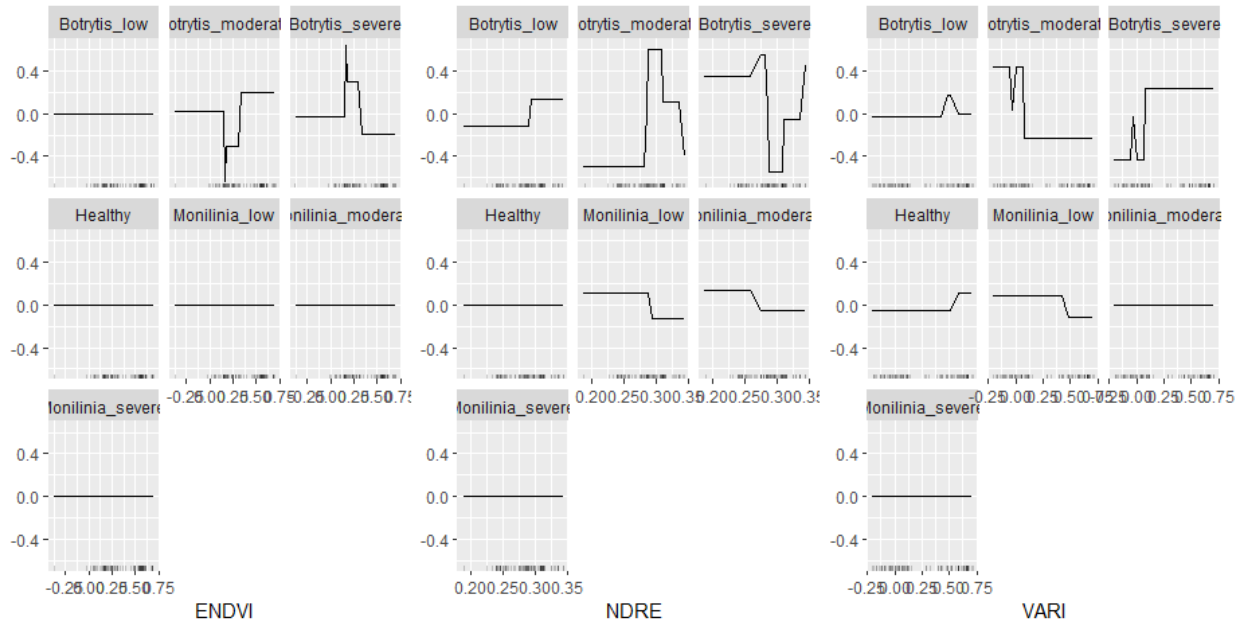

Figure A 5. ALE plot of ENVI, NDRE, and VARI under the different levels of disease severity using the SVM classifier

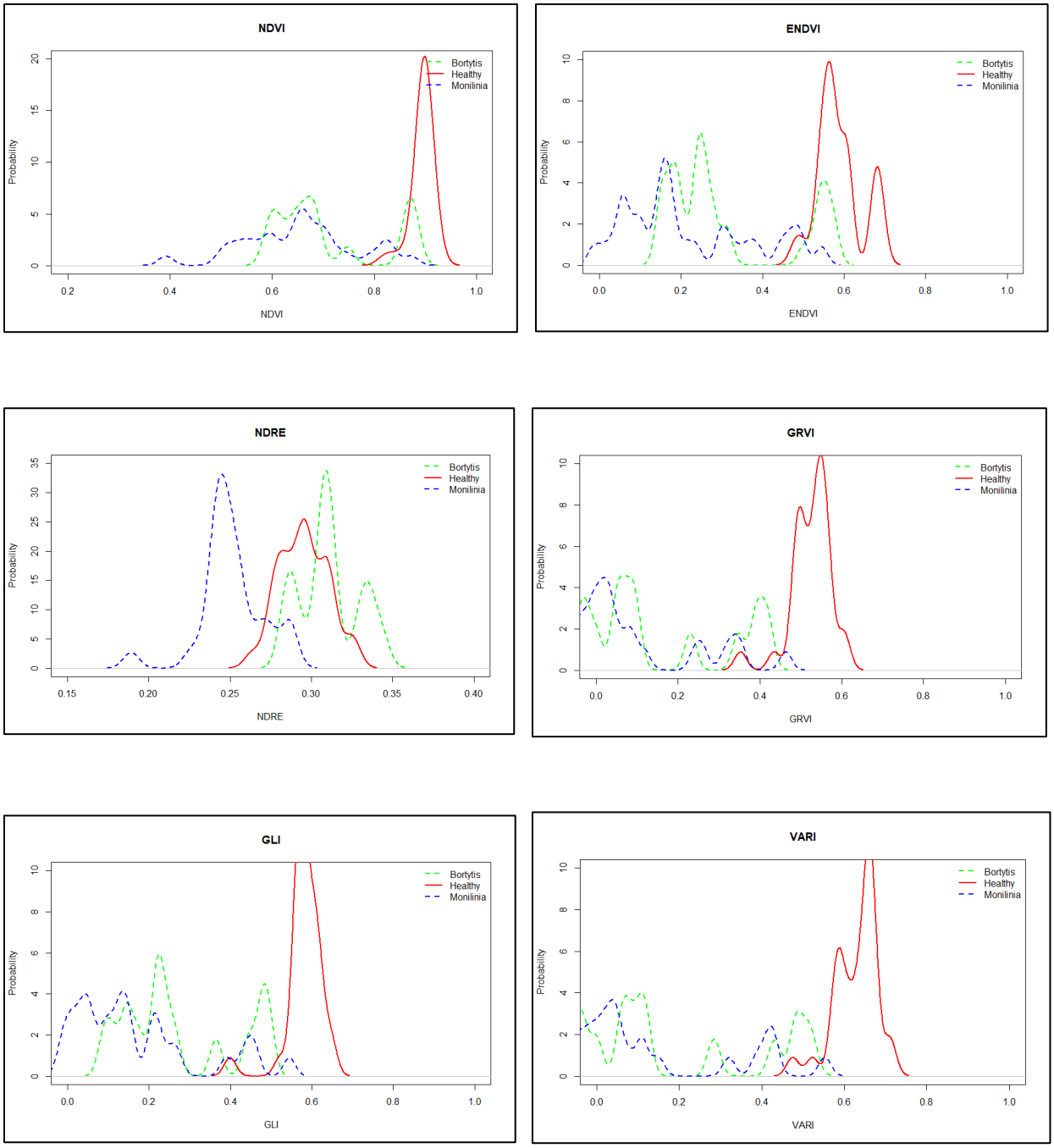

Figure A 6. Probability density function (PDF) plot on all six VIs under the three (3) conditions

Table A 8. Aerial vegetative indices (VI's) observed from Farmington after 3rd fungicide application. Image samples for this observation were collected on [19th June 2019].

Treatment	Green Leaf (GL)	GRVI	VARI
Untreated Control	0.261	0.109	0.137
Monilinia Control	0.266	0.113	0.140
Botrytis Control	0.254	0.101	0.126
Monilinia & Botrytis Control	0.247	0.092	0.116
ANOVA Results[1]	**NS**	**NS**	**NS**

1 Analysis of variance (ANOVA) results refer to treatment effects that were either not significant (NS) or significant at $p<0.05$. Mean separation was completed using Fisher's multiple means comparison test procedure ($\acute{a}=0.05$).

Table A 9. Aerial vegetative indices (VI's) observed from Farmington after 4th fungicide application. Image samples for this observation were collected on [3rd July 2019].

Treatment	Green Leaf (GL)	GRVI	VARI
Untreated Control	0.308	0.189	0.244
Monilinia Control	0.340	0.219	0.277
Botrytis Control	0.311	0.194	0.250
Monilinia & Botrytis Control	0.320	0.204	0.262
ANOVA Results[1]	**NS**	**NS**	**NS**

1 Analysis of variance (ANOVA) results refer to treatment effects that were either not significant (NS) or significant at $p<0.05$. Mean separation was completed using Fisher's multiple means comparison test procedure ($\acute{a}=0.05$).

Table A 10. Aerial vegetative indices (VI's) observed from Lemmon Hill after 3rd fungicide application. Image samples for this observation were collected on [19th June 2019].

Treatment	Green Leaf (GL)	GRVI	VARI
Untreated Control	0.189	0.077	0.103
Monilinia Control	0.226	0.100	0.129
Botrytis Control	0.216	0.090	0.118
Monilinia & Botrytis Control	0.220	0.096	0.124
ANOVA Results[1]	**NS**	**NS**	**NS**

1 Analysis of variance (ANOVA) results refer to treatment effects that were either not significant (NS) or significant at $p<0.05$. Mean separation was completed using Fisher's multiple means comparison test procedure ($\acute{\alpha}=0.05$).

Table A 11. Aerial vegetative indices (VI's) observed from Lemmon Hill after 4th fungicide application. Image samples for this observation were collected on [3rd June 2019].

Treatment	Green Leaf (GL)	GRVI	VARI
Untreated Control	0.389	0.375	0.499
Monilinia Control	0.458	0.457	0.596
Botrytis Control	0.440	0.428	0.568
Monilinia & Botrytis Control	0.435	0.427	0.564
ANOVA Results[1]	**NS**	**NS**	**NS**

1 Analysis of variance (ANOVA) results refer to treatment effects that were either not significant (NS) or significant at $p<0.05$. Mean separation was completed using Fisher's multiple means comparison test procedure ($\acute{\alpha}=0.05$).

Table A 12. Aerial vegetative indices (VI's) observed from Kemptown after 3rd fungicide application. Image samples for this observation were collected on [10th June 2020].

Treatment	Green Leaf (GL)	GRVI	VARI	NDVI	NDRE	ENDVI	SAVI
Untreated Control	0.185	0.077	0.105	0.761	0.357	0.757	0.926
Monilinia Control	0.238	0.141	0.192	0.803	0.362	0.790	0.934
Botrytis Control	0.196	0.095	0.129	0.750	0.354	0.746	0.908
Monilinia & Botrytis Control	0.247	0.158	0.218	0.809	0.368	0.794	0.764
ANOVA Results[1]	**NS**	**NS**	**NS**	**NS**	**NS**	**NS**	**NS**

[1] Analysis of variance (ANOVA) results refer to treatment effects that were either not significant (NS) or significant at $p<0.05$. Mean separation was completed using Fisher's multiple means comparison test procedure ($\acute{a}=0.05$).

Table A 13. Aerial vegetative indices (VI's) observed from Kemptown after 4th fungicide application. Image samples for this observation were collected on [18th June 2020].

Treatment	Green Leaf (GL)	GRVI	VARI	NDVI	NDRE	ENDVI	SAVI
Untreated Control	0.195	0.196	0.318	0.426	0.056	0.334	0.634
Monilinia Control	0.241	0.254	0.408	0.501	0.078	0.385	0.734

Botrytis Control	0.222	0.229	0.362	0.434	0.056	0.345	0.592
Monilinia & Botrytis Control	0.261	0.278	0.436	0.510	0.084	0.396	0.727
ANOVA Results[1]	**NS**	**NS**	**NS**	**NS**	**NS**	**NS**	**NS**

[1] Analysis of variance (ANOVA) results refer to treatment effects that were either not significant (NS) or significant at p<0.05. Mean separation was completed using Fisher's multiple means comparison test procedure (ά=0.05)

Table A 14. Aerial vegetative indices (VI's) observed from Lemmon Hill after 3rd fungicide application. Image samples for this observation were collected on [9th June 2020].

Treatment	Green Leaf (GL)	GRVI	VARI	NDVI	NDRE	ENDVI	SAVI
Untreated Control	0.312	0.243	0.318	0.836	0.360	0.801	0.763
Monilinia Control	0.306	0.236	0.309	0.831	0.355	0.797	0.752
Botrytis Control	0.310	0.236	0.321	0.839	0.355	0.808	0.918
Monilinia & Botrytis Control	0.300	0.226	0.293	0.830	0.348	0.799	0.761
ANOVA Results[1]	**NS**	**NS**	**NS**	**NS**	**NS**	**NS**	**NS**

[1] Analysis of variance (ANOVA) results refer to treatment effects that were either not significant (NS) or significant at p<0.05. Mean separation was completed using Fisher's multiple means comparison test procedure (ά=0.05).

Table A 15. Aerial vegetative indices (VI's) observed from Lemmon Hill after 4th fungicide application. Image samples for this observation were collected on [17th June 2020].

Treatment	Green Leaf (GL)	GRVI	VARI	NDVI	NDRE	ENDVI	SAVI
Untreated Control	0.337	0.261	0.334	0.846	0.402	0.821	0.702
Monilinia Control	0.335	0.258	0.330	0.848	0.403	0.824	0.702
Botrytis Control	0.341	0.264	0.350	0.856	0.398	0.831	0.875
Monilinia & Botrytis Control	0.338	0.260	0.342	0.852	0.394	0.828	0.867
ANOVA Results[1]	**NS**	**NS**	**NS**	**NS**	**NS**	**NS**	**NS**

[1] Analysis of variance (ANOVA) results refer to treatment effects that were either not significant (NS) or significant at $p<0.05$. Mean separation was completed using Fisher's multiple means comparison test procedure ($\acute{a}=0.05$)

Table A 16. Aerial vegetative indices (VI's) observed from Mount Thom after 4th fungicide application. Image samples for this observation were collected on [12th June 2021].

Treatment	Green Leaf (GL)	GRVI	VARI
Untreated Control	0.144	-0.073	-0.087
Monilinia Control	0.160	-0.068	-0.079

Botrytis Control	0.156	-0.059	-0.069
Monilinia & Botrytis Control	0.157	-0.065	-0.076
ANOVA Results[1]	**NS**	**NS**	**NS**

[1] Analysis of variance (ANOVA) results refer to treatment effects that were either not significant (NS) or significant at p<0.05. Mean separation was completed using Fisher's multiple means comparison test procedure (ά=0.05).

Table A 17. Aerial vegetative indices (VI's) observed from Farmington after 3rd fungicide application. Image samples for this observation were collected on [3rd June 2022].

Treatment	Green Leaf (GL)	GRVI	VARI	NDVI	NDRE	ENDVI	SAVI
Untreated Control	0.309	0.208	0.271	0.848	0.339	0.840	0.655
Monilinia Control	0.343	0.248	0.320	0.856	0.335	0.845	0.672
Botrytis Control	0.304	0.206	0.270	0.842	0.326	0.832	0.652
Monilinia & Botrytis Control	0.328	0.233	0.303	0.849	0.330	0.837	0.666
ANOVA Results[1]	**NS**	**NS**	**NS**	**NS**	**NS**	**NS**	**NS**

[1] Analysis of variance (ANOVA) results refer to treatment effects that were either not significant (NS) or significant at p<0.05. Mean separation was completed using Fisher's multiple means comparison test procedure (ά=0.05).

Table A 18. Incidence and severity of Monilinia and *Botrytis* blight disease observed from Webb Mountain before fungicide application. Plant samples for this observation were collected on [13th June 2023, 4th Collection].

Treatment	*Monilinia* incidence of floral nodes (%)[1]	*Monilinia* incidence of vegetative nodes (%)[2]	Monilinia severity of floral node[3]	Monilinia severity of Vegetative node[4]	*Botrytis* incidence of floral nodes (%)[5]	*Botrytis* incidence of vegetative nodes (%)[6]	Botrytis severity of floral node[7]	Botrytis severity of vegetative node[8]
Untreated Control	0.429	0.04	0.714	0.944	5.850	0	9.465 a	0
Monilinia Control	0.571	0	0.952	0	3.754	0	3.262 b	0
Botrytis Control	0	0	0	0	5.726	0	5.707 ab	0
Monilinia & Botrytis Control	0	0	0	0	2.241	0	2.389 b	0
ANOVA Results[9]	**NS**	**NS**	**NS**	**NS**	**NS**	**NS**	**p<0.0020**	**NS**

[1,2,5,6] % Incidence = 0 to 100% where 0 = no blossoms/leaves affected and 100 = all blooms/leaves are affected with at least one lesion.

[3,4,7,8] Severity = 0 to 9 rating scale where 0 = no disease and 9 >= 90% of each blossom/leaf tissue is affected.

[9] Analysis of variance (ANOVA) results refer to treatment effects that were either not significant (NS) or significant at $p<0.05$. Mean separation was completed using Duncan's multiple means comparison test procedure ($\acute{a}=0.05$).

Table A 19. Incidence and severity of Monilinia and *Botrytis* blight disease observed from Fox Point before fungicide application. Plant samples for this observation were collected on [12th June 2023, 5th collection].

Treatment	*Monilinia* incidence of floral nodes (%)[1]	*Monilinia* incidence of vegetative nodes (%)[2]	Monilinia severity of floral node[3]	Monilinia severity of Vegetative node[4]	*Botrytis* incidence of floral nodes (%)[5]	*Botrytis* incidence of vegetative nodes (%)[6]	Botrytis severity of floral node[7]	Botrytis severity of vegetative node[8]
Untreated Control	0	0	0	0	0.922	0	0.500	0
Monilinia Control	0.080	0	0.940	0	0	0	0	0
Botrytis Control	0	0	0	0	0	0	0	0
Monilinia & Botrytis Control	0.040	0	0.180	0	0	0	0	0
ANOVA Results[9]	**NS**	**NS**	**NS**	**NS**	**NS**	**NS**	**NS**	**NS**

[1,2,5,6] % Incidence = 0 to 100% where 0 = no blossoms/leaves affected and 100 = all blooms/leaves are affected with at least one lesion.

[3,4,7,8] Severity = 0 to 9 rating scale where 0 = no disease and 9 >= 90% of each blossom/leaf tissue is affected.

[9] Analysis of variance (ANOVA) results refer to treatment effects that were either not significant (NS) or significant at $p<0.05$. Mean separation was completed using Duncan's multiple means comparison test procedure ($\acute{a}=0.05$).